Acta morphologica et anthropologica (21)

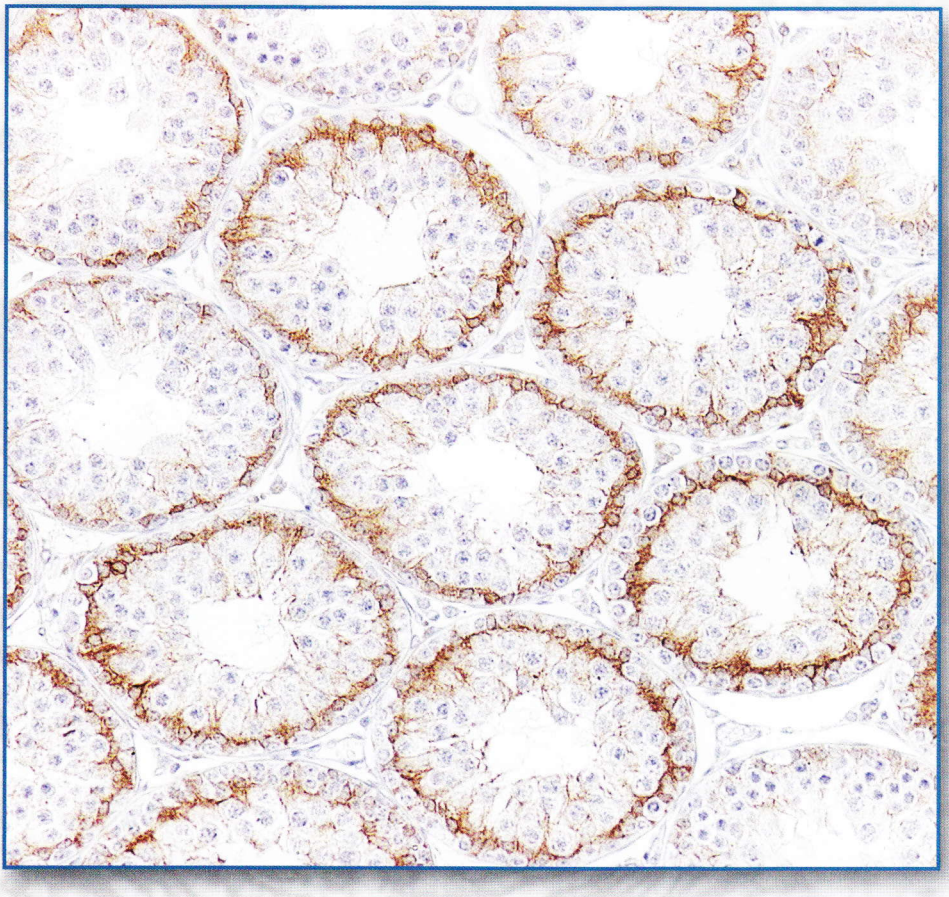

Prof. Marin Drinov Publishing House
of Bulgarian Academy of Sciences

Acta morphologica et anthropologica

is the continuation of
Acta cytobiologica et morphologica

Издаването на настоящия брой на списанието е осъществено с финансовата подкрепа на Фонд „Научни изследвания".

Prof. Marin Drinov Publishing House of Bulgarian Academy of Sciences
Bulgaria, 1113 Sofia, Acad. Georgi Bonchev Str., Bl. 6

Editor *B. Kremenski* Graphic designer *Desislava Georgieva*
Format 70×100/16 Printed sheets 10.63

Printing-office of Prof. Marin Drinov Publishing House of Bulgarian Academy of Sciences
1113 Sofia, Acad. Georgi Bonchev Str., Bl. 5

ISSN 0861-0509

Acta morphologica et anthropologica (21)

21 ● Sofia ● 2015
Institute of Experimental Morphology, Pathology and Anthropology with Museum
Bulgarian Anatomical Society

Contents

Institute of Experimental Morphology, Pathology and Anthropology with Museum
Bulgarian Anatomical Society

Acta morphologica et anthropologica, 21
Sofia ● 2015

Editorial

6th Morphological Days in Sofia
10th National Conference of Anthropology
6-8 of June, 2014

N. Atanassova

Director of Institute of Experimental Morphology, Pathology and Anthropology with Museum, Bulgarian Academy of Sciences, 1113 Sofia, Bulgaria

During 6-8 of June, 2014 two traditional meetings – the 6th Morphological Days and the 10th National Conference of Anthropology were held in the National Anthropological Museum of the Institute of Experimental Morphology, Pathology and Anthropology with Museum at Bulgarian Academy of Sciences in Sofia. The organizers of this event were the Institute of Experimental Morphology, Pathology and Anthropology with Museum and Bulgarian Anatomical Society.

The Conference was dedicated to 145th anniversary of foundation of Bulgarian Academy of Sciences and to 40th anniversary of the first anthropological reconstruction "Ancient Bulgarian women" made by Professor Yordan Yordanov.

More than 100 scientists took part in the Conference – cytologists, histologists, anatomists and anthropologists from all the morphological research groups in Bulgaria – Medical Faculties of Medial Universities in Sofia, Plovdiv, Varna, Pleven, Stara Zagora, Faculty of Biology and Faculty of Medicine of Sofia University St. Kliment Ohridski, Faculty of Biology of Plovdiv University Paisii Hilendarski, Faculty of Medicine and Faculty of Veterinary Medicine of Trakia University in Stara Zagora, Faculty of Veterinary Medicine of University of Forestry in Sofia.

International participants form Russia, Germany, USA, Slovakia, and Macedonia took also part in the Conference.

The opening ceremony started by welcome addresses presented by Professor Nina Atanassova, Director of IEMPAM-BAS, Professor Yordan Yordanov, Head of National Anthropological Museum. Three plenary lectures were given by Invited Speakers from Sofia and Varna.

During the seven Sessions of the Conference, 67 reports were presented followed by discussions. Many young researches and PhD students got opportunity to present their results and to talk with famous scientists. The meeting always provides great time for all the participants to share their research progress and ideas and to make fruitful collaborations.

The Conference was sponsored by Microoptica Ltd. and FOT Ltd.

Institute of Experimental Morphology, Pathology and Anthropology with Museum
Bulgarian Anatomical Society

Acta morphologica et anthropologica, 21
Sofia ● 2015

Morphology

Experimental Approaches for Identification of Biomarkers for Male Infertility

N. Atanassova

Dept. Experimental Morphology, Institute of Experimental Morphology, Pathology and Anthropology with Museum, Bulgarian Academy of Sciences, 1113 Sofia, Bulgaria

The incidence of disorders of human male reproductive health has increased more than double in the past 30 years while sperm counts have declined by about half. Similar abnormalities occur in sons of women treated with estrogenic hormones during pregnancy and they can be experimentally induced in animals by brief exposure to exogenous estrogens during perinatal life [6]. Hormones (mainly estrogens) determine subsequent risk of cancers of the male reproductive organs, e.g. testicular and prostate cancers. Endocrine disrupting chemicals that are widely spread in the environment act as weak hormones being estrogen or androgen receptor agonists or antagonists. Hence, they cannot be ignored as a potential involvement in human reproductive disease [7].

A complex system of morphological, quantitative and functional criteria was developed for identification and evaluation of androgen and estrogen action and the balance between both of hormones in the male reproductive system applying experimental approach involving single or combined treatments with different doses potent (DES) or weak estrogens (Bisphenol-A, Octylphenol, phytoestrogen-Genistein), GnRH-antagonist and anti-androgen Flutamide [2]. The role of each somatic cell types of the testis (Sertoli cells, Leydig cells, peritubular cells, testicular arteriole smooth muscle cells) in androgen signaling was established via comparative and detailed studies on genetic model total and selective targeted disruption of androgen receptor (AR) in these cells [1, 2, 5, 8, 9, 10]. Another experimental model, complementary to the latter, is androgen withdrawal after selective ablation of Leydig cells by ethane dimethanesulfonate (EDS) [2, 3].

Another risk factor for male infertility is diabetes mellitus (DM), but the underlying mechanisms involved are poorly understood. Recently, experimental model was developed for induction of hyperglycaemia in neonatal (on day 1), peripubertal/developing (on day 10) and adult (on day 60) rats by treatment with streptozotocin [4].

Schematic demonstration of treatment regimens was shown in **Table 1** together with semiquantitative presentation of plasma levels of steroid hormones and gonadotrophins.

Table 1. Schematic demonstration of treatment regimens and semiquantitative presentation of plasma levels of steroid hormones (testosterone and estradiol) and gonadotrophins (FSH and LH). DES – diethylstilboestrol; GnRHa – GnRH-antagonist; EDS – ethane dimethanesulfonate; ARKO – AR knockout; pnd – postnatal day; N – normal; nm – non measured

	Treatments	**Doses**	**Regimen**	**Androgen**	**Estrogen**	**FSH**	**LH**
1	Control	20 µl corn oil	2-12 pnd	N	N	N	N
2	DES-10	10 µg	2-12 pnd	↓↓↓↓↓	↑↑↑↑↑↑	↓↓↓↓	↓↓↓↓
3	DES-1/0.1	1 µg/ 0.1µg	2-12 pnd	↓-N	↑↑↑↑/ ↑↑	N/ ↑	↓/ N
4	Bisphenol-A	0.5 mg	2-12 pnd	↑	↑	↑	N
5	Octylphenol	150 mg/kg	2-12 pnd	↑	↑	↑	nm
6	Genistein	4 mg/kg	2-18 pnd	nm	↑	N	nm
7	GnRHa	10 mg/kg	2, 5 pnd	↓↓↓↓↓		↓↓↓↓	↓↓↓↓
8	Flutamide	50 mg/kg	2-12 pnd	AR↓↓↓		N	N
9	Testosterone	200 µg	2-12 pnd	↑↑		↓↓↓↓	nm
10	DES+T	as 2 and 9	as 2 and 9	↑↑	↑↑↑↑↑↑	↓↓↓	↑↑↑
11	DES-0.1+GnRHA	as 3 and 7	as 3 and 7	↓↓↓↓↓	↑↑	↓↓↓↓	↓↓↓
12	DES-10+GnRHA	as 2 and 7	as 2 and 7	↓↓↓↓↓	↑↑↑↑↑↑	↓↓↓↓	↓↓↓↓
13	DES+Flutamide	as 3 and 8	as 3 and 8	AP↓↓↓	↑↑	N	N
14	EDS	75 mg/kg	60 pnd	↓↓↓↓↓↓	↓↓↓↓↓↓	↑↑	↑↑↑
15	streptozotocin	65 mg/kg	1/10 pnd	↓/N	nm	nm	nm
16	AP -/- ARKO	total		↓/N	nm	↑↑	↑↑
17	AP -/- SCARKO	Selective in Sertoli cells		N	nm	N	N
18	AP -/- PTMARKO	Selective in Peritubular cells		N	nm	↑↑	↑↑↑
19	AP -/- LCARKO	Selective in Leydig cells		N	N	N	N
20	AP -/- SMARKO	Selective in testicular arteriole smooth muscle cells		N	nm	N	↑↑

Detailed studies were performed on the testes and male reproductive tracts from rats subjected on treatment regiments shown in **Table 1**, as well as from AR-knockout mice. They involved stereological analysis, immunohistochemistry and measurement of plasma levels testosterone, FSH and LH [1, 2]. Based on data obtained quantitative and cellular markers was identified for experimentally induced male reproductive abnormalities that lead to infertility. They are summarized below:

I. Testicular biomarkers:

1. Quantitative macro-biomarkers of the testis:

a. Testis weight (mg) – indicative for total germ cell number;

b. Luminal percentage volume – indicative for Sertoli cells (SC) function to produce seminiferous tubule fluid.

2. Quantitative micro-biomarkers of spermatogenesis:

a. Absolute nuclear volume (ANV)/Number of Sertoli cells per testis indicative for SC function to produce Inhibin-B and is also used for monitoring of spermatogenesis;

b. Absolute nuclear volume/Number of Leydig cells (LC) per testis indicative for Testosterone production;

c. Germ cell apoptotic index = apoptotic cell /total germ cell number;

d. Absolute nuclear volume of germ cells population and their subtypes:

– Spermatogonia – type A and type In+B;

– Spermatocytes – early (leptotene+zygotene) and late meiotic (pachytene+diplotene);

– Spermatids – round (steps 1-7) and elongating (steps 8-19).

e. Cell ratios – Germ cell ANV/Sertoli cells ANV indicative for supporting function of Sertoli cells toward germ cells and hence for efficiency of spermatogenesis.

3. Cellular biomarkers:

a. Sertoli cell markers:

– nuclear: Androgen Receptor (AR), 27 kD Cyclin-dependent kinase inhibitor protein ($p27^{Kip1}$), Wilms' Tumor suppressor protein 1 (WT-1), GATA-4, Placentae and Embryos Oncofetal gene (Pem, marker for androgen regulation);

cytoplasmic: Anti Müllerian Hormone (AMH), Sulfated Glycoprotein-2 (SGP-2), Inhibin-α, – Retinoic Acid Receptor-α (RARα);

b. Leydig cell (LC) markers:

– nuclear: – Chicken Ovalbumin Upstream Promoter Transcription-Factor II (COUP TF-II) as marker for LC progenitor cells;

– cytoplasm: 3βHydroxysteroid Dehydrogenase (3βHSD) as marker for androgen production and steroidogenic capacity of LC; Insulin-like 3 factor (Insl-3) and 11βHSD (markers for LC differentiation), Estrogen Recepto-α (ERα).

c. Peritubular markers: α-Smooth Muscle Actin (αSMA), Desmin, Laminin, β-Tubulin isotype 3;

d. Germ cell markers: p63 (marker for meiotic spermatocytes); Testicular Angiotensin Converting Enzyme (tACE, marker for postmeiotic elongating spermatids step 8-19).

II. Biomarkers of male reproductive tract.

a. Quantitative measurements: area of rete testis and ductuli efferentes (indicative for accumulation of seminiferous tubule fluid); epithelial cell high of rete testis, ductuli efferentes, epididymis and ductus deferens; number of basal epithelial cell per μm length;

b. Epithelial cells: AR, ERα, ERβ, pan-cytokeratins;

c. Basal epithelial cells: p63 and Cytokeratin High Molecular Weight (CKHMW) – indicative for hyperplasia;

d. Stromal and periductal cells: αSMA, desmin.

III. Hormonal profiles.

a. Testosterone: indicative for LC steroidogenesis and androgen production;
b. FSH: indicative for adequate spermatogenesis;
c. LH: indicative for LC responsiveness to androgen;
d. Inhibin-B: indicative for Sertoli cell function and monitoring of spermatogenesis.

Acknowledgement: The author thanks to Professor Richard Sharpe for providing samples from experimental models for hormonal manipulations, to Professor Guido Verhoven, Dr. Karel DeGent and Professor Lee Smith for samples from AR knockout models and to Chris McKinnel for technical expertise in immunohistochemistry. I am also grateful to Professor Michail Davidoff, Professor Yvetta Koeva and Assoc. Professor Mariana Bakalska for studies on EDS experimental model as well as to Assoc. Professor Emilia Lakova for studies on streptozotocin induced DM model. Authors' work was supported in part by Grant DEER # 212844 funded by FP7-ENV-CP and by Grant # DO 02/113 funded by NF "Scientific Research" of Ministry of Education Youth and Science in Bulgaria.

References

1. **Atanassova, N., K. De Gendt, K. A. L. Tan, L. R. De Franca, G. G. Parreira, C. McKinnell, R. M. Sharpe, P. T. K. Saunders, J. I. Mason, S. Hartung, R. Ivell, E. Denolet, G. Verhoeven.** Development and function of the adult generation of Leydig cells in mice with Sertoli cell-selective or total ablation of the androgen receptor. – Endocrinology, **146**, 2005, 4117-4126.
2. **Atanassova, N.** Morpho-functional aspects of androgen/estrogen regulation of the testis and male reproductive tract. D. Sci Thesis, 2007, 346 pages.
3. **Atanassova, N., Y. Koeva.** Hydrohysteroid Dehydrogenases – biological role and clinical importance. Review (Chapter 6). – In: Dehydrogenases (Ed. R. A. Canuto), Rijeka, Croatia, InTech, 2012, 115-16.
4. **Lakova, E., S. Popovska, I. Gencheva, M. Donchev, G. Krasteva, E. Pavlova, D. Dimova, N. Atanassova.** Experimental Model for Streptozotocin – induced diabetes mellitus neonatally or in adulthood – comparative study on male reproduction in condition of hyperglycaemia. – Acta Morphol. Anthropol., **19**, 2012, 122-126.
5. **O'Hara, L., K. McInnes, I. Simitsidellis, S. Morgan, N. Atanassova, J. Slowikowska-Hilczer, K. Kula, M. Szarras-Czapnik, L. Milne, R. Mitchell, L. B. Smith.** Autocrine androgen action is essential for Leydig cell maturation and function, and protects against late-onset Leydig cell apoptosis in both mice and men. – FASEB J., **29**, 2014, 894-890.
6. **Sharpe, R. M., N. E. Skakkebaek.** Are oestrogen involved in falling sperm counts and disorders of the male reproductive tract? – Lancet, **341**, 1993, 1392-1395.
7. **Sharpe, R. M.** Pathways of endocrine disruption during male sexual differentiation and masculinization.– Best Practice & Research Clinical Endocrinology & Metabolism, **20** (1), 2006, 91-110.
8. **Tan, K., K. De Gent, N. Atanassova, M. Walker, R. M. Sharpe, P. T. K., Saunders, E. Denolet, G. Verhoeven.** The role of androgens in Sertoli cell proliferation and functional maturation: studies in mice with total or Sertoli cell-selective ablation of the androgen receptor. – Endocrinology, 2005, **146**, 2674-2683.
9. **Welsh, M., P. T. K. Saunders, N. Atanassova, R. M. Sharpe, L. B. Smith.** Androgen action via testicular peritubular myoid cells is essential for male fertility. – FASEB J., **23** 2009, 4218-4230.
10. **Welsh, M., R. M. Sharpe, L. Moffat, N. Atanassova, P. T. K. Saunders, S. Kilter, A. Bergh, L. B. Smith.** Androgen action via testicular arteriole smooth muscle cells is important for Leydig cell Function, vasomotion and testicular fluid dynamics. – Plos One, **5**, 2010, 1-12.

Institute of Experimental Morphology, Pathology and Anthropology with Museum
Bulgarian Anatomical Society

Acta morphologica et anthropologica, 21
Sofia ● 2015

Comparative Study on Cell Lines Established from Retrovirus-Induced Transplantable Chicken Liver Cancer

R. Alexandrova[*], T. Zhivkova[*], L. Dyakova[**], I. Dankov[,***], P. Jordanova[*], V. Altanerova[****], C. Altaner[****]*

[*]Institute of Experimental Morphology, Pathology and Anthropology with Museum, Bulgarian Academy of Sciences, Acad. Georgi Bonchev Str., Block 25, Sofia, Bulgaria;
[**]Institute of Neurobiology, Bulgarian Academy of Sciences;
[***]Faculty of Medicine, Sofia University St. Kl. Ohridski
[****]Cancer Research Institute, Slovak Academy of Sciences, Bratislava, Slovakia

The cell lines LSCC-PR2-Mc29 and LSCC-SF-Mc29 were established from a transplantable liver cancer in chicken induced by the myelocytomatosis virus Mc29. The aim of the present study was to evaluate comparatively some biological characteristics of these cells. Both cell lines have been found to grow as monolayer cultures and form 3D colonies in semi-solid medium, express v-myc (gag-myc) gene; are sensitive to the cytotoxic/cytostatic effects of the widely used commercial anticancer drug cisplatin. On the other hand, these cells differ in their tumorigenic potential *in vivo*.

Key words: myelocytomatosis virus Mc29, transplantable chicken liver cancer, cell line.

Introduction

Avian myelocytomatosis virus Mc29 was isolated in Bulgaria in 1961 from a Rhode Island Red chicken with spontaneous mielocytomatosis [3]. It belongs to the group of defective avian leukemia retroviruses (ALVs). It has been shown that all three genes essential for the replication of ALVs, i.e. *gag*, *pol* and *env*, are defective in Mc29 virus (gene *pol* is completely missing). The virus possesses a specific oncogene – *v-myc* [5, 8]. *In vitro* the virus Mc29 induces transformation of fibroblasts, epithelial cells and macrophages. *In vivo* transmission causes primarily myelocytomatosis and myelocytomas in chickens but it is also responsible for a broad spectrum of leukemias and tumor growths, including endothelioma, mesothelioma sarcoma and erythroblastosis. Of particular interests are some epithelial cell tumors in the kidney, pancreas and especially in the liver [4, 6, 8]. LSCC-PR2-Mc29 [9] and LSCC-SF-Mc29 [1] are cell lines derived from Mc29 virus-induced transplantable chicken liver cancer. The aim of the present study was to compare some biological characteristics of these cell lines.

Materials and Methods

The cells were grown as monolayer cultures in D-MEM medium, supplemented with 5-10% fetal bovine serum, 100 U/ml penicillin and 100 μg/ml streptomycin. The cultures were maintained at 37 °C in a humidified CO_2 incubator. For routine passages adherent cells were detached using a mixture of 0.05% trypsin – 0.02% ethylendiaminotetraacetic acid (EDTA). The investigations were carried out by colony-forming method [2], karyological analysis and polymerase chain reaction (PCR). The influence of cisplatin on cell viability and proliferation was evaluated by thiazolyl blue tetrazolium bromide test (MTT) [7]. *In vivo* experiments were performed using inbred 15I White leghorn chickens.

Chromosome analysis is performed according to the standard procedure. Briefly, the cells have been arrested in metaphase with 0.02 μg/ml Colcemide for 2 h. Chromosome spreads are prepared by hypotonic treatment, fixation and Giemsa staining. Fifty well spread metaphases have been analyzed following the standard nomenclature for chicken chromosomes.

The DNA isolation was carried out by the method of phenol: chloroform: isoamyl alcohol extraction. PCR was performed in DNA thermal cycler (Perkin Elmer). Primers specific for chicken Mc29 virus gag-myc gene were designed: 5'-GAC GGG GGG AAC GGA CTA ACT T-3' (forward) and 5'-TTC CAG ATG TCC TCG GAC GG-3' (reverse). The resulted PCR product was 535 base pairs (bp) in length and contained region from 1707 to 2241 nucleotide positions. An initial step for denaturation of dsDNA was performed at 94 °C for 2 min. Amplification was carried out for 35 cycles consisting of: denaturation at 94 °C for 40 sec, annealing at 66 °C for 1 min, synthesis at 72 °C for 50 sec and prolongation of DNA synthesis at 72 °C for 7 min. Then reaction mixture was cooled to 4 °C. Separation of PCR products was provided by electrophoresis in 1% agarose gel. Smart ladder (Eurogentech) was used as a molecular weight marker.

Results and Discussion

Both cell lines have been found to share the following common characteristics: they grow as monolayer cultures and form 3D colonies in semi-solid medium, express v-myc (gag-myc) gene; they are sensitive to the cytotoxic/cytostatic effects of the widely used commercial anticancer drug cisplatin. On the other hand, these cells differ in their tumorigenic potential in vivo. The results obtained are summarized in **Tables 1** and **2**.

Table 1. LSCC-SF-Mc29 and LSCC-PR2-Mc29 chicken liver cancer cell lines – comparison of some biological characteristics

Cell line	LSCC-SF-Mc29	LSCC-PR2-Mc29
Establishment of the cell line	After trypsinization of tumor explants*	After culturing of tumor explants**
Karyotype	Diploid and threeploid	Hypodiploid**
Formation of 3D colonies in semi-solid medium	Yes	Yes
Presence of *v-myc* (*gag-myc*) gene	Yes	Yes
Sensitivity to cis-platin (CC_{50}, μg/ml)	Yes (< 0.7)	Yes (< 0.7)
Tumor growth at the site of s.c. cancer cell inoculation	Yes	No
Tumor growth outside the place of s.c. cancer cell transplantation	Rare	Yes

* - According to Alexandrova, Ogneva [1]; ** - According to Sovova et al. [9];
CC_{50} – concentration of the compound that reduces the number of viable cells by 50% as compared to the untreated control. CC_{50} was determined by MTT test after 24 and 48 h treatment.

In order to investigate the *in vivo* tumorigenic potential of LSCC-SF-Mc29 and LSCC-PR2-Mc29 cell lines, the viable cancer cells (in 0.5 ml phosphate saline buffer) were transplanted s.c. into the knee flexure of 7- to 14-day-old 15I White leghorn chickens (**Table 2**).

Table 2. Tumorigenicity in vivo of cell lines LSCC-SF-Mc29 and LSCC-PR2-Mc29 in 15I White Leghorn chickens

Cell line	Age at the time of inoculation (days)	Number of inoculated cells	Latent period (days)	Number of tumor-bearing chickens***/ total number of inoculated chickens
LSCC-SF-Mc29	7	5.0×10^6	6–9	5/7 (71.4%)
	8	7.0×10^6	5–8	7/7 (100%)
	11	2.5×10^6	12–14	3/5 (60%)
	11	5.0×10^6	12	5/5 (100%)
	12	7.5×10^6	9–10	4/5 (80%)
	13-14	5.0×10^6	10–12	5/5 (100%)
LSCC-PR2-Mc29	7	2.5×10^6	–	0/5 (0 %)
	7	5.0×10^6	–	0/4 (0 %)
	7	7.5×10^6	–	0/5 (0 %)
	7	10.0×10^6	–	0/4 (0 %)
	7	20.0×10^6	–	0/2 (0 %)
	14	7.5×10^6	–	0/4 (0 %)
	14	10.0×10^6	–	0/4 (0 %)
	14	20.0×10^6	–	0/2 (0 %)

*** - The tumors observed are at the site of cancer cell inoculation.

In the case of LSCC-SF-Mc29 cell line, tumor growth was observed at the site of cancer cell inoculation in 60-100% of the transplanted chickens. In one of the chickens (transplanted with 2.5×10^6 cells) tumor growth was observed also in the liver.

The situation with LSCC-PR2-Mc29 cell line was different. Tumor growth at the site of transplantation was not detected in anyone of the cases. Part of the chickens (19/30) were euthanized and autopsied 14-18 days after implantation of cancer cells – no significant visible changes were noticed in tissues and organs of these chickens. The rest (11/30) of the chickens were monitored over a longer period of time: ≥ 34 days. In part (9/11) of them solid tumors were found in the thymus (tightly elastic consistency, measuring 1-4 mm in diameter, sometimes bilateral). In one chicken tumor growth (two nodes with weight of 1.5 g and 18.8 g) was observed also in one kidney.

Our data confirm the results published by Sovova et al. [9] – after inoculation of 5×10^6 or 5×10^7 LSCC-PR2-Mc29 cells into the wing web of 1-day-old Brown leghorn chickens, the authors did not usually find tumors at the site of inoculation. While Sovova and collaborators [9] found tumor growths mainly in the mesentery and liver of Brown leghorn chickens transplanted with LSCC-PR2-Mc29 cells, the main location of tumors observed in 15I White leghorn chickens implanted with the same cells in our experiments was thymus.

It can be suggested that the differences between these cell lines (LSCC-SF-Mc29 and LSCC-PR2-Mc29) could be explained at least partially by:

1. A different approach applied for the preparation of cell lines – with and without chemical (enzyme) treatment – which can result in the isolation and selection of different cell populations;

2. Both lines have been established independently of each other at different times and in different laboratories from transplantable chicken liver cancers that undergone large number of *in vivo* passages. During these passages under the influence of various factors (such as tumor-host relationships) may have become a selection of different cell subpopulations;

3. The high mutation capacity of cancer cells and the tumor cell heterogeneity phenomenon which converts any malignant neoplasm (resp. tumor cell line) in a unique system.

In conclusion, both cell lines have their specific characteristics and can be used for various scientific and biotechnological purposes. The presence of v-myc gene makes them valuable experimental models – the disturbed regulation of its cellular analogues (c-myc, L-myc, N-myc) is involved in pathogenesis of > 80% of human cancers.

Acknowledgement: Tanya Zhivkova is supported by Grant No BG051PO001-3.3.06-0048 from 04.10.2012; European Social Fund and Republic of Bulgaria, Operational Programme "Human Resources Development", 2007-2013 framework.

References

1. **Alexandrova, R., V. Ogneva.** Transplantable chicken hepatoma as a model for tumor heterogeneity investigations. – In: The Proceedings of the First Joint Meeting of Departments of Animal Sciences of the Balkan Countries. BALNIMALCON, 2-8 June 2001, Tekirdag, Turkey, 127-131**.**
2. **Alexandrova, R., A. Vacheva, M. Kirilova**, **G. Miloshev, E.-M. Mosoarca, R. Tudose, O. Costisor.** Investigations on cytotoxic and antiproliferative effects in vitro of a newly synthesized mixed ligand copper (II) complex. – Acta Morphol. Anthropol., **12**, 2007, 72-78.
3. **Ivanov, X., Z. Mladenov, S. Nedyalkov, T. Todorov, M. Yakimov.** – Bulletin de l'Institute de Pathologie Comparee des Animaux, **10**, 1964, 5-38 (In Bulgarian).
4. **Law, W., M. L. Linial.** Transforming ability of Gag-Myc fusion proteins correlates with Gag-Myc protein stability and transcriptional repression. – Oncogene, **20**(9), 2001, 1118-1127.
5. **Lee, C. M., E. P. Reddy.** The v-myc oncogene. – Oncogene, **18**, 1999, 2997-3003.
6. **Mladenov, Z.** Comparative Pathology of Avian Leukoses. – Sofia, Publishing House of the Bulgarian Academy of Sciences, 1974 (In Russian).
7. **Mossman, T.** Rapid colorimetric assay for cellular growth and survival: Application to proliferation and cytotoxicity assays. – J. Immunol. Meth., **65**(1), 1983, 55-63.
8. **Payne, L. N.** Biology of avian Retroviruses. – In: Levy, (Ed. A. Jay), New York and London, The Retroviridae. Plenum Press, **1**, 1992, pp. 299-404.
9. **Sovova, V., I. Hlozanek, H. Cerna, V. Dostalova, H. Sainerova.** Analysis of a cell line derived from a chicken hepatoma induced by virus Mc29. – Avian Pathol., **10**, 1981, 461-469.

Institute of Experimental Morphology, Pathology and Anthropology with Museum
Bulgarian Anatomical Society

Acta morphologica et anthropologica, 21
Sofia ● 2015

Apoptotic Changes in Aging Testis

D. Barbutska, Y. Koeva

Department of Anatomy and Histology, Medical University, Plovdiv, Bulgaria

Cell apoptosis is an active process which occurs in the course of aging. The direct result of the aging of the testis is reduction in levels of testosterone (T) and results of this are disrupting of physiological processes and dramatically worsened the quality of life for millions of older men. According to the theory of oxidative stress, with the leading factors free radicals (ROS- Reactive oxygen species), mitochondria are the biological clock of aging and the main place of oxidative injury in the course of this process. ROS attack primarily mitochondria and their DNA (mt DNA), increased permeability of the mitochondrial membrane, reduced membrane potential of mitochondria and these are the early signs of beginning apoptotic changes in the cells. Mitochondrial damage caused by ROS disrupts steroidogenesis in the testis and at the same time the process of steroidogenesis generates sub-products, which could also be responsible for functional insufficiency and apoptotic changes in aging LC. Apoptosis is a complex process which is regulated from multiple levels pro-and anti-apoptotic proteins and long-term damage to the balance between the two groups causes apoptotic changes in cells. One of this proteins is tumor suppressive protein p53 – promotes the expression of a number apoptotic genes. At this stage, the role of p53 in the control of apoptosis in human steroidogenic LC in the aging testis is not well investigated which determines the aim of the present study. We used material from human testis of patients between 56, 68 and 80 years old, embedded in paraffin and prepared for immunohistochemistry. Our results demonstrated the increased intensity of the immunoexpression of p53 in the course of the aging and these findings categorically point out the role of this protein in the regulation of testis apoptosis.

Key words: apoptosis, Leydig cells, aging, immunoexpression, p53.

Introduction

A lot of external factors and intracellular mechanisms occurring in the course of aging lead to a flow of active processes in the cells as apoptosis that affects the cells of the germinative epithelium and endocrine Leydig cells (LC). The direct result of the aging of the testis is reduction in levels of testosterone (T), such as changes in hormonal values, disrupting a number of physiological processes and dramatically worsened quality of life for millions of older men.

Well known is the theory of oxidative stress with the leading factors free radicals (ROS- Reactive oxygen species), influencing a wide range of physiological and pathological processes, including aging. According to this theory, mitochondria are the biological clock of aging and the main place of oxidative injury in the course of this

process [10]. ROS attack primarily mitochondria and their DNA (mt DNA) as oxidative lesions accumulate with age, losses of mt DNA are often more critical, than those of the nuclear DNA. The increased permeability of the mitochondrial membrane and the reduced membrane potential of mitochondria are the early signs of beginning apoptotic changes in the cells [10]. Mitochondrial damage caused by ROS, together with the deterioration of the synthesis of ATP, as well as participation in the steroidogenic process enzyme P-450 are key factors not only in the process of aging, but in general in the process of apoptosis [7]. The mitochondria of endocrine cells like LC release free radicals which exceed the antioxidant cellular protection and this fact is the basis of mitochondrial theory of aging [10]. The process of steroidogenesis as a cascade of several enzymatic activities generates so-called sub-products, which could also be responsible for functional insufficiency of aging LC and for apoptotic changes in it [7].

Apoptosis is a complex process involving two main paths – indoor and outdoor, each of which is regulated at multiple levels by a wide spectrum-pro-and anti-apoptotic proteins [14]. Long-term damage to the balance between the two groups causes apoptotic changes in cells [5]. Bcl-2 family is the main regulator of the internal apoptotic way in the testis, essential for the normal balance between survival and death of germ cells [1, 2, 12, 13]. The internal mechanism of apoptosis is regulated by the tumor suppressive protein p5 – which promotes the expression of a number apoptotic genes (transcription factor), also directly modulates the activity of theBcl-2 family members [3, 6, 8, 9]. Reported on the important role of p53 in apoptosis in normal spermatogenesis and in response to DNA damage [2, 4, 11], facts demonstrating the importance of p53 gene in the modulation of apoptosis and spermatogenesis.

At this stage, the role of p53 in the control of apoptosis in human steroidogenic LC in the aging testis is not well investigated that determines the aim of the present study.

Materials and Methods

In the present study, material was used from human testis of patients aged between 56 and 80 years, obtained after an orchidectomy in connection with the treatment of prostate carcinoma (Urology Clinic at the Medical University, Plovdiv). Testicular fragments (4-5 mm thick) were fixed by immersion in Bouin's fluid for 24 hours, embedded in paraffin and prepared for routine histological analysis and immunohistochemistry. Expression of p53 in aging testis was visualized by ABC method with kit Immuno-Cruz™ rabbit ABC Staining System (Santa Cruz Biotechnology, Inc., USA), with DAB chromogen and primary polyclonal anti-p53 antibody (Santa Cruz Biotechnology, Inc., USA; 1: 100). As negative controls were used cuts in which the primary antibody was replaced with phosphate buffered saline (PBS).

Results

By using light microscopic observation and immunohistochemical analysis we determine significant immunoexpression of p53 in the curved seminal tubules and greatly reduced immunostaining in the testis interstitium, that indicates that the control of cell death of LC, does not include only the p53 and probably involved and other gene products.

We observed atrophy of LCs with aging (56, 68 and 80 years of age) rather than reduction in their numbers and as consequence the interstitium of aging testis appeared enlarged (**Fig. 1A-C**).

Our results demonstrated the increased intensity of the immunoexpression of p53 in the course of aging (**Fig. 1A-C**) fact which categorically points out the role of this protein in the regulation of testis apoptosis.

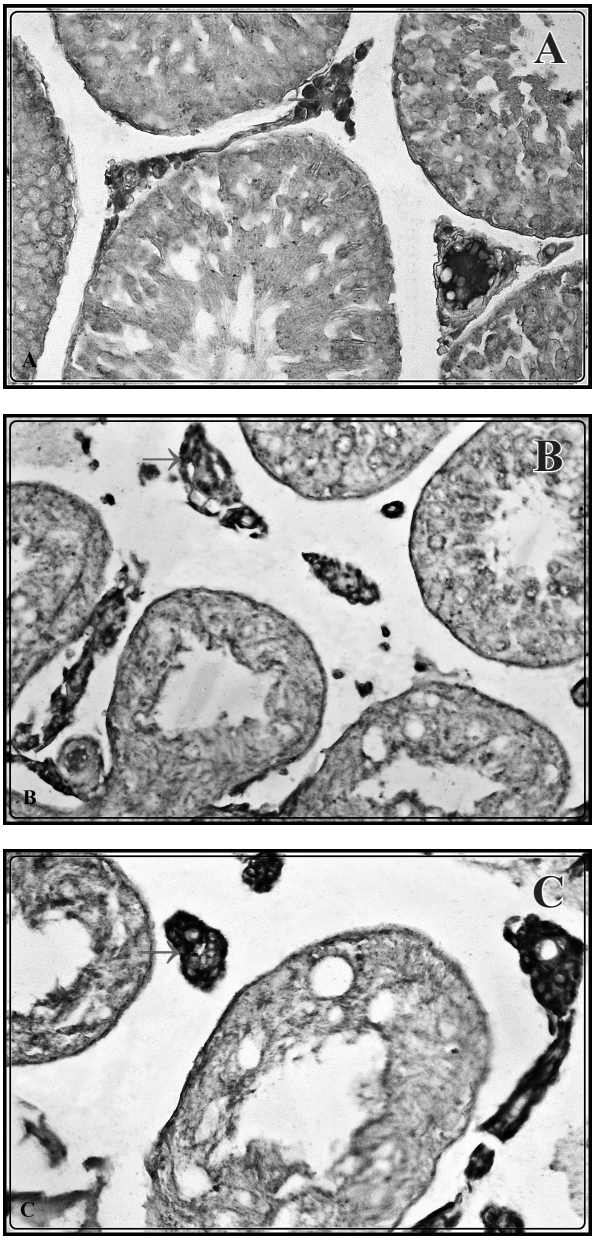

Fig. 1. A, B, C – Immunohistochemistry for p-53. Expression of p-53 increased in testis 80 years (C) compared to 56 and 68 years (A, B)

Discussion

External factors and intracellular mechanisms occurring in the course of aging lead to active processes in the cells as apoptosis, and this affects not only the cells of the germ epithelium and endocrine Leydig cells (LC). The theory of oxidative stress with the leading factors free radicals (ROS- Reactive oxygen species), is known and ROS influencing a wide range of physiological and pathological processes, including the process of aging [10]. ROS attack mitochondria and mt DNA. Increased permeability of the mitochondrial membrane and the reduced membrane potential of mitochondria are the early signs of beginning apoptotic changes in the cells [10]. Pro-and anti-apoptotic proteins and long-term damage to the balance between the two groups caused apoptotic changes in cells [5, 14]. Tumor suppressive protein p53 promotes the expression of numerous apoptotic genes in the processes of cellular differentiation and cellular life cycle, as well as in response to different stress signals [3, 6, 8, 9]. P53 affects programmed cell death through direct interaction with cellular proteins or directly with DNA and this makes it a unique marker for development of apoptosis in cells [2, 4, 11]. Our study revealed the role of this protein in the regulation of testis apoptosis.

References

1. **Adams, J. M., S. Cory.** The Bcl-2 protein family: arbiters of cell survival. – Science, **28**, 1998, 1322-1326.
2. **Baum, J. S., J. P. St George, K. McCall.** Programmed cell death in the germline. – Semin. Cell. Dev. Biol., **16**, 2005, 245-259.
3. **Bennett, M., K. Macdonald, S. W. Chan, J. P. Luzio, R. Simari, P. Weissberg.** Cell surface trafficking of Fas: a rapid mechanism of p53-mediated apoptosis. – Science, **282**, 1998, 290-293.
4. **Beumer, T. L., H. L. Roepers-Gajadien, I. S. Gademan, P. P. van Buul, G. Gil-Gomez, D. H. Rutgers, D. G. de Rooij.** The role of the tumor suppressor p53 in spermatogenesis. – Cell. Death. Differ., **5**, 1998, 669-677.
5. **Bozec, A., F. Chuzel, S. Chater, C. Paulin, R. Bars, M. Benahmed M, C. Mauduit.** The mitochondrial-dependent pathway is chronically affected in testicular germ cell death in adult rats exposed in utero to anti-androgens. – Journal of Endocrinology, **183**, 2004, 79-90.
6. **Chipuk, J. E., T. Kuwana, L. Bouchier-Hayes, N. M. Droin, D. D. Newmeyer, M. Schuler, D. R. Green.** Direct activation of Bax by p53 mediates mitochondrial membrane permeabilization and apoptosis. – Science, **303**, 2004, 1010-1014.
7. **Lacombe, A., V. Lelievre, C. E. Roselli, W. Salameh, Y-H. Lue, G. Lawson, J-M. Muller, J. A. Waschek, E. Vilain.** Delayed testicular aging in pituitary adenylate cyclase-activating peptide (PACAP) null mice. – PNAS, **103**(10), 2006, 3793-3798.
8. **Miyashita, T., J. C. Reed.** Tumor suppressor p53 is a direct transcriptional activator of the human bax gene. – Cell., **80**, 1995, 293-299.
9. **Oda, E., R. Ohki, H. Murasawa, J. Nemoto, T. Shibue, T. Yamashita, T. Tokino, T. Taniguchi, N. Tanaka.** Noxa, a BH3-only member of the Bcl-2 familyand candidate mediator of p53-induced apoptosis. – Science, **288**, 2000, 1053-1058.
10. **Sastre, J., F. V. Pallardo, G. J. De la Asuncion.** Mitochondria, oxidative stress and aging. – Free Radic. Res., **32**(3), 2000, 189-198.
11. **Schwartz, D., N. Goldfinger, Z. Kam, V. Rotter.** p53 Controls low DNA damage-dependent premeiotic checkpoint and facilitates DNA repair during spermatogenesis. – Cell. Growth. Differ., **10**, 1999, 665-675.
12. **Taylor, M. F., I. Woolveridge, A. D. Metcalfe, C. H. Streuli, J. A. Hickman, I. D. Morris.** Leydig cell apoptosis in the rat testes after administration of the cytotoxin ethane dimethanesulphonate: role of the Bcl-2 family members. – Journal of Endocrinology, **157**, 1998, 317-326.

13. **Tsujimoto, Y.** Cell death regulation by the Bcl-2 protein family in the mitochondria. – J. Cell. Physiol., **195**, 2003, 158-167.
14. **Xu, G., K. S. Vogel, C. A. McMahan, D. C. Herbert, C. A. Walter.** BAX and Tumor Suppressor TRP53 are important in regulating mutagenesis in spermatogenic cells in mice. – Biology of Reproduction, **83**, 2010, 979-987.

Corresponding author:
Assist. Prof. Darina Barbutska, DM
Medical University, Plovdiv
Department of Anatomy,
Histology and Embryology
15A Vassil Aprilov Str., Plovdiv
tel: 032602304,
e-mail: darinas5@abv.bg

Institute of Experimental Morphology, Pathology and Anthropology with Museum
Bulgarian Anatomical Society

Acta morphologica et anthropologica, 21
Sofia ● 2015

Effects of Aronia Melanocarpa on the Process of Thymic Involution in Aging Rats

E. Daskalova[*], S. Delchev[*], D. Staribratova[**]

[*]*Department of Anatomy, Histology and Embryology, Medical University, Plovdiv*
[**]*Department of Pathology, Medical University, Plovdiv*

Progressive thymic involution, a sign of aging leads to loss of immune function associated with T-cell immunity and increased susceptibility to infections, risk for development of autoimmune diseases and neoplasms in adults. It has been shown that the thymic tissue is a plastic tissue and the process of involution can be delayed and even therapeutically reversed. The use of antioxidants is one potential therapeutic approach for slowing aging of immunity. The purpose of this study is to determine the effect of Aronia melanocarpa juice either pure or enriched with 1% pectin on the thymus involution in aging rats. The results show differences in thymus weight index**,** weight and size between the groups of treated rats and normal controls. The thymus of treated animals along with the usual age-related changes shows increased cortical apoptosis similar to the extent seen in young controls and is suggested as an expression of remodeling or even rejuvenating.

Key words: Thymic involution, Antioxidants, Aronia melanocarpa.

Introduction

One of the most significant changes occurring in the process of normal aging is immune aging affecting all the cells and organs of innate and acquired immunity. Progressive thymic involution, a definite sign of aging, leading to loss of immune functions associated with T-cell-mediated immunity is generally associated with increased susceptibility to infections as well as increase in risk of autoimmune diseases and neoplasms in adults [8]. There is a growing evidence that the thymus tissue is plastic and that the process of involution can be therapeutically influenced and even reversed [6, 7]. At present, there are several potential therapeutic approaches for slowing aging of immunity, including the use of antioxidants [2]. The morphological changes occurring in the involuting rat thymus are similar to those in humans, and as such rats are an appropriate model for studying the process of immune senescence [9]. The anthocyanin fruit Aronia melanocarpa is ranked first in its antioxidant potential as confirmed by several different methods. A number of in vitro and in vivo studies have demonstrated the wide range of applications of the juice extracts or the dry substance of the fruits of Aronia melanocarpa, as anti-mutagenic, anti-cancer, lipid-lowering, antidiabetic, antihyperten-

sive, hepatoprotective, immunomodulatory effects etc. [3]. The literature provides only limited data on the effect of its application on aging and in particular on age related involution of the thymus. The purpose of this study is to determine the influence of Aronia melanocarpa as pure juice or in combination with pectin on thymic involution in rats.

Materials and Methods

Fruit juices of Aronia melanocarpa – pure and enriched with 1% pectin were provided by "VITANEA-Ltd", Plovdiv and were stored at 6 °C. Total content of anthocyanins in the first was 305.6 mg/l, in the second 598.5 mg/l, and the polyphenol content was respectively 5069.3 mg/l and 2571 mg/l, as reported from the assays performed in LBAV (Laboratory of biologically active substances) affiliation of Bulgarian Academy of Science. The study included 24 male Wistar rats, 18 of them at the age of 10 months with initial body weight 350g ± 50; 6 animals of 2 months of age and body weight 100 ± 10. Animals were provided by and bred in the vivarium of the Medical University in Plovdiv under standard laboratory conditions. The rats were divided into 4 groups: two control groups – the one defined as young (Cy) – 2-month-old, and the other as old (Co) - 10-month-old, which had been put on a standard diet and tap water ad libitum. The study included two experimental groups: (A) and (A+P), age matched to the older controls which received ad libitum Aronia melanocarpa juice (for group A) and Aronia melanocarpa with addition of 1% pectin (for group A+P). Juices were diluted 1:1 in drinking water. The experiment lasted 90 days [11]. The experimental protocol was approved by the Committee on Ethical Treatment of Animals from the Bulgarian Agency for Food Safety. At the end of the experimental period the animals were euthanized with T61. The rats of all groups were measured to establish body weight (g), thymus weight (g), thymus length and width (mm) and the thymus index (as organ weight(g)/ weight of animal(g).100). After dissection and fixation in formalin, thymus sections were subjected to routine paraffin embedding, cutting and staining with hematoxylin and eosin. Tissue sections of 5 μm thickness were incubated with a ready-to-use Bcl-2 (mouse antibody sc-509, Santa Cruz Biotechnology, Inc. USA) and visualizing kit "ABC Staining system" (sc-2017, Santa Cruz Biotechnology, Inc. USA). The enclosed photomicrographs were taken on microscope Nikon Microphot SA (Japan), equipped with a digital camera Camedia-5050Z (Olympus, Japan). The data were processed by non-parametric analysis (Kruskal-Wallis test) and multiple comparison analysis (Dunnett T3 test). Statistical significance between experimental groups was determined by u-criterion of Mann-Withney, the differences were considered significant at $p < 0.05$. Data are presented as mean±SD.

Results

Thymus Weight

The average weight of the thymus in the elderly controls and in both groups treated rats was significantly lower than in young controls (0.2133 g for group Co, 0.2450 g for group A and 0.2360 g for group A+P v/s 0.3471 g for group Cy; $p < 0.05$), which is concordant with the chosen experimental model. There was a tendency to increase the weight of the thymus in the groups treated with Aronia only and Aronia and pectin compared to adult controls without statistically significant differences in the different values ($p > 0.05$).

Thymus length

The average length in young controls was significantly higher compared to old controls (18.00 mm for group Cy v/s 14.33mm for group Co*;* $p < 0.05$) and compared to Aronia with pectin group (18.00 mm for group Cy v/s 15.60 mm for group A+P; $p < 0.05$).

Thymus width

The average width in young controls was significantly higher than old controls (14.00 mm for group Cy v/s 10.66 mm for group Co; $p < 0.05$) and than Aronia with pectin group (14 mm for group Cy v/s 10.40 mm A+P for group; $p < 0.05$).

The average length and width of the thymus in the groups receiving Aronia and Aronia with pectin compared to adult controls tend to increase without statistically significant differences ($p > 0.05$).

Thymus weight index

With respect to thymus weight index between young and old controls the differences were statistically significant, which confirms the process of age involution of the thymus. There was a statistically significant difference between the young controls compared to elderly controls (0.33 for group Cy v/s 0.61 for group Co; $p < 0.05$) and between young controls in comparison to the two treated groups (0.33 for group Cy v/s 0.58 for group A and 0.58 for group A+P; $p < 0.05$). No significant differences were found between the groups treated with Aronia juicescompared to the old controls ($p > 0.05$).

Histology of rat thymus

The thymus of young rats (2 months old) was characterized by oval thymic lobules with broad cortex area rich in thymocytes, clear and distinct cortico-medullary border, presence of medulla and outside thin capsule with interlobular loose connective tissue (**Fig. 1A**). At month 13 the controls show a marked decrease in the density of the

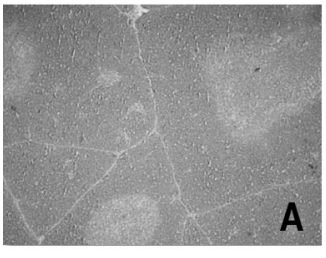

Fig. 1A. Thymus of 2-month-old rat, CY group (HE, ×40)

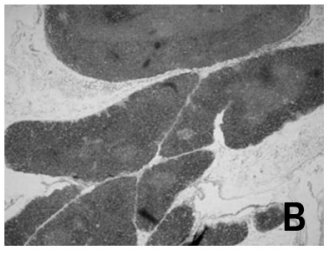

Fig. 1B. Thymus of 13-month-old rat, CO group (HE, ×40)

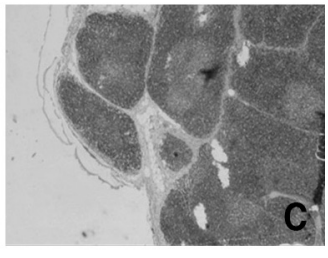

Fig. 1C. Thymus of 13-month-old rat, Aronia group (HE, ×40)

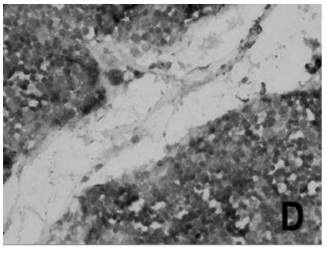

Fig. 1D. Bcl-2, young controls (×100)

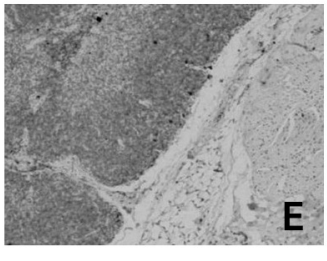

Fig. 1E. Bcl-2, old controls group (×40)

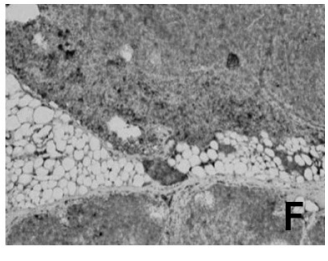

Fig. 1F. Bcl-2, Aronia and pectin group (×40)

thymocytes in the outer and inner cortical regions with thinning and sharpening of the lobules. The cortico-medullary border becomes obscure. Interlobular amount of connective and fatty tissue is increased, the thymus capsule is thickened (**Fig. 1B**). When comparing the older controls with treated with Aronia animals parallel to age-related changes is noticed an enhanced apoptosis, particularly in cortical areas, forming the characteristic picture of starry sky appearance (**Fig. 1C**). Vigorous apoptosis is represented both in Aronia and in Aronia and pectin treated rats.

Immunohistochemistry

Young controls showed an increased immune expression of Bcl-2, as a feature of the normal physiological process of apoptosis (**Fig. 1D**). In the adult controls is noticed only weak and scattered immune expression of Bcl-2 (**Fig. 1E**). Both groups of treated animals was found strongly positive for Bcl-2 similar in intensity to that in younger controls (**Fig. 1F**).

Discussion

Apoptosis is an essential physiological process during differentiation and maintenance of immune cells including the thymocytic population. Apoptosis in thymus can be induced by stimuli such as high dose of corticosteroids, gamma radiation, immunosuppressives and oxidants [1]. As some of the polyphenols, the predominant group bioactive substances in Aronia may have bidirectional effect – as anti- and pro-oxidants, which is dose dependent and ion specific [5]. Induction of apoptosis in lymphoid cells underlies their antitumoral effect, but in our case it refers to normal lymphoid cells [5]. The anti-apoptotic marker Bcl-2 is represented to its highest extend by the T lymphocytes at an early stage in their differentiation - the double negative T-cells stage, and also in their final stage – the double positive T-cells stage, as a sign of the active T lymphocytes proliferation in the young thymus [11]. The presence of increasing apoptosis and the simultaneous activation of the anti-apoptotic protein Bcl-2 of the treated animals suggests different hypotheses. On one hand, the enhanced apoptosismay be a result from pro-oxidant effect of Aronia melanocarpa and the higher immunoexpression of Bcl-2 could be a result of a defense reaction to the first process. On the other hand, this apoptosis may come as a result of a thymus remodeling that has already began by losing its adult lymphocytes and activating a proliferation for producing new T lymphocytes at the same time. These results put many questions, the answers to which demand additional functional study of the thymus in the treated and untreated adult animals.

References

1. **Burikhanov, R., K.Wakame, Y. Igarashi, S.Wang, S. Matsuzaki.** Suppressive effect of active hexose correlated compound (AHCC) on thymic apoptosis induced by dexamethasone in the rat. – Endocr. Regul., **34**, 2000, 180-188.
2. **De la Fuente, M., J. Cruces, O. Hernandez, E. Ortega.** Strategies to improve the functions and redox state of the immune system in aged subjects. – Curr. Pharm. Des., **17**, 2011, 3966-3993.
3. **Denev, P., Ch. Kratchanov, M. Ciz, A. Lojek, M. Kratchanova.** Bioavailability and antioxidant activity of black chokeberry (aronia melanocarpa) polyphenols: in vitro and in vivo evidences and possible mechanisms of action: a review. – Compr. Rev. Food Sci. F., **11**, 2012, 472-489.
4. **Feng, R., H. Ni, S. Wang, I. Tourkova, M. Shurin, H. Harada, X. M. Yin.** Cyanidin-3-rutinoside, a natural polyphenol antioxidant selectively kills leukemic cells by induction of oxidative stress. – J. Biol. Chem., **282**, 2007, 13468-13476.

5. **Halliwell, B.** Review: Are polyphenols antioxidants or pro-oxidants? What do we learn from cell culture and in vivo studies? – Arch. Biochem. Biophys., **476**, 2008, 107-112.
6. **Lynch, H., G. Goldberg, A. Chidgey, M. van den Brink, S. Boyd, G. Sempowski.** Thymic involution and immune reconstitution. – Trends. Immunol., **30**(7), 2009, 366-373.
7. **Mennen, L, I., R. Walker, C. Bennetau-Pelissero, A. Scalbert.** Risks andsafety of polyphenol consumption. – Am. J. Clin. Nutr., **81**(suppl), 2005, 326S-329S.
8. **Montecino-Rodriguez, E., B. Berent-Maoz, K. Dorshkind.** Causes, consequences, and reversal of immune system aging. – J. Clin. Invest., **123**(3), 2013, 958-965.
9. **Obukhova, L., V. Skulachev, N. Kolosova.** Mitochondria-targeted antioxidant SkQ1 inhibits age-dependent involution of the thymus in normal and senescence-prone rats. – Aging, **1**, 2009, 389-401.
10. **Plećas-Solarović, B., V. Pesić, K. Radojević, G. Leposavić.** Morphometrical characteristics of age-associated changes in the thymus of old male Wistar rats. – Anat. Histol. Embryol., **35**(6), 2006, 380-386.
11. **Renault, T., J. Chipuk.** Getting away with murder: how do the BCL-2 family of proteins kill with immunity? – Ann. N.Y. Acad Sci., **1285**(1), 2013, 59-79.
12. **Sharif, T., M. Alhosin, C. Auger, C. Minker, J. Kim, N. Selloum, P. Bories, H. Gronemeyer, A. Lobstein, C. Bronner, G. Fuhrmann,V. Schini-Kerth.** Aronia melanocarpa juice induces a redox-sensitive p73-related caspase 3-dependent apoptosis in human leukemia cells. – Plos One, **7**(3), 2012, 1-11.
13. **Балански, Р., Г. Ганчев, И. Стойчев, М. Илчева, А. Томова, П. Денев, М. Крачанова, Хр. Крачанов**. Ефект на натурален сок от Арония, обогатен с пектин върху канцерогенното действие на 1,2-диметилхидразин в интестиналния тракт на плъхове. – Българско дружество по хранене и диететика, **1**, 2008, 220–227.

Institute of Experimental Morphology, Pathology and Anthropology with Museum
Bulgarian Anatomical Society

Acta morphologica et anthropologica, 21
Sofia ● 2015

Markers of Metabolic Adaptation in Gastrocnemius Muscle after Administration of Antiandrogen in Endurance Trained Rats

S. Delchev[*], K. Georgieva[**], Y. Koeva[*], F. Gerginska[*], D. Terzieva[***]

Department of Anatomy, Histology and Embryology[*], Department of Physiology[**], Department of Clinical Chemistry[***], Medical University, Plovdiv, Bulgaria

We studied the effect of Flutamide, an androgen receptor (AR) blocker, on glycogen content, the glycogen synthase (GS) and irisin expression in gastrocnemius muscles of rats undergoing endurance training for 8 weeks. Trained animals were found to have a higher glycogen content and stronger expression of GS and irisin than untrained animals. The higher glycogen content in gastrocnemius corresponds to the increased expression of GS in trained rats, which indicates that this enzyme takes part in the adaptation processes. Flutamide treatment increased the serum testosterone levels and decreased glycogen and irisin expressions. Glycogen and irisin in the muscle decreased when training was combined with administration of Flutamide, without any significant effect on GS, compared to those in untrained animals, but their levels were higher than those in Flutamide-treated untrained animals. These results suggest that endurance training can be used as a non-drug therapeutic modality to lessen the negative effects of antiandrogen therapy on skeletal muscles.

Kew words: endurance training, Flutamide, glycogen, glycogen synthase, irisin.

Introduction

Endurance training induces adaptations in skeletal muscles and increases the aerobic physical performance. Testosterone plays a key physiologic role in maintaining the proper function of skeletal muscle [9, 11] and the glycogen metabolism [5]. Depletion of muscle glycogen is an accurate marker of the onset of exhaustion in aerobic training exercises. Glycogen synthase (GS) is a key enzyme in the synthesis of glycogen. Its activity has been demonstrated to be dependent on the initial glycogen depots content and the muscle contraction itself [6, 7, 10]. Myocytes have been shown to release irisin when stimulated in physical exercise – the peptide increases the thermogenesis in white adipose cells and the total energy expenditure [2].

AR blockers are used in the treatment of prostate cancer [8]. Their long-term use has been associated with reduced capacity of physical performance [3]. It is not clear whether this side effect is associated with changes in the glycogen depots of skeletal muscles. There are no data in the available literature what effect anti-androgens have on glycogen content, the expression of GS and irisin in the muscles during endurance training.

The aim of the present study was to investigate the effect of androgen receptor blockers on the glycogen content, the expression of glycogen synthase and irisin in gastrocnemius muscle in endurance trained rats.

Materials and Methods

Male Wistar rats were allocated into two groups (n=12): a group of trained animals (T), and a group of sedentary animals (NT). Trained rats underwent 8-week submaximal treadmill training at 70-75% of VO_{2max} for 5 days per week. Half of the trained and untrained rats were treated with the androgen receptor blocker Flutamide (15 mg·kg^{-1}) dissolved in sesame oil and administered subcutaneously (T+F and NT+F); the remaining animals were given only sesame oil. Mixed blood and gastrocnemius muscle tissue samples were obtained from each rat at the end of experiment: a part of the muscle samples was frozen in liquid nitrogen, and another part – in the Bouin's fixative. We measured the levels of total testosterone in serum (Testosterone rat ELISA kit, Biotrend Chemikalien, Gmbh, Germany). The cryostatic sections were tested for glycogen using the PAS reaction. The paraffin sections (5 μm) were studied immunohistochemically (ABC Staining System, ImmunoCruz, Santa Cruz Biotechnology, USA) using the following antibodies: anti-glycogen synthase CT (04-357, Chemicon Millipore, USA), dilution 1:100; irisin rat antibody (42-112, Phoenix Pharmaceuticals, USA), dilution 1:100. The preparations were analysed using a special software program (DP-Soft 3.2, Olympus, Japan). We measured the intensity of the reactions (in relative units, RU) of 50 fibers of a muscle. The results were analysed statistically using two-way ANOVA. The data are presented as mean ± SEM.

Results

Administration of AR blocker affected the serum levels of testosterone. The Flutamide treated animals had higher concentrations of testosterone than the rats receiving placebo (8.48 ± 0.91 ng·ml^{-1} vs 1.83 ± 0.97 ng·ml^{-1}; $p < 0.001$). These findings were the result of the blocking of the hypothalamus-hypophysis-gonadal axis and show the efficiency of the drug dose we used in the experiment (**Fig. 1**).

We found no effect both of the training in comparison with the untrained rats (1.86 ± 0.26 g vs 1.92 ± 0.47 g; $p > 0.05$), and of the treating with AR blocker in com-

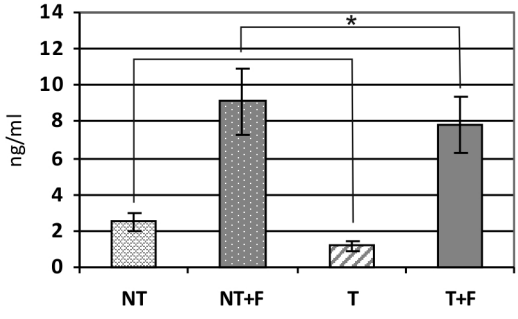

Fig. 1. Serum testosterone levels (ng·ml^{-1}) at the end of the experiment. *$p < 0.001$ in comparison with the placebo treated animals

parison with the placebo treated animals (1.90 ± 0.24 g vs 1.89 ± 0.46 g; $p > 0.05$) on the muscle mass of gastrocnemius muscle.

Aerobic training had a significant main effect on glycogen content in gastrocnemius muscle (**Fig. 2**). Trained animals were found to have a higher content of glycogen than that in the untrained rats (33.03 ± 1.33 RU vs 22.44 ± 1.33 RU, $p < 0.001$). Glycogen tended to decrease in the Flutamide treated rats ($p = 0.069$). We found a significant interaction of training and Flutamide treatment ($p = 0.001$). The highest glycogen content was found in the gastrocnemius of the endurance trained animals that received placebo. The AR blocker reduced the glycogen content in the trained animals ($p = 0.057$) in comparison with the single effect of endurance training.

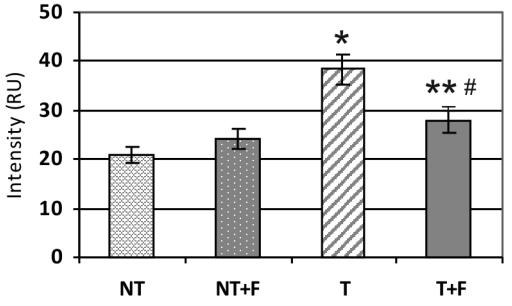

Fig. 2. Glycogen content (RU) in gastrocnemius m. *$p < 0.01$ in comparison with NT; **$p < 0.05$ in comparison with NT; #$p = 0.057$ in comparison with T

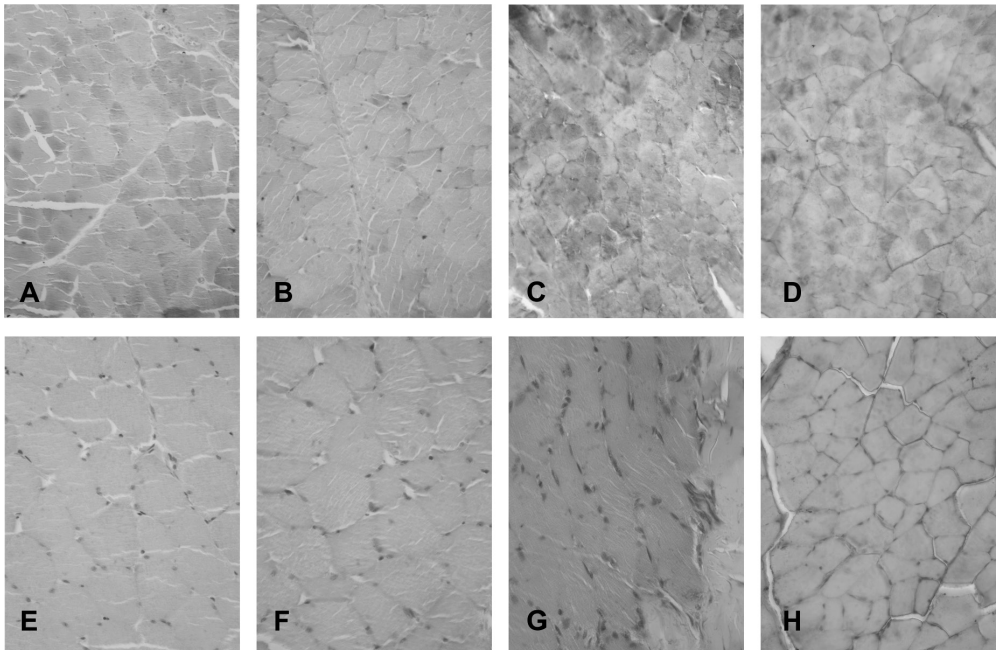

Fig. 3. Immunohistochemical reactions for glycogen synthase (A-D, ×200) and irisin (E-H, ×400) in gastrocnemius m. of animals of the experimental groups: NT (A, E), NT+F (B, F), T (C, G), T+F (D, H)

Analysis of the immunoreactions showed that the trained animals had stronger expression of glycogen synthase than the untrained rats (91.88 ± 1.57 RU vs 86.30 ± 1.57 RU; $p < 0.05$). Treatment with AR blocker induced no statistically significant main effect on this parameter ($p > 0.05$), (**Fig. 3**).

Endurance training had a significant effect on the expression of irisin. The trained animals showed a stronger immune expression in comparison with the untrained rats (81.49 ± 0.84 RU vs 75.69 ± 0.84 RU; $p < 0.001$) (**Fig. 3**). Administration of AR blocker also exerted an effect: the irisin expression was lower in the Flutamide treated animals than it was in the animals receiving placebo. We also found a significant two-way interaction ($p < 0.01$). The irisin reaction was strongest in the gastrocnemius of trained control animals. The combining effect of training and Flutamide treatment lead to a decrease of irisin expression compared with the effect of the training itself ($p < 0.001$).

Discussion

Our results showed that glycogen content in muscles at rest was higher in trained animals than it was in the untrained rats, a finding confirmed by other researchers as well [4]. GS activation after a single bout training session is important for so called glycogen overcompensation. The increased expression of GS in trained rats we found in the study shows that this enzyme takes part in the adaptation processes in endurance training. Blocking the androgen receptors in trained rats reduces the glycogen content in the gastrocnemius, which proves that the androgen receptors and androgens are involved in these processes of adaptation. The fact that Flutamide has no effect on GS expression shows that the effect of training on this enzyme is AR independent.

Irisin has been demonstrated to have a very low expression in the skeletal muscle of untrained animals [2], a finding which is corroborated by the results in the present study concerning the gastrocnemius muscle. Endurance training upregulated the irisin expression in the gastrocnemius which is consistent with the data provided by other researchers [1]. Administration of an AR blocker into trained rats lead to reduction of irisin expression in comparison with that in trained controls (T) which shows for the first time participation of AR in the processes of increased synthesis of irisin during training.

Conclusions

AR blocking reduces the glycogen content and irisin when aerobic training is combined with an AR blocker administration, which is one of the possible mechanism by which physical capacity is decreased. The glycogen content and irisin expression remain high in comparison with these in untrained animals treated with an AR blocker. On the basis of these results we can conclude that endurance training can be used as a non-drug therapeutic modality to lessen the negative effects of anti-androgen therapy on skeletal muscles. Our results show for the first time the role of androgens in irisin production during aerobic training.

Acknowledgements: This study was supported by Medical University – Plovdiv, Bulgaria, Grant 35/2012.

References

1. **Aydin, S., T. Kuloglu, S. Aydin, M. N. Eren, A. Celik, M. Yilmaz, M. Kalayci, I. Sahin, O. Gungor, A. Gurel, M. Ogeturk, O. Dabak.** Cardiac, skeletal muscle and serum irisin responses to with or without water exercise in young and old male rats: Cardiac muscle produces more irisin than skeletal muscle. – Peptides, **52** C, 2013, 68-73.
2. **Boström, P., J. W, M. P. Jedrychowski, A. Korde, L. Ye, J. C. Lo, K. A. Rasbach, E. A. Boström, J. H. Choi, J. Z. Long, S. Kajimura, M. C. Zingaretti, B. F. Vind, H. Tu, S. Cinti, K. Hojlund, S. P. Gygi, B. M. Spiegelman.** A PGC1α-dependent myokine that drives browning of white fat and thermogenesis. – Nature, **481**(7382), 2012, 463-468.
3. **Chu, C. W., S. J. Hwang, J. C. Luo, S. H. Tsay, C. P. Li, Y. S. Huang, F. Y. Chang, S. D. Lee.** Flutamide-induced liver injury: a case report. – Zhonghua Yi Xue Za Zhi, **61**(11), 1998, 678-82.
4. **Holloszy, J. O., W. M. Kohrt.** Regulation of carbohydrates and fat metabolism during and after exercise. – Annu. Rev. Nutr., **16**, 1996, 121-38.
5. **Kelly, D. M., T. H. Jones.** Testosterone: a metabolic hormone in health and disease. – J. Endocrinol., **217**, 2013, R25-R45.
6. **Lai, Y. C., J. T. Stuenaes, C. H. Kuo, J. Jensen.** Glycogen content and contraction regulate glycogen synthase phosphorylation and affinity for UDP-glucose in rat skeletal muscles. – Am. J. Physiol., Endocrinol Metab., **293**, 2007, E1622-E1629.
7. **Lai, Y. C., F. C. Lin, J. Jensen.** Glycogen content regulates insulin- but not contraction-mediated glycogen synthase activation in the rat slow-twitch soleus muscles. – Acta Physiol., **197**(2), 200, 139-150.
8. **Lekas, E., A. Bergh, J. E. Damber.** Effects of finasteride and bicalutamide on prostatic blood flow in the rat. – BJU International, **85**, 2000, 962-965.
9. **Mänttäri, S., K. Anttila, M. Järvilehto.** Testosterone stimulates myoglobin expression in different muscles of the mouse. – J. Comp. Physiol. B, **178**, 2008, 899-907.
10. **Nielsen, J. N., W. Derave, S. Kristiansen, E. Ralston, T. Ploug, E. A. Richter.** Glycogen synthase localization and activity in rat skeletal muscle is strongly dependent on glycogen content. – J. Physiol., **531**, 2001, 757-769.
11. **Salehzadeh, F., A. Rune, M. Osler, L. Al-Khalili.** Testosterone or 17 β-estradiol exposure reveals sex-specific effects on glucose and lipid metabolism in human myotubes. – J. Endocrinol., **210**, 2011, 219-229.

Institute of Experimental Morphology, Pathology and Anthropology with Museum
Bulgarian Anatomical Society

Acta morphologica et anthropologica, 21
Sofia ● 2015

Comparative Study of the Activity Levels and Localization of Tripeptidyl Peptidase I in Rat and Mouse Brain

M. Dimitrova[*], D. Deleva[*], I. Ivanov[**]

[*]*Institute of Experimental Morphology, Pathology and Anthropology with Museum, Bulgarian Academy of Sciences, Acad. G. Bonchev Str., Bl. 25, 1113 Sofia*
[**]*Medical University - Sofia, 2 Zdrave Str., 1431 Sofia*

Tripeptidyl peptidase I is a lysosomal protease, crucial for the brain function. Its genetically determined deficiency causes the late infantile form of classical neuronal ceroid lipofuscinosis – a serious neurodegenerative disorder, connected with severe symptoms and early death at puberty. Since most of the brain diseases are now studied using animal models, it is important to identify the enzyme locations and activity levels in healthy laboratory animals' brain regions. However, TPPI locations and activity levels in mesencephalon, thalamus and pons are still largely unknown. In the present paper we determine the enzyme activity levels and localization pattern in the above three brain regions of healthy adult rats and mice. The results show species differences in TPPI activity levels. All the studied types of neurons show high enzyme activity in both species. Those results would be important in view of the use of animal models for studying neurodegenerative disorders.

Key words: tripeptidyl peptidase I, enzyme histochemistry, enzyme kinetics, central nervous system.

Introduction

Tripeptidyl peptidase I (TPPI, E.C. 3.4.14.9) is a lysosomal enzyme – a protein product of the *cln2* gene, mutations in which are known to cause the recessive neurodegenerative disease late infantile neuronal ceroid lipofuscinosis (LINCL) or Jansky-Bielschowsky disease [9]. LINCL is connected with pathological accumulation of autofluorescent lipopigment in the neurons and photoreceptor cells leading to their degeneration and progressive loss [11]. Recently, a mouse model of LINCL has been established [10] and used for testing different therapeutic strategies [8]. On the other hand, changes in TPPI activity levels in human brain have been found in many diseases like Alzheimer disease, Down syndrome, other forms of neuronal ceroid lipofuscinosis, sclerosing panencephalitis and brain infarctions [5]. Some of the above disorders are also studied using animal models, particularly mice and rats. Therefore, it is important to identify the enzyme activity levels and localization pattern in normal rats and mice brains for comparative purposes. TPPI activity studies have been performed in cerebral cortex, cerebellar cor-

tex and spinal cord of adult rats and mice using biochemical assays [2, 6], immunohistochemistry [6] and enzyme histochemistry [3]. However, the enzyme localization and activity levels in rat or mouse thalamus, mesencephalon and pons are largely unknown.

The aim of the present study is to determine TPPI activity levels and cell localization in the normal adult rat and mouse thalamus, mesencephalon and pons. The results can be useful for the study of different brain diseases using mammalian models.

Materials and Methods

Adult Balb/C mice (3-month-old) and Wistar rats (5-month-old) of both sexes were decapitated in deep anesthesia.

Enzyme assays in tissue homogenates. Mesencephalon, thalamus and pons were extracted and the enzyme assays were performed exactly according to the procedure described in [2]. Briefly, the brain parts were homogenized in lysis buffer (1% Triton ×100 and 0.15 M NaCl, disolved in 0.05 M sodium acetate buffer, pH 4.5) on ice. The lysates were diluted with 0.4 M sodium acetate buffer, pH 4.5, supplied with 4 mM EDTA. After centrifugation at 4000 rpm, supernatants were diluted with 0.2 M sodium acetate, pH 4.5, containing 2 mM EDTA and the protein content was determined by measuring the samples absorption at 260 and 280 nm on a spectrophotometer Speckol 1500 (Analitjk, Jena) and calculations as described by Dawson et al. [4]. The activity of TPPI in tissue homogenates was assayed in incubation solutions, containing 0.5 mM substrate alanyl-alanyl-phenylalanine-p-nitroanilide (AAF-*p*NA, Bachem-Switzerland) at 37 ºC. Aliquots were collected every 15 minutes, in which the reaction was stopped with equal volume of 0.1 M chloroacetic acid in 0.1 M sodium acetate, pH 4.4. Absorption of the samples at 405 nm was measured spectrophotometrically against a control of freshly prepared incubation solution, in which the reaction was immediately stopped as above. The results were statistically estimated by regression analysis and curves showing the time-dependence of the absorption at 405 nm were built by means of Sigma Plot 9.0. One unit of enzyme activity was defined as the amount of enzyme liberating 1 μM product – *para*-nitroaniline (*p*NA) per minute per 1 mg protein at 37 ºC.

Enzyme histochemistry. Thalamus, mesencephalon and pons were extracted and fixed in 0.067 M phosphate buffer, pH 7.0 containing 4% sucrose for 18 h at 4 °C. Then, the brain parts were washed with 30% aqueous solution of sucrose supplied with 1% gum arabic for 48 h at 4 °C. Finally, the samples were frozen in liquid nitrogen. Tissue sections (10 μm) were cut on cryotome Reichert Jung 2800 (FRG) and mounted on gelatinized glass slides. They were covered by celoidine (1% in acetone : diethyl ether : absolute ethanol 4:3:3) for a minute at room temperature just before use. The enzyme localization was performed as described previously [1]. Briefly, the sections were incubated in a substrate medium consisting of 0.5 mmol enzyme substrate Gly-Pro-Met-(1-anthraquinonyl hydrazide) (GPM-AH), synthesized after Dikov et al. [1], and 0.5 mg/ml 4-nitrobenzaldehyde in 0.1 M acetate buffer, pH 4.5 for 70 min at 37 °C. Then, they were post-fixed in 4% neutral formalin for 15 min at room temperature. The sections were stained by haematoxylin according to the classical methods of histology and embedded in glycerol/gelatin.

Histochemical controls. Control sections were incubated in 0.1 M acetate buffer, pH 4.5 containing 1 μM inhibitor Ala-Ala-Phe-chloromethyl ketone (AAF-CMK) (Bachem, Switzerland) for 45 min at room temeperature. Then, they were transferred to the full substrate medium supplied with 1 μM inhibitor and incubated for 70 min at 37 °C. After the incubation, they were treated as the other sections.

All the sections were studied under the microscope Leica DM5000B (New York, USA).

Results

TPPI biochemical assays revealed high enzyme activity in the three studied brain regions of both mice and rats (**Fig. 1**). The enzyme activity per mg protein in the mice brain decreased in the following order: mesencephalon > thalamus > pons, whereas in the rat brain this order was different: thalamus > mesencephalon > pons.

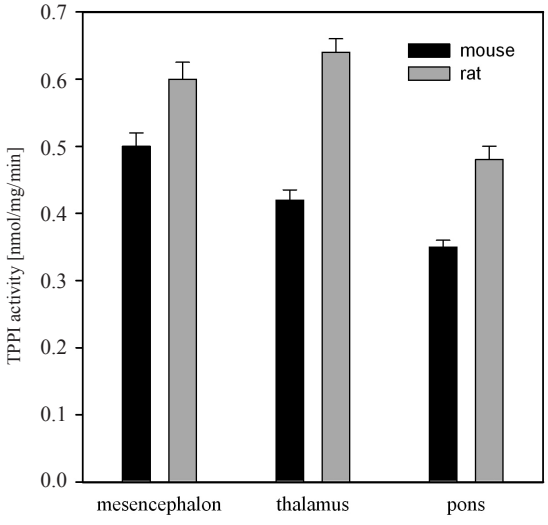

Fig. 1. Biochemical analysis of TPPI activity in rat and mouse brain regions using the substrate AAF-*p*NA in tissue homogenates. Each value was obtained as a mean of five separate experiments using adult animals of the respective species

Histochemical studies showed that TPPI was highly active in the neurons of both nucleus rubber (**Fig. 2A, B**) and substantia nigra (**Fig. 2C, D**) in mesencephalon of the two species. The enzyme activity was visualized as numerous orange-brown granules filling the cell cytoplasm. TPPI-positive granules were visible in the glial cells as well. All the neurons of the mouse (**Fig. 3A**) and rat (**Fig. 3B**) thalamic region were also highly positive for the enzyme as well as the neurons of the pons nuclei of the gray matter (**Fig. 2C, D**). In the thalamus and pons the enzyme activity was also visualize in the form of dark granules, which corresponds to the lysosomal localization of TPPI. Similarly high reaction for TPPI was observed in the glial cells too.

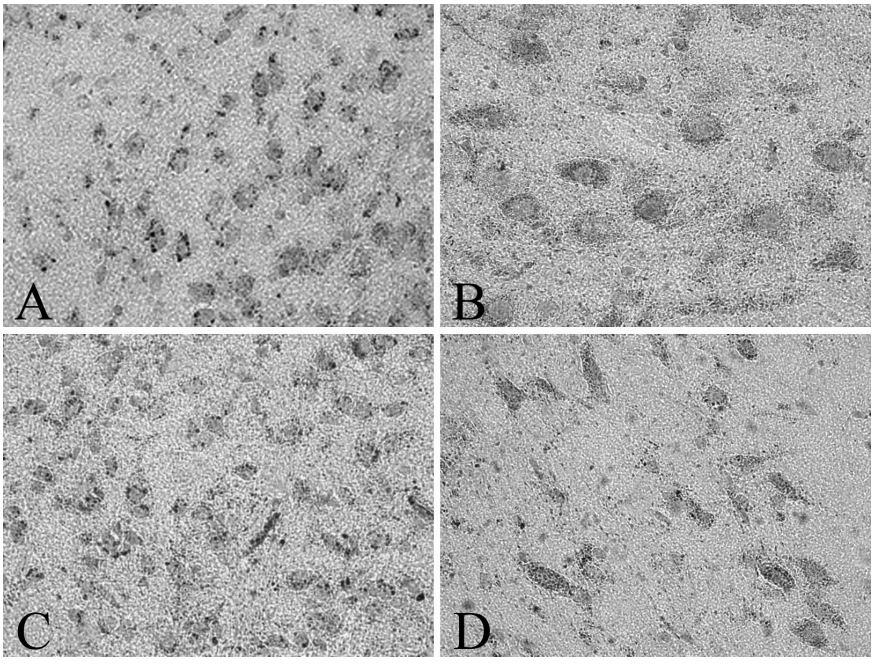

Fig. 2. Localization of TPPI activity in mouse (A, C) and rat (B, D) mesencephalon. High enzyme activity in the neurons of nucleus ruber (A, B) and substantia nigra (C, D). 400 ×

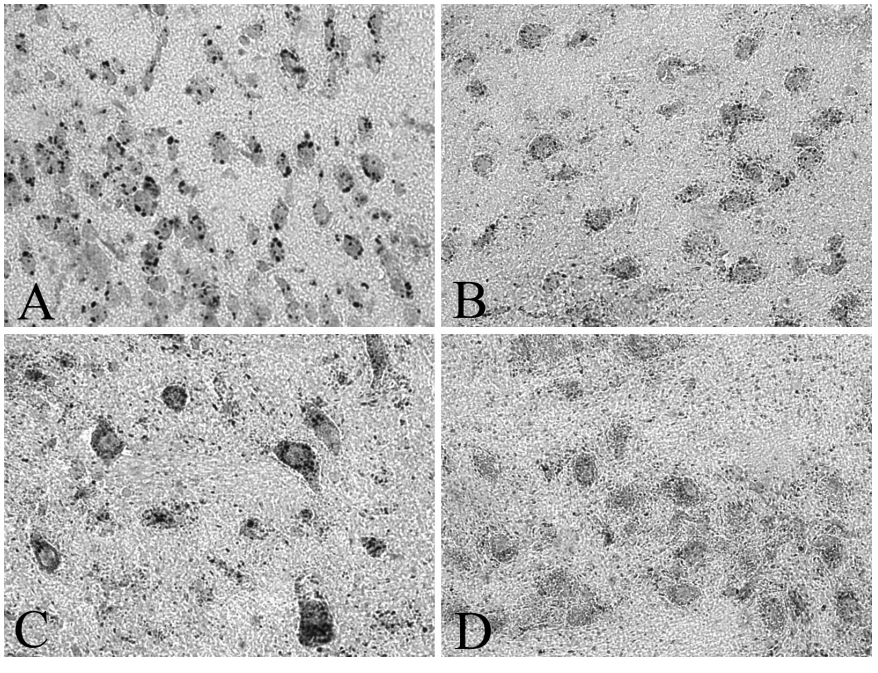

Fig. 3. Localization of TPPI activity in mouse (A) and rat (B) thalamus as well as in mouse (C) and rat (D) pons. High enzyme activity in the thalamis' (A, B) and pons' (C, D) neurons of nuclei of the gray matter. 400 ×

Discussion

TPPI activity is vital for the neuronal functions. The genetically determined enzyme deficiency leads to the development of the recessive neurodegenerative disease LINCL. LINCL is characterized by coupling of undegraded material in the lysosomes and lysosomal dysfunction, enhanced mitochondrial fragmentation and subsequent neuronal death. Clinical symptoms include severe epileptic seizures, ataxia, mental deterioration and progressive visual failure resulting in an early death in puberty [7]. The recently developed mouse model of LINCL [10] opens new possibilities for finding therapeutic approaches for the treatment of this serious genetic disorder [8]. On the other hand, many other brain diseases, also studied by mammalian models are connected with abnormally high or low TPPI activity levels [5]. In that respect, it is important to identify both normal enzyme activity levels and normal enzyme locations in all the brain regions of mostly used laboratory animals, i.e. rats and mice.

In the present paper we report TPPI activity levels and tissue distribution in three brain regions of rats and mice – mesencephalon, thalamus and pons. The enzyme in those brain parts have not been studied thus far. Our results show high enzyme activity levels. However, whereas in mouse the highest enzyme activity per mg protein was detected in the mesencephalon, in rat TPPI activity was most elevated in the thalamic region. This difference between species should be kept in mind when interpreting the results of studies using mouse and/or rat models for different disorders. On the other hand, the enzyme distribution is largely similar in the neurons of the two species. The enzyme was highly active in all the studied types of neurons as well as in glial cells of the three brain regions. This result points out at the crucial role of TPPI in rat and mouse brain as well.

In conclusion, the results presented here would be important in view of the use of animal models for studying LINCL as well as other neurodegenerative disorders.

References

1. **Dikov, A., M. Dimitrova, I. Ivanov, R. Krieg, K.-J. Halbhuber.** Original method for the histochemical demonstration of tripeptidyl aminopeptidase I. – Cell. Mol. Biol., **46**, 2000, 1219-1225.
2. **Dimitrova, M., D. Deleva, V. Pavlova, I. Ivanov.** Developmental study of tripeptidyl peptidase I activity in the mouse central nervous system and peripheral organs. – Cell Tissue Res., **346**, 2011, 141-149.
3. **Dimitrova, M., I. Ivanov, D. Deleva.** Distribution of tripeptidyl peptidase I activity in the rat brain and spinal cord. – Compt. rend. Acad. bulg. Sci., **62**, 2009, 729-734.
4. **Dawson, R., D. Elliot, W. Elliot, K. Jones.** – In: Biochemists manual, Moscow, Mir, 1991, 301.
5. **Kida, E., A. Golabek, M. Walus, P. Wujek, W. Kaczmarski, E. K. Wisniewski.** Distribution of tripeptidyl peptidase I in human tissues under normal and pathological conditions. – J. Neuropathol. Exper. Neurol., **60**, 2001, 280-292.
6. **Koike, M., M. Shibata, Y. Ohsawa, S. Kametaka, S. Waguri, E. Kominami, Y. Uchyiama.** The expression of tripeptidyl peptidase I in various tissues of rats and mice. – Arch. Histol. Cytol., **65**, 2002, 219-232.
7. **Mole, S., R.Williams, H. Goebel.** Correlations between genotype, ultrastructural morphology and clinical phenotype in the neuronal ceroid lipofuscinoses. – Neurogenetics, **6**, 2005, 107-126.
8. **Passini, M., J. Dodge, J. Bu, W. Yang, Q. Zhao, D. Sondhi, N. Hackett, S. Kaminsky, Q. Mao, L. Shihabuddin, S. Cheng, D. Sleat, G. Stewart, B. Davidson, P. Lobel, R. Crystal.** Intracranial delivery of CLN2 reduces brain pathology in a mouse model of classical late infantile neuronal ceroid lipofuscinosis. – J. Neurosci., **26**, 2006, 1334-1342.

9. **Sleat, D., R. Donnelly, H. Lackland, C.-G. Liu, I. Sohar, R. Pullarkat, P. Lobel.** Association of mutations in a lysosomal protein with classical late-infantile neuronal ceroid lipofuscinosis. – Science, **277**, 1997, 1802-1805.
10. **Sleat, D., J. Wiseman, M. El-Banna, K.-H. Kim, Q. Mao, S. Price, S. Macauley, R. Sidman, M. Shen, Q. Zhao, M. Passini, B. Davidson, G. Stewart, P. Lobel.** A mouse model of classical late-infantile neuronal ceroid lipofuscinosis based on targeted disruption of the CLN2 gene results in a loss of tripeptidyl-peptidase I activity and progressive neurodegeneration. – J. Neurosci., **24**, 2004, 9117-9126.
11. **Steinfeld, R., J. Fuhrmann, J. Gartner.** Detection of tripeptidyl peptidase I activity in living cells by fluorogenic substrates. – J. Histochem. Cytochem., **54**, 2006, 991-996.

Institute of Experimental Morphology, Pathology and Anthropology with Museum
Bulgarian Anatomical Society

Acta morphologica et anthropologica, 21
Sofia ● 2015

The Many Faces of Urticaria

M.Gantcheva

Institute of Experimental Morphology, Pathology and Antropology with Museum, Bulgarian Academy of Sciences, Sofia

Urticaria is a heterogeneous group of diseases that result from a large variety of underlying causes. It is characterized by the development of wheals, angioedema, or both. Urticaria needs to be differentiated from other medical conditions where hives and angioedema can occur as a symptom. Urticaria and angioedema may have diverse pathogenesis and clinical course and are usually the clinical consequence of vasoactive mediators derived from mast cells in the skin or mucosal tissues. Skin biopsies from lesions are important to make an appropriate diagnosis and particular therapy. Our cases demonstrate that predominance of lymphocytes and neutrophils in histological examination is important for therapeutic response. Antihistamines may not work if the infiltrate consists mainly of neutrophils. In such cases the right answer could be treatment with colchicin, dapsone or short course with steroids.

Key words: urticaria, angioedema.

Introduction

Urticaria is a disease characterized by the development of wheals, angioedema, or both. A wheal is a superficial skin-colored or pale skin swelling, usually surrounded by erythema. It may have a burning sensation or is very itchy. It has a fleeting nature, with the skin returning to its normal appearance, usually within 1-24 h. Sometimes wheals resolve even more quickly. Angioedema is deeper swelling within the skin or mucous membranes, and can be skin-colored or red. It resolves within 72 hours. Angioedema is more often asymptomatic and rarely painful.

It is very important urticaria to be differentiated from other medical conditions where wheals and/or angioedema can occur as a symptom, for example skin prick test, anaphylaxis, auto-inflammatory syndromes, or hereditary angioedema (bradykinin-mediated angioedema) [3].

It is not easy to be classified the subtype of the disease. Urticaria can be spontaneous, physical, or other, based on duration, frequency, and causes of symptoms.

Spontaneous urticaria occurs in the absence of external physical stimuli. According to the duration of the hives urticaria is: acute – when they last less than 6 weeks and often have gone within hours to days, and chronic – with a more than 6 weeks duration of the lesions.

Physical urticaria is caused by external physical stimuli. Some cases of physical urticaria may be considered chronic. However, physical urticaria is distinguished from chronic urticaria based on clear evidence that physical factors are eliciting urticaria.

Other urticaria disorders are those induced by exercise or contact, anaphylactic reactions, cholinergic mechanisms, and aquagenic factors.

We analyze five patients with hives or edema on the lips, suspected at first sight as suffering from urticaria or angioedema. After careful anamnestic and histopathological examination the diagnosis were re-examined.

Case Reports

We analyze four patients – two of them with clinical manifestations of angioedema and three patients with wheals, characterized as clinical marker for urticaria.

The patiens with angioedema had edema of lips with pain and discomfort. They were young women, aged 33 and 38. The first one had an anamnesis for lip augmentation with dermal filler before 4 days. She developed swelling of the lips 8 hours after the injection and 3 days after the procedure the conditions worsed. She refused a biopsy and was treated with parenteral steroids and antihistamins. The other patient had swelling on the lips an around the eyes. She also had lip augmentation before 6 months. A biopsy was performed and the result demonstrates labial edema with mild vessel ectazia, without granuloma or inflammatory reaction (**Fig.1**). The treatment was intravenous steroids.

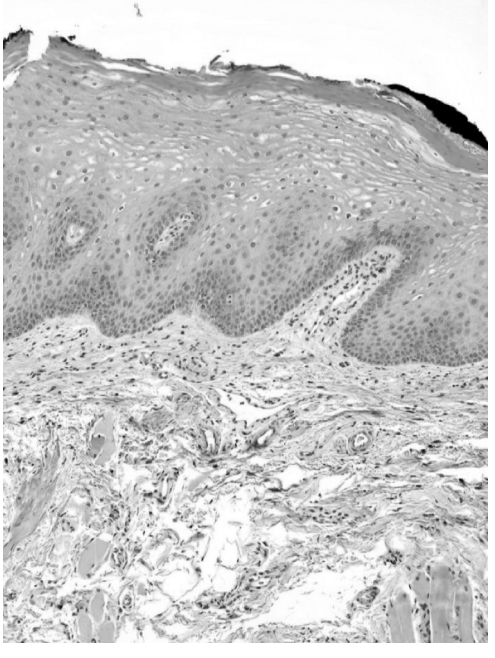

Fig. 1. Labial edema with mild vessel ectazia, without granuloma and inflammatory reaction

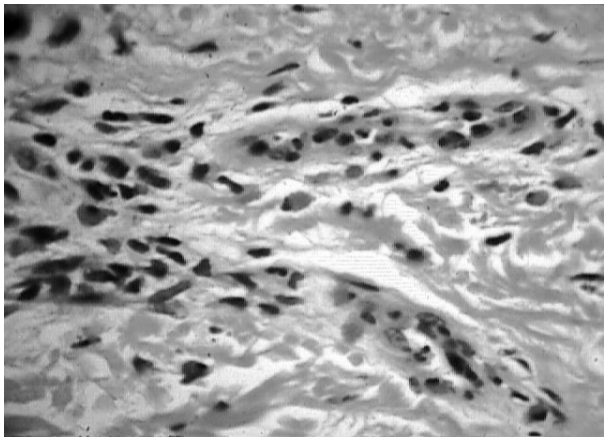

Fig. 2. Dermal edema, slight dilatation of superficial dermal vessels and slender perivascular infiltrate of macrophages, lymphocytes and granulocytes

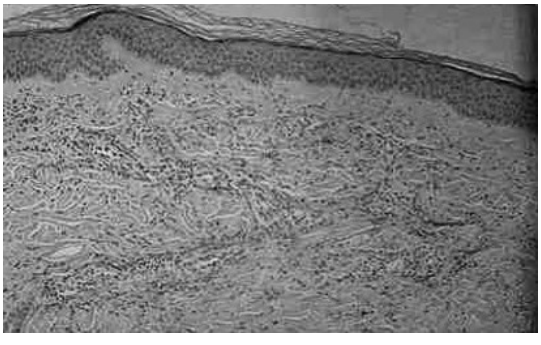

Fig. 3. Leucocytoclastic vasculitis with distroyed blood vessels and neutrophilic infiltrate

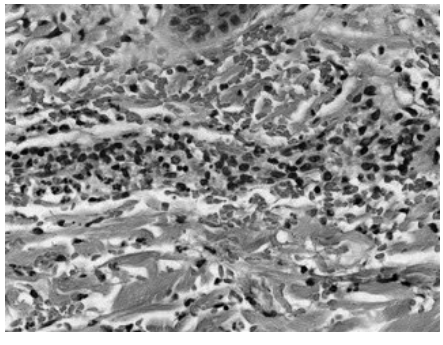

Fig. 4. Mixed inflammatory infiltrate in upper derma composed mainly of neutrophils and eosinophils

Three other patients were with hives all over the skin without mucosal involvement. Histopathological investigations were performed. One patient showed characteristic features of the urticaria with dermal edema, slight dilatation of superficial dermal vessels and slender perivascular infiltrate of macrophages, lymphocytes and granulocytes. (**Fig.2**). The biopsy specimens from the other two patiens were quite different from the typical picture for urticaria. They showed leucocytoclastic vasculitis with distroyed blood vessels and neutrophylic infiltrate (**Figs. 3, 4**).

Results and Discussion

The both patients with lips swelliing raise the question wheather the reason for mucous edema is because of the filler. Some transient swelling in the immediate postprocedural period is normal and occurs with all dermal fillers. This type of edema happens shortly

after injection and is related to injection volume and technique. It is so called short-term posttraumatic edema.

Another subtype of angioedema is antibody-mediated edema. This may occur after initial or repeated exposure to dermal fillers, which are essentially foreign bodies. Some patients may develop hypersensitivity to injected products due to an immunoglobulin E-mediated immune response (Type I hypersensitivity reaction). IgE stimulates mast cells to degranulate, releasing proteases, heparin, histamine, cytokines, prostaglandins, leukotrienes, and platelet-activating factor, which result in the edema, erythema, pain, and itching characteristic of an allergic response. Angioedema occurs within hours of exposure. Reactions can be severe and can last for several weeks [4].

Nonantibody-mediated (delayed) edema is characterized by induration, erythema, and edema, and are mediated by T lymphocytes rather than antibodies. They typically occur 1 day after injection, but may be seen as late as several weeks after injection and may persist for many months [1]. Delayed hypersensitivity reactions are nonresponsive to antihistamines. The allergen should be removed. In the case of HA, this will involve treatment with hyaluronidase.

We think our first patient had a severe short-term posttraumatic edema even the clinical picture was supposed to be angioedema. The second one had typical angioedema despite the anamnesis for dermal filler in her lips, which was confirmed with the histopathological findings. The biopsy was very important in this case as this reaction could be assosiated also with granuloma but fortunately this was rejected with the morphology.

The other three patiens with the clinical manifestation of urticaria with wheals involving all over the skin were diagnosed as urticaria. The interesting finding is that two of them had leucitoclastic vasculitis on the biopsy speciments and only one of them was confirmed to have real urticaria with dermal edema and without vessel involment. The presence of leukocytoclastic vasculitis in persistent lesions indicates an underlying immune complex disease[2]. The patients were reexamined as suffered from urticaria vasculit. It was very important for the therapy for these patients, where corticosteroids are indicated. Cytotoxic drugs may be required for adequate treatment in such cases.

According to the latest guidelines, urticaria pigmentosa, urticarial vasculitis, familial cold urticaria and nonhistaminergic angioedema are no longer considered to be subtypes of urticaria [5].

References

1. **Arron, S. T., I. M. Neuhaus.** Persistent delayed-type hypersensitivity reaction to injectable non-animal-stabilized hyaluronic acid. – J. Cosmet. Dermatol., **6**, 2007, 167-171.
2. **Brodell, L. D., L. A. Beck.** Differential diagnosis of chronic urticaria. – Ann. Allergy. Asthma Immunol., **100**, 2008, 181-188.
3. **Peroni, A. et al.** Urticarial lesions: If not urticaria, what else? The differential diagnosis of urticaria. – JAAD, **62**, 2010, 557-570.
4. **Van Dyke, S., G. P. Hays, A. E .Caglia, M. Caglia.** Severe acute local reactions to a hyaluronic acid-derived dermal Filler. – J. Clin. Aesthet Dermatol., **3** 2010, 32-35.
5. **Zuberbier, T. T., W. Aberer, R. Asero, C. Bindslev-Jensen et al.** The AACI/GA^{2}LEN/EDF/WAO Guideline for the definition, classification, diagnosis, and management of urticaria: the 2013 revision and update. – Allergy, **69**, 2014, 868-887.

Institute of Experimental Morphology, Pathology and Anthropology with Museum
Bulgarian Anatomical Society

Acta morphologica et anthropologica, 21
Sofia ● 2015

In Vitro Effect of Temperature and Cobalt Chloride Treatment on Human Red Blood Cells' Morphology and Indices

Y. Gluhcheva[*], *I. Ivanov*[**]

[*]*Institute of Experimental Morphology, Pathology and Anthropology with Museum, Bulgarian Academy of Sciences*
[**]*Institute of Mechanics, Bulgarian Academy of Sciences*

Changes of erythrocyte morphology induced by exposure of blood to cobalt chloride ($CoCl_2$) and/or various degrees of temperature are poorly studied. The aim of the study was to investigate the *in vitro* effect of $CoCl_2$ on erythrocyte morphology and indices of red blood cell suspensions after incubation at different temperatures. Human erythrocyte (RBC) suspensions were treated with 50 μM or 500 μM $CoCl_2$ and incubated for one hour at 4 ºC, room temperature and 40 ºC. After incubation the morphological changes were studied. Morphological studies showed RBC aggregates at 4 ºC while elyptocytes were mainly observed at 40 ºC. Thermal treatment induced anisocytosis leading to increased RDW and decreased MCV. The results indicate that both $CoCl_2$ and temperature affect erythrocyte morphology and indices of RBC suspensions possibly by inducing structural, biomechanical and biochemical changes in the erythrocyte membrane.

Key words: RBC suspensions, *in vitro* treatment, cobalt chloride, erythrocyte morphology, temperature incubation.

Introduction

Cobalt chloride ($CoCl_2$) is a water soluble hypoxia-mimicking agent shown to improve hematological parameters [1]. Recent data show that athletes use the compound to stimulate endogenous erythropoietin production, thus erythropoiesis [4].

Temperature, on the other hand, induces changes in cell membrane composition and permeability. The literature data suggest that it affects primarily the membrane protein component and not the lipids [3]. No significant morphological changes are observed when erythrocytes are exposed *in vitro* to 42 ºC [2].

Changes in the hematological parameters induced by exposure of blood to varying degrees of temperature are poorly studied. Alterations in red blood cell (RBC) properties – morphology and viscoelasticity is one of the basic indicators for human health, disease diagnosis, treatment, etc [6].

The aim of the present study was to investigate the *in vitro* effect of $CoCl_2$ treatment on erythrocyte morphology and some erythrocyte indices of RBC suspensions

after incubation at different temperatures.

Materials and Methods

Human erythrocytes (RBC) from a healthy donor, obtained from the National Center for Hematology and Transfusiology in Sofia, Bulgaria were washed in 0.9% NaCl, hematocrit was adjusted to 40% and treated with 50 μM or 500 μM $CoCl_2 \times 6H_2O$ (Reahim). The RBC suspensions (n = 5) were incubated for one hour at 4 ºC, room temperature and/or 40 ºC. The morphological changes were studied on blood smears stained with May-Grünwald-Giemsa (Merck, Germany) and observed on a light microscope Leica DM 5000B (Leica Microsystems, USA). Erythrocyte indices such as hematocrit (Hct), mean corpuscular volume (MCV), mean corpuscular hemoglobin (MCH), mean corpuscular hemoglobin concentration (MCHC) and red blood cell distribution width (RDW) were obtained using automated hematological analyzer BC-2800Vet (Mindray, China). Changes were compared against control samples of RBC suspensions (n = 5) incubated at the same temperatures.

Statistical Analysis

The obtained results are presented as mean value ± SD. Statistical significance between the experimental groups was determined using Student's *t*-test. Difference was considered significant at $p < 0.05$.

Results and Discussion

Preliminary results showed that RBC morphological alterations were detected when different $CoCl_2$ concentrations were added. Thermal treatment induced anisocytosis leading to increased RDW and decreased MCV. The highest RDW values were measured at 40 ºC. Incubation at room temperature or 40 ºC decreased MCH and MCHC ($p < 0.03$). Addition of $CoCl_2$ to the RBC suspensions increased insignificantly both parameters when the samples were incubated at 4 ºC. On the other hand, at room temperature and at 40 ºC MCH and MCHC decreased significantly in the presence of the cobalt compound compared to the samples incubated at 4 ºC with 50 and/or 500 μM $CoCl_2$. The results suggest a relationship between cobalt and hemoglobin content which is temperature dependent. Changes in MCH and MCHC could be explained by the results of Simonsen et al. [5] demonstrating that ^{57}Co co-migrates with hemoglobin when added *in vitro* to a lysate of unlabeled cells or to a solution of purified hemoglobin. Addition of $CoCl_2$ increased MCV in samples incubated at 4 ºC or 40 ºC compared to controls. The parameter though was significantly decreased when samples treated with the compound but incubated at different temperatures were compared. Morphological studies showed RBC aggregates (**Fig. 1a**) and echinocytes at 4 ºC while elyptocytes were mainly observed at 40 ºC (**Fig. 1b, c**). Incubation at different temperatures and treatment with $CoCl_2$ did not affect Hct values of RBC suspensions compared to the control samples. Dose-dependent effect was not observed.

According to the literature data changes in hematological parameters and erythrocyte morphology are found when blood is exposed to 50 ºC [2]. These results indicate significant stability of the RBC membrane at high temperature. Incubation of RBC with $CoCl_2$ leads to accumulation of cobalt in the cells in a time-dependent manner [5]. The

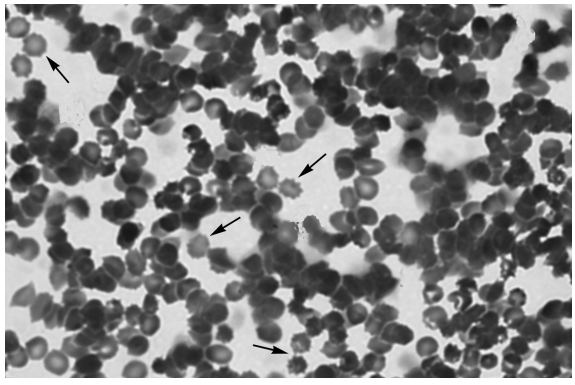

(a)

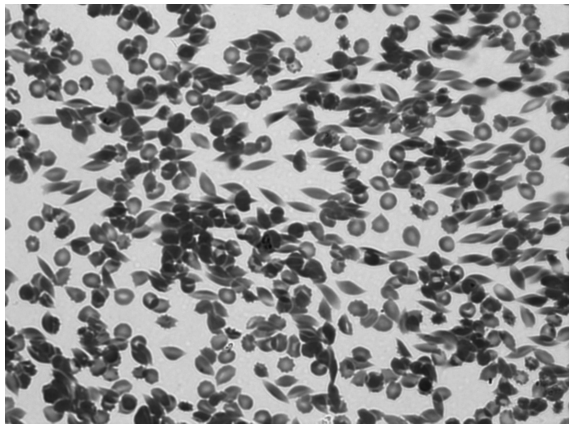

(b)

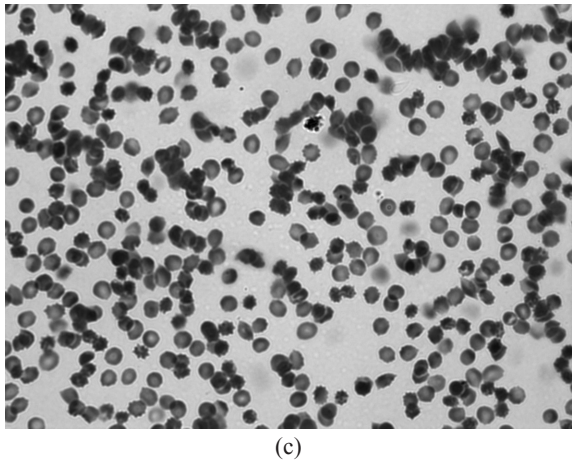

(c)

Fig. 1. RBC smears stained with May-Grünwald-Giemsa, × 200. RBC aggregates and echinocytes (arrow) are observed after incubation at 4 °C (a); Eliptocytes are found mainly in control smears incubated at 40 °C (b); Individual echinocytes are observed in smears treated with $CoCl_2$ (c)

temperature treatment possibly affects cobalt ion influx in the cells. Cobalt ion concentration up to 0.1 mM is regarded as non-cytotoxic. Incubation of RBC suspensions with 500 μM $CoCl_2$ for one hour in our experiment possibly is not long enough to induce apoptotic changes. Therefore, significant changes in erythrocyte morphology are not expected. The effect in this case would be mainly due to heat treatment. The experimental data suggest that the temperature of the solution is an important factor and should be considered when applying $CoCl_2$ treatment.

Conclusions

The results indicate that both $CoCl_2$ and temperature affect erythrocyte morphology and indices of RBC suspensions possibly by inducing structural, biomechanical and biochemical changes in the erythrocyte membrane.

Acknowledgements: The work is supported by grant No DO02 - 351/2008 from the Bulgarian National Science Fund.

References

1. **Bowie, E. A., P. J. Hurley.** Cobalt chloride in the treatment of refractory anaemia in patients undergoing long-term haemodialysis. – Aust. N. Z. J. Med., **5**, 1975, 306-314.
2. **Choi, J. W., S. H. Pai.** Changes in hematologic parameters induced by thermal treatment of human blood. – Ann. Clin. Lab. Sci., **32**, 2002, 393-398.
3. **Ho, K.-C., P.-S. Lin.** Response of erythrocytes to heat in the presence of D_20, glycerol, and anisotonic saline. – Radiat. Res., **125**, 1991, 20-27.
4. **Lippi, G., M. Franchini, G. C. Guidi.** Cobalt chloride administration in athletes: a new perspective in blood doping. – Br. J. Sports Med., **39**, 2005, 872-873.
5. **Simonsen, L. O., A. M. Brown, H. Harbak, B. I. Kristensen, P. Bennekou.** Cobalt uptake and binding in human red blood cells. – Blood Cells Mol Dis., **46**, 2011, 266-276.
6. **Wu, Y., Y. Hu, J. Cai, S. Ma, X. Wang, Y. Chen, Y. Pan.** Time-dependent surface adhesive force and morphology of RBC measured by AFM. – Micron, **40**, 2009, 359-364.

Address for correspondence:
e-mail: ygluhcheva@hotmail.com

Institute of Experimental Morphology, Pathology and Anthropology with Museum
Bulgarian Anatomical Society

Acta morphologica et anthropologica, 21
Sofia ● 2015

MMP-2 and MMP-9 in Drug-Provoked Developmental Neuroapoptosis

V. Goranova[*], O. Uckermann[**], H. Luksch[**], J. Marzahn[**], Y. Hoehna[**], C. Ikonomidou[***]

[*]*Department of Anatomy, Histology and Embryology, Medical University, Varna, Bulgaria*
[**]*Department of Pediatric Neurology, University Children's Hospital, Dresden, Germany*
[***]*Department of Neurology, University of Wisconsin, Madison, USA*

Matrix metalloproteinases (MMPs) are zinc-dependent endoproteases with multiple roles in morphogenesis, cell death, and tissue regeneration. The aim of the present study was to investigate potential role of MMP-2/-9 in the pathogenesis of neuroapoptosis provoked by MK-801 or phenobarbital in the developing rodent brain. Seven-day-old rats or mice were drug-injected and pups were sacrificed at different survival times. Tissues from various brain regions were studied for expression of MMP-2/-9 by standard RT-PCR, western blotting, gelatin zymography and TUNEL immunohistochemistry. We found an increased number of TUNEL-positive cells 24 h after administration of MK-801 or phenobarbital. There was no significant increase in MMP-2/-9 mRNA expression, protein level or gelatinolytic activity observed in conjunction with drug-induced neuroapoptosis. The extent of neurodegeneration was not altered in MMP-9 TG rats and was increased in MMP-9 KO mice. Treatment with the broad metalloproteinase inhibitor GM6001 did not protect against drug-induced apoptosis. Our results suggest that activation of MMP-2/-9 does not contribute to pathogenesis of neuroapoptosis caused by NMDA antagonists or $GABA_A$ agonists in the developing rodent brain.

Key words: Matrix metalloproteinases, neuroapoptosis, MK-801, phenobarbital, GM6001.

Introduction

MMPs play an essential role in extracellular matrix remodeling and modulation of signaling pathways [4, 6]. They are known to be involved in the cleavage of cell surface receptors, release of apoptotic ligands, and chemokine-cytokine inactivation. MMPs are involved in various normal and pathological processes such as cell proliferation, migration, differentiation, angiogenesis, tissue repair, inflammation, tumor invasion, and apoptosis by degrading all kinds of extracellular matrix proteins and processing a number of bioactive molecules [10].

Our previous findings on the effects of N-methyl-D-aspartate (NMDA) antagonists, especially MK801 (dizocilpine), and $GABA_A$ agonist phenobarbital have shown that they cause a widespread neuroapoptosis in the infant mammalian brain [2, 3]. There exist data that MMP-9 control NMDA receptors [5].

The aim of the present study was to investigate potential involvement of selected MMPs in the pathogenesis of neuronal apoptosis induced by the NMDA antagonist MK-801 (dizocilpine) or the $GABA_A$ agonist phenobarbital in infant rats, transgenic (TG) rats overexpressing MMP-9 and MMP-9 knockout (KO) mice.

Materials and Methods

We used 7-day-old Wistar rats, MMP-9 TG rats and MMP-9 KO mice. Standard RT-PCR, western blotting, gelatin zymography and TUNEL immunohistochemistry were applied. The following drugs: 1 mg/kg MK-801 (dizocilpine), 50 mg/kg phenobarbital, 50 mg/kg GM6001 (ilomastat, a broad MMP inhibitor), dissolved in 0.1% DMSO 2 h later were i.p. injected. Fresh tissue frozen in liquid nitrogen from cortex, hypothalamus, and thalamus 1, 4, 12, 24, 48 or 72 h after injection of drugs were used for molecular/biochemical studies. For TUNEL peroxidase staining perfusion of brains with 4% paraformaldehyde in 0.1M PB under chloral hydrate anesthesia was performed 24 h after drug application followed by postfixation and embedding in paraffin. Paraffin sections were used for stereological quantification of neurodegeneration in different 13 brain regions evaluated in a blinded fashion.

Results

MK-801 and phenobarbital caused a widespread neuronal apoptosis throughout various regions of the immature rodent brain (**Fig. 1**). There is a more significant increase of cell death following treatment with MK-801 as compared to phenobarbital.

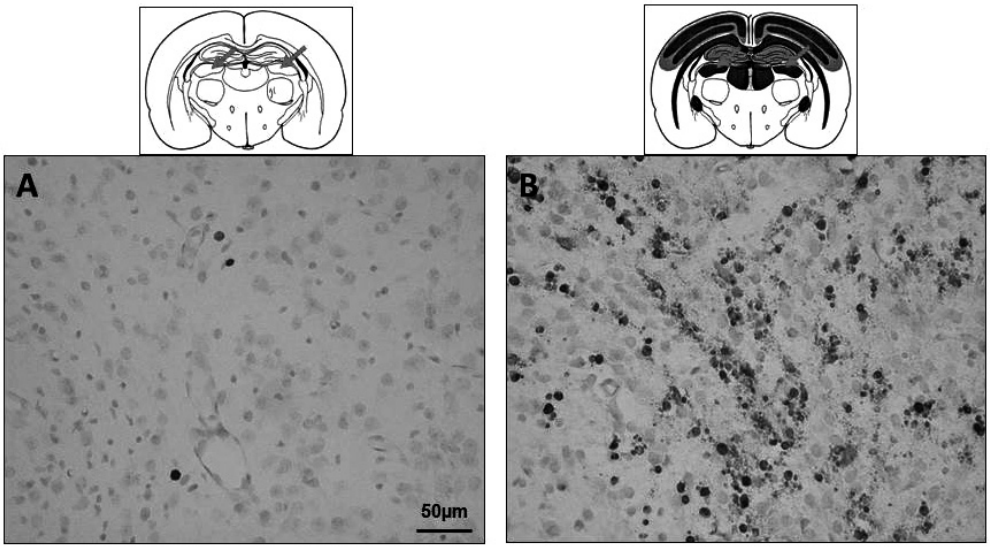

Fig. 1. Degenerated neurons detected by TUNEL staining in the laterodorsal thalamus (arrows) of control animals **(A)**, and 24 h after treatment with MK-801 **(B)**. DAB substrate, methyl green counterstaining

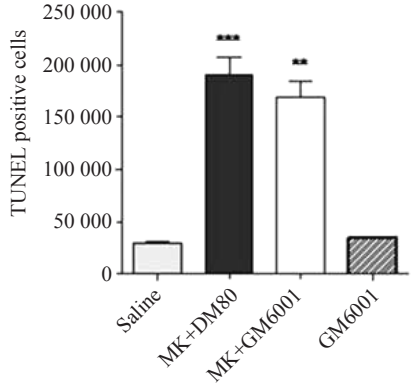

Fig. 2. Stereologic quantification of degenerating cells in the brain detected by TUNEL-staining 24 h after treatment with saline, MK-801 + 0.1% DMSO, MK-801 + GM6001 or GM6001. Values are means ± SEM. ** $P < 0.01$, *** $P < 0.001$, one-way ANOVA and Tukey's post-hoc test, n = 6 per each group

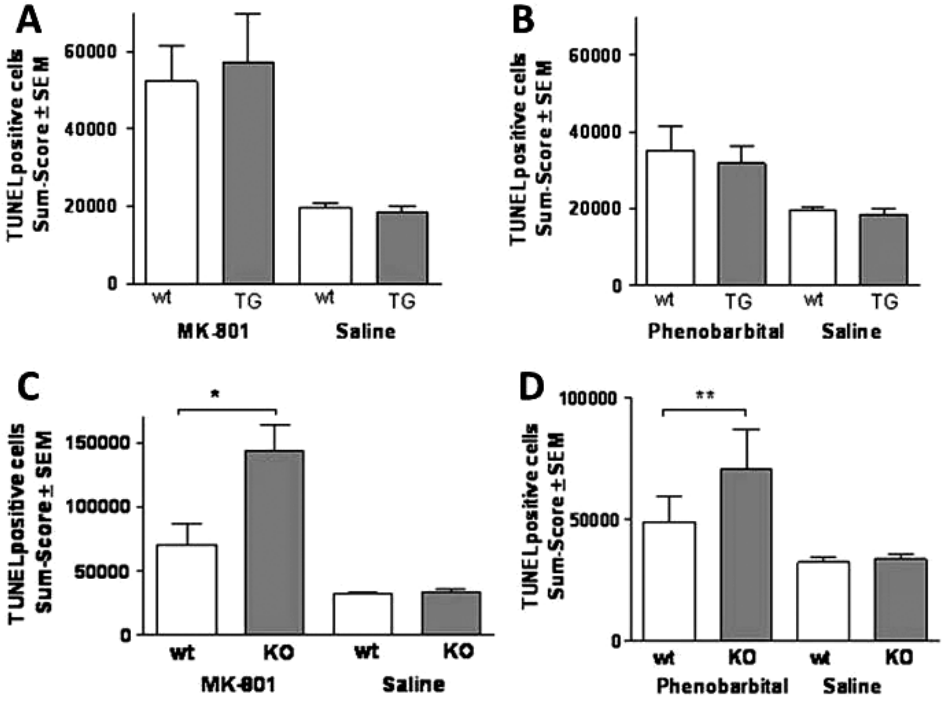

Fig. 3. Statistical analysis of the brain damage in TG rats and wild-type animals after treatment with MK-801 **(A)** or phenobarbital **(B)** and MMP-9 KO mice after treatment with MK-801 **(C)** or phenobarbital **(D)**. Values are means ± SEM. wt - wild type, TG - transgenic, KO - knockout, * $P < 0.05$, ** $P < 0.01$, unpaired t-test, n = 6 per each group

Stereologic quantification of degenerating cells in 13 brain regions detected by TUNEL-staining 24 h following treatment showed a significant increase of cell death. The application of GM6001 did not ameliorate the extent of brain damage induced by MK-801 (**Fig. 2**) or phenobarbital.

Drug-induced apoptosis was not altered in MMP-9 overexpressing rat brain. Statistical analysis revealed that the extent of brain damage indicated by number of TUNEL-positive cells was similar in transgenic rats and wild-type animals after treatment with MK-801 (**Fig. 3 A**) or phenobarbital (**Fig. 3 B**). We found a significantly enhanced drug-induced apoptosis in brains of MMP-9 KO mice for both drugs. The extent of neurodegeneration was statistically increased in MMP-9 KO mice than in brains of wild-type animals after treatment with MK-801 (**Fig. 3 C**) or phenobarbital (**Fig. 3 D**).

The expression of MMP-2 and MMP-9 were studied also at transcriptional, protein, cellular and functional level. No significant increase in MMP-2/-9 mRNA expression, protein level or gelatinolytic activity, observed in conjunction with drug-induced neuronal apoptosis, were found (data not shown).

Discussion

Our present findings confirm the effect of the NMDA antagonist MK-801 and $GABA_A$ agonist phenobarbital as potent neurotoxic agents that exert severe damage in the infant rodent brain. We did not found any morphological, molecular or biochemical data by the methods applied that MMP-2 and MMP-9 are pathogenetically involved in the developmental neuronal apoptosis induced by MK-801 or phenobarbital. The metalloproteinase inhibitor GM6001 does not prevent MK-801-induced neurodegeneration in the developing rat brain. Drug-induced brain apoptosis was not altered in MMP-9 TG rats but it was increased in MMP-9 KO mice compared to wild-type animals. This corresponded to previous data indicating a protective effect of MMP-9 after cerebral hypoxia-ischemia [9]. MMPs are important mediators in various neurodegenerative disorders [8] but they are known to contribute to neurogenesis and regeneration of the nervous system [1, 7, 11]. Additional experiments may reveal a potential beneficial or detrimental role of MMP-2/-9 or other members of the large family of MMPs in the immature brain.

Acknowledgements: Supported by BMBF grant No 01GZ0702.

References

1. **Agrawal, S. M., L. Lau, V. W. Yong.** MMPs in the central nervous system: where the good guys go bad. – Semin. Cell. Dev. Biol., **19**, 2008, 42-51.
2. **Bittigau, P., M. Sifringer, K. Genz, E. Reith, D. Pospischil, S. Govindarajalu, M. Dzietko, S. Pesditschek, I. Mai, K. Dikranian, J. W. Olney, C. Ikonomidou.** Antiepileptic drugs and apoptotic neurodegeneration in the developing brain. – Proc. Natl. Acad. Sci., **99**, 2002, 15089-15094.
3. **Ikonomidou, C., F. Bosch, J. Miksa, P. Bittigau, J. Vöckler, K. Dikranian, T. I. Tenkova, V. Stefovska, L. Turski, J. W. Olney.** Blockade of NMDA receptors and apoptotic neurodegeneration in the developing brain. – Science, **283**, 1999, 70-74.
4. **Klein, T., R. Bischoff.** Physiology and pathophysiology of matrix metalloproteases. – Amino Acids, **41**, 2011, 271-290.
5. **Michaluk, P., L. Mikasova, L. Groc, R. Frischknecht, D. Choquet, L. Kaczmarek**. Matrix metalloproteinase-9 controls NMDA receptor surface diffusion through integrin beta1 signaling. – J. Neurosci., **29**, 2009, 6007-6012.

6. **Nagase, H., R. Visse, G. Murphy.** Structure and function of matrix metalloproteinases and TIMPs. – Cardiovasc. Res., **69**, 2006, 562-573.
7. **Rivera, S., M. Khrestchatisky, L. Kaczmarek, G. A. Rosenberg, D. M. Jaworski.** Metzincin proteases and their inhibitors: foes or friends in nervous system physiology? – J. Neurosci., **30**, 2010, 15337-15357.
8. **Rosenberg, G. A.** Matrix metalloproteinases and their multiple roles in neurodegenerative diseases. – Lancet Neurol., **8**, 2009, 205-216.
9. **Svedin, P., H. Hagberg, K. Sävman, C. Zhu, C. Mallard.** Matrix metalloproteinase-9 gene knock-out protects the immature brain after cerebral hypoxia-ischemia. – J. Neurosci., **27**, 2007, 1511-1518.
10. **Verslegers, M., K. Lemmens, I. van Hove, L. Moons.** Matrix metalloproteinase-2 and -9 as promising benefactors in development, plasticity and repair of the nervous system. **–** Prog. Neurobiol., **105**, 2013, 60-78.
11. **Yong, V. W**. Metalloproteinases: mediators of pathology and regeneration in CNS. – Nat. Neurosci., **6**, 2005, 931-944.

Institute of Experimental Morphology, Pathology and Anthropology with Museum
Bulgarian Anatomical Society

Acta morphologica et anthropologica, 21
Sofia ● 2015

In vitro Maturing Mouse Oocytes Treated by Okadaic Acid – Effect on Cytoskeletal Structures and the Chromosome Spread

V. Hadzhinesheva, V. Nikolova, I. Chakarova, M. Markova, S. Delimitreva, R. Zhivkova

Department of Biology, Medical Faculty,
Medical University of Sofia, Bulgaria

Okadaic acid (OA) was applied in different concentrations for 1 or 2 hours on *in vitro* maturing and ovulated mouse oocytes. Actin, tubulin and chromatin were fluorescently stained and chromatin condensation, chromosome spreading, presence and morphology of meiotic spindle and actin cap were analyzed. One hour OA treatment of *in vitro* maturing oocytes produced slender spindles and was not enough for chromosome condensation. *In vitro* maturing oocytes treated for 2 h had abnormal or destroyed spindles and often condensed chromatin. When chromosomes were well spread, actin cap was lacking and actin was distributed uniformly in cortical cytoplasm. These changes preceded changes in meiotic spindle and chromatin. Chromatin condensation was higher for *in vivo* ovulated oocytes and good quality chromosome plates were obtained from them. In conclusion, OA treatment of oocytes affects the actin cap first, causes spindle abnormalities depending on meiotic maturation stage and provides good chromosome spreading and condensation.

Key words: oocyte, actin, tubulin, metaphase plate, okadaic acid.

Introduction

Okadaic acid ($C_{44}H_{68}O_{13}$) is a cytotoxin produced by dinoflagellates. It is named after the marine sponge *Halichondria okadai,* from which this compound was first isolated. Its hydrophobic backbone enables it to enter cells where it stimulates intracellular protein phosphorylation. Okadaic acid (OA) is a reversible, potent and selective inhibitor of serine threonine protein phosphatases PP2A and PP1, especially the former [6]. In oocytes, OA induces activation of MPF, entry to M-phase and chromosome condensation. In *Xenopus* eggs, OA provokes lamin depolymerization and nuclear envelope breakdown and strongly affects the microtubule organizing center [5]. Because of its effect on chromosome condensation, okadaic acid was applied on human second polar bodies to obtain readable metaphase plates as an approach for preimplantation diagnostics in assisted reproduction [7]. The authors reported some benefits of OA treatment (no need of hypotonic incubation during oocyte fixation) but also a disadvantage (cell

fragmentation). According to [1], OA prevents polar body extrusion and causes ruffling of cell membrane and formation of large vacuoles in the ooplasm. Treatment of canine oocytes of different sizes with 0.5 μM OA for 1 h reportedly improves meiotic maturation [2]. These data, however, are still preliminary and no benefit of OA as methodological tool for oocytes is generally accepted. To study the potential of okadaic acid in this respect, we investigated its effects on chromosome condensation and spreading as well as on tubulin and actin cytoskeleton in ovulated and *in vitro* maturing mouse oocytes.

Materials and Methods

The study used 141 mouse oocytes obtained after hormonal stimulation of the animals. Ninety-one oocytes were obtained by ovarian section and subjected to *in vitro* maturation (IVM). Fifty oocytes were isolated from the oviduct after their *in vivo* ovulation. The stimulation was carried out by FSH (Follicle Stimulating Hormone) treatment of animals for the oocytes subjected to *in vitro* maturation and a combination of FSH/hCG (human Chorionic Gonadotropin) for ovulated oocytes.

Three different concentrations (0.4 μM, 2 μM and 5 μM) of okadaic acid were applied for 1 or 2 hours to mouse oocytes at different maturation stages (in vitro maturing or ovulated). Oocytes were then subjected to fluorescent detection of tubulin, actin and chromatin or to classical karyotyping. In the latter case, hypotonic incubation was omitted in some samples. Chromatin was visualized by Giemsa for karyotyping and by HOECHST 33258 (Sigma-Aldrich) for fluorescent analysis. Monoclonal mouse anti-α-tubulin antibody followed by FITC-conjugated goat antibody (Sigma-Aldrich) were used for detection of tubulin. Fibrillar actin was visualized using its specific reaction with phalloidin-TRITC (Sigma-Aldrich).

The results were analyzed regarding chromatin condensation, chromosome spreading, presence and morphology of meiotic spindle and actin cap.

Results

In vitro maturing oocytes

Incubation of in vitro maturing oocytes with OA in different concentrations for 1 hour did not cause chromosome spreading. A slender meiotic spindle containing few fibers was present in these oocytes. The proportion of oocytes with visible spindles was comparable between samples exposed to low and high concentration of OA: 36.36% of oocytes treated by 0.4 μM OA and 32-34% of cells treated by 2 μM or 5 μM OA.

Chromosome spreading was obtained in 26.67% of oocytes incubated for 2 h in 5 μM OA, 30.77% of oocytes incubated in 2 μM OA and 31.25% of oocytes incubated in 0.4 μM OA. The chromosomes were condensed at regard-

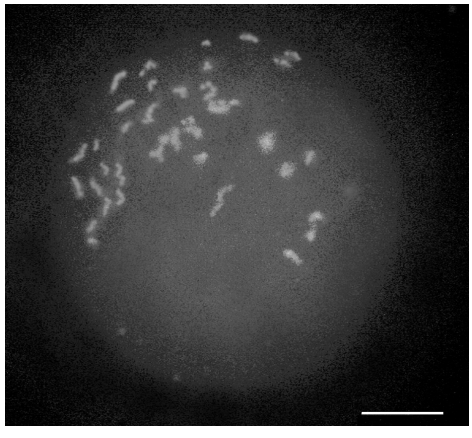

Fig. 1. Spread of chromosomes in an *in vitro* maturing oocyte treated by 5 μM OA for 2 h. The chromosomes are well condensed and distributed in the ooplasm. Most of them are seen represented by single chromatids and their number is corresponding to the diploid set. Bar = 20 μm

less of the stage of meiotic maturation and the spread occupied nearly half of the oocyte volume (**Fig. 1**).

Meiotic spindles had abnormal shape and/or length or were fully destroyed. The low (0.4 μM) or high (2 μM and 5 μM) concentration of OA had different effect on tubulin: spindles were present in 43.75% of oocytes incubated in 0.4 μM OA compared to 23% and 20% respectively of cells treated by 2 μM and 5 μM OA.

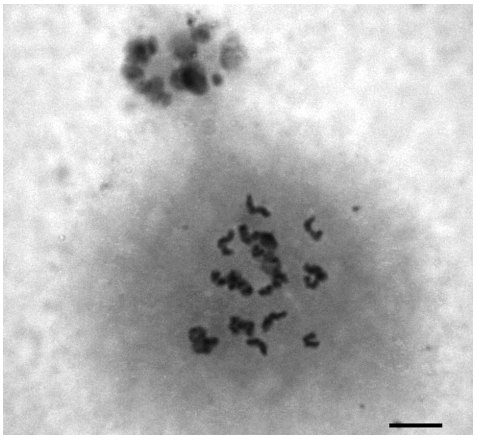

Fig. 2. Good quality chromosome spread of an *in vivo* ovulated oocyte incubated in 2 μM OA for 2 h. Chromosomes have good morphology and condensation and are suitable for classical cytogenetics. Bar = 20 μm

***In vivo* ovulated oocytes**

The incubation in OA for two hours resulted in very good chromosome spreading. Ovulated mouse oocytes had well spread metaphase chromosomes after incubation with OA for 2 hours at concentrations of 2 μM (60%) and 5 μM (75%). No microtubules were observed in these cells. In cases when chromosomes were not spread, the peripheral region adjacent to the chromosomes showed diffuse fluorescence for tubulin.

Good quality chromosome spreads suitable for classical cytogenetic analysis (**Fig. 2**) were obtained from *in vivo* ovulated oocytes incubated in OA for 2 h (58.33% of cells treated by 5 μM OA and 56.25% of those treated by 2 μM OA).

The quality of spreads was slightly variable: most of them had well condensed chromosomes but some had chromosomes longer than normal or not well condensed. On average, spreading was better in cells subjected to hypotonic incubation, therefore this protocol was used for most samples.

Actin cap was lacking in cells with well spread chromosomes and actin was distributed uniformly in the cortical cytoplasm. These changes in actin cytoskeleton preceded changes in meiotic spindle and chromatin.

All groups of oocytes treated by OA had intact cell membrane and no vacuoles or cell fragments were observed.

Discussion

Our study provides data about the sequence of effects caused by OA on actin and tubulin cytoskeleton and their relation to chromosome condensation. Treatment by okadaic acid affects the actin cytoskeleton first and causes abnormalities of meiotic spindle depending on the maturation stage of the oocyte. By our opinion, these dramatic cytoskeletal changes make controversial the stimulating effects of OA on oocyte maturation [2] even if reversibility of the treatment is taken into account.

While okadaic acid suitability to improve the outcome of assisted mammalian reproduction is questionable, it has a potential use in cytogenetic analysis by increasing the yield of good metaphase plates from oocytes. In our study, chromosome condensation was achieved for both mature and immature mouse oocytes after treatment by okadaic acid. The main obstacles in mammalian oocyte cytogenetic analysis are the low number of cells for analysis (especially for human oocytes) and the quality of chromo-

some spreads [8]. Increasing the number of analyzable cells could improve both classical and molecular cytogenetic analysis.

The advantage of OA treatment cited in [7] – skipping of hypotonic incubation, was not confirmed by this study. Our previous experience with mammalian oocyte chromosome spreads [3, 4] has shown strain-dependent differences in chromosome clumping. In the present study, spreading of mouse chromosomes fixed for cytogenetics was better when hypotonic incubation was applied during fixation.

The data reported in [1, 7] concerning changes of oocyte membrane or integrity caused by OA were also not supported by our results. Even after oocyte incubation for 2 hours in the highest (5 μM) concentration of OA, cell membrane was intact and no vacuoles or cell fragments were formed.

In conclusion, our study of the effects of okadaic acid treatment on oocyte chromosomes and cytoskeleton showed that this procedure can be used to obtain metaphase plates suitable for karyotyping from both mature and immature oocytes.

Acknowledgements: This work was supported by Grant No 29/2014 of the Counsel of Medical Science in Medical University – Sofia, Bulgaria.

References

1. **Alexandre, H., A. van Cauwenberge, Y. Tsukitani, J. Mulnard.** Pleiotropic effect of okadaic acid on maturing mouse oocytes. – Development, **112**, 1991, 971-980.
2. **Ariu, F., S. Fois, D. Bebbere, S. Ledda. I. Rosati, M. T. Zedda, S. Pau, L. Bogliolo.** The effect of okadaic acid on meiotic maturation of canine oocytes of different size. – Theriogenology, **77**, 2012, 46-52.
3. **Delimitreva, S., M. Markova, R. Zhivkova.** Optimal metaphase plate preparation in mouse oocytes requires specific conditions for spindle disintegration. – Compt. rend. Acad. bulg. Sci., **52**, 1999, 105-108.
4. **Delimitreva, S., R. Zhivkova, E. Isachenko, N. Umland, P. L. Nayudu.** Meiotic abnormalities in in vitro-matured marmoset monkey (*Callithrix jacchus*) oocytes: development of a non-human primate model to investigate causal factors. – Hum. Reprod., **21**, 2006, 240-247.
5. **Rime, H., D. Huchon, C. Jessus, J. Goris, W. Merlevede, R. Ozon.** Characterization of MPF activation by okadaic acid in *Xenopus* oocyte. – Cell. Differ. Dev., **29**, 1990, 47-58.
6. **Valdiglesias, V., M. V. Prego-Faraldo, E. Pásaro, J. Méndez, B. Laffon.** Okadaic acid: more than a diarrheic toxin. – Mar. Drugs, **11**, 2013, 4328-4349.
7. **Verlinsky, Y., S. Evsikov.** Karyotyping of human oocytes by chromosomal analysis of the second polar bodies. – Mol. Hum. Reprod., **5**, 1999, 89-95.
8. **Zhivkova R. S., S. M. Delimitreva, D. I. Toncheva, I. T. Vatev.** Analysis of human unfertilized oocytes and pronuclear zygotes-correlation between chromosome/chromatin status and patient-related factors. – Eur. J. Obstet. Gynecol. Reprod. Biol., **130**, 1, 2007, 73-83.

Corresponding author:
Ralitsa Zhivkova
Department of Biology, Medical Faculty
Medical University of Sofia
1 Sv. Georgi Sofiiski Street, 1431 Sofia
e-mail: rzhivkova@yahoo.com

Institute of Experimental Morphology, Pathology and Anthropology with Museum
Bulgarian Anatomical Society

Acta morphologica et anthropologica, 21
Sofia ● 2015

Expression of Ghrelinpositive Cells in the Stomach of the Rat

S. Hamza[*], I. Vulkova[*], M. Gulubova[**], P. Atanasova[***], D. Sivrev[*]

[*]*Department of Anatomy, Faculty of Medicine, St. Zagora, Bulgaria*
[**]*Department of General and Clinical Pathology, Faculty of Medicine, St. Zagora, Bulgaria*
[***]*Department of Anatomy, Histology and Embryology, University of Medicine, Plovdiv, Bulgaria*

Ghrelin is a relatively new-found hormone. The cells which express ghrelin in the largest amount are in the ventricular fundus. The aim of the study was by immunocytochemical methods to establish the presence of ghrelinpositive cells in the lining of the stomach. Ghrelinpositive cells are visualized in the deeper parts of the lining taken from the area of ventricular fundus. Their amount is greater near the border with the muscle sheath. Individual cells containing granules with ghrelin was found in the superficial parts of the muscular coat and close to the surface of the lining.

Key words: ghrelin, stomach, ghrelinpositive cells, expression.

Introduction

Following the discovery of new hormone ghrelin by Kojima et al. [8] research on it increases every year [9]. Ghrelin is a hunger hormone with gastroprokinetic properties [5] but the factors controlling ghrelin secretion from the stomach are not too elucidated. Malik et al. [10] showed that even in the absence of caloric deficiency, ghrelin may favor food consumption by enhancing the hedonic and incentive responses to food-related cues. Ghrelin also has important effects on gastrointestinal (GI) motility, which may contribute to appetite signaling [5].

Most researchers have focused on the impact of hormones on metabolism, energy balance, the level of blood sugar, gastric emptying etc. [1, 2, 3, 12]. Kojima and Kandala continues his research on the structure and function of the newly hormone [8]. There are many studies on the physiological effects and potential clinical applications of ghrelin but too few are purely theoretical developments on the expression of ghrelinpositive cells in the body [11, 13, 14]. The aim of the study was to establish the expression of ghrelinpositive cells in the lining of the stomach. For the implementation of the objective identified the following main tasks: 1) to visualize any ghrelin productive cells in the fundus by immunocytochemical methods; 2) to determine their localization in the gastric mucosa by light microscopy.

Materials and Methods

We examined the expression of ghrelinpositive cells in mucosa of the rat ventricular fundus by immunohistochemistry. Stomach tissue samples were collected from the fundus region of 3 male mature rats strain Wistar subject to the European Directive 2010/609 for animal welfare and with the permission of the Ethics Committee at the Faculty of Medicine – Stara Zagora.

We applied the "dropping" of ultra-thin (4 μm) sections with antibody Ghrelin (H-40) SC-50 297, produced by Santa Cruz, USA, and visualization ghrelin positive cells – detection system Daco - En Vision FLEX - Mini Kit.

Results

Immunostaining of ghrelin was detected in the deeper parts of the lining taken from the area of ventricular fundus. Immunohistochemistry demonstrated the presence of ghrelin cells near the proper gastric glands. Their amount is greater near the border with the muscle sheath (**Fig. 1**).

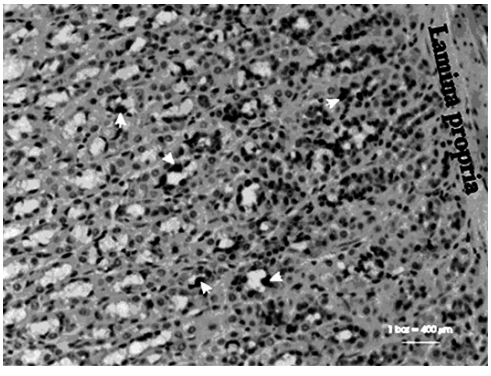

Fig 1. Ghrelinpositive cells near the border with the muscle sheath

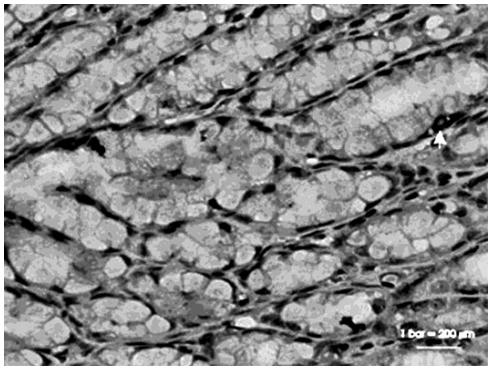

Fig 2. Ghrelinpositive cells near the border with the muscle sheath

A few cells containing ghrelin granules were found in the deep layers of the mucous membrane of the stomach, superficial parts of the muscular tunic and close to the surface of the lining (**Fig. 2**).

Discussion

Ghrelin is a 28-amino acid peptide with an octanoyl modification, which is mainly produced by the "X/A-like" cells of the oxyntic glands of the stomach [8, 9] in response to conditions of negative energy balance.

According to Abbuki et al. [15] the localization of ghrelin cells in the stomach was similar in mice, rats and hamsters. No immunoreactivities were detected in any animals when antiserum absorbed by excessive ghrelin was used [15]. Most authors describe expression of ghrelin positive cells in the deep part of the gastric mucosa, but no reports of the existence of such cells in the muscle layer.

Hayashida et al. [4] investigate ghrelin in domestic animals, its distribution in stomach and a possible role. Jason [6] searches ghrelin in the summer flounder – immunolocalization to the gastric glands and action on plasma cortisol levels. Their reports were similar to our results of the ghrelin cellpositive expression [7].

Conclusions

1. Ghrelin-producing cells are characteristic of the venter and operate basic on digestive system.
2. Greatest amount ghrelinpositive cells found in the gastric mucosa of ventricular fundus.
3. Some cells are visualized in the deep layers of the mucous membrane of the stomach, near the glands, but there are single cells in muscle sheath.

References

1. **Asakawa, A., A. Inui, T. Kaga, H. Yuzuriha, T. Nagata, N. Ueno, S. Makino, M. Fujimiya, A. Niijima, M. Fujino, and M. Kasuga.** Ghrelin is an appetite-stimulatory signal from stomach with structural resemblance to motilin. – Gastroenterology, **120**, 2001, 337-345.
2. **Broglio, F., E. Arvat, A. Benso, C. Gottero, G. Muccioli, M. Papotti, A. van der Lely, R. Deghenghi, E. Ghigo.** Ghrelin, a natural GH secretagogue produced by the stomach, induces hyperglycemia and reduces insulin secretion in humans. – J. Clin. Endocrinol. Metab., **86**, 2001, 5083-5086.
3. **Dornoville, C., E. Lindström, P. Norlén, R. Håkanson.** Ghrelin stimulates gastric emptying but is without effect on acid secretion and gastric endocrine cells. – Regul. Pept., **120**, 2004, 23-32.
4. **Hayashida, T., K. Murakami, K. Mogi, M. Nishihara, M. Nakazato, M. S. Mondal, Y. Horii, M. Kojima, K. Kangawa, N. Murakami.** Ghrelin in domestic animals: distribution in stomach and its possible role. – Domest. Anim. Endocrinol., **21**, 2001, 17-24.
5. **Janssen, S., J. Laermans, P. Verhulst, T. Thijs, J. Tack, I. Depoortere.** Bitter taste receptors and α-gustducin regulate the secretion of ghrelin with functional effects on food intake and gastric emptying. – PNAS, **108**(5), 2011, 2099.
6. **Jason, P., A. Philip, J. Specker.** Ghrelin in the summer flounder: Immunolocalization to the gastric glands and action on plasma cortisol levels. – Comparative Biochemistry and Physiology: Part A. – Molecular & Integrative Physiology, 152, 2009, 268-272.
7. **Kaya, H., I. Sakata, K. Yamamoto, A. Koda, T. Sakai, K. Kangawa, S. Kikuyama.** Identification of immunoreactive plasma and stomach ghrelin, and expression of stomach ghrelin mRNA in the bullfrog, Rana catesbeiana. – General and Comparative Endocrinology, **148**, 2006, 236-244.
8. **Kojima, M., H. Hosoda, Y. Date, M. Nakazato, H. Matsuo, K. Kangawa.** Ghrelin is a growth-hormone-releasing acylated peptide from stomach. – Nature, **402**, 1999, 656–660.
9. **Kojima, M., K. Kangawa.** Ghrelin: structure and function. – Physiol. Rev., **85**, 2005, 495-522.
10. **Malik, S., F. McGlone, D. Bedrossian, A. Dagher.** Ghrelin modulates brain activity in areas that control appetitive behavior. – Cell. Metab., **7**, 2008, 400-409.
11. **Matsubara, M., I. Sakata, R. Wada, M. Yamazaki, K. Inoue, T. Sakai.** Estrogen modulates ghrelin expression in the female rat stomach. – Peptides, **25,** 2004, 289–297.
12. **Sakata, I., J. Yang, C. Lee, S. Osborne-Lawrence, S. Rovinsky, J. Elmquist, J. Zigman.** Colocalization of ghrelin O-acyltransferase and ghrelin in gastric mucosal cells. – Am. J. Physiol. Endocrinol. Metab., **297**, 2009, 134-141.
13. **Sakata, I., K. Nakamura, M. Yamazaki, M. Matsubara, Y. Hayashi, K. Kangawa, T. Sakata, I., T. Tanaka, M. Matsubara, M. Yamazaki, S. Tani, Y. Hayashi, K. Kangawa, T. Sakai.** Postnatal changes in ghrelin mRNA expression and in ghrelin-producing cells in the rat stomach. – J. Endocrinol., **174**, 2002, 463-471.
14. **Sakata, I., T. Mori, H. Kaiya, M. Yamazaki, K. Kangawa, K. Inoue, T. Sakai.** Localization of Ghrelin-Producing Cells in the Stomach of the Rainbow Trout (Oncorhynchus mykiss). – Zoological Science, **21**(7), 2004, 757-762.

15. **Yabuki, A., T. Ojima, M. Kojima, Y. Nishi, H. Mifune, M. Matsumoto, R. Kamimura, T. Masuyama, S. Suzuki.** Characterization and species differences in gastric ghrelin cells from mice, rats and hamsters. – J. Anat., **205**, 2004, 239-246.

Address for correspondence
Sevinch Hamza
Department of Anatomy
Faculty of Medicine
11 Armeyska Str.
6000 Stara Zagora
Bulgaria
e-mail: dsivrev@abv.bg

Institute of Experimental Morphology, Pathology and Anthropology with Museum
Bulgarian Anatomical Society

Acta morphologica et anthropologica, 21
Sofia ● 2015

Model Systems and Approaches to Study the Metabolism of Alzheimer's Amyloid Precursor Protein

L. Kirazov[*], E. Kirazov[*], C. Naydenov[**], V. Mitev[**]

[*]Institute of Experimental Morphology, Pathology and Anthropology with Museum, Bulgarian Academy of Sciences, Acad. G. Bonchev Str. Bl. 25, 1113 Sofia, Bulgaria
[**]Department of Chemistry and Biochemistry, Medical University, Sofia, 2 Zdrave Str., 1431 Sofia, Bulgaria

It is believed that amyloid precursor protein has a central role in the etiology of Alzheimer's disease, because of the β amyloid peptide contained in its structure. Here we present different methods employed to study the metabolism of APP, such as the use of native brain slices, isolated synaptosomal fractions, specific cholinergic immunotoxins, transgenic animals and monitoring the expression of amyloid precursor protein during ontogenesis.

Key words: Alzheimer's disease, APP, Aβ, animal models, ontogenesis.

Introduction

Alzheimer's disease is the most common degenerative disease of the human brain. The major risk factor in this disease is age and the incidence of the disease increases and reaches 50% in people older than 85 years. By the constant change of the demographic structure of the society toward the older group of people the number and percentage of sufferers is increasing steadily and Alzheimer's disease (AD) is becoming a serious social and economic problem.

Alois Alzheimer first described in 1906 the morphological changes in the brain characteristics for this type of dementia – degeneration of cortical neurons, extracellular neuritic plaques and intracellular neurofibrillary tangles. Neurofibrillary tangles are constituted of the abnormally phosphorylated cytoskeletal τ-protein that participates in the formation of the cytoskeleton and the core of senile plaques is composed of aggregated amyloid β peptide (Aβ).

Some 80 years later, it was clarified that Aβ is part of a larger protein – the amyloid precursor protein (APP). APP is an integral membrane glycoprotein and consists of a large extracellular portion, a transmembrane portion and a short intracellular carboxy-terminal portion. It contains the amino acid sequence of Aβ, which has 39 to 43 amino acids.

The main route of degradation of APP in a healthy brain is via an enzyme called α-secretase, which cuts within the sequence of Aβ and thus makes impossible its aggregation to form the core of senile plaques. There are alternative ways of degradation, which are much less active. There are the β- and γ-secretases that cut at the amino, respectively at the carboxy terminus of Aβ. In sufferers of AD the balance between these enzymes is impaired and β- and γ-secretase activities are increased. As a result Aβ remains intact and can be aggregated as the core of senile plaques.

Therefore, the mechanisms which regulate the processing of APP are of particular interest, since an error in the cascades that regulate, respectively modulate its secretion could lead to a change in the balance between these enzymes.

Materials and Methods

Studies on the processing of APP are preferably carried out on cell cultures, which are often transfected. This method has its drawbacks. Cell cultures do not always reproduce exactly the processes in the brain tissue. Various cell types and various culturing conditions may affect the manner of processing of APP.

We established a relatively easy model to study the secretion of APP in native brain slices, i.e. under conditions much closer to those in the intact brain tissue [3].

For this purpose cortex of rat brain was dissected and cut on a McIlwain tissue chopper in 300 μm thick slices. They were washed in Krebs-Ringer solution at 37ºC, pH 7.4, in a cell culture incubator (O_2/CO_2 = 95%/5%) with repeated change of buffer. The dynamics of release of APP in the incubation medium showed that during the first 15-20 min there is a rapid increase, then it decreases and reaches a constant value after 45-60 min. For this reason we chose an equilibration time of 1h. Then, 3 slices were transferred to 250 μl Krebs-Ringer solution containing an appropriate agent, resp. Krebs-Ringer solution without additives as a control, and were incubated for 30 min.

Incubation was terminated by centrifugation whereby the slices were pelleted and the incubation medium was collected and lyophilized to concentrate the contained protein and the lyophilisates were prepared for immunoblotting.

Our first task was to prove that in the incubation medium there are only secreted forms of APP, i.e. cut from the C-terminal end. The group of Prof. Konrad Beyreuther from Heidelberg University provided us with polyclonal antibodies recognizing the C- and N-ends of APP and with them we performed immunoprecipitation once in the incubation medium and once in the slices and investigated the precipitants. We were able to demonstrate that in the incubation medium there are only secreted forms of APP truncated at the C-terminus.

Results and Discussion

It is reported that many transmitter systems are affected in AD. The most studied one is the cholinergic system and the different types of cholinergic receptors. In patients with AD a hypofunction of the glutamate neurotransmitter system was also observed. We performed a series of experiments to establish whether glutamate is modulating the secretion of APP, using the model of native brain slices.

The stimulation with different concentrations of glutamate showed glutamate influences the secretion of APP in a concentration dependent manner (**Fig. 1**). It could be expected that, upon reaching the most effective glutamate concentration (50 μM) a plateau would be reached. The reduction of the secretion at higher concentrations

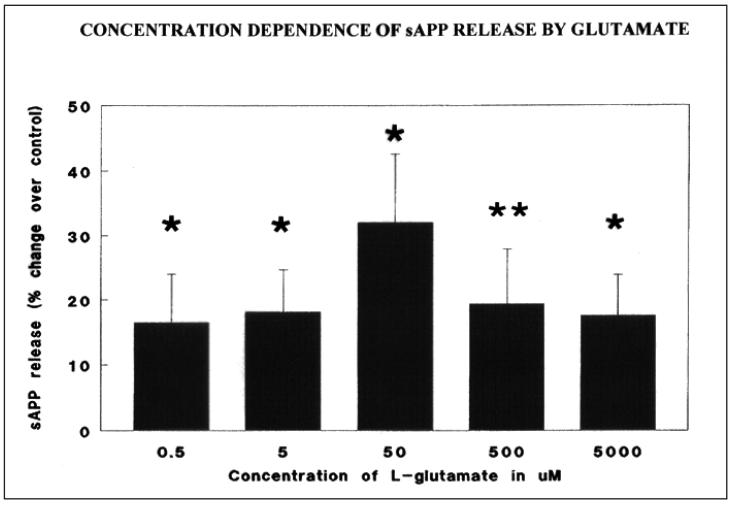

Fig. 1. Quantification of the effect of various concentrations of glutamate on the release of secretory forms of APP

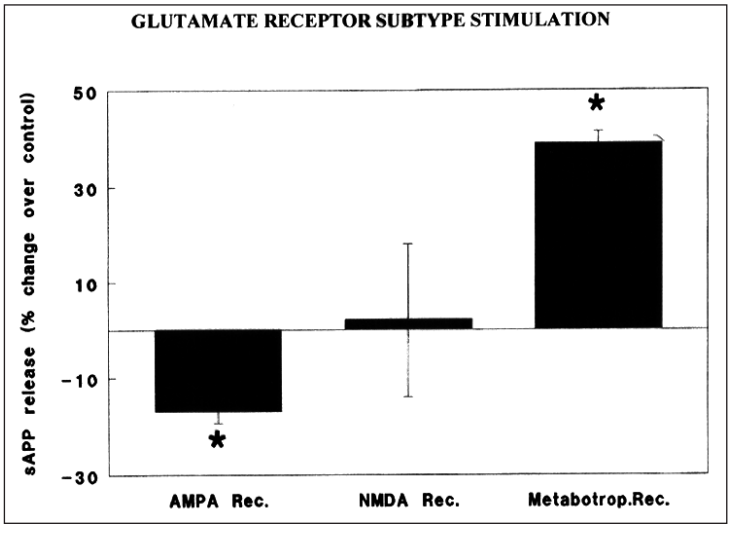

Fig. 2. Effect of the stimulation of different glutamate receptors on the APP secretion

could mean that at different concentrations, different subtypes of glutamate receptors are affected. To clarify this, in the next series of experiments we stimulated different glutamate receptors with their agonists.

Stimulating the AMPA-receptor results in a decrease of the secretion of APP, the stimulation of the NMDA-receptor had no effect, and the stimulation of the metabotropic Glu-receptor lead to increased secretion (**Fig. 2**). These findings can explain the biphasic character of the glutamate concentration dependence of APP release.

The data for neurotransmitter control of APP secretion directed us to choose isolated synaptosomes as the next model system for its study [5]. Synaptosomes were isolated from rat forebrain by homogenizing the tissue and separation of the homogenate

in subcellular fractions by density gradient centrifugation. Aliquots of the synaptosomal fraction were stimulated with different glutamate concentrations (**Fig. 3**).

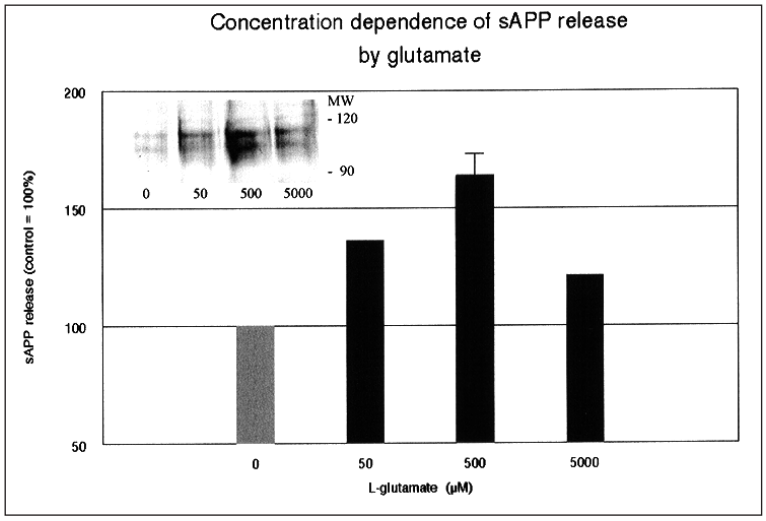

Fig. 3. Stimulation of sAPP release in synaptosomal fractions by different glutamate concentrations

Compared to the stimulation of native brain slices we observed a two-fold increase of the secretion. The weaker effect of glutamate on the slices may be due to the complex relationships between various cell populations; to the more difficult penetration of glutamate in the tissue; to difficulties of detecting of the APP metabolites because of their internalization into cell populations or to binding to the extracellular matrix.

Protein kinase C (PKC) participates in the metabotropic glutamate receptor cascade. In cell culture studies it has been shown that stimulation of other neurotransmitter receptors, which interact with PKC, leads to an increase in the secretion of APP. Direct stimulation of PKC brings about the same result. Therefore, we performed a direct stimulation of PKC with phorbol ester in the synaptosomal fraction.

It can be seen that direct stimulation of PKC has a stronger stimulating effect on the secretion than glutamate (**Fig. 4**). This is probably due to the fact that only part of the synaptosomal population possesses receptors responsive to stimulation by glutamate, and a larger portion are more responsive to stimulation with PKC.

These studies show that native synaptosomes and brain slices are suitable models for studying the secretion of APP, as well as the role of the different types of receptors in this process.

The model with brain slices was also used to study the effects of the vascular endothelial growth factor (VEGF) on the metabolism of APP [1]. For this purpose we used transgenic mice (Tg2576) containing human APP, carrying the double mutation of the so-called Swedish type. The mutation was named so because it was found in a large family in Sweden, where an early development of AD was observed. The children have a 50% chance to develop AD and to lose their memory about their 50th anniversary. The discovery of this family type mutation is of great importance to the study of AD, because mice transfected with this mutation develop with age morphological and behavioral changes corresponding to those of AD (plaques, memory loss) and therefore are a good animal model of the disease.

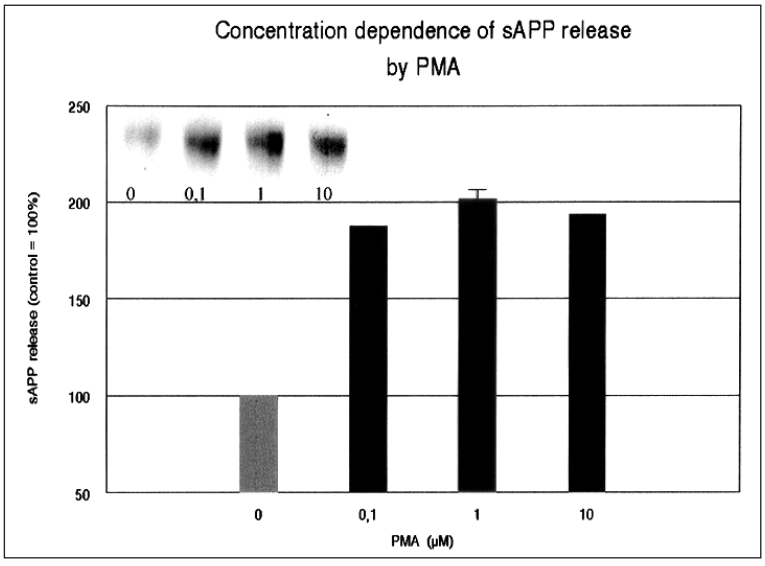

Fig. 4. Stimulation of sAPP release in synaptosomal fractions by different phorbol-12-miristrate-13-acetate (PMA) concentrations

Brain slices were prepared from 17-month-old animals, incubated with VEGF and the secretion of APP, Aβ formation and activity of α- and β-secretases were examined.

The results give reason to believe that VEGF is involved in the processing of Aβ – at least *in vitro*.

We established a further model system in which we used the properties of the immunotoxin 192IgG-Saporin, which consists of a monoclonal antibody against the low-affinity nerve growth factor receptor (LNGF-R), and is conjugated with the ribosome inactivating protein Saporin. The specific location of the LNGF-R on cell bodies and synaptic terminals of cholinergic neurons in the basal forebrain allows to deliver 192IgG-Saporin to that cholinergic population by an intracerebroventricular injection, without affecting cholinergic populations in other areas of the brain and non-cholinergic neurons in the basal forebrain.

The modulation of APP processing by cholinergic activity is shown in several cell cultures, transfected cell lines as well as in native brain slices, but a demonstration of receptor mediated control of APP metabolism under *in vivo* conditions is lacking. To achieve this we specifically reduced cortical cholinergic innervation in rats by partial immunolesion with 192IgG-Saporin. Subsequently the cholinergic function in lesioned rats was restored by transplantation of NGF-producing fibroblasts [6].

The total APP fraction in the cortex was not affected by this deinervation, but there was a marked reduction in the secreted APP-form accompanied by an increase in membrane-bound APP. These changes were reversible with transplantation of NGF-producing fibroblasts.

This in vivo model shows that the processing of APP in the cortex is under cholinergic control from the basal forebrain.

The same type of transgenic mice (Tg2575) were used for the creation of another animal model of AD. The cholinergic immunotoxin mu p-75-Saporin was injected in the 3rd ventricle of 6- to 8-month-old Tg2575 mice to cause cholinergic denervation. Four weeks later there was a 14-fold increase in soluble Aβ1-42 (the most active form in AD) [2].

The lesion leads to atrophy of the hippocampus and to reduction of the expression of synaptophysin, which indicates the degeneration of synaptic contacts – a feature of AD.

The cholinergic agonist carbachol counteracts these effects, indicating that the use of drugs supporting cholinergic transmission (cholinomimetics) must be taken into account in the treatment of AD.

The hippocampus (Hp) is innervated by cholinergic neurons in the basal forebrain and the disruption of their function, respectively of the cholinergic innervation of the Hp and the cerebral cortex is considered to be one of the causes of AD.

This animal model encompasses both the amyloid pathology, characteristic of Tg2575 mice, and the atrophy of the Hp, combined with synaptic dysfunction, which are also characteristic for AD. This makes the model an exceptionally suitable system for studying the etiology of AD.

Recently in a joint work with colleagues from the Paul Flechsig Institute for Brain Research, Leipzig, we conducted research on the role of the Smad family of proteins in AD (results not published). Smad proteins are transcription factors which also control the expression of APP. We used three types of transgenic animals – with increased expression of wild-type APP; with Swedish mutation; and triple transgenic: with Swedish mutation, mutation of τ-protein leading to another prominent morphological change in the brain – neurofibrillary tangles, and mutation of presenilin, which is part of the γ-secretase. A mutation in the presenilin-genes in familial forms of AD is found and it is believed that it results in increased formation of Aβ.

To get more information on the physiological role of APP, we studied the changes in the expression of APP in ontogeny [4]. The data of APP content in brain homogenate from embryonic day 20 to day 400 after birth are presented on the next figure. There is an increase during the period around the peak of synaptogenesis (**Fig. 5**).

We also examined the content of APP in isolated growth cones and synaptosomes (**Fig. 6**).

The pronounced increase of the concentration of APP in homogenate, growth cones and synaptosomes during the most intense establishment of cell contacts un-

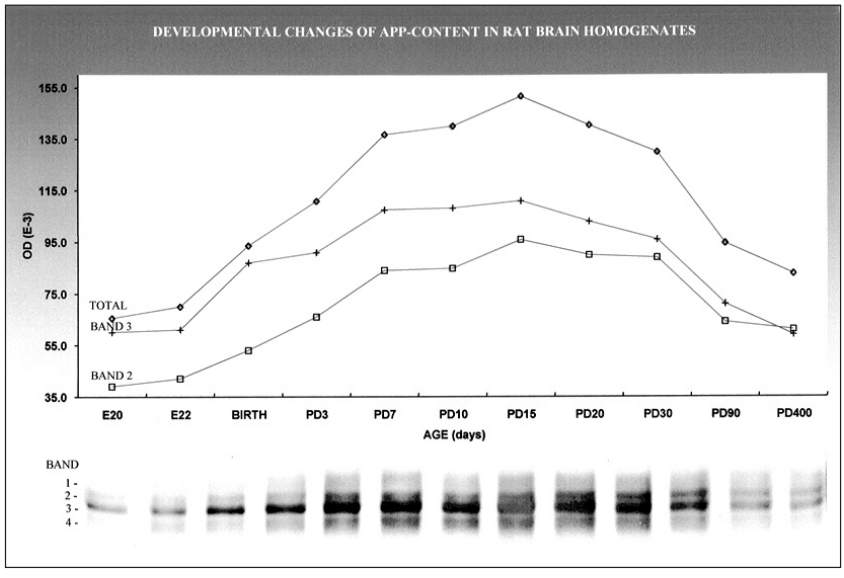

Fig. 5. Changes in APP content in rat forebrain during pre- and postnatal development

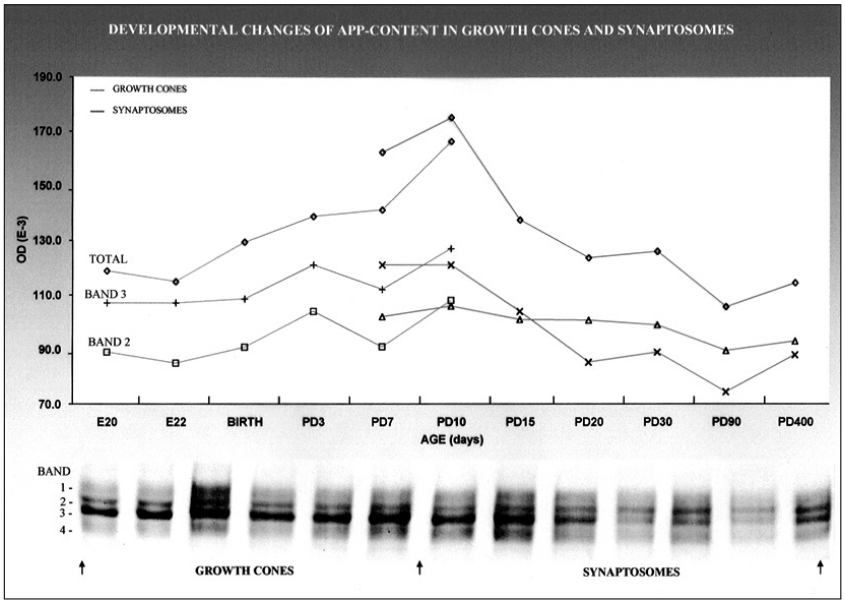

Fig. 6. Changes in APP content in growth cones and synaptosomes isolated from rat forebrain

derlines the importance of APP for the processes of synaptogenesis. APP is probably actively involved in finding the path from growth cones, the establishment of synaptic contacts and the maintenance of normal synaptic functions.

References

1. **Buerger, S., M. Noack, L. Kirazov, E. Kirazov, C. Naydenov, E. Kouznetsova, Y. Yafai, R. Schliebs.** Vascular endothelial growth factor (VEGF) affects processing of amyloid precursor protein and β-amyloidogenesis in brain slice cultures derived from transgenic Tg2576 mouse brain. – Int. J. Devl. Neurosci., **27**, 2009, 517-523.
2. **Gil-Bea, F. J., G. Gerenu, B. Aisa, L. P. Kirazov, R. Schliebs, M. J. Ramirez.** Cholinergic denervation exarbates amyloid pathology and induces hippocampal atrophy in Tg2576 mice. – Neurobiology of Disease, **48**(3), 2012, 439-446.
3. **Kirazov, L., T. Loeffler, R. Schliebs, V. Bigl.** Glutamate-stimulated secretion of amyloid precursor protein from cortical rat brain slices. – Neurochem. Int., **30**, 1997, 557-563.
4. **Kirazov, E., L. Kirazov, V. Bigl, R. Schliebs.** Ontogenetic changes in protein level of amyloid precursor protein (APP) in growth cones and synaptosomes from rat brain and prenatal expression pattern of APP mRNA isoforms in developing rat embryo. – Int. J. Devl. Neurosci., **19**, 2001, 287-296.
5. **Kirazov, L., E. Kirazov, R. Schliebs.** L-Glutamate and phorbol ester stimulate the release of secretory amyloid precursor protein from rat cortical synaptosomes. – Acta Biol. Hung., **56**(3-4), 2005, 177-183.
6. **Rossner, S., U. Ueberham, J. Yu, L. Kirazov, R. Schliebs, J. R. Perez-Polo, V. Bigl.** In vivo regulation of amyloid precursor protein secretion by cholinergic activity. – Eur. J. Neurosci., **9**, 1997, 2125-2134.

Corresponding author
e-mail: lkirazov@yahoo.com

Institute of Experimental Morphology, Pathology and Anthropology with Museum
Bulgarian Anatomical Society

Acta morphologica et anthropologica, 21
Sofia ● 2015

Serum IgG Antibodies to GM1, GM3 and GD1a Gangliosides in Patients with Relapsing Remitting Multiple Sclerosis under Treatment with Interferon, Copaxone and Laquinimod – Preliminary Data

V. Kolyovska, D. Maslarov[*], I. Dokova[**], S. Todorov, I. Iliev, S. Engibarov[***], R. Eneva[***]

Institute of Experimental Morphology, Pathology and Anthropology with Museum, Bulgarian Academy of Sciences, Sofia 1113 Acad. G. Bonchev Str., Bl. 25
[*] Medical University of Sofia, Neurology Clinic, First MHAT – Sofia
[**] Multiprofile hospital for active treatment in neurology and psychiatry "St. Naum", Accredited university hospital, Sofia
[***] The Stephan Angeloff Institute of Microbiology, Bulgarian Academy of Sciences, Sofia 1113, Acad. G. Bonchev Str., Bl. 26

Multiple sclerosis (MS) is an inflammatory disease in which the myelin sheaths around the axons of brain and spinal cord's neurons are damaged by autoantibodies, resulting in demyelination and scarring. Our previous studies have shown that the amount of ganglioside in the brain may serve as a hallmark for the disease. Serum IgG anti-GM1 antibodies are associated as potential biomarkers for the diagnosis of demyelination. Serum IgG anti-GM3 antibodies may be accepted as biomarker for BBB integrity. Autoantibodies against gangliosides GD1a are associated with acute motor axonal neuropathy and acute motor-sensory axonal neuropathy. Interferons (INFs) and Glatiramer acetate (Copaxone) are immunomodulators. Laquinimod is a new experimental immunomodulator investigated as an oral treatment for MS.

Key words: multiple sclerosis treatment, serum IgG anti-ganglioside antibodies, Interferon, Copaxone, Laquinimod.

Introduction

Multiple sclerosis (MS) is a chronic inflammatory disorder of the central nervous system (CNS), traditionally considered to be an autoimmune, demyelinating, inflammatory and neurodegenerative disease. The initial MS therapeutic strategies were directed at immune modulation and inflammation control. Disease-modifying drugs (DMDs) require long-term, regular injection or monthly parenteral infusions, which may impact the patient's compliance. The aim is to prevent demyelination and to reduce axonal loss. During the different MS phases patients use various drugs: in attacks – Corticosteroids; immunomodulators -Interferon beta-1a, Interferon beta-1b (INFs) and Glatiramer ace-

tate (Copaxone). Five oral therapies are in Phase III clinical trial development or have recently been approved for the treatment of relapsing-remitting MS. One of them is Laquinimod (ABR-215062), (ALLEGRO and BRAVO clinical studies). For evaluating the level of gangliosides in the brain, the titer of antibodies against them may be used, as they are produced due to long excess release of CNS, in case of damage of the integrity of the blood brain barrier (BBB).

Interferons (IFNs, scarce and expensive until 1980**)** are proteins made and released by host cells in response to the presence of pathogens such as viruses, bacteria, parasites or tumor cells. IFNs also activate immune cells, such as natural killer cells and macrophages; they increase host defenses by up-regulating antigen presentation by virtue of increasing the expression of major histocompatibility complex (MHC) antigens. They allow the communication between cells to trigger the protective defenses of the immune system that eradicate pathogens or tumors.

Glatiramer acetate (licensed in 1996) is an immunomodulator drug currently used to treat multiple sclerosis. It is a random polymer of four amino acids found in myelin basic protein, namely glutamic acid, lysine, alanine, and tyrosine, and may work as a decoy for the immune system. Glatiramer acetate is approved by the Food and Drug Administration (FDA) for reducing the frequency of relapses, but not for reducing the progression of disability. Glatiramer acetate has also been shown to limit the formation of new MS-related lesions in the CNS and to reduce brain atrophy.

Laquinimod is an experimental immunomodulator developed by Active Biotech and Teva. It is being investigated as an oral treatment for multiple sclerosis. Laquinimod has a high level of oral bioavailability, a small distribution volume, and a low rate of total clearance. Laquinimod is an orally administered quinoline-3-carboxamide small-molecule derivative of the parent compound, the immunomodulator linomide. In preclinical studies, evidence has accumulated suggesting that laquinimod may exhibit immunomodulatory and potentially neuroprotective properties [8]. The molar mass of laquinimod is 356.803 g/mol. As a small molecule, Laquinimod diffuses freely across the BBB without any known active transport by extra- or intracellular receptor [2]. The last studies provide evidence of the broad impact that laquinimod has on brain tissue damage [3, 9].

Materials and Methods

The MS patient's sera were provided from Multiprofile hospital for active treatment in neurology and psychiatry "St. Naum"– Sofia and from Neurology Clinic, First MHAT –Sofia. After informed consent seven patients from each group were tested. The titers of serum IgG anti-GM1, anti-GM3 and anti-GD1a antibodies were estimated by the enzyme-linked immunosorbent assay (ELISA). The results were accounted on the ELISA reader TECAN TM, Sunrise, Austria. We conclude that high serum titers IgG anti-GM3 antibodies correspond with a presence of BBB integrity damage [12]. The neurodegeneration may be presented with numerical values of the serum IgG titers of anti-GD1a antibodies but high titers IgG anti-GM1 antibodies correspond with a presence of demyelination [1, 4, 7, 10, 11].

ELISA Protocol

We made slight modifications of the Mizutamari method [5]. Briefly, 1000 ng of GD1a (or GM1 or GM3) ganglioside in 100 ml of methanol were pipetted into microtitre plate wells. After air drying, the wells were blocked with BSA-PBS (1% bovine serum

albumin in phosphate-buffered saline) for 1 h. After sixfold washing with PBS, 100 μl of sera, diluted 1:20 to 1:5000 in BSA-PBS, were added to each well and incubated overnight. After that the plates were washed sixfold thoroughly with PBS. Binding was detected following a 2 h incubation period with BSA-PBS diluted (1/3200) peroxidase-conjugated goat anti-human IgG antibodies and with BSA-PBS diluted (1/4800) peroxidase conjugated goat anti-human IgM antibodies. All the incubation steps were performed at 4 °C. After sixfold washing with PBS, color development was achieved in a substrate solution containing 15 mM O-phenilendiamine and 0.015% H_2O_2 in 0.1 M sodium acetate buffer, pH 5.0 at room temperature. The reaction was stopped after 30 min by addition of 50 μl of 1N H_2SO_4 and the optical density (OD) was measured and read spectrometrically at 490 nm in a ELISA reader (TECAN, Sunrise TM, Austria). Non specific antibody binding (OD value in a well not containing GD1a) was subtracted for each measurement. Adult patients were considered strongly positive only if the mean OD of their sera exceeded $x \pm 2$ SD (standard deviation) of the healthy controls. Determinations were carried out in duplicate [6, 10].

Results and Conclusions

The aim of the treatment is to prevent demyelination and to reduce axonal loss. Interferons are reliable and accessible drug, with good perspective for the course of the disease. All investigated medicines are shown for long-term treatment and should not be interrupted. The levels of the serum IgG anti-GD1a antibodies titers in two groups Interferons and Glatiramer acetate patients are different, but showing Interferons and Glatiramer acetate demonstrate to an equal extent, partial influence on demyelination, BBB integrity and neurodegeneration the preliminary results of this study at this stage demonstrates significantly elevated serum IgG anti-GM1 titers in Laquinimod treated patients. This implicates the presence of demyelination. On the other hand, the low titers of other antibodies demonstrate that in the Laquinimod treated patients we have full BBB integrity and indications for lack of neuronal damage. It can be concluded that Laquinimod has a neuroprotective action, although the treatment does not lead to remyelination, hence combined therapy is proposed to affect all the damages. The serum IgG titers of anti-GM1, anti-GM3 and anti-GD1a antibodies demonstrates all investigated medicines are not 100% effective in all patients. Unfortunately in some patients relapses can occur, despite the continuous treatment with a suitable medicine. The presented results are preliminaries, further researches with bigger number of patients need to be conducted to confirm the findings.

References

1. **Brettschneider J, A. Petzold, A. Junker, H. Tumani.** Axonal damage markers in the cerebrospinal fluid of patients with clinically isolated syndrome improve predicting conversion to definite multiple sclerosis. – Mult. Scler., **12**(2), 2006, 143-148.
2. **Brück, W., C. Wegner.** Insight into the mechanism of laquinimod action. – J. Neurol. Sci., **306**, 2011, 173-179.
3. **Hughes, S.** Laquinimod in MS: Latest safety data 'reassuring'. The latest data from long-term follow-up of patients receiving laquinimod. – BOSTON, Nerventra, Teva Pharmaceutical Industries Ltd/Active Biotech, 2014
4. **Kolyovska, V., D. Deleva.** Serum IgG and IgM antibodies to GD1a ganglioside in adults – preliminary data. – Acta morphol. et anthropol., **19**, 2012, 114-117.

5. **Mizutamari, R., H. Wiegandt, G. Nores.** Characterization of antiganglioside antibodies present in normal human plasma. – J. Neuroimmunol., **50**(2), 1994, 215-220.
6. **Ravindranath, M., S. Muthugounder.** Human antiganglioside autoantobodies: validation of ELISA. – Ann. N. Y. Acad. Sci., **1050**, 2005, 229-242.
7. **Susuki, K., N. Yuki, D. P. Schafer, K. Hirata, G. Zhang, K. Funakoshi, M. Rasband.** Dysfunction of nodes of Ranvier: a mechanism for anti-ganglioside antibody-mediated neuropathies. – Exp. Neurol., **233**(1), 2012, 534-542.
8. **Thöne, J., R. Gold.** Review of laquinimod and its therapeutic potential in multiple sclerosis. **–** Expert. Opin. Pharmacother, **14**(18), 2013, 2545-2552.
9. **Tur, C.** Oral laquinimod for multiple sclerosis: beyond the anti-inflammatory effect. **–** J. Neurol. Neurosurg. Psychiatry, **85**(8), 2014, 833.
10. **Uncini, A.** A common mechanism and a new categorization for anti-ganglioside antibody-mediated neuropathies. – Exp. Neurol., **235**(2), 2012, 513-516.
11. **Zaprianova, E., K. Majtenyi, D. Deleva, O. Mikova, A. Filchev, B. Sultanov, V. Kolyovska, E. Sultanov, L. Christova, X. Kmetska and D. Georgiev.** Serum IgG and IgM ganglioside GM1 antibodies in patients with multiple sclerosis. – Clin. Neurosci., **57,** 2004, 94-99.
12. **Zaprianova, E., D. Deleva, B. Sultanov, V. Kolyovska.** Serum ganglioside GM3 changes in patients with early multiple sclerosis. – Acta morphol. et anthropol., **15,** 2010, 16-18.

Institute of Experimental Morphology, Pathology and Anthropology with Museum
Bulgarian Anatomical Society

Acta morphologica et anthropologica, 21
Sofia ● 2015

Neurodegenerative Changes in Aging Rats

V. Kolyovska, V. Ormandzhieva, D. Deleva, I. Iliev, S. Engibarov[*]*, R. Eneva*[*]

Department of Experimental Morphology, Institute of Experimental Morphology, Pathology and Anthropology with Museum, BAS, Sofia 1113, Acad. G. Bonchev Str., Bl. 25
[*] *The Stephan Angeloff Institute of Microbiology, BAS, Sofia 1113, Acad. G. Bonchev Str., Bl. 26*

The choroid plexus in the brain ventricles consists of epithelial cells, fenestrated blood vessels, and the stroma, dependent on various physiological conditions. Changes of the rat choroid plexus, characterized by reduction of the capillaries (20%) and atrophy of epithelial cells, are evidence of aging degeneration processes. GD1a gangliosides could be used as biomarkers of the neurodegeneration. Serum IgG anti-GD1a titer was determined in young and aging rats to establish the existence of neurodegeneration process. Serum IgG anti-GM1 titer correlated with demyelination and serum IgG anti-GM3 titer correlated with loss of integrity of the blood brain barrier (BBB). Our morphological and immunological studies demonstrated that changes in the structure of the plexus choroideus, neurodegeneration, demyelination and damage of the integrity of the BBB are available in adult rats.

Key words: aging rats, choroid plexus blood vessels, morphometric analysis, serum IgG anti-ganglioside antibodies, neurodegeneration.

Introduction

The choroid plexuses are specialized highly vascular anatomycal structure which protrude into the lateral ventricle, as well as in the third ventricle and fourth ventricle. As a secretory source of vitamins, peptides and hormones for neurons, the choroid plexus provides substances for brain homeostasis [2].

The auto-antibodies against GD1a gangliosides are associated with acute motor axonal neuropathy and acute motor-sensory axonal neuropathy [8]. Anti-gangliosides complex antibodies may be useful diagnostic and prognostic markers of the demyelination, neurodegeneration and correlated with the loss of integrity of the blood brain barrier (BBB) [3, 4, 9]. Patients with a positive titer of anti-ganglioside antibodies have significant alterations of motor conduction parameters and contribute to the neuropathy [10]. GM1 are the main myelin gangliosides and the high titer of IgG anti-GM1 antibodies is correlated with the demyelination [11]. Serum gangliosides GM3 could be used as biomarkers of BBB destruction [12].

The aim of the present investigation is to establish the changes of the microvasculature and to value the titers of the IgG anti-GD1a, anti-GM1 and anti-GM3 antibodies in aging rats.

Materials and Methods

Wistar rats aged 1, 13, 18, 22 and 32 months (five animals per group) were used in the present study. The animals were fixed by intracardial perfusion, embedded in Durcupan and examined with JEOL JEM 1200EX transmission electron microscope and Light microscope Carl Zeiss Jena (morphometric analysis) and Leica DM5000B. Results are reported as mean values ± SEM and as relative part in %, and statistically analyzed by Student's t-test using statistical package. Differences were regarded as significant at $p < 0.05$.

We made slight modifications of the method of Mizutamari et al. [5]. The serum titers of IgG anti-GD1a, anti-GM1 and anti-GM3 were estimated by the enzyme-linked immunosorbent assay (ELISA) [8]. The results were accounted on the ELISA reader TECAN TM, Sunrise, Austria.

Results

Changes in relative part of the blood vessels divided in four subgroups in young (1 month) and adult rats (13 and 22 months) were analyzed and comprised (**Fig. 1**). Blood vessels with luminal diameter >30 μm have not been found in young rats. This may be related to a large number of the blood vessels with small luminal diameter, i.e. capillaries (85.80%) and blood vessels of 15.5-30.0 μm in diameter (14.20%). Relative part of the capillaries in adult rats (13 and 22 months) was 71.75% and 65.70% respectively.

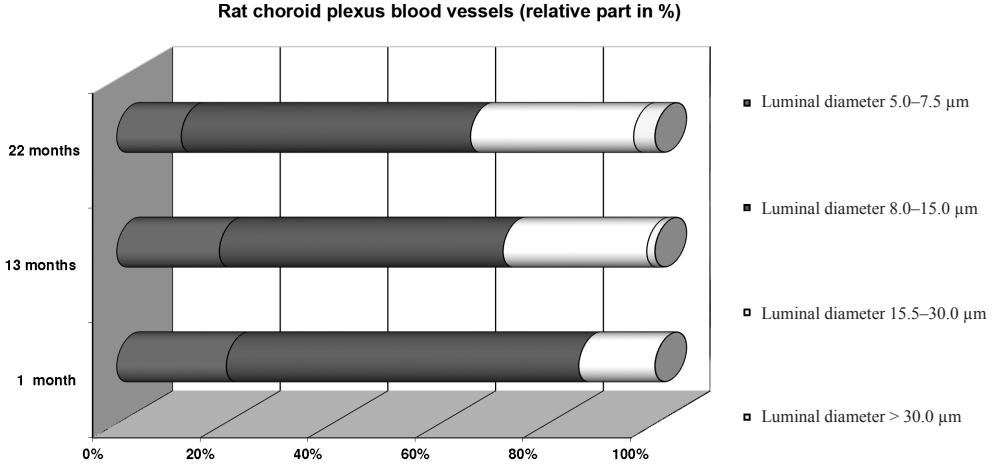

Fig. 1. Comparative analyses of the number (%) of choroid plexus blood vessels in young and adult rats

The surface of the young rat choroid plexus consists of small villi each covered with a single layer of large cuboidal epithelial cells, electron-dense epithelial cytoplasm, well differentiated connective tissue elements and capillary with many fenestrations (**Fig. 2**). In the epithelial cytoplasm of the aging rat choroid plexus were observed many lipid droplets, imbibing mitochondria and dense bodies (13, 22 months).

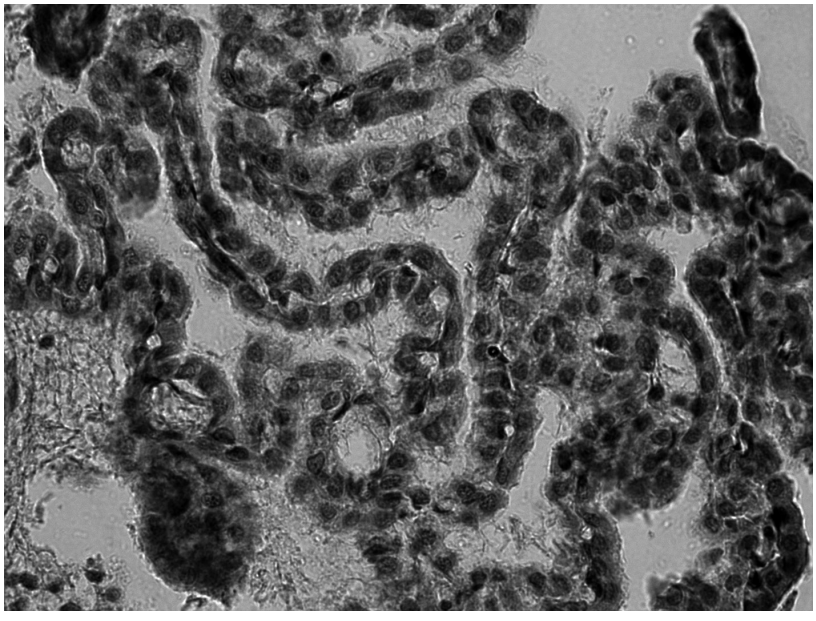

Fig. 2. Choroid plexus in the IV ventricle of the young rat brain. H&E stain, × 40

There was a significant increase in the titers value of the IgG anti-GD1a, anti-GM1 and anti-GM3 only in adults – 32 month rats. These changes began in rats after the 22nd month and are probably related to the beginning of neurodegenerative changes in brain at this age.

Discussion

Normal aging is associated with various metabolic and vascular changes, which are systemic and organ-specific [1]. In the brain, both structure and function are altered with age. In the present study quantitative information has been available regarding the vessels of the brain, in particular, regarding the vessels of the rat choroid plexus. Blood vessels with luminal diameter >30 μm have not been found in young rats. In our previous study the blood vessels with luminal diameter >30 μm were found for the first time in rats aged 2 months [7]. This may be related with a larger number of the blood vessels with small luminal diameter, i.e. capillaries (85.80%) and blood vessels of 15.5-30.0 μm in diameter (14.20%). The capillaries number was reduced by 20% in old rats and this compensatory reaction may be related with structural changes with age. The choroid plexus epithelium constitutes a physical barrier between blood and cerebrospinal fluid (the blood-CSF barrier – BCSFB) by virtue of the complexity of the tight junctions between adjacent epithelial cells. The age-related changes (22-month-old rats) might indicate a gradual change in function or at least a decrease in efficiency of the choroid plexus and may be evidence of slow degeneration of the rat choroid plexus [6,13]. The value of IgG anti-GD1a, anti-GM1 and anti-GM3 titers determined by ELISA technique revealed the presence of the immune-mediated neurodegeneration, concomitant demyelination, growing with age, and impaired integrity of the BBB.

Conclusion

Our morphological and immunological studies demonstrated that in adult rats changes in the structure of the plexus choroideus are present also demyelination, neurodegeneration and damage of the integrity of the BBB are present. The observed changes are evidence of age-related neurodegenerative changes, which are important for the homeostatic regulation of CNS.

Acknowledgement: This study was supported by the project funded by Bulgarian Academy of Sciences, Sofia, Bulgaria. The authors are grateful to L. Voyvodova, M. Pavlova and G. Zaharieva for the technical assistance.

References

1. **Desjardins, M., R. Berti, J. Lefebvre, S. Dubeau, F. Lesage.** Aging-related differences in cerebral capillary blood flow in anesthetized rats. – Neurobiology of Aging**, 35**(8), 2014, 947–1955.
2**. Johanson, C., J. Duncan, P. Klinge, T. Brinker, E. Stopa, G. Silverberg.** Multiplicity of cerebrospinal fluid functions: New challenges in health and disease. – Cerebrospinal Fluid Research, **5**(1), 2008, 10.
3. **Kolyovska, V., D. Deleva.** Serum IgG and IgM antibodies to GD1a ganglioside in adults – preliminary data. – Acta morphol. et anthropol., **19**, 2012, 114-117.
4. **Kusunoki, S.** Immune-mediated neuropathies. Clinical Neurology, **49**(11), 2009, 956-958.
5. **Mizutamari, R., H. Wiegandt, G. Nores.** Characterization of antiganglioside antibodies present in normal human plasma. – J. Neuroimmunol., **50**(2), 1994, 215-220.
6. **Ormandzhieva, V. K.** Rat choroid plexus: morphometric characteristics. – Medical Data, **2**(1), 2010, 9-12.
7. **Ormandzhieva, V. K.** Morphometric parameters of rat choroid plexus blood vessels. – Acta Morphol. Anthropol., **17**, 2011, 56-61.
8. **Ravindranath, M., S. Muthugounder.** Human antiganglioside autoantobodies: validation of ELISA. – Ann. New York Acad. Sci., **1050**, 2005, 229-242.
9. **Susuki, K., N. Yuki, D. Schafer, K. Hirata, G. Zhang, K. Funakoshi, M. Rasband.** Dysfunction of nodes of Ranvier: a mechanism for anti-ganglioside antibody-mediated neuropathies. – Exp. Neurol., **233**(1), 2012, 534-542.
10. **Uncini, A.** A common mechanism and a new categorization for anti-ganglioside antibody-mediated neuropathies. – Exp. Neurol., **235**(2), 2012, 513-516.
11. **Zaprianova, E., K. Majtenyi, D. Deleva, O. Mikova, A. Filchev, B. Sultanov, V. Kolyovska, E. Sultanov, L. Christova, X. Kmetska, D. Georgiev.** Serum IgG and IgM ganglioside GM1 antibodies in patients with multiple sclerosis. – Clin. Neurosci., **57**, 2004, 94-99.
12. **Zaprianova, E., D. Deleva, B. Sultanov, V. Kolyovska.** Serum ganglioside GM3 changes in patients with early multiple sclerosis. – Acta morphol. et anthropol., **15**, 2010, 16-18.
13. **Орманджиева, К. В.** Електронномикроскопски и хистометрични изследвания на plexus choroideus в мозъка на плъх в онтогенеза и при експериментални въздействия. – София: АИ „Проф. Марин Дринов“, 2014.

Institute of Experimental Morphology, Pathology and Anthropology with Museum
Bulgarian Anatomical Society

Acta morphologica et anthropologica, 21
Sofia ● 2015

Thermal Stress-Induced Expression of CB1 Cannabinoid Receptors in the Rat Rostral Pons

N. Lazarov [*], D. Atanasova[**], A. Ivanov[*]

[*] *Department of Anatomy and Histology, Medical University of Sofia, Sofia, Bulgaria*
[**] *Institute of Neurobiology, Bulgarian Academy of Sciences, Sofia, Bulgaria*

Endocannabinoids are a family of biologically active lipids in the brain that mediate the psychoactive effects of cannabis by two distinct receptors, cannabinoid receptor type I (CB1) and type II (CB2). It has been shown that the CB1 is the major cannabinoid receptor in the brain and is highly expressed in areas that are involved in pain modulation. There is also recent evidence that its activation reduces nociceptive processing in acute and chronic animal pain models. In this study, we demonstrate that thermal stress induces the expression of CB1 cannabinoid receptors in certain brainstem regions associated with pain sensation in the rat rostral pons, using light microscopic immunohistochemistry with a subtype-specific antibody. In particular, we were able to reveal that the pontine gray matter, the locus coeruleus, the parabrachial nuclear complex and the pontine raphe nuclei show high levels of CB1 cannabinoid receptors with a possible role in specific brain functions, such as nociception. The present results suggest that in addition to their known expression in excitatory glutamatergic and inhibitory GABAergic neuronal subpopulations, the CB1 receptors are also present in a subset of noradrenergic, cholinergic and serotonergic neurons in the rat rostral pons. It can be inferred that CB1 receptors may have divergent roles in nociceptive processing in a broad brainstem area, depending on the exact neurotransmitter system they modulate.

Key words: cannabinoid receptors, endocannabinoids, locus coeruleus, parabrachial nuclear complex, periventricular gray, pontine raphe nuclei, rat.

Introduction

The endocannabinoid system is a recently discovered neuromodulatory system implicated in a multitude of physiological and pathophysiological functions by influencing the activity of diverse neurotransmitter systems, including GABA, noradrenaline, dopamine, glutamate and acetylcholine [9]. This system consists of endogeneous ligands, i.e. endocannabinoids, the enzymes for their biosynthesis and degradation, and their specific cannabinoid receptors [15, 18].

Endogenous cannabinoids (endocannabinoids) are a group of neuromodulatory lipids that mediate the psychoactive effects of cannabis and participate in a variety of physiological processes including appetite, pain sensation and memory [6]. They exert their physiological actions by at least two G protein-coupled receptors that inhibit adenylate cyclase activity. To date, two receptor subtypes, the cannabinoid receptor type 1

(CB1) and type 2 (CB2), have been described with regard to their primary structure, ligand-binding properties, and signal transduction systems [10, 14].

The CB1 is the major cannabinoid receptor in the brain while CB2 cannabinoid receptors are widely distributed in the peripheral nervous and immune systems [2, 8, 18]. Specifically, CB1 receptors are highly expressed in rat brain areas that are involved in pain modulation, including the periaqueductal gray [20, 22] and the dorsal horn of the spinal cord [7] whereas the brainstem exhibits low levels of CB1 receptor activity [18, 20]. Recent studies have also shown that their activation reduces nociceptive processing in acute and chronic animal pain models [reviewed in 17]. Our study was thus designed to test whether thermal stress induces the expression of CB1 receptors in other brainstem regions associated with pain sensation in the rat brain.

Materials and Methods

The experiments were carried out on adult Wistar rats of both sexes, weighing 250-300 g. The animals were divided into three experimental groups of 3 rats: rats after thermal stress exposure, ones treated with the cannabinoid receptor agonist anandamide, and untreated controls. Thermal stress nociception was induced using the hot plate test as previously described by Bocheva et al. [3]. One group of rats (n = 3) received subcutaneous injections of anandamide (10 mg/kg b.w.) dissolved in physiological saline. All the procedures were performed according to a standard protocol established by the Bioethical Commission of the Biomedical Research at the Institute of Neurobiology of the Bulgarian Academy of Sciences. All efforts were made to minimize the number of animals used and their suffering.

For the immunohistochemical experiments, the rats were deeply anesthetized and transcardially perfused first with 0.05 M phosphate-buffered saline (PBS), pH 7.4, followed by 4% paraformaldehyde (PFA) in 0.01 M phosphate buffer (PB), pH 7.4. The brain was dissected out, sliced at the level of the rostral pons and postfixed in the same fixative overnight at 4ºC. Thereafter, the tissues were embedded in paraffin and cut into 5 μm thick sections. The samples were then deparaffinized with xylene and ethanol, and subsequently processed for avidin-biotin-horseradish peroxidase complex (ABC) immunohistochemistry using an ImmunoCruz™ goat ABC Staining System (Santa Cruz Biotechnology, Inc., Santa Cruz, CA, USA). Briefly, the sections were treated with hydrogen peroxide (1% in absolute methanol; 30 min) to inactivate endogenous peroxidase and the background staining was blocked with 1.5% normal goat serum (NGS) in PBS for 1 hour. Between the separate steps, the sections were rinsed with cold PBS/Triton X-100. Afterwards, they were incubated with a polyclonal goat anti-CB1 receptor antibody (diluted 1:500, Santa Gruz Biotechnology) overnight at 4 °C in a humid chamber, followed by biotinylated donkey anti-goat IgG (Santa Gruz Biotechnology, 1:500) for 2 h at room temperature, and lastly the AB enzyme reagent was applied for 30 min at room temperature. Finally, the peroxidase activity was visualized by 1-3 drops of peroxidase substrate using diaminobenzidine as a chromogen. After the immunoreaction, the sections were dehydrated in ethanols, cleared in xylene and coverslipped with Entellan (Merck, Darmstadt, Germany). The slides were observed and photographed with a Nikon research microscope equipped with a digital camera DXM1200c. The brainstem structures were identified according to the rat brain atlas of Paxinos and Watson [13].

The specificity of the immunostaining was controlled by omission of the primary antiserum from the incubation medium or its replacement with PBS. No immunoreactivity was detected in either case.

Results

The immunohistochemical experiments demonstrated staining for CB1 in the thin layer of cells in the dorsal pontine tegmentum called the central pontine gray. The cell bodies and proximal processes of the neurons were strongly immunostained (**Fig. 1A**), in comparison with these in the untreated control rats. Many intensely stained neurons were also observed in the locus coeruleus and the subcoeruleus nucleus (**Fig. 1B**). In addition, moderately stained neurons were found in the pontine parabrachial nuclear complex, comprising the medial parabrachial nucleus and lateral parabrachial nucleus (**Fig. 1C**). A number of neurons in the raphe nuclei of the pontine reticular formation

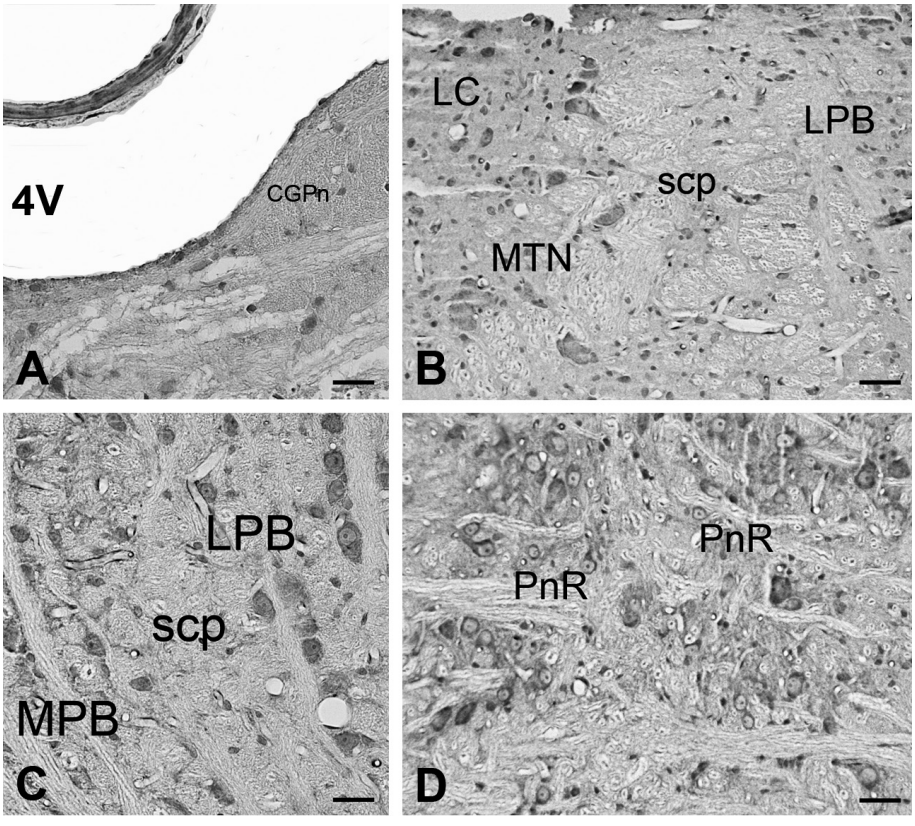

Fig. 1. Expression of CB1 cannabinoid receptors in the rat rostral pons. (**A**) Immunohistochemical staining for CB1 in the central pontine gray (CGPn). Note that both perikarya and proximal processes of cholinergic neurons around the fourth ventricle (4V) are intensely immunostained. (**B**) Low-magnification photomicrograph of the pons demonstrating CB1 immunoreactivity in the locus coeruleus (LC) and adjacent nuclei. The majority of noradrenergic cerulean neurons and their proximal axonal profiles are strongly CB1-immunostained. (**C**) Higher magnification of the parabrachial nuclear complex showing that neurons in both medial parabrachial nucleus (MPB) and lateral parabrachial nucleus (LPB) express CB1 immunoreactivity. (**D**) Serotonergic reticular neurons in the pontine raphe nucleus (PnR) also exhibit strong CB1 immunostaining. MTN, mesencephalic trigeminal nucleus, scp, superior cerebellar peduncle. Scale bars = 200 μm (**A**); 100 μm (**B, D**); 50 μm (**C**).

and, in particular, the pontine raphe nucleus and inferior central nucleus were CB1-immunopositive as well.

Discussion

It is well known that the endocannabinoids bind to type I cannabinoid receptors, located at the presynaptic level, and exert important control upon some neuronal functions by modulating the release of several neurotransmitters [1, 4, 16]. Previous investigations have focused on the distribution of CB1 receptors in rat brainstem regions such as the periaqueductal gray traditionally associated with pain transmission in relation with opioids [22]. It has also been revealed that the CB1 cannabinoid receptors are expressed solely in the gray matter around the fourth ventricle under normal conditions in rats [18, 20]. Here we report the contribution of certain rostral pons-located nuclei and their possible role for pain inhibition by administration of cannabinoids. The present data demonstrate that mild thermal stress induces high expression of CB1 cannabinoid receptors in other rat brainstem regions associated with pain sensation such as the pontine gray matter, locus coeruleus, parabrachial nuclear complex and pontine raphe nuclei.

Furthermore, the presence of CB1 receptors in the rodent brain has been verified in certain glutamatergic, GABAergic, dopaminergic and adrenergic neurons [5, 11, 21] and recently in septohippocampal cholinergic [12] and raphal serotonergic neurons in mice [9]. Our results provide immunohistochemical evidence that CB1 receptors are also present in a subset of noradrenergic, cholinergic and serotonergic neurons in the rat rostral pons. In particular, the central gray of the pons, known as the cholinergic Ch6 cell group, is the site of origin of the descending pain control pathway that relays to the raphe nuclei of the rostral medulla and caudal pons. In turn, the raphe nuclei of the pontine reticular formation, the pontine raphe nucleus and the inferior central nucleus which are serotonin-containing (B5 and B8 cell groups, respectively) are implied in the regulation of anxiety and depression. On the other hand, the locus coeruleus is considered the most important pain-related nucleus in the pons and the major noradrenergic nucleus in brain (cell group A6). It is believed that its activation by noxious stimuli leads to inhibition of perceived pain [19]. Last but not least, our findings also indicate that noradrenergic neurons in the rat pontine parabrachial nuclear complex which usually contain endogenous opioids and their receptors possibly plays important roles in pain modulation via activation of CB1 receptors, thus implying probable functional interactions between cannabinoids and opioids within the complex.

Conclusion

Our data support the existence of an extended brainstem cannabinoid system that possibly has a role relevant for nociception. It can be inferred that CB1 receptors may have divergent functions in nociceptive processing in this broad area, depending on the exact neurotransmitter system they modulate.

References

1. **Alger, B. E.** Retrograde signaling in the regulation of synaptic transmission: focus on endocannabinoids. – Prog. Neurobiol., **68**, 2002, 247-286.
2. **Berdyshev, E. V.** Cannabinoid receptors and the regulation of immune response. – Chem. Phys. Lipids, **108**, 2000, 169-190.

3. **Bocheva, A., H. Nocheva, I. Jlalia, N. Lensen, G. Chaume, T. Brigaud.** Effects of enantiopure (S)-a-trifluoromethyl proline containing MIF-1's analogue on stress-induced analgesia. – Med. Chem., **3**, 2013, 206-209.
4. **Chevaleyre, V., K. A. Takahashi, P. E. Castillo.** Endocannabinoid-mediated synaptic plasticity in the CNS. – Annu. Rev. Neurosci., **29**, 2006, 37-76.
5. **De Novellis, V., L. Mariani, E. Palazzo, D. Vita, I. Marabese, M. Scafuro, F. Rossi, S. Maione.** Periaqueductal grey CB1 cannabinoid and metabotropic glutamate subtype 5 receptors modulate changes in rostral ventromedial medulla neuronal activities induced by subcutaneous formalin in the rat. – Neuroscience, **134**, 2005, 269-281.
6. **Di Marzo, V., D. Melck , T. Bisogno, L. De Petrocellis.** Endocannabinoids: endogenous cannabinoid receptor ligands with neuromodulatory action. – Trends Neurosci., **21**, 1998, 521-528.
7. **Farquhar-Smith, W. P., M. Egertova, E. J. Bradbury, S. B. McMahon, A. S. Rice, M. R. Elphick.** Cannabinoid CB(1) receptor expression in rat spinal cord. – Mol. Cell. Neurosci., **15**, 2000, 510-521.
8. **Gong, J.-P., E. S. Onaivi, H. Ishiguro, Q.-R. Liu, P. A. Tagliaferro, A. Brusco, G. R. Uhl.** Cannabinoid CB2 receptors: Immunohistochemical localization in rat brain. – Brain Res., **1041**, 2006, 10-23.
9. **Häring, M., G. Marsicano, B. Lutz, K. Monory.** Identification of the cannabinoid receptor type 1 in serotonergic cells of raphe nuclei in mice. – Neuroscience, **146**, 2007, 1212-1219.
10. **Howlett, A. C., F. Barth, T. I. Bonner, G. Cabral, P. Casellas, W. A. Devane, C. C. Felder, M. Herkenham, K. Mackie, B. R. Martin, R. Mechoulam, R. G. Pertwee.** International Union of Pharmacology. XXVII. Classification of cannabinoid receptors. Pharmacol. Rev., **54**, 2002, 1161-1202.
11. **Kathmann, M., U. Bauer, E. Schlicker, M. Göthert.** Cannabinoid CB1 receptor-mediated inhibition of NMDA- and kainate-stimulated noradrenaline and dopamine release in the brain. – Naunyn Schmiedebergs Arch. Pharmacol., **359**, 1999, 466-470.
12. **Nyiri G., E. Szabadits, C. Cserep, K. Mackie, R. Shigemoto, T. F. Freund.** GABAB and CB1 cannabinoid receptor expression identifies two types of septal cholinergic neurons. – Eur. J. Neurosci., **21**, 2005, 3034-3042.
13. **Paxinos, G., C. Watson.** The rat brain in stereotaxic coordinates. New York, Academic Press, 1998.
14. **Pertwee R. G.** Cannabinoid receptor ligands. London, Academic Press, 1995.
15. **Salzet, M.** Invertebrate molecular neuroimmune processes. – Brain Res. Rev., **34**, 2000, 69-79.
16. **Schlicker, E., M. Kathmann.** Modulation of transmitter release via presynaptic cannabinoid receptors. – Trends Pharmacol. Sci., 22, 2001, 565-572.
17. **Starowicz, K., N. Malek, B. Przewlocka.** Cannabinoid receptors and pain. – WIREs Membr. Transp. Signal, **2**, 2013, 121-132.
18. **Svíženská, I., P. Dubový, A. Šulcová.** Cannabinoid receptors 1 and 2 (CB1 and CB2), their distribution, ligands and functional involvement in nervous system structures-a short review. – Pharmacol. Biochem. Behav., **90**(4), 2008, 501-511.
19. **Szabadi, E.** Modulation of physiological reflexes by pain: role of the locus coeruleus. – Front. Integr. Neurosci., **6**, 2012, 94.
20. **Tsou, K., S. Brown, M. C. Sañudo-Peña, K. Mackie, J. M. Walker.** Immunohistochemical distribution of cannabinoid CB1 receptors in the rat central nervous system. – Neuroscience, **83**, 1998, 393-411.
21. **Wallmichrath, I., B. Szabo.** Cannabinoids inhibit striatonigral GABAergic neurotransmission in the mouse. – Neuroscience, **113**, 2002, 671-682.
22. **Wilson-Poe, A. R., M. M. Morgan, S. A. Aicher, D. M. Hegarty**. Distribution of CB1 cannabinoid receptors and their relationship with mu-opioid receptors in the rat periaqueductal gray. – Neuroscience, **213**, 2012, 191-200.

Institute of Experimental Morphology, Pathology and Anthropology with Museum
Bulgarian Anatomical Society

Acta morphologica et anthropologica, 21
Sofia ● 2015

Abnormal Maximum in the Current during Isoelectric Focusing and Certain Possibilities to Control and Utilize It

C. L. Naydenov[*], E. P. Kirazov[**], L. P. Kirazov[**], V. I. Mitev[*]

[*]*Department of Chemistry and Biochemistry, Medical University Sofia, 2 Zdrave Str., Sofia 1431, Bulgaria*
[**]*Institute of Experimental Morphology, Pathology and Anthropology with Museum, Bulgarian Academy of Sciences, Acad. G. Bonchev Str., Bl. 25, Sofia 1113, Bulgaria*

Studying the influence of the electrochemical reactions occurring at the electrodes on the attainment of steady state we found that an additional process occurs at the electrodes, causing an abnormal increase of the current. Since the magnitude of the current determines the progress of IEF, knowledge gained from studies on its nature and generation reveals a possibility for this entity to be controlled. We observed that the addition of gelatin into the electrode solutions suppresses the magnitude of the current flowing through the system, which allows the IEF system to approach steady state for a shorter time.

Key words: isoelectric focusing, abnormal current, control of the electric current.

Introduction

Svensson formulated the basic concept of isoelectric focusing, according to which at steady state a dynamic equilibrium between the thermal diffusion and electrophoretic migration in the direction of the isoelectric state is attained, where the amphoteric molecules should remain indefinitely [16, 17, 18]. One of the important considerations in Svensson's theory concerns the electrochemical reactions which take place at the electrodes. The significant feature is that under the influence of the electric field water decomposition commences and the anode naturally becomes acidic, while the cathode naturally becomes alkaline. According to this concept, the continuous production of water ions causes a very steep micro pH gradient only in the near vicinity of the electrodes, which does not spread over the whole carrier matrix. Thus the large part of the gel remains neutral. However, a number of studies have shown that the steady state postulated by the theory is never attained [1, 9]. Furthermore, during IEF the measured pH gradient, created only by the electrode solutions, has a rather different profile along the carrier than that of the carrier ampholytes. These pH gradients, termed "primary", are characterized by a specific dynamics that provokes corresponding changes of the ampholyte pH gradient [7, 8]. These findings prompted us to study more closely the

"background" processes occurring in the electrode solutions, which have a bearing to the current flowing through the electrophoretic system.

Electrode Solutions used in IEF

Non-volatile solutions of acids and bases are used routinely in IEF, as summarized by Righetti [14]. This author does not recommend water as electrode solution. However, in another paper [15] the same author offers a list of electrode solutions commonly used for electrophoresis in Immobiline gels and specifies that water is applicable only when samples with high salt concentration are analyzed. A number of other authors have also employed water as electrode solutions [3, 4, 5, 6, 10, 12].

Water Decomposition and Transport phenomena during IEF

In a recent paper [8] we discussed the kinetics of the electrochemical reactions transferring electrons during IEF. Routinely, in the isoelectric focusing numerous acids and bases are employed as electrode solutions and a porous barrier of polyacrylamide gel separates them. There are many IEF techniques, but in the popular implementation of this method a thin platinum wire is laid on paper strips, soaked with electrode solutions that are in contact with the carrier gel, or the electrodes are immersed into appropriate electrode reservoirs. In all cases the products of water electrolysis are liberated into the electrode solutions, thus influencing their physicochemical properties during the process, by alteration of their pH.

Studying the process of water electrolysis it was found that there is a non symmetrical acidification and alkalization of both electrode solutions [8]. When an electric field is applied a two-way process begins, whereby the migration of the produced water ions is accompanied by diffusion of charge-compensating particles originating from the electrode solutions, and/or some constituents of the carrier matrix [7]. This process determines the conductivity of the system, and thus the magnitude of the current flowing through the system. As we reported earlier [8], the electrode current represents the reaction rate at which water is discharged on the platinum wire, which can be calculated applying the equation

$$i \sim k \frac{\Delta \mathrm{pH}}{\sqrt{t}}, \qquad (1)$$

where the rate constant k includes the number of transferred electrons, Faraday's constant, the electrode surface and diffusion coefficient of the respective particle, $\sqrt{t}$ is the duration of the electrophoresis and ΔpH is the difference between the initial pH of a definite electrode solution and the pH measured after a definite interval of time during the IEF process.

Steady state Condition

Irrespectively of the type of electrode solutions employed, when electrophoresis is carried out in power mode the current gradually decreases, tending to reach a minimal value. We observed the same correlation for the yield of water ions, which decreases during the process, following a non-linear relationship similar to that of the current. As we concluded in a preceding paper [8], as long as the electrode solutions are a continuous source of hydrogen and hydroxide ions the electrophoretic system will go through a sequence of transient states, gradually approaching steady state ($i = 0$), when the equal-

ity $i_{anode} = i_{cathode}$ should be valid. Thus studying the pH alterations when water alone is used as electrode solutions we formulated a criterion for the attainment of steady state, based on the proximity of the sum $pH_{anode} + pH_{cathode}$ to 14.

Alteration in the Electrode Current during IEF

Studying the processes occurring on both electrodes we observed that during the early stage of the experiment the current changes abnormally reaching unusually high values (**Fig. 1**). This side effect cannot be predicted by the theory [8]. After a relatively short interval of time the current decreases to a definite value from which asymptotically tends to zero, while the system is driving slowly toward a steady state. Analyzing the relationship between the electrode current and the pH of the electrode solutions we reached the conclusion that the attainment of steady state requires an indefinitely long isoelectric focusing process, the duration of which is proportional to the applied voltage [8]. A similar conclusion was reached earlier by Bier and Palusinski et al. [2, 11].

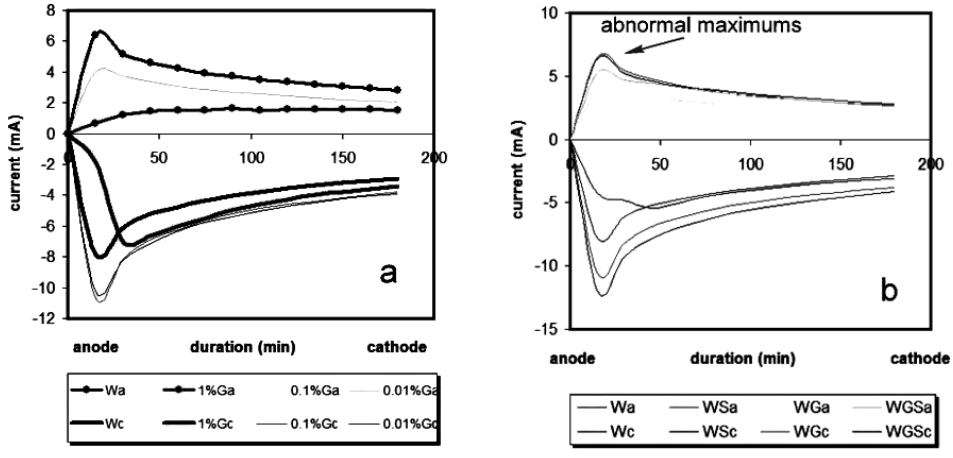

Fig. 1. a) Comparison of the electrode current when different electrode solutions are applied: W_a, W_c – distilled water alone; G_a, G_c – 1%, 0.1% and 0.01% (m/V) solution of gelatin. The anode and cathode currents are denoted by the indexes ($_a$) and ($_c$) respectively. PAG was prepared in the absence of carrier ampholytes. The extrapolation of the curves to current zero shows that the duration of electrophoresis needed to reach steady state should be different. The presence of 1% (m/V) gelatin brings about considerable decrease of both electrode currents;
b) Comparison of the electrode current when different electrode solutions are applied: W_a, W_c – distilled water alone; WS_a, WS_c – 0.1 M solution of Na_2SO_4; WG_a, WG_c – 0.1% (m/V) solution of gelatin; WGS_a, WGS_c – the solution contains 0.1 M Na_2SO_4 and 0.1% (m/V) gelatin. The anode and cathode currents are denoted by the indexes ($_a$) and ($_c$). PAG was prepared in the absence of carrier ampholytes

Therefore we can suggest that any substance present in the electrode solutions, which can suppress the electrolysis of water, will be suitable to bring the system nearer to steady state for a shorter time, which is the essence of the present study.

pH gradient Drifts

In a recent paper we discussed widely the reasons for the pH gradient drift during the IEF process. The considerations presented there enabled us to be the first to arrive at

the conclusion, that the gradient drift can be explained and predicted with a very good approximation by the alteration of both most important electrical parameters of the system: electrode potential and current [8]. The analysis of this phenomenon showed that during the early phase of the electrophoretic process the acidity of the electrode solutions changes asymmetrically and the system is strongly diverted from its steady state ($i_{anode} \neq i_{cathode}$). With time the change of the reaction rate of the electrolytic processes shows a clearly defined tendency for equalization of the electrode currents ($i_{anode} = i_{cathode}$), which is the reason for the observed decrease of the pH changes, occurring in the electrode solutions. Concomitantly with the processes of electron transfer, corresponding changes in mass transport take place in the system, which is the reason for the observed gradient drift.

Materials and Methods

Materials

Polyacrylamide gel slabs were prepared as previously described [8]. 2.2 ml of carrier ampholytes (CA) "Ampholyte high-resolution 3-10", Fluka & Riedel (catalogue No. 39878) per 60 ml gel were introduced, followed by 20 mg ammonium persulfate and 0.06 ml TEMED. Solutions of 0.1 M phosphoric acid (Merck, Germany) and sodium hydroxide (Reanal, Hungary) or distilled water alone (pH=6.75) were used as electrode solutions. In some instances 0.01%, 0.1% or 1% (m/v) gelatin (for electrophoresis, type A, G8150, Sigma) or Triton X-100 (CAS number 9002-93-1, laboratory grade, Sigma Chemical) and/or 0.1 M Na_2SO_4 were added to the electrode solutions. The total volume of each electrode solution was 100 ml. Each electrode solution was bubbled with argon prior to use for about 15 minutes. 5 µl of 5% (m/v) solution of Protein Test Mixture 9 ("wide-range" pI-Marker Proteins), purchased from Serva (catalogue No. 39206) were used as a protein standard. To avoid the interaction between the electrode solutions and the gel with atmospheric carbon dioxide, electrophoresis and measurements were performed under argon.

Equipment and Isoelectrophoretic conditions

We should stress that we selected the conditions for IEF so as to be able to register the changes of pH of the electrode solutions, and to ensure a satisfactory separation of the standard protein mixture employed by us. The choice of a rather larger volume of the electrode solutions is due to the technical characteristics of the electrophoresis bath used by us, as well as to ensure a reliable and easy measurement of pH without interrupting the IEF process.

Electrophoresis was carried out using a Pharmacia ECPS 3000/150 Power Supply (Sweden) and an LKB 2117 Multiphor (Sweden) apparatus cooled by running water. The gel was maintained at a temperature of about 10 °C. Platinum electrodes (thin platinum wire – 0.3 mm in diameter, 26 cm length) hanging on a plastic plate (LKB, Sweden) were immersed to the bottom of both electrode solution reservoirs, where the electrode strips were soaked in the corresponding electrode solution. The strips were connected to the gel ends by Whatman 3MM chromatographic paper. The power supply was set to the limiting values of 800 V, 20 mA and 15 W. The duration of the process was read from the moment when the apparatus was switched on only when the purpose of the electrophoretic run was to calculate the alteration of the electrode current during the process. Routinely the duration was read from the moment when the voltage reached the limiting value of 800 V. A pH-meter for water with low conductivity

780 pH meter Metrohm (Switzerland) equipped with Aquatrode plus combined LL pH glass electrode was used.

Measuring Procedure

To follow up the pH changes occurring in the electrode solutions composed of water alone, or containing gelatin or Triton X-100 and in the absence or in the presence of sodium sulfate, we performed a series of experiments as follows: at regular 15 min intervals during the IEF process 6 ml samples were withdrawn from the electrode solutions and were transferred to tightly capped vials. The pH was measured and the samples were returned to the electrode reservoirs. The temperature of the electrode solutions was 22 °C. The electrode current was calculated using equation (1).

Staining and destaining was performed according to the method described by Righetti and Drysdale [13].

Results and Discussion

Physicochemical Influence on the Electrode Current

Studying the electrochemical reactions occurring on the electrode surface and taking into consideration their relationship with the electrode current we reached the conclusion that under the conditions of IEF the abnormal maximum, which is always registered, is analogous to the same phenomenon observed in polarography. In polarography the abnormal jump of the current is suppressed by addition of small amounts of certain substances like the non-ionic detergent Triton X-100 or gelatin. In this paper we turned our attention to the analogous side effect observed by us, which is registered for both electrode currents in electrophoresis. We tried to resolve this problem adapting the knowledge gained from polarographic studies in an attempt to find a way for effective suppression of the electrolysis of water, which in its turn will bring about a decrease of current.

Influence of Gelatin added to the Electrode Solutions on the Electrode Current

We studied the influence of gelatin contained in the electrode solutions on the current flowing through the electrophoretic system. The obtained data presented in **Fig. 1a** show that the decrease of the anode current is proportional to the concentration of the gelatin dissolved in electrode solutions of distilled water. Furthermore, the decrease of the anode current leads to a corresponding increase of the cathode current when the concentration of gelatin is in the range of 0.01-0.1%. However, when the highest feasible 1% concentration of gelatin was employed there was a considerable lowering of both currents.

Unfortunately, when electrode solutions similar to the widely used phosphoric acid and sodium hydroxide are employed, because of their masking role it is not possible to follow up the changes in pH during electrophoresis. However, it is beyond doubt that as a result of the ongoing electrolysis of water there is continuous release of hydrogen and hydroxide ions into the electrode solutions [7, 8]. Considering that the presence of an acid and/or a base increases the intensity of water electrolysis, as a substitute of the routinely used electrode solutions, we employed water solutions of the non-hydrolyzing salt sodium sulfate, which only brings about increased water electrolysis and higher conductivity, without hampering the measurement of pH. The obtained results showed that when sodium sulfate is introduced into the electrode solutions the anode current increases become higher than those calculated when distilled water alone was used. However, at the cathode this effect is very small (**Fig. 1b**). Indeed, when the anodal cur-

rent increases the current at the opposite electrode compensatory decreases during the early stage of the experiment.

When in addition to the salt gelatin is introduced in the electrode solutions to a final concentration of 0.01% or 0.1%, the abnormal maximum, as well as the anode current as a whole, slightly decreases, but the registered decrease becomes greater at high gelatin concentration of 1%. These experimental facts gave us good reason to conclude, that the presence of gelatin in electrode solutions composed of phosphoric acid and sodium hydroxide will ensure the attainment of the maximal preset voltage for a shorter run time, i.e. the electrophoretic system will approach steady state faster. Furthermore, our data clearly show that there is a direct relationship between the concentration of gelatin and the decrease of the electrode current, which leads to faster equalization of anode and cathode currents, i.e. to steady state, where $i = 0$.

We can now propose that the current flowing through both electrodes can be decreased efficiently by adding 1% gelatin to the electrode solutions, so that steady state is attained for a shorter run time.

Influence of Triton X-100 on the Electrode Current

On the basis of the experience in polarography next we studied the influence of 0.01%, 0.1% or 1% concentrations of Triton X-100 introduced in the electrode solutions on the electrode current. Contrary to the results obtained with gelatin containing electrode solutions, in the case of Triton X-100 we found a reciprocal relationship. The data presented in **Fig. 2** show that there is a directly proportional relationship between the concentration of Triton X-100 and the magnitude of both electrode currents, which means that the electrophoretic system will be diverted significantly away from the steady state. This result can be exploited in some analytical cases, since it can be employed as a tool to manage the electrode currents according to our needs.

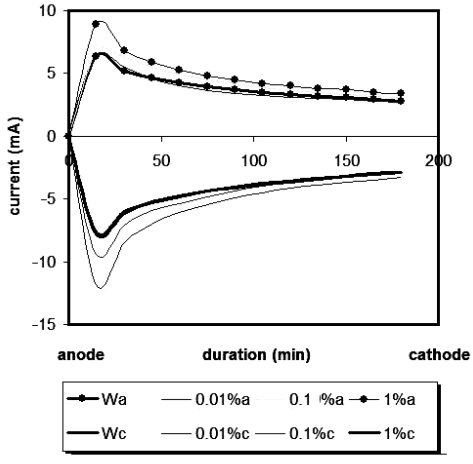

Fig. 2. Comparison of the electrode current when different electrode solutions are applied: W_a, W_c – distilled water alone; 0.01%, 0.1% and 1% solutions of Triton X-100. The anode and cathode currents are denoted by the indexes ($_a$) and ($_c$) respectively. PAG was prepared as in Fig. 1

IEF in the presence of Gelatin or Triton X-100 in the Electrode Solutions

To further verify the influence of gelatin added to the electrode solutions consisting of phosphoric acid and sodium hydroxide, we carried out IEF of a standard protein mixture. For the purposes of comparison we used two types of electrode solutions – the first contained 1% gelatin and in the second gelatin was omitted. It was established that the maximal preset voltage is reached 30 min faster when gelatin is introduced into the electrode solutions, as compared to the case when gelatin is absent. Electrophoresis was continued for two hours after the maximal preset voltage was reached when the process was interrupted and the electrophoregrams were compared. As can be seen in **Fig. 3** the focused protein bands have a very similar separation concerning the number of separated bands, however, their position along the gel is different. This result apparently reflects the pH gradient drift during electrophoresis, which is influenced by the electrochemical processes occurring at the electrodes [8].

Obviously, the presence of gelatin in the electrode solutions brings about suppression of the electrolysis of water, which results in a reduction of the amounts of hydrogen and hydroxide ions liberated in the electrode solutions. At this stage of our investigations we cannot rule out the possibility for a certain buffering action of gelatin, which can bring about a smaller alteration of the pH of the electrode solutions, as compared to the case when gelatin is absent. Moreover, this fact is closely related to the changes of the electrode potentials during the IEF process, which are a function of pH electrode solutions [8].

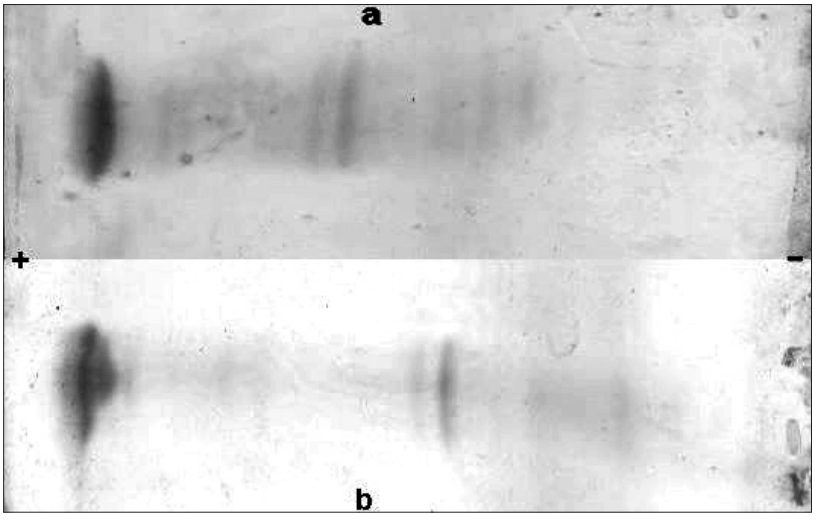

Fig. 3. IEF of Protein standard mixture. Two types of electrode solutions were employed: 0.1 M phosphoric acid and sodium hydroxide (a), and 0.1 M phosphoric acid and sodium hydroxide in the presence of 1% gelatin (b). PAG was prepared in the presence of carrier ampholytes. The maximal preset voltage is reached 30 min faster when gelatin is introduced into the electrode solutions, and then the ectrophoresis was continued for two hours at 800 V. The focused protein bands have an almost identical separation and sharpness, however, their position along the gel differs, which is caused by the pH gradient drift. Running conditions: 800 V, 20 mA, 15 W. The letters denoting the electrophoregrams correspond to the electrode solutions employed

The same electrophoretic system was studied, where gelatin was replaced with 0.01%, 0.1% or 1% concentrations of Triton X-100. We found that the time needed to reach the preset limiting voltage is proportional to the concentration of Triton X-100. Carrying out IEF in the presence of 1% Triton X-100 we observed a considerable prolongation of the time for which the voltage reaches the preset limiting value, approximately 90 min. At the same time the magnitude of the current was very high throughout the process. In addition we observed that the electrophoresis was accompanied by a considerable transport of water toward the anode, which caused a swelling of the carrier gel. Under these conditions the anodal proteins precipitate, thus compromising the electrophoretic separation.

The statistical treatment of the results on the time taken by the electrophoretic system to attain the preset maximum voltage of 800 V shows that in the presence of gelatin in the electrode solutions the decrease is 30 ± 4 min, as compared to electrophoretic runs performed in the absence of gelatin. This 10% decrease of the duration of electrophoresis apparently reflects the contribution of the electrolysis processes, occurring at the electrodes, to the deviation of the system from its steady state.

The comparative analysis of the electrophoregrams obtained in the presence and in the absence of gelatin shows that no additional protein bands can be found. Therefore, the inclusion of gelatin into the electrode solutions only influences the reaction rate of water electrolysis and reduces selectively the quantity of the ions H^+ and HO^- produced during the IEF process.

We found that the addition of Triton X-100 to the electrode solutions brings about the considerable increase of 90 ± 7 min of the time taken by the system to reach 800 V. Presently we cannot assess the significance of this result for the practice of IEF, however, we believe that it has a potential application.

Concluding Remarks

Contemporary IEF applications are typically characterized by a plethora of physical phenomena. This, in addition to their ever-increasing scope and complexities, makes their realistic modeling a daunting task. Central to modeling electrophoresis is the understanding of both transport and stoichiometric behavior of analytes in the electrolyte system in the presence of numerous driving forces. This work is a continuation of our efforts towards developing a comprehensive, and at the same time, a sufficiently simple model for realistic IEF applications and techniques, supplementing certain substances into the electrode solutions. The core of the present work, however, is to stress again the importance of the electrode solutions for the entire IEF process, which so far appears to be overlooked. In this paper we offer a simple modification of the electrophoretic method, allowing to predict and control the electrode current. We believe that the results reported in the present paper are a further contribution toward the elucidation of the role of the electrode solutions in the isoelectrophoretic process.

References

1. **Baumann, G. A., A. Chrambach.** An idealized model of IEF. – In: Progress in Isoelectric Focusing and Isotachophoresis, (Ed. P. Righetti), Holland, Elsevier Excerpta Medica, 1975, 13-19.
2. **Bier, M., R. A. Mosher, O. A. Palusinski.** Computer simulation and experimental validation of isoelectric focusing in ampholyte-free systems. – J. Chromatogr., **211**, 1983, 313-335.

3. **Demianova, Z., M. Shimmo, E. Pöysä, S. Franssila, M. Baumann.** Toward an integrated microchip sized 2-D polyacrylamide slab gel electrophoresis device for proteomic analysis. – Electrophoresis, **28**, 2007, 422-428.
4. **Fredriksson, S.** Scanning isoelectric focusing in small density-gradient columns. IV. The use of deuterium oxide for preparing the density gradient and its effects on isoelectric points of proteins. **–** J. Chromatogr., **108**, 1975, 153-167.
5. **Hashimoto, K., K. Sato, Y. Nakamura, K. Ohtsuki.** Development of continuous type apparatus for ampholyte-free isoelectric focusing (autofocusing) of peptides in protein hydrolysates. **–** J. Agric. Food Chem., **54**, 2006, 650-655.
6. **Macounova, K., C. R. Cabrera, M. R. Holl, P. Yager.** Generation of natural pH gradients in microfluidic channels for use in isoelectric focusing. – Anal. Chem., **72**, 2000, 3745-3751.
7. **Naydenov, C. L., E. P. Kirazov, L. P. Kirazov, T. T. Genadiev.** New approach to calculating and predicting the ionic strength generated during carrier ampholyte isoelectric focusing. – J. Chromatogr. A, **1121**, 2006, 129-139.
8. **Naydenov, C. L., E. Kirazov, V. Lozanov, L. Kirazov, V. Mitev.** Novel methods to control the current during isoelectric focusing. – Chromatographia, **69**, 2009, 887-895.
9. **Nguyen, N. Y., A. Chrambach.** Electrofocusing on flat pH gradients: Systematic pH gradient modification leading to improved protein separation. – Electrophoresis, **1**, 1980, 14-22.
10. **Ogasawara, A., T. Odake, T. Umemura, K. Tsunoda.** A new isoelectric focusing system for fast two-dimensional gel electrophoresis using a low-concentration polyacrylamide gel supported by a loose multifilament string. – Anal. Sci., **20**, 2004, 1673-1679.
11. **Palusinski, O. A., T. T. Allgyer, R. A. Mosher, M. Bier, D. A. Saville.** Mathematical modeling and computer simulation of isoelectric focusing with electrochemically defined ampholytes. – Biophys. Chem., **13**, 1981, 193-202.
12. **Rademacher, B. E., W. J. Steele.** Modifications and additions to the ISO-DALT system for two-dimensional gel electrophoresis. – Anal. Biochem., **167**, 1987, 37-46.
13. **Righetti, P. G., J. W. Drysdale.** Isoelectric focusing in gels. – J. Chromatogr., **98**, 1974, 271-321.
14. **Righetti, P. G.** In: Isoelectric Focusing: Theory, Methodology and Applications. Mir, Moscow (in Russian), 1986, 191-204.
15. **Righetti, P. G.** In: Immobilized pH gradients: Theory and Methodology. Elsevier, Amsterdam, New York, 1990, 139-148.
16. **Svensson, H.** Isoelectric fractionation, analysis, and characterization of ampholytes in natural pH gradients. I. The differential equation of solute concentrations at a steady state and its solution for simple cases. – Acta Chem. Scand., **15**, 1961, 325-341.
17. **Svensson, H.** Isoelectric fractionation, analysis, and characterization of ampholytes in natural pH gradients. II. Buffering capacity and conductance of isoionic ampholytes. – Acta Chem. Scand., **16**, 1962, 456-466.
18. **Svensson, H.** Isoelectric fractionation, analysis, and characterization of ampholytes in natural pH gradients. III. Description of apparatus for electrolysis in columns stabilized by density gradients and direct determination of isoelectric points. – Arch. Biochem. Biophys., Suppl. **1**, 1962, 132-136.

Corresponding author:
Fax: +359-2-91-72-513
e-mail: cyrill@mbox.contact.bg

Institute of Experimental Morphology, Pathology and Anthropology with Museum
Bulgarian Anatomical Society

Acta morphologica et anthropologica, 21
Sofia ● 2015

Modulation of Intestinal Alkaline Phosphatase and Lactase Activities in Organ Culture by Growth Factors

V. Pavlova[*], V. Petrova[*], I. Ivanov[**], M. Dimitrova[*], E. Nikolova[*]

[*] *Institute of Experimental Morphology, Pathology and Anthropology with Museum, Bulgarian Academy of Sciences, Acad. G. Bonchev Str., Bl. 25, 1113 Sofia, Bulgaria*
[**] *Department of Chemistry and Biochemistry, Medical University Sofia, 2 Zdrave Str., Sofia 1431, Bulgaria*

Colostrum and milk are rich sources of nutrients and biologically active substances. Among these substances growth factors are present that are crucial for the proper development of neonates. These growth factors include EGF, SCF, aFGF, bFGF, TNF-alpha and several others. The exact biological role of the latter factors is still under investigation. We have hypothesized that EGF, SCF, TNF-alpha, aFGF and bFGF could influence the activity and distribution of two important intestinal enzymes namely lactase and intestinal alkaline phosphatase. Using biochemistry protocols to measure the total enzyme activities we determined different types of dependence between the growth factors and the enzymes studied.

Key words: growth factors, intestinal alkaline phosphatase, lactase.

Introduction

Colostrum is the first milk that is produced after parturition. It contains high levels of growth factors and components with immunomodulatory properties. These bioactive substances have different origin – some are produced by the mammary epithelium, some are produced by cells within milk or originate from the maternal serum [5]. Some of the growth factors like tumor necrosis factor-alpha (TNF-alpha) could be classified as cytokines – substances with autocrine or paracrine functions. It has been shown that over time their levels in mature milk lower [13]. The precise role of cytokines found in human milk remains under investigation. They are linked to the recruitment of neutrophils, and to the process of intestinal development. Other growth factors in colostrum and milk as epithelial growth factor (EGF), stem cell factor (SCF) or fibroblast growth factors (FGFs) are linked to maturation and healing of the intestinal mucosa [1], or are potent mitogen agents for diverse cell types [6].

Two of the key enzymes that function at the neonatal intestine are lactase and intestinal alkaline phosphatase (iAP). They are considered marker enzymes for the stage of development of enterocytes – absorptive cells that line the lumen of the small intestine. Lactase is a neutral β-galactosidase that hydrolyzes lactose to glucose and galac-

tose that are absorbed by intestinal enterocytes into the bloodstream. Lactase is present on the apical surface of enterocytes. Its activity in most mammals decreases following weaning. iAP is a hydrolytic enzyme crucial for the intestinal homeostasis. It regulates lipid absorption in enterocytes, limits bacterial passage through intestinal epithelium and detoxifies bacterial endotoxins. Dietary components were shown to modulate the expression and activity of iAP [8]. The modulation of lactase activity was detected to be thyroxine dependent [4].

Little information could be found regarding the possible effect of growth factors derived from colostrum or milk on the activity of intestinal enzymes.

The aim of the present work was to follow up the changes in intestinal alkaline phosphatase and lactase enzyme levels provoked by several growth factors from milk: EGF, SCF, TNF-alpha, aFGF and bFGF in organ culture.

Materials and Methods

Organ culture

Small intestinal organ explants (1.0 cm long pieces of duodenum, jejunum and ileum) from 5-day-old Balb/c mice (weaning period) were cultivated separately with different milk growth factors: EGF (50 ng/ml, 48 h), SCF (20 ng/ml, aFGF (10 ng/ml, 24 h), bFGF (10 ng/ml, 24 h) or TNF-alpha (30 pg/ml, 48 h) in RPMI1640 at 37 °C, 5% CO_2 and 95% humidity.

Biochemical assay

After the cultivation, the explants were homogenized in buffer solutions suitable for the respective enzyme (see below) for 10 min on electrical homogenizer. Protein content of homogenates was assessed after Dawson et al. [2] by measuring absorption of the samples at 260 nm and 280 nm on spectrophotometer Specol 1500 (Analitjk, Jena) and calculations, as follows: mg protein/ml = 1.55×A280 – 0.76×A260.

Enzyme activity

The enzyme activities were determined by incubation of tissue homogenates with substrate solutions containing the following substrates:

– for iAP: 20 mM 4-nitropheyilphosphate disodium salt in 0.1 M Tris/HCl, pH 10.00;

– for Lactase: 20 mM 2-Nitrophenil-β-D-galactopyranoside in 0.1 M citrate/phosphate buffer, pH 6.0.

Aliquots were gathered every 5 min (for iAP) or every 30 min (for lactase) in which the reaction was stopped by applying stopping solutions: for iAP – 0.5 M NaOH (10:1), and for lactase – 4% K_2CO_3 (1:1). Spectrophotometric measurements of the samples were performed at 410 nm for iAP; and at 450 nm for lactase using the same spectrophotometer as above. The curves showing the quantity of enzymatically released colorful product per min were built using SigmaPlot 9.0. The enzyme activity was obtained from the curves by regression analysis and was expressed as mg colorful product per min per mg protein.

Results and Discussion

An increasing body of evidence has indicated that growth factors play an important role in cell growth and differentiation. EGF, aFGF and bFGF have crucial role in the development of mammary epithelial cells. Their concentrations in colostrum and milk are dependent on the physiological stage of development [9]. TNF-alpha is also linked to mammary gland development but at the same time it is able to induce apoptotic cell death [14, 10]. SCF is linked to the process of normal development of mammary gland and its loss is associated with malignant transformations [12]. Once introduced into the developing gut, those growth factors enhance the maturation of intestinal cells. Little is known about the role of growth factors in the activation/deactivation of intestinal enzymes. Studies have shown that only high physiological levels of EGF could recover lactase activity after infections [15]. Other studies reported that epithelial growth factor had vague effect on the activity of iAP [3]. Our results indicated that after stimulation of small intestinal explants with EGF in organ culture the activities of both iAP and lactase were augmented (as seen in **Fig. 1** and **Fig. 2)**.

A possible explanation could be the ability of EGF to modify gene expression outside of the crypt region. TNF-alpha release in murine gut was shown to be dependent on iAP levels in inflammatory bowel disease [11]. Lactase activity was augmented in a study dealing with intestinal maturation in rats [7]. In our study iAP activity was increased in duodenum but not in jejunum or ileum. The activity of lactase was decreased in all three parts of the small intestinal specimens. These results suggest that this inflammatory cytokine could cause enzyme deficiencies by down regulating lactase activities. In our study SCF lowered the activity of iAP in all parts of gut explants, whereas for lactase we noticed increased activity for jejunum and for ileum specimens only. Unfortunately, no data is available to compare our results with. Stimulation with aFGF showed increased activity of iAP in duodenum and decreased activity of the enzyme in

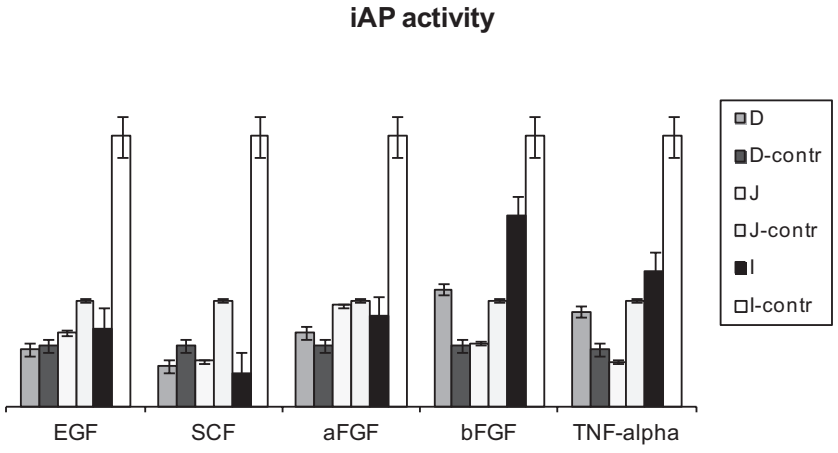

Fig. 1. Intestinal alkaline phosphatase activity in neonatal murine intestinal explants after stimulation with EGF, SCF, aFGF, bFGF and TNF-alpha

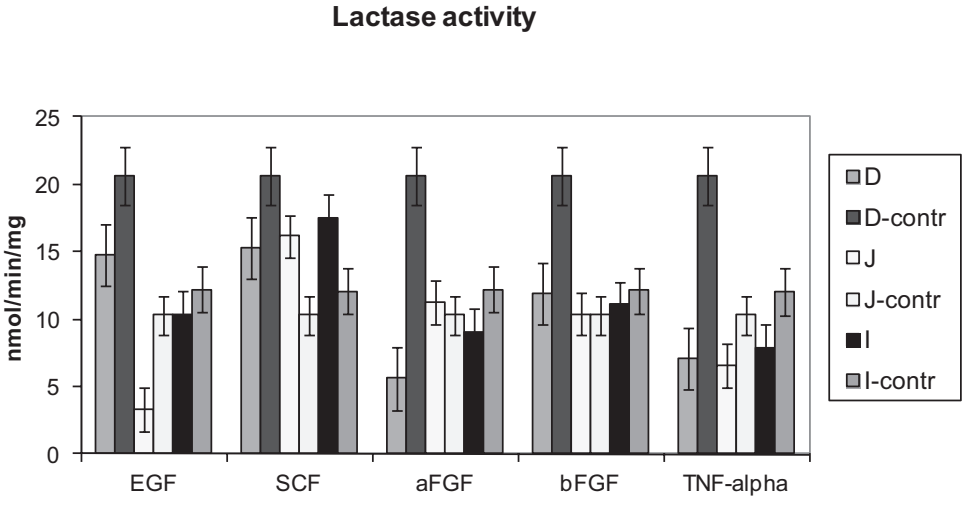

Fig. 2. Lactase activity determined after stimulation of neonatal murine gut explants with EFG, SCF, aFGF, bFGF or with TNF-alpha

jejunum and in ileum. Lactase activity was slightly increased for jejunum and decreased for duodenum and for ileum. Enzyme activities of lactase were not affected by the incubation of neonatal murine gut explants in presence of bFGF whereas iAP levels were increased for duodenal specimens.

Colostrum and milk are dynamic fluids that contain nutrients and bioactive substances needed for the proper development and health of neonates. Growth factors may modulate the activity of key intestinal enzymes in organ culture to different extent. Future studies are needed to investigate the regulatory effect of the growth factors towards the regulation of intestinal cells and the outcomes of their supplementation in infant formulas.

Acknowledgements: This work was supported by the European Social Fund and Republic of Bulgaria, Operational Programme "Human Resources Development" 2007-2013 framework, Grant No BG-051PO001-3.3.06-0048 from 04.10.2012. This work was also supported by grant DFNI B 01/30 from the National Science Fund of Republic of Bulgaria.

References

1. **Chang, C. Y., J. J Chao.** Effect of human milk and epidermal growth factor on growth of human intestinal caco-2 cells. – JPGN, **34**, 2002, 394-401.
2. **Dawson, R., D. Elliot, W. Elliot, K. Jones.** Handbook of Biochemist. (In Russian). Moscow, Mir, 1991, 301 p.
3. **Falcone, R. A. Jr, C. E. Shin, C. R. Erwin, B. W. Warner.** The effect of epidermal growth factor on differentiation of isolated enterocytes after small bowel resection. – J. Pediatr. Surg., **34**(1), 1999, 209-213.
4. **Freund, J. N., I. Duluc, F. Raul.** Discrepancy between the intestinal lactase enzymatic activity and mRNA accumulation in sucklings and adults. Effect of starvation and thyroxine treatment. – FEBS Lett, **248**(1-2), 1989, 39-42.
5. **Garofalo, R.** Cytokines in human milk. – The Journal of Pediatr., **156**(2), 2010, S36–40.
6. **Gospodarowicz, D., G. Neufeld, L. Schweigerer.** Fibroblast growth factor. – Mol. Cell. Endocrinol., **46**, 1986, 187-204.

7. **Kaouass, M., P. Deloyer, I. Gouders, O. Peulen, G. Dandrifosse.** Role of interleukin-1 beta, interleukin-6, and TNF-alpha in intestinal maturation induced by dietary spermine in rats. – Endocrine, **6**(2), 1997; 187-194.
8. **Lalles, J. P.** Intestinal alkaline phosphatase: multiple biological roles in maintenance of intestinal homeostasis and modulation by diet. – Nutr. Rev., **68**(6), 2010, 323-332.
9. **Lavandero, S., A. Chappuzeau, M. Sapag-Hagar, T. Oka.** *In vivo*- and *in vitro*-evidence of basic fibroblast growth factor action in mouse mammary gland development. – FEBS Lett., **439**(3), 1998, 351-356.
10. **Locksley, R. M., N. Killeen, M. J. Lenardo.** The TNF and TNF receptor superfamilies: integrating mammalian biology. – Cell. **104**, 2001, 487–501.
11. **Moss, A. K., S. R Hamarneh., M. M. Mohamed, S. Ramasamy, H. Yammine, P. Patel, K. Kaliannan, S. N. Alam, N. Muhammad, O. Moaven, A. Teshager, N. S. Malo, S. Narisawa, J. L. Millán, H. S. Warren, E. Hohmann, M. S. Malo, R. A. Hodin.** Intestinal alkaline phosphatase inhibits the proinflammatory nucleotide uridine diphosphate. – Am. J. Physiol. Gastrointest. Liver Physiol., **304**(6), 2013, G597-604.
12. **Ulivi, P., W. Zoli, L. Medri, D. Amadori, L. Saragoni, F. Barbanti, D. Calistri, R. Silvestrini.** c-kit and SCF expression in normal and tumor breast tissue. – Breast Cancer Res. Treat., **83**(1), 2004; 33-42.
13. **Ustundag, B., E. Yilmaz, Y. Dogan, S. Akarsu, H. Canatan, I. Halifeoglu, G. Cikim, A. D. Aygun.** Levels of cytokines (IL-1beta, IL-2, IL-6, IL-8, TNF-alpha) and trace elements (Zn, Cu) in breast milk from mothers of preterm and term infants. – Mediators of inflammation, **6**, 2005, 331–336.
14. **Warren, M. A., S. F. Shoemaker, D. J. Shealy, W. Bshar, M. M. Ip.** Tumor necrosis factor deficiency inhibits mammary tumorigenesis and a tumor necrosis factor neutralizing antibody decreases mammary tumor growth in neu/erbB2 transgenic mice. – Mol. Cancer. Ther., **8**, 2009, 2655–2663.
15. **Zijlstra, R. T., J. Odle, W. F. Hall, B. W. Petschow, H. B. Gelberg, R. E. Litov.** Effect of orally administered epidermal growth factor on intestinal recovery of neonatal pigs infected with rotavirus. – J. Pediatr. Gastroenterol. Nutr., **19**(4), 1994, 382-90.

Institute of Experimental Morphology, Pathology and Anthropology with Museum
Bulgarian Anatomical Society

Acta morphologica et anthropologica, 21
Sofia ● 2015

A Morphological Study on the Effect of Liposomally Administered Albendazole on the *Trichinella spiralis* Muscle Stage in Mice

S. Petkova, V. Dilcheva, E. Gabev

Institute of Experimental Morphology Pathology and Anthropology with Museum, Bulgarian Academy of Science, Acad. G. Bonchev Str., Bl.25,1113 Sofia Bulgaria

The aim of the present morphological study is to establish the effect of the liposomally encapsulated and separately applied albendazol during the muscle stage of Trichinella infection. The therapy was applied once a week at doses of 24 mg/kg body weight for the liposome encapsulated albendazol, the separately applied albendazol and the control groups. The corresponding medications were injected intraperitoneally once a week. The treatment was started on day 35-38 after the infection when the larvae are localized in the muscle tissue (muscle stage of Trichinellosis). The efficiency of the conducted therapy is measured as follows: liposome-encapsulated albendazol shows a statistically significant efficiency of 69 percent for the 24 mg/kg dose while albendazol applied separately indicates a statistical significance of 36 percent for the 24 mg/kg dose. The pathomorphological impact obtained as a result from the action of the antihelminthics shows that in the different groups there are differences only as to the numbers of the living and dead larvae. According to pathomorphological changes of the capsules, the parasites and the spaces around them are identical both for the liposome-encapsulated and the separately applied albendazol. The muscle samples for the histological study were removed from the thoracic musculature of the experimental animals.

Key words: pathomorphology, liposomes, *Trichinella spiralis*, albendazole.

Introduction

Trichinellosis is a parasitic disease spread throughout the world. It is caused by various representatives of the Trichinella genus after consumption of infected meat or meat products insufficiently cooked.

The modern therapy of Trichinellosis is being carried out by means of antihelminthics from the benzamidazole group with mebendazole, albendazole, flubendazole, etc. [4]. The intestinal phase of the ailment is prone to treatment but unfortunately it is diagnosed rather late when the parasite is already encapsulated in the muscle cells. At that stage, the treatment requires high doses of the preparation which in most cases leads to undesired side effects [7].

Recently it became possible to solve some of the problems associated with the usage of the therapeutic agents through a system of carriers in the organism. These systems

optimize the action of the medicament and direct it to the target parts of the organism in order to overcome the cell barriers.

Liposomes as the most promising carriers are biodegradable, easy-to-prepare and also diverse in terms of composition, size and other structural parameters defining the various putative mechanisms of interaction of the liposomes with the biological entities [10].

For the first time, liposomes were received and used by the team of A. Bangham [2]. Originally, they were used for modeling ionic transport via the cell membrane due to their structural similarity with the lipid bilayer membrane of the cell. Later on, Gregoriadis et al. have found application of the different types of liposomes for improving the therapy of various diseases and their diagnostics [10]. Liposomal encapsulation of the antihelminthics helps the therapy, decreases the resistance and creates the so-called depot-effect (the corresponding medicines are introduced once per week).

The purpose of current study is to compare morphologically the action of the liposome-encapsulated and free-applied albendazol in the muscular stage of Trichinellosis caused by *Tr. spiralis*.

Materials and Methods

Experimental animals and concept of experiment

White mice weighing about 30 g on average were infected per os with about 100 *Trichinella* larvae of the *Tr. spiralis* species. On day 35 after the infection with the well expressed muscle stage of the disease the corresponding experimental groups were formed – one for the free applied albendazole and the other for the liposome-encapsulated albendazole respectively. Each group numbered 30 mice. Albendazole at a dose of 24 mg/kg body weight was used i.p. introduced in the course of nine weeks. A control group was injected with saline.

Biotechnological methods: Liposomal encapsulation of albendazole

The technology encompasses three stages: The production of multilamellar liposomes of the Banghams type [2]. For this purpose, the corresponding amounts of albendazole (pharmaceutically pure substances Cypla, India) were dissolved in a chloroform solution of the lipid, evaporated on a vacuum evaporator until the final elimination of the solvent and the lipid film such obtained was hydrated by the addition of the water liposomal phase 150 ml saline. A thermal cycle of freezing (in liquid nitrogen) and defrosting of the obtained liposomal suspension was carried out and subjected to extrusion through 100 nm of polycarbonate membranes by an extruder Emulsiflex C5 of the Avestin firm. Thus obtained liposomal medicament containing albendazole was kept in the presence of an inert gas at – 25 °C and used for treating the experimental animals.

Preparation of non-liposomal albendazole

Immediately prior to the experiment the needed amounts of albendazole were dissolved in saline with an ensuing intermittent ultrasonic processing twice for 20 sec with a 1-minute pause between both sonifications.

Pathomorhological methods

Histological studies on thoracic musculature from control and experimental animals were carried out. Material was removed from the experimental animals in the ninth week after the beginning of the therapy with the corresponding preparation.

Fixation and embedding

The material was fixed in the medium of Serra for 45 min up to 1 hour. After the fixation, the samples were dehydrated in a series of alcohols with growing concentrations (70%, 80%, 96% and 100%). Impregnation in cedar oil was performed for 12-18 h followed by embedding in paraffin. The material was cut out on a microtome and sections of a 6 μ thickness were prepared and then mounted on slides. Then staining was performed with hematoxylin – eosin with the sections first deparaffinized in xylol, whereafter dehydrated in a series of alcohols, washed in water and stained with the hematoxylin of Maier for 5 to 7 min and counterstained with 1% water solution of eosin for 1-2 min and embedded in Canadian balm. As a result of the staining the nuclei were colored in blue and the cytoplasm of the cells in pink.

Results and Discussion

The following results were obtained upon comparing the therapeutic activity of liposomal albendazol and free (non-encapsulated in liposomes) albendazol on a murine experimental model. The exact efficacy of the preparations is 69% for the dose of 24 mg/kg body weight in the case of the liposome-encapsulated antihelminthics, while for the free applied albendazol the efficiency is 36% per dose of 24 mg/kg body weight, respectively.

The conducted morphological research definitely confirms the destructive action of the antihelminthic medicines over the Trichinella larvae encapsulated in the muscle. The obtained results are shown in **Figs. 1-6**.

The pathomorphological pattern in the separate experimental groups shows that differences are found only in the numbers of the live and dead larvae. The samples for the histological studies were taken from the pectoral musculature of the experimental animals. This is in accordance with the observations of other authors who have found that the larvae of the *Tr. spiralis* species have a predilection to the tonic muscles with good blood supply – the diaphragm, pectoral musculature, the masseter muscles, tongue and intercostals musculature [1, 6].

A structure typical for the muscle phase of trichinellosis is observed in the tissues of the control animals: a well-shaped capsule of connective tissue around an intact Trichinella larva which is lemon-shaped and with a thick matrix (**Fig. 1**).

Inflammatory cells are not found in the surrounding muscular tissue. After mebendazole treatment a multitude of pathomorphological alterations are established affecting the capsules, the parasite itself, and the spaces around them. A strong inflammatory reaction is observed in the infected zones expressed in an augmentation of the macrophage and polymorphonuclear numbers (**Figs. 2, 3**). The reaction of inflammation is localized around and inside the Trichinella capsules. This is due to progressive destruction of the capsule wall and the following resorption which allows the inflammatory cells to penetrate into it (**Figs. 3, 4)** The matrix is strongly reduced and modified as the capsule is filled with cell detritis (**Fig. 4).** Parallelly to this process, the parasite larvae inside the capsule are also subject to changes. Initially, the cuticle is injured which is expressed in the damage of its integrity. Gradually, the parasite larvae die out and destroyed capsules containing residual parasitic material are observed (**Figs. 3, 4**). The process is terminated by a complete destruction of the Trichinella larvae and their total lysis (**Fig. 6**). In most cases the striation of miofibres adjacent to the capsules is lost (**Fig. 3**). The application of the liposome-encapsulated medicament with albendazol over a seven-day interval in the course of 9 weeks has led to the killing of the Trichi-

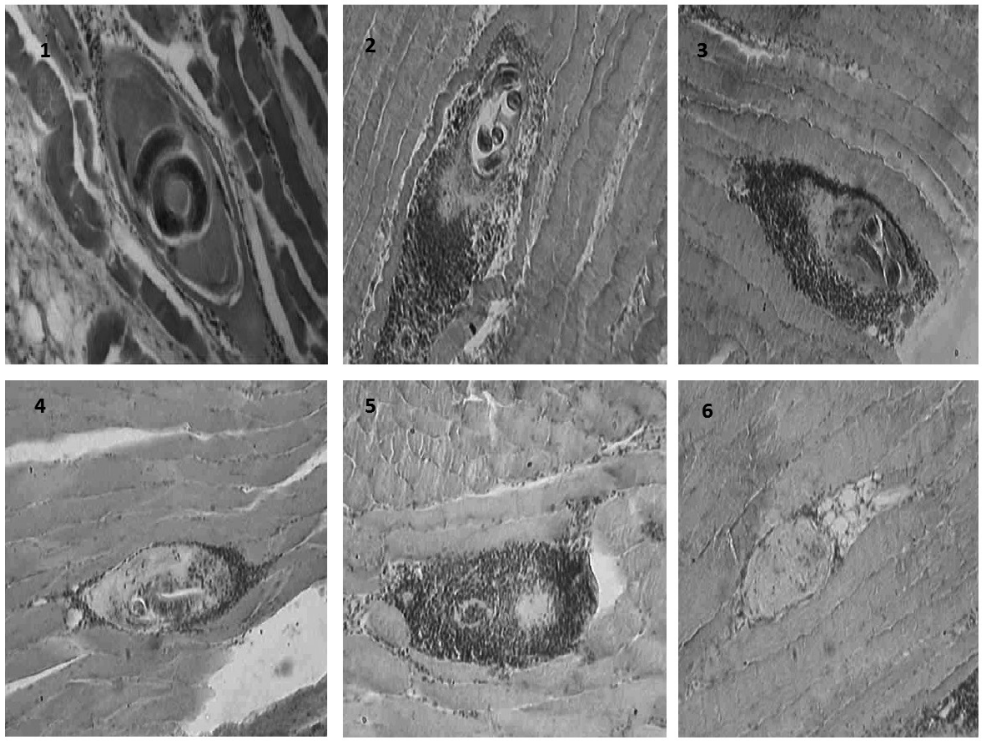

Figs. 1-6. Major morphological changes in the chest musculature of mice infected with *Tr. spiralis* following albendazole treatment. Hematoxylin-eosin staining: 1. – A control group – well formed capsule containing an undamaged larva; 2. – A capsule with lytic changes and an abundant intra – and pericapsular infiltration with inflammatory cells; 3. – A total resorption of the capsule wall infiltrated by a great number of macrophages and polymorphonuclears; 4. – A capsule with strongly attenuated matrix filled with cell detritis; 5. – Totally destroyed larvae in capsules infiltrated with inflammatory cells; 6. – A total lysis of a capsule and a larva, 10×

nella larvae – 69% at the dose of 24 mg/kg (**Fig. 6**). Such a result was not recorded in any of the controls. In all groups treated with the liposome-encapsulated antihelminthic a progressive development of the pathomorphological changes in the encapsulated larvae was observed ending with destruction of the trichinellae. According to Despommier [5], the infective larva of *Tr. spiralis* causes a redifferentiation of the muscle fibres expressed in an augmentation of the nuclei and the mitochondria numbers. The nurse cells maintain the biochemically compatible environment which is needed for the development and the continuous existence of the parasite allowing it to assimilate nutrients and to remove waste products. In that respect the development and encapsulation of the Trichinella larvae does not cause an inflammatory process in the entire tissue only with a local character. The immune response of the tissues of the host against the parasites usually is very weak and it is reinforced by the negative chemotaxis of the leucocytes and platelets, secretory or excretory products of the parasite and the immunosuppressive action of the larvae. The application of albendazole changes the character and the intensity of the cellular inflammatory reaction [8]. Albendazole is considered to be one of the most efficient antihelminthics but it has a low solubility in water solutions. Therefore after an oral application of the medicine only a small part of it reaches the parasite

while the majority of the substance remains in the intestines and is disposed from the body undigested [9]. Consequently, increasing doses of the benzimidazole preparations is acceptable especially in the treatment of the muscle stage of trichinelosis but is accompanied by the risk of side effects for the host. According to Bogan and Mariner [3] the higher activity of the benzimidazole preparations leads to greater toxicity. Such disadvantage can be resolved by the encapsulation of much lower concentrations of the medicament in a suitable carrier such as the liposome. In this way the biological activity of the medicine is definitely enhanced [8].

The results obtained by us confirm the higher efficiency of the liposome-encapsulated albendazole compared to that applied in the free state.

References

1. **Bangham, D.** Membrane models with phospholipids. – Prog. Biophys. Mol. Biol., **18**, 1968, 29-95.
2. **Bangham, D., W. Hill, G. Mill.** – In: Methods in Membrane Biology (Ed. E. D. Korn), New York, Plenum Press, 1974, 1-68.
3. **Bogan, J. A., S. E. Mariner.** – In: Albendazole in Helminthiasis (Ed. H. J. C. Etang), 1983, 13-21.
4. **Cabie, A., O. Bouchaud, S. Houze, M. Khuong, C. Ruggeri, T. Ancelle, S. Matheron, J. Coulaud.** Albendazole versus thiabendazole as therapy for trichinosis: a retrospective study. – Clin. Infect. Dis., **22**, 1996, 1033-1035.
5. **Despommier, D.** Trichinella spiralis: The worm that would be virus. – Parasitology Today, **6**, 1990, 193-196.
6. **Gould, E.** Trichinosis in man and animals (Ed. S. E. Gould). Charles C. Thomas, Publisher, Springfield, Illinois, **3**, 1970, 190.
7. **Horton, J.** The development of albendazole for lymphatic filariasis. – Ann Trop. Med. Parasitol., **103**, 2009, 33-40.
8. **Hrčkova, G., S. Velebny, J. Horák.** A morphological study of the effects of liposomized albendazole on the muscle phase of Trichinella spiralis in mice. – Journal of Helminthology, **67**, 1993, 24-30.
9. **Lacey, E.** Mode action of benzimidazes. – Parasitol. Today, **6,** 1990, 112-115.
10. **Грегориадис, Г., А. Аллисона.** Липосомы в биологических системах. Москва, Медицина, 1993.

Institute of Experimental Morphology, Pathology and Anthropology with Museum
Bulgarian Anatomical Society

Acta morphologica et anthropologica, 21
Sofia ● 2015

Study on the localization of Aminopeptidase A in Invasive Carcinoma of Mammary Gland in Human

V. Petrova[*], M. Dimitrova[*], I. Ivanov[**], V. Cenova[***]

[*]*Institute of Experimental Morphology, Pathology and Anthropology with Museum, Bulgarian Academy of Sciences, Acad. G. Bonchev Str., Bl. 25, 1113 Sofia, Bulgaria*
[**]*Department of Chemistry and Biochemistry, Medical University Sofia, 2 Zdrave Str., 1431 Sofia, Bulgaria*
[***]*Specialized Hospital for Active Treatment in Oncology, Sofia, Bulgaria*

Aminopeptidase A (APA) has a broad tissue distribution in both animals and humans. The enzyme is a part of renin-angiotensin system (RAS) and plays a role in blood pressure regulation. It participates also in other physiological functions such as processing of primary urine in kidneys and protein digestion in small intestine. APA expression has been studied in several types of malignant neoplastic lesions to show that it can serve as a biomarker for certain of them, particularly for active neoangiogenesis. In the present paper APA localization is studied in 5 cases of human invasive carcinoma of mammary gland using enzyme histochemistry. The results show elevated APA activity in the area of newly forming blood vessels as well as in tumor cells. A possible role of APA as a marker enzyme in this type of cancer is suggested.

Key words: Aminopeptidase A, blood vessels, mammary gland, invasive carcinoma.

Introduction

Aminopeptidase A (APA, EC 3.4.11.7) is a membrane-bound zinc metallopeptidase of M1 family [2]. The enzyme cleaves specifically the N-terminal glutamyl or aspartyl residues from peptide substrates, such as angiotensin II, chromogranin A, neurokinin B and cholecystokinin-8 [4]. APA is expressed normally in the brush-border membrane of renal tubules and is overexpressed in clear cell renal cell carcinoma [7]. APA is highly active in neoplastic lesions of the uterine cervix [6], human malignant gliomas and metastatic carcinomas of the brain [3]. Studies show that APA is overexpressed in stromal cells of prostatic carcinoma and show no expression in benign prostatic stroma [1]. Our recent studies indicate that APA is weakly expressed in normal mouse fibroblasts but is active in fibroblasts from mouse fibrosarcoma (unpublished results). Thus, it is possible that APA is involved in the formation of malignant tumors stromae. The enzyme is upregulated and overexpressed in blood vessels of some human tumors and is believed to play a role in pathological angiogenesis [3]. It is also highly expressed in pericytes in vasculature of tumors and wound healing tissues which shows that APA may be in-

volved in neovascularization, as well [5]. No data exist about the enzyme distribution and activity levels in mammary gland carcinomas.

The aim of the present study is to determine the localization of aminopeptidase A in cases of invasive carcinoma of mammary gland in humans. The results are expected to show whether the enzyme deserves to be studied in more details as a possible biological marker for mammary gland carcinoma.

Materials and Methods

Studies were made on anonymous cryostat sections of invasive carcinoma of mammary gland and lymph nodes with metastases, taken from 5 women 53 years middle-aged. The sections were provided by Specialized Hospital for Active Treatment in Oncology, Sofia. Before the enzyme reaction, all the sections were covered by celloidin (1% celloidin in absolute ethanol/diethyl ether/acetone 3:3:4) for a minute at room temperature. The sections were incubated in a substrate medium consisting of 0.5 mM fluorogenic enzyme substrate 4-(α-glutamylhydrazido)-N-hexyl-1,8-naphthalimide (α-Glu-HHNI) and 0.5 mg/ml piperonal in 0.1 M cacodylate/HCl buffer (pH 7.4), supplied with 5 mM of calcium ions, for 20 hours at 37 ºC. Then, the sections were post-fixed in neutral formaline for 15 min at room temperature, stained with haematoxyline consistent with classical methods of histology and embedded in glycerol/jelly. All the sections were studied under the fluorescent microscope Leica DM5000B (New York, USA).

Results and Discussion

Many metalloproteinases are known to participate in tumorigenesis and tumor progression and some of them are identified as targets for therapy. APA localization and activity levels have been studied in several types of tumors such as clear cell renal cell carcinoma [7], uterine carcinomas [6], gliomas [3], prostatic carcinoma [1], etc. Most of the studies show elevated enzyme expression although the pathophysiological significance of APA activation in those cases is not fully understood. Recent studies show that APA is involved in both angiogenesis [3] and neovascularization [5] in some types of human tumors. APA distribution and activity levels in human mammary gland carcinomas have not been examined thus far.

In the present work, the APA activity localization was studied in cryostat sections of invasive carcinoma of mammary gland in human and in lymph nodes with metastases using enzyme histochemistry with the novel fluorogenic substrate α-Glu-HHNI, recently developed by us (design and synthesis of the substrate as well as development of the histochemical method will soon be published elsewhere). APA activity was evaluated semi-quantitatively according to the intensity of fluorescent light emitted from the final product of the enzyme reaction.

In tissue sections of invasive carcinoma of mammary gland, tumor foci consisting of cells with different shape, size and degree of staining were observed (**Fig. 1**). The enzyme histochemistry revealed APA overexpression mainly in the region of blood vessels (**Fig. 1**).

A much lower enzyme reaction was visible also in the tumor foci. In the metastatic lymph nodes a considerable APA activity was detected in tumor cells (**Fig. 2**). Thus, our results show increased enzyme activity in the blood vessels region to suggest a possible role of APA in neoangiogenesis in this type of tumors, as well.

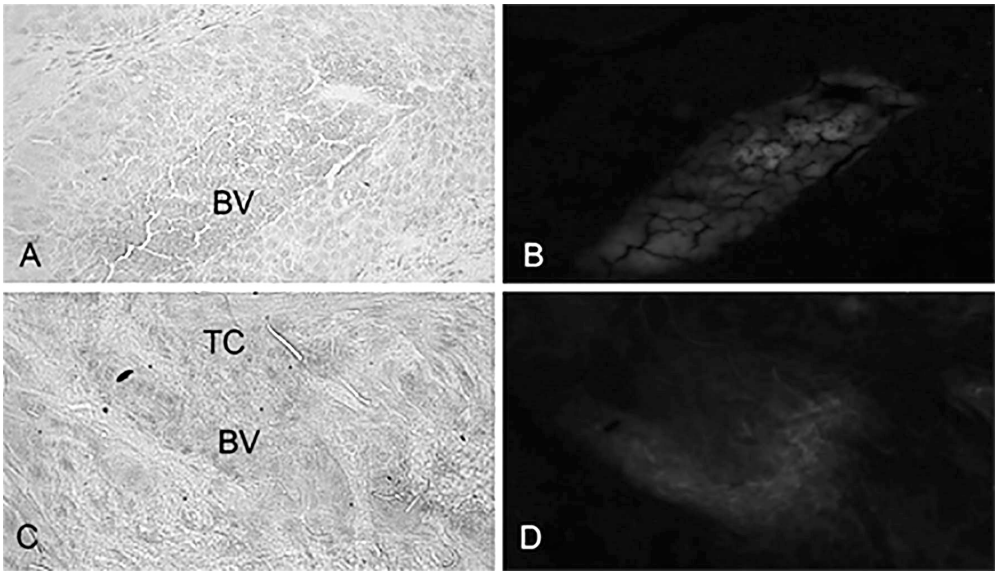

Fig. 1. APA activity in mammary gland carcinoma. Enzyme reaction in the area of blood vessels (BV). Lower reaction in tumor cells (TC). A, C – light microscopy; B, D – fluorescent microscopy. Magn. 200×

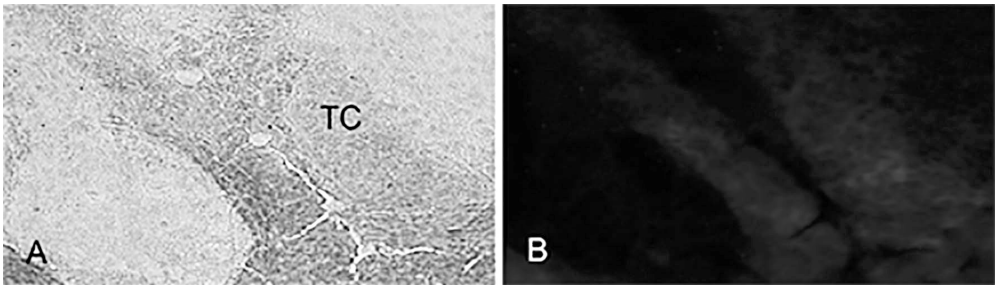

Fig. 2. APA activity in metastatic lymph node. Enzyme reaction in tumor cells (TC).
A – light microscopy; B – fluorescent microscopy. Magn. 200×

In conclusion, our results show high expression of APA in invasive carcinoma of mammary gland in human as well as in lymph nodes with metastases. It is possible that the degree of APA activation can serve to predict the degree of aggression of the tumors. This possibility remains to be explored in our future studies.

References

1. **Bogenrieder, T., C. L. Finstad, R. H. Freeman,C. N. Papandreou, H. Scher, A. Albinol, V. Reuter, D. Nanus.** Expression and localization of aminopeptidase A, aminopeptidase N, and dipeptidyl peptidase IV in benign and malignant human prostate tissue. – The Prostate, **33**, 1997, 225-232.
2. **David, C., L. Bischoff, H. Meudal, A. Mothe, N. de Mota, S. DaNascimento, C. Llorens-Cortes, M. C. Fournie-Zaluski, B. Roques.** Investigation of subsite preferences in aminopeptidase A (EC 3.4.11.7) led to the design of the first highly potent and selective inhibitors of this enzyme. – J. Med. Chem., **42**, 1999, 5197-5211.

3. **Marchio, S., J. Lahdenranta, R. Schlingemann, D. Valdembri, P. Wesseling, M. Arap, A. Hajitou, M. Ozawa, M. Trepel, R. Giordano, D. Nanus, H. Dijkman, E. Oosterwijk, R. Sidman, M. D. Cooper, F. Bussolino, R. Pasqualini, W. Arap.** Aminopeptidase A is a functional target in angiogenic blood vessels. – Cancer cell, **5**, 2004, 151-162.
4. **Rozenfeld, R., X. Iturrioz, M. Okada, B. Maigret, C. Llorens-Cortes.** Contribution of Molecular Modeling and Site-Directed Mutagenesis to the Identification of a New Residue, Glutamate 215, Involved in the Exopeptidase Specificity of Aminopeptidase A. – Biochemistry, **42**, 2003, 14785-14793.
5. **Schlingemann, R., E. Oosterwijk, P. Wesseling, F. Rietveld, D. Ruiter.** Aminopeptidase A is a constituent of activated pericytes in angiogenesis. – The Journal of Pathology, **179**, 1996, 436-442.
6. **Suganuma, T., K. Ino, K. Shibata, S. Nomura, H. Kajiyama, F. Kikkawa, N. Tsuruoka, S. Mizutani.** Regulation of aminopeptidase A expression in cervical carcinoma: role of tumor–stromal interaction and vascular endothelial growth factor. – Laboratory Investigation, **84**, 2004, 639-648.
7. **Varona, A., L. Blanco, J. Lopez, J. Gil, E. Agirregoitia, J. Irazusta, G. Larrinaga.** Altered levels of acid, basic, and neutral peptidase activity and expression in human clear cell renal cell carcinoma. – Am. J. Physiol. Renal. Physiol., **292**, 2007, 780-788.

Institute of Experimental Morphology, Pathology and Anthropology with Museum
Bulgarian Anatomical Society

Acta morphologica et anthropologica, 21
Sofia ● 2015

Structural Organization of Renal Medulla in Domestic Swine

I. Stefanov, A. Vodenicharov

Department of Veterinary Anatomy, Histology and Embryology, Faculty of Veterinary Medicine, Trakia University, 6000 Stara Zagora, Bulgaria

The morphological and physiological features of kidney in humans and different animals have been determined over the years. However, the detailed data about the structural organization of the porcine renal medulla are absent. In the present study it was established that in the outer stripe of outer medulla, the diameter and the number of proximal straight tubules were larger than in distal straight tubules. The number and the diameter of collecting ducts (CD) in the outer and in the inner stripe of the outer medulla were the same. The height and number of epithelial cells of CD increased towards the inner medulla. The diameter of *Ductus papillaris* was the largest. The diameter of thin limbs of Henle in the inner stripe and in the inner medulla unchanged, but in the tip of papilla it increased.

The pattern of the tubular and vascular organization of medulla that was established by the current study is evidence that porcine renal medulla belongs to the simple type of renal medulla.

Key words: renal medulla, morphometry, swine.

Introduction

Many studies have paid attention to the structural organization of the mammalian kidney [1, 2, 3]. The morphological and physiological features of this organ is studied in detail in rat, mouse, rabbit, guinea pig, minipig, cat, dog, horse and human [2, 8, 3, 13].

According to the urine concentrating ability the authors divide the kidneys into three types: the first type has a high urine concentrating ability (rat, mouse, golden hamster, Pammomys, Meriones), but the second one has a low concentrating ability (mountain beaver, muskrat). In comparison with other species, cats and dogs have an average urine concentrating ability. According to Kokubo et al. [8] the concentration ability of the urine is the highest in hamster, followed in order by dog, man and swine. Swine share a number of anatomic and physiologic characteristics with humans that make swine potentially a better model for some procedures and studies compared with other large animal species [16]. Pig has a true multirenculate, multipapillate kidney with true calices as in humans [17]. Systems that are most commonly cited as being suitable models include the cardiovascular, urinary, integumentary, and digestive systems. These features have led to the increasing use of swine as a major species in preclinical toxicology testing [16]. Histologically, both the proximal and distal tubules in the pig appear

dilated when the lumen diameter is compared with other experimental species such as the dog or the rodent, but this is a normal finding in pigs and minipigs. Similarly, glomeruli tend to have a greater degree of apparent dilation of the capillary [17].

The aim of the current work was to study the light microscopical tubular organization of the renal medulla in domestic swine.

Materials and Methods

Animals

The material was obtained from the kidneys of 10 castrated male pigs (Landras × Bulgarian White), aged 6 months, slaughtered for meat consumption in a slaughterhouse.

Hematoxylin and eosin staining of tissue samples

Immediately after death, the samples were immersed in 10% neutral formalin for 48 h. Then they were soaked in tap water, dehydrated and embedded in paraffin. Serial longitudinal sections through the cortex and medulla of the renal lobus and cross-sections at different level of renal medulla (from the tip of papilla to the corticomedullary border) were prepared. The paraffin sections were stained with hematoxylin and eosin for light microscopy measurements.

Micromorphometrical investigation

In the outer stripe of the outer medulla, the diameter and the number of proximal straight tubules (PST, S3 segment - thick descending limb), distal straight tubules (DST, thick ascending limb), vessel bundles (VB), outer medullary collecting ducts (OMCD) per 1 mm^2 were estimated. In the inner stripe of the outer medulla, the diameter and the number of DST, TLH, VB and OMCD were determined. In the inner medulla at the border to the outer medulla, the diameter and the number of the TLH, VB and the inner medullary collecting ducts (IMCD) were measured. In the renal papilla it was established the diameter and the number of TLH and the papillary ducts (DP).

Statistics

Data for number and dimensions are given as mean ± SD (Standard deviation). For that purpose was used a light microscope (ZEISS Primo Star, Germany), camera (Progres, Capture 2.6 - JENOPTIK) and software analysis programme (Soft Imaging Sistem GmbH). Statistical data processing was done using Data Analysis tool and Student's t-test by means of the StatMost for Windows software and the difference was considered significant when P-values were less than 0.05.

Results

Light microscopic observation showed that the tubules in outer and in inner medulla were located around vascular bundles (**Fig. 1** and **Fig. 2**). The diameter of PST (61.75 ± 11.92 μm) was greater than those of DST (49.63 ± 3.12 μm) with statistically significant difference $P < 0.01$. The number of PST per mm^2 (26.80 ± 0.79) was more than those (26.80 ± 0.79) of DST, $P < 0.001$ but the number of the cells (11.1 ± 2.64) of PST per 1 tubule was less than those of the cells of DST (15.30 ± 1.70), $P < 0.01$.

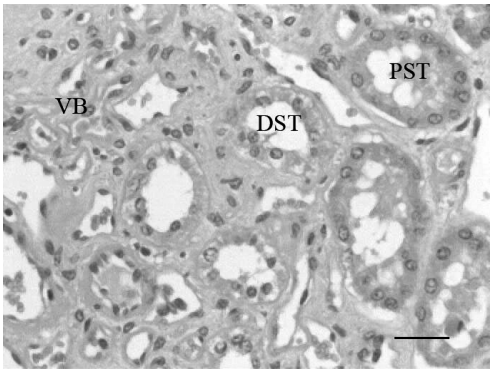

Fig. 1. Proximal (PST) and distal (DST) straight tubules situated around vascular bundles (VB) consist of arterioles and venules in the outer medulla. Bar = 25 μm

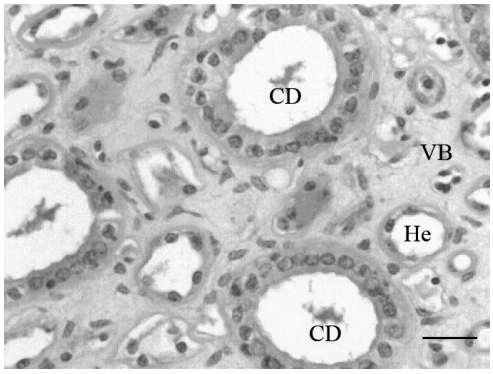

Fig. 2. Collecting ducts and thin limbs of Henle near the arterioles and venules of vascular bundles in the inner medulla. Bar = 25 μm

The number and the diameter of OMCD in the outer (16.40 ± 0.69 and 62.06 ± 7.12 μm, respectively) and in the inner stripe (16.4 ± 0.70 μm and 62.01 ± 7.29 μm, respectively) of the outer medulla were the same. The height and number of simple columnar epithelial cells of collecting ducts increased towards the inner medulla (from 11.92 ± 0.45 μm and 16.2 ± 2.15 μm in the outer stripe to 14.16 ± 1.10 μm and 48.10 ± 7.75 μm, respectively in the inner medulla). However, the width of this epithelium decreased to the inner medulla. In the tip of the papilla the columnar epithelial cells of IMCD is replaced by higher (25.82 ± 2.19 μm) transitional epithelium of *Ductus papillaris*. In the papillary duct, the number of epithelial cells increased to 54.20 ± 5.14. The diameter of DP was the largest (136.56 ± 13.07 μm). The distance between OMCD in the outer stripe (40.90 ± 21.11 μm) and in the inner stripe (40.45 ± 20.03 μm) remained the same but the distance between the IMCD decreased in the inner medulla at the border to the outer medulla. In the papilla, the distance between the DP was 106.55 ± 28.58 μm which is longer than those between IMCD, on the one hand, and those between OMCD, on the other hand. In the inner stripe the number of DST increased to 49.30 ± 1.16 but the number of DST cells remained the same. The OMCD cells are almost as high as in the outer stripe. The diameter of TLH in the inner stripe (19.01 ± 1.30 μm) and in the inner medulla at the border to the outer medulla (19.23 ± 0.67 μm) unchanged, but in the tip of papilla it increased to 32.18 ± 32.15 μm. The number of TLH increased from the inner stripe (11.50 ± 1.35) to the inner medulla (16.6 ± 1.26) at the border to the outer medulla but decreased in the tip of papilla to 8.70 ± 0.20. The ratio between TLH and CD increased from the inner stripe (2.40 ± 1.08 to 1, respectively) to the inner medulla (3.40 ± 0.52 to 1, respectively) at the border with outer medulla. In the tip of papilla this ratio was the smallest (1.80 ± 0.79 to1, respectively).

The diameter and the number of VB per 1 mm^2 in the outer (292.64 ± 12.63 μm and 1.00±2.34, respectively) and in the inner stripe (287.99 ± 35.63 μm and 1.00 ± 2.34, respectively) of the outer medulla were the same. In the inner medulla at the border with the outer medulla their diameter decreased to 225.77 ± 51.89 μm and their number increased to 3.40 ± 0.52. In the papilla only single arterioles were found. In this part of medulla, the capillaries dominated.

Discussion

The results of our research on the structural features of the porcine renal medulla using light microscopy correlate with studies on renal medulla in species which possess both long- and short-looped nephrons by several authors. Most species have both short- and long-looped nephrons. However, cats, dogs, and many species native to arid climates have only long-looped nephrons, which conserve water more efficiently than short-looped nephrons. Conversely, beavers, which live in fresh water, have only short-looped nephrons [3].

The inner medulla of porcine kidney was located deep to the outer medulla. It contains no thick ascending limb segments, only collecting ducts and descending and ascending thin limbs of Henle's loop in addition to capillaries. As it can be seen in the reports by Dellman and Eurell [3], the inner medulla can be subdivided into the base and the papilla. The base is adjacent to the outer medulla. The papilla, is the terminal portion of the inner medulla, which extends into the renal calices.

Compared to the medullary architecture of other mammalian species (rat [9], mouse [10] and Psammomys [6]) investigated in detail the rabbit renal medulla is the most simply organized. In the rabbit kidney all the vascular bundles are of the same small size and are regularly distributed throughout a cross-section of the inner stripe. They do not fuse, reflecting in the whole medulla the state of the bundles as originally developed in the outer stripe. In the current study, the same pattern of vascular bundles organization was observed in swine. This fact is evidence that the vascular architecture of porcine renal medulla is much closer to those of rabbit than the other rodents.

The inner stripe of the outer medulla is the most constant part of the renal medulla [4, 5, 9]. The tubules are arranged around these bundles in a pattern similar to that found in the outer stripe. This pattern of the tubular and vascular organization of medulla was confirmed by the current study, which means that porcine renal medulla belongs to the simple type of renal medulla.

The inner medulla is very differently developed among species. Species (mountain beaver, muskrat) with only short loops of Henle do not have an inner medulla and their urine-concentrating ability is poor [11, 14]. All species with high urine-concentrating ability have a well developed inner medulla [1, 13, 15].

Regarding the ratio between Henle's loops and collecting ducts along the inner medulla, considerable differences are found when comparing the base with the tip of the inner medulla; there are interspecies differences [7]. Our findings are closer to those in rat than those in rabbit.

The final sodium concentration of the interstitial tissue of the inner medulla is the result of the interaction of sodium and water transport from both Henle's loops and collecting tubules. According to Kokubo et al. [8], the rabbit kidney is structurally similar to those of man and swine. Sasaki and Suwa [12] calculated that this structural feature counteracts the effect of producing a gradient of sodium concentration towards the medullary apex on the basis of the countercurrent multiplier system. They regarded the Henle's thin segment as an exchanger, sodium depriving system. However, in contrast to man and swine, thin loops of Henle was less than collecting ducts along the entire length of the inner medulla in dog and hamster. According to Kokubo et al. [8], this finding indicates that in the pile of Henle's loop, short loops predominate over long ones. The concentration ability of the urine is the highest in hamster, followed in order by dog, man and swine.

Conclusion

In this study, the tubular and vascular architectural pattern of porcine renal medulla showed that it belongs to simple type of renal medulla and is structurally similar to that of man and rabbit, as a whole. However, it was established that some differences from this pattern exist, such as the ratio between Henle's loops and collecting ducts along the inner medulla is closer to that in rat than in rabbit. It was observed that in the outer and inner medulla of swine, the collecting ducts were situated almost regularly and did not tend to form groups of four ducts as they do in rabbit and man. So we can assume that the domestic swine renal medulla has specific tubular organization which defines the differences in concentration ability in comparison with other mammals.

References

1. **Altschuler, E. M., R. B. Nagle, E. J. Braun, S. L. Lindstedt, P. H. Krutzsch.** Morphological study of the desert heteromyid kidney with emphasis on the genus perognathus. – Anat. Rec., **194**, 1979, 461-468.
2. **Beeuwkes, R. and J. V. Bonventre.** Tubular organization and vascular-tubular relations in the dog kidney. – Am. J. Physiol., **229**, 1975, 695-713.
3. **Dellman, H. D., J. Eurell.** Textbook of Veterinary Histology, 1st edition. Lippincott Williams & Wilkins, 1998, 203-223.
4. **Dobyan, D. C., R. Bulger.** Morphology of minipig kidney. – J. Electron. Microsc. Tech., **9**, 1988, 213-234.
5. **Kaissling, B., W. Kriz.** Structural analysis of the rabbit kidney. – Adv. Anat. Embryol. Cell Biol., **56**, 1979, 1-123.
6. **Kaissling, B., C. de Rouffignac, J. M. Barrett, W. Kriz.** The structural organization of the kidney of the desert rodent Psammomys Obesus. – Anat. Embryol., **148**, 1975, 121-143.
7. **Knepper, M. A., R. A. Danielson, G. M. Saidel, R. S. Post.** Quantatative analysis of renal medullary anatomy in rats and rabbits. – Kidney Int., **12**, 1977, 313-323.
8. **Kokubo, T., M. Tauanashi, F. Furukawa, K. Nagano, Y. Hayasi, T. Takanashi.** A Comparative Histometrical Analysis of Renal Inner Medulla of Man, Swine, Dog and Hamster. – Tohoku J. Exp. Med., **142**, 1984, 77-88.
9. **Kriz, W.** Structural organization of renal medulla: Comparative and functional aspects. – Am. J. Physiol., **241**, 1981, R3-R16.
10. **Kriz, W., J. Schnermann, H. Koepsell.** The position of short and long loops of Henle in the rat kidney. – Z. Anat. Entwicklungsgesch., **138**, 1972, 301-319.
11. **Pfaller, E. W., W. C. Nungesser, D. A. Iverson, J. F. Wallerrius.** The renal anatomy of primitive rodent, Aplodontia rufa, and a consideration of its functional significance. – Anat. Rec., **137**, 1960, 227 -235.
12. **Sasaki, Y., N. Suwa.** Functional model of inner medulla of rabbit kidney based on its structural principle. – Tohoku J. Exp. Med., **98**, 1969, 33-63.
13. **Schmidt-Nielsen, B., R. O'Dell.** Structure and concentrating mechanism in the mammalian kidney. – Am. J. Phisyol., **200**, 1961, 1119-1124.
14. **Schmidt-Nielsen, B., E. W. Pfeiffer.** Urea and urinary concentrating ability in the mountain beaver Aplodontia rufa. – Am. J. Phisyol., **218**, 1970, 1370-1375.
15. **Sperber, J.** Studies on the mammalian kidney. – Zool. Bidrag., **22**, 1944, 249-431.
16. **Swindle, M. M., A. Makin, A. J. Herron, F. J. Clubb Jr, K. S. Frazier.** Swine as models in biomedical research and toxicology testing. – Vet. Pathol., **49**(2), 2012, 344-356.
17. **Swindle M. M., A. C. Smith.** Comparative anatomy and physiology of the pig. – Scand. J. Lab. Anim. Sci., **25**(1), 1998, 1-10.

Corresponding author:
e-mail: iv_stefanov@uni-sz.bg

Institute of Experimental Morphology, Pathology and Anthropology with Museum
Bulgarian Anatomical Society

Acta morphologica et anthropologica, 21
Sofia ● 2015

Anthropology and Anatomy

Morphometric Characteristics of the Brain Ventricular System Based on the Magnetic Resonance Imaging Data

S. Baybakov, L. Gorbov

Kuban State Medical University, Krasnodar, Russia, Dept. of Normal Anatomy

In this study there are presented the results of a morphometric description of brain ventricle sizes based on the data collected via the magnetic resonance imaging in 60 men and 60 women of early adulthood. Study includes the magnetic resonance imaging scans of the heads of people who were specifically proven not to have any cerebral pathology. There were studied the linear sizes of the liquor system objects, the comparison of those parameters in men and women was carried out as well. For those objects that have a chiral symmetry, the bilateral differences were also determined.

Key words: magnetic resonance imaging, brain ventricles, early adulthood, bilateral symmetry, gender differences.

Introduction

Magnetic resonance imaging (MRI) is one of the new methods that provides the imaging that is used in medicine. In its physical and technical basis it is drastically different from the other methods used up to this day. It is based on the combined use of the magnetic field and radiofrequent impulses. MRI and its modifications allow to collect valuable data about anatomical systems and organs in vivo. The ways that the MRI may be used in anatomy are: a) anatomical interpretation of the MRI scans in preparation of cadaver slices in the dimensions, examined by the MRI; b) using the MRI scans as the source of the anatomical information, thus when determining a diagnosis the clinicist should compare the image of the pathological object to that of a normal one. Thus, one of the goals of modern human anatomy is to determine the quantitative and qualitative characteristics of various organs in vivo via the MRI in order to form a system of traits that characterize a normal live human organ.

Magnetic resonance imaging is a highly informative method when observing organs with a high water content. One of the most commonly studied objects is the central nervous system. MRI can be used to observe almost any part of the brain [2, 3]. Almost all parts of the brain relief can be seen. Individual and age-related features of the fissures and the gyri can be defined as well as the ratio between grey and white matter on different levels. Due to the high intensity of the signal sent by the cerebrospinal fluid, the ventricular system of the brain can be clearly visualized.

Materials and Methods

The goal of this study was to observe the morphometric characteristics of the ventricular system of the brain in patients of the early adulthood via the MRI. This research was carried out on the magnetic resonance images from a private archive. 120 images were studied (T1 and T2) in 60 men and 60 women aged 25. The application of the morphometric techniques followed the recommendations of the encephalometrics guidelines [1].

Results and Discussion

In men the length of the anterior horn of the right lateral ventricle (LV) is 29.3 ± 2.74 mm, of the left – 28.6 ± 2.78 mm. In women the length of the anterior horn of the right LV is 27.4 ± 2.73 mm, the left one – 26.3 ± 2.52 mm, which is 4.18% less, than that of a right LV ($p < 0.05$). Thus, the length of the anterior horn of the right and the left LV of men is respectively 6.93% and 8.47% more than that of women ($p < 0.05$).

The width of the anterior horn of the LV of the right hemisphere in men equals 7.8 ± 1.69 mm, in the left hemisphere – 7.2 ± 1.14 mm. Gender and interhemispheric variability has not been determined.

The length of the central part of the LV in the right hemisphere of men equals 38.8 ± 5.14 mm, in the left hemisphere – 39.4 ± 6.37 mm. In women the length of the central part of the right LV equals 41.4 ± 6.93 mm, the left LV – 42.4 ± 4.85 mm. Interhemispheric asymmetry was not present, although, the length of the central part of the left LV of women is 7.61% higher than that of men ($p < 0.05$).

The width of the central part of the right LV in men is 11.3 ± 2.64 mm, in women – 11.1 ± 1.94 mm. The width of the central part of the left LV in men equals 10.8 ± 2.53 mm, in women – 11.2 ± 2.20 mm. Gender and interhemispheric variability hasn't been statistically determined.

The length of the posterior horn of the right LV in men was 34.8±8.49 mm, the left LV – 33.8 ± 6.97 mm. In women there was noted an interhemispheric asymmetry: the length of the left posterior horn is 25.5 ± 8.87 mm, the right one – 27.3 ± 9.17 mm, which is higher by 7.06% ($p < 0.05$). Gender variability presents: the length of the right and left posterior horns of men is higher by 27.47% and 32.55% respectively than those of the posterior LV horns of women ($p < 0.05$).

The width of the posterior LV horn in the right hemisphere in men equals 10.4 ± 2.23 mm, in women – 9.6 ± 1.87 mm; in the left hemisphere of men – 9.9 ± 1.86 mm, of women – 8.7 ± 2.18 mm. Interhemispherical variability was not noted among men, although in women the size of the right posterior horn is 10.34% more than that of the left. Also the length of the left posterior horn of the LV in men is 13.79% is higher than that of women ($p < 0.05$).

In men the length of the inferior horn of the LV in the right hemisphere is 45.3 ± 6.34 mm, in the left hemisphere – 47.8 ± 5.27 mm, which is 5.52% higher ($p < 0.05$). In

women the length of the inferior horn of the right hemisphere is 44.7 ± 4.87 mm, in the left hemisphere – 46.5 ± 4.73 mm. Gender differences were not noted.

The anteroposterior size of the right LV of men equals 89.4 ± 10.9 mm, of women – 84.5 ± 10.00 mm. The anteroposterior size of the left ventricle of men equals 88.3 ± 11.2 mm, of women – 81.7 ± 10.11 mm. Thus, in women the anteroposterior size of the right ventricle is 3.48% bigger than that of the left ventricle ($p < 0.05$). In men the anteroposterior size of the right ventricle is 8.08% bigger than that of the left ventricle ($p < 0.05$).

The distance between the anterior horns of the LV equals in men – 33.2 ± 2.51 mm, in women – 32.1 ± 3.23 mm.

The distance between the posterior horns of the LV is: in men – 47.6 ± 8.80 mm, in women – 45.4 ± 9.82 mm.

The length of the III ventricle in men equals 32.7 ± 3.68 mm, and in women – 28.6 ± 2.75 mm which is less than that of the men by 14.33% ($p < 0.05$).

The height of the III ventricle is also 13.70% higher in men than in women: in men – 24.9±2.78 mm, in women – 21.9 ± 3.54 mm ($p < 0.05$).

The width of the III ventricle in men equals 4.6 ± 0.17 mm, in women – 4.6 ± 0.18 mm.

The length of the aqueduct in men is 14.4 ± 2.00 mm, in women – 13.8 ± 1.64 mm.

The sizes of the IV ventricle also had no gender features. The length of the IV ventricle in men equals 44.3 ± 5.60 mm, in women – 44.4 ± 4.21 mm. The height of the IV ventricle in men is 11.8 ± 2.03 mm, in women – 11.2 ± 1.87 mm.

Thus, this study has determined the morphometric parameters of the brain ventricles in a live human. It has shown the morphometric criteria of the gender and interhemispheric variability of the ventricular system of the brain. The data received may be interesting for the medical anthropology specialists as well as for the neurosurgeons because it may help in determining the stage of the hydrocephalus and in order to objectify the stereotaxic calculations.

References

1. **Moller, T., E. Reif.** Pocket atlas of cross-sectional anatomy: Computer tomography and magnetic resonance imaging. New York, Thieme, 1994. 264 p.
2. **Yock, D. H.** Magnetic resonance imaging of CNS disease. Mosby, St. Louis, 1995. 351 p.
3. **Кандель, Э. И.** Функциональная и стереотаксическая нейрохирургия. Москва, Медицина, 1981. 368 с.

Institute of Experimental Morphology, Pathology and Anthropology with Museum
Bulgarian Anatomical Society

Acta morphologica et anthropologica, 21
Sofia ● 2015

Free Nerve Endings in Biological Active Point ST_{36} of Rat

N. Dimitrov[*], *D. Atanasova*[**], *D. Sivrev*[*]

[*]*Department of Anatomy, Faculty of Medicine, St. Zagora, Bulgaria*
[**]*Institute of Neurobiology, Bulgarian Academy of Sciences, Sofia, Bulgaria*

Point Stomach 36 (ST_{36}) is one of the most important and most commonly used in acupuncture biological active point (BAP). The aim of the study is to determine the presence or absence of free nerve endings in the area of acupuncture point ST_{36}. Free nerve endings are unencapsulated, they are the most common type of nerve ending, and are most frequently found in the skin. Free nerve endings infiltrate the epidermis and surround hair follicles. We observe a large amount of hair follicles in the dermis with sebaceous glands. We observe accumulation of free nerve endings around the hair follicles. The nerve innervations in the hair follicles possibly play a role for the effect of acupuncture at point ST_{36} in rats.

Key words: acupuncture, BAP – biological active point, histology, rat, ST_{36}, free nerve endings.

Introduction

In the last century, the traditional Chinese medicine has been increasingly used for treatment or improvement of the general state of chronic diseases, as well as an additional physio-therapeutic agent, enhancing the primary therapeutic methods [2]. Point ST_{36} is one of the most important and most commonly used biological active points (BAP) in acupuncture. Free nerve endings in the skin play an important role in the effects of acupuncture [3]. Receptors and free nerve endings in the skin play an important role in the effects of acupuncture and interpretation of responses to mechanical signals [1, 2, 4]. The aim of the study was to determine the presence or absence of free nerve endings in the area of acupuncture point ST_{36}. For the implementation of the objective we identified the following main tasks: 1) by appropriate specific staining techniques to visualize any free nerve endings in the ST_{36}, 2) by light microscopy to determine the presence or absence of free nerve endings in the area of acupuncture point ST_{36}.

Materials and Methods

We observed 12 adult normotensive rats, Wistar strain of either sex weighing ranging between 220 and 350 g. The area around the BAP was epilated, defined and marked with the method of standard proportion of anatomical structures [5] under the control

of the apparatus KWD-808 measuring skin resistance. Point ST_{36} had been previously marked and we put acupuncture needle in it for some time. The material was taken and treated without removing the needle for better visualization of the acupuncture channel. The samples were cut into freezing microtomes with thickness of 15, 20 to 40 μm. We used the following 2 stains: Bodian and Bielschowsky.

Results

We observe a large amount of hair follicles in the dermis with sebaceous glands (**Figs. 1, 3**)**.** Free nerve endings infiltrate the epidermis and surround hair follicles. We observe accumulation of free nerve endings around the hair follicles (**Figs. 2, 4, 5, 6**).

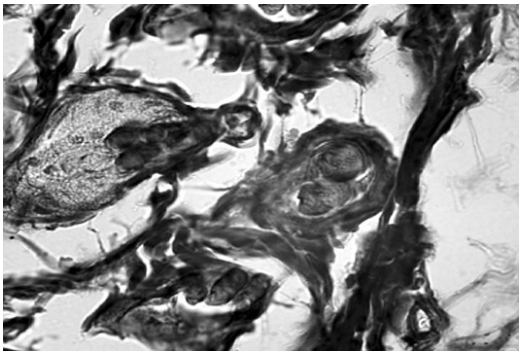

Fig. 1. Free nerve ending around hair follicles (Bielschowsky*)*

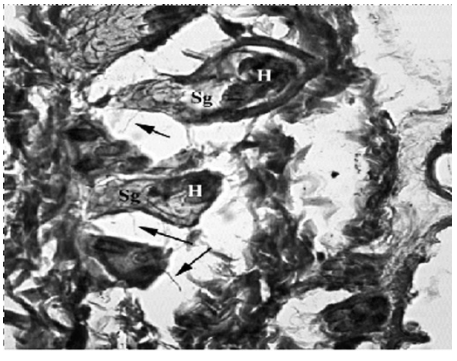

Fig. 2. Free nerve ending around hair follicles (Bielschowsky) free nerve ending around hair follicles (arrow), H. hair follicles, Sg. sebaceous gland

Fig. 3. Free nerve ending around hair follicles (Bielschowsky)

Fig. 4. Free nerve ending around hair follicles (arrow). (Bielschowsky) *H.* hair follicles*, Sg.* sebaceous gland

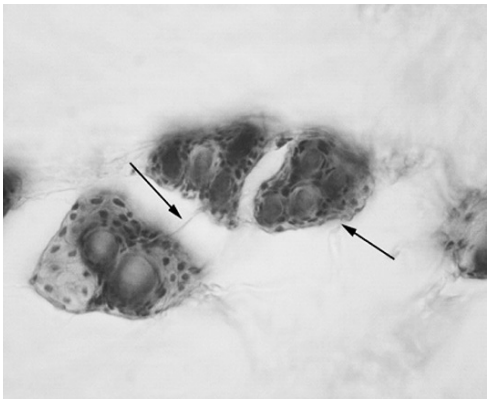

Fig. 5. Free nerve ending around hair follicles (arrow) (Bodian)

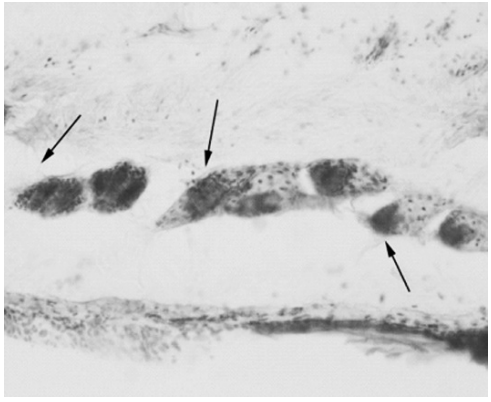

Fig. 6. Free nerve ending around hair follicles (arrow) (Bodian)

Discussion

Concentration of free nerve ending around hair follicles has been observed by other authors [4, 6]. Hair follicles and piloerection muscles associated with meridian and acupuncture effect [5]. We cannot confirm at this stage the difference in the number of free nerve endings at the point and the surrounding tissues. The nerve innervations in the hair follicles possibly play a role for the effect of acupuncture at point ST_{36} in rats.

Conclusions

We observe concentration of free nerve endings in the dermis around the hair follicles at the point ST_{36} in rats. The nerve innervations in the hair follicles possibly play a role for the effect of acupuncture at point ST_{36} in rats.

References

1. **Banes, A., M. Tsuzaki, J. Yamamoto, T. Fischer, B. Brigman, T. Brown, M. Miller.** Mechanoreception at the cellular level: the detection, interpretation and diversity of responses to mechanical signals. – Biochem. Cell. Biol., **73**, 1995, 349-365.
2. **Dimitrov, N., D. Sivrev, N. Pirovski, A. Georgieva.** Methods for localization of BAP of the human body. – Journal of Biomedical & Clinical Research, **2**(1), Pleven, 2009, 19-21.
3. **Langevin, H., D. Churchill, J. Fox, G. Badger, B. Garra, M. Krag.** Biomechanical response to acupuncture needling in humans. – J. Appl. Physiol., **91**(6), 2001, 2471-8.
4. **Liyuan, L.** Hair follicles and piloerection muscles associated with meridian and acupuncture effect. – Journal of Accord Integrative Medicine, **5**(1), 2009, 37-44.

5. **Liyuan, L., P. Juan, H. Zhang, Y. Limin.** The Morphological structure of the skin along the meridian and the transmitting mechanism of arrector pili muscle-sympathetic axon reflex. – Acupuncture Research, 04, 2002. (http://en.cnki.com.cn/Article_en/CJFDTOTAL-XCYJ200204006.htm).
6. **Zhang, K., R. Dang, L. Guan.** A morphological study on the receptors of acupuncture points. – J. Trad. Chin. Med., **2**(4), 1982, 251-260.

Address for correspondence:
Dr Nikolay Dimitrov
Department of Anatomy
Faculty of Medicine
11 Armeyska Str.
6000 Stara Zagora, Bulgaria
e-mail: nikolaydd@abv.bg

Institute of Experimental Morphology, Pathology and Anthropology with Museum
Bulgarian Anatomical Society

Acta morphologica et anthropologica, 21
Sofia ● 2015

Changes in Collagen and Elastic Fibers in Biological Active Point ST_{36} of Rats after Experimental Acupuncture

N. Dimitrov[*], , D. Atanasova[**], J. Staykova[***], N. Pirovski[****], D. Sivrev[*]

[*]*Department of Anatomy, Faculty of Medicine, St. Zagora, Bulgaria*
[**]*Insitute of Neurobiology, Bulgarian Academy of Sciences, Sofia, Bulgaria*
[***]*Department of General Medicine, Faculty of Medicine, St. Zagora, Bulgaria*
[****]*Department of Anatomy, Medical College, University of Thrace, St. Zagora, Bulgaria*

One of the most used methods of Chinese medicine is acupuncture. Point ST_{36} is one of the most important and most commonly used in acupuncture biologically active points (BAP). The target of this study is, by using the classic histological techniques, to identify any changes that occur in the elastic and collagen fibers under the influence of acupuncture needle. We observe deformation and partial demolition of adjacent elastic and collagen fibers and the fascia. In the needle canal elastic and collagen fibers are destroyed**.** Particles of loose connective tissue and fascia, collagen and elastic fibers fall into striated muscle, located in the depth of the point. Changes in the structure of elastic and collagen fibers are most clearly differentiated near the channel formed by the acupuncture needle, but also occur in adjacent areas of skin. The defect seen is with a minimum size and the tissue integrity recovers fast after the removal of the needle.

Key words: acupuncture, BAP – biologically active point, histology, rat, ST_{36}, elastic and collagen fibers.

Introduction

The beginning of the traditional Chinese medicine (TCM) dates back to antiquity [1]. One of the most used methods of Chinese medicine is acupuncture [1, 2]. There is a correlation between the location of acupuncture points and channels in humans and animals [2, 8]. Point ST_{36} is one of the most important and most commonly used [11] in acupuncture biologically active points (BAP). Using the classic histological techniques the aim of this study is to identify changes that occur in the elastic and collagen fibers under the influence of acupuncture needle. For the implementation of the objective we identified the following main tasks: 1) through various coloring methods to visualize the state of the tissues in ST_{36} before and after acupuncture; 2) with a light microscope to identify changes in the state of collagen and elastic fibers in the area of ST_{36} after experimental acupuncture.

Materials and Methods

We carried out the experiments on 14 normotensive rats, Wistar strain of either sex weighing 220-350 g. The point ST_{36} was localized by determining the ratio of standard anatomical structures and with the help of device KWD-808 to measure the skin resistance. Point ST_{36} had been previously marked and we put acupuncture needle for some time. The material was taken and treated without removing the needle for better visualization of the acupuncture channel. The material was cut into paraffin cut with a thickness of 5, 7 to 10 μm. Five different types of staining were applied. We used the following 5 stains: van Gieson, V. G & Elastin, Asan, Mallory, Masson.

Results

After the acupuncture we observed thickening of loose connective tissue adjacent to the acupuncture channel (**Fig. 1**). We observe deformation and partial demolition of adjacent elastic and collagen fibers and the fascia (**Fig. 6**). In the needle canal elastic and collagen fibers are destroyed (**Fig. 3, Fig. 5**). Particles of loose connective tissue and fascia, collagen and elastic fibers fall into striated muscle, located in the depth of the point (**Fig. 2**). Changes in the structure of elastic and collagen fibers are most clearly differentiated near the channel formed by the acupuncture needle, but also occur in adjacent areas of skin (**Fig. 4**). The defect seen is with a minimum size and the tissue integrity recovers fast after the removal of the needle.

Fig. 1. Thickening of loose connective tissue adjacent to the acupuncture channel (van Gieson)

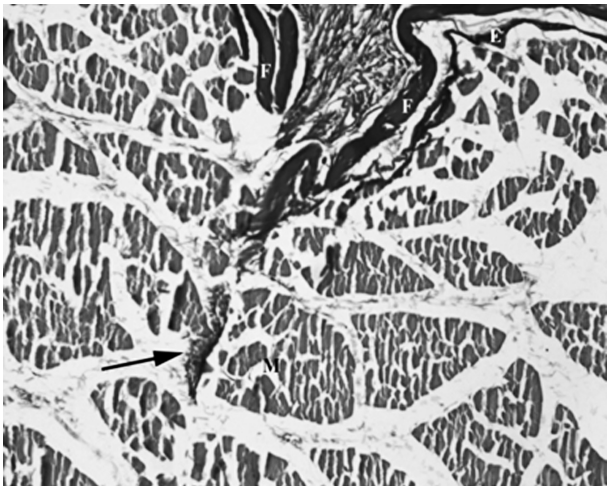

Fig. 2. Deformation and partial demolition of adjacent elastic and collagen fibers and the fascia. M – striated muscle, E – epimysium, F – fascia (arrow) (V. G & Elastin)

Fig. 3. The acupuncture channel (arrow) (Mallory)

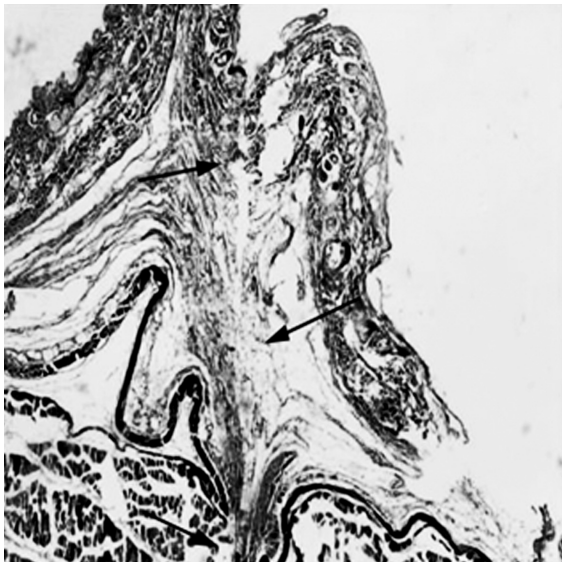

Fig. 4. Deformation of loose connective tissue adjacent to the acupuncture channel (arrow) (Asan)

Fig. 5. The acupuncture channel (arrow) (Masson) A. dermis, B. subcutaneous tissue, C. striated muscle

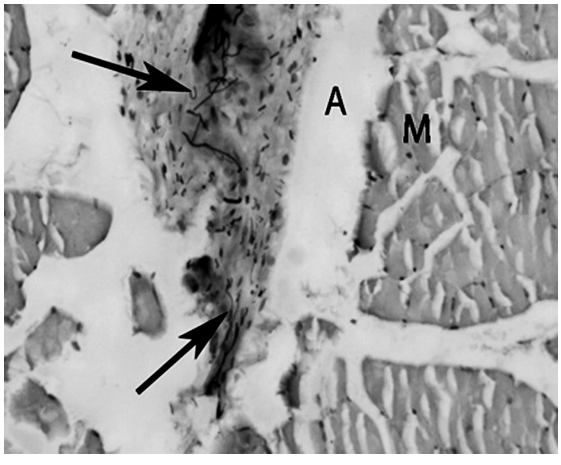

Fig. 6. Deformation and partial demolition of adjacent elastic fibers and the fascia (arrow) (Orcein) A. acupuncture channel, M. striated muscle

Discussion

The results obtained by other authors confirm the destruction to elastic and collagen fibers in the acupuncture channel formed by the needle and there is deformation in the adjacent layers and tissues are confirmed [6, 7, 4, 9, 10]. The defect seen is with a minimum size and the tissue integrity recovers fast after the removal of the needle.

Authors recognize that changes in the elastic and collagen fibers have important effect in acupuncture [3, 5, 8, 11].

Conclusions

As a result of the experimental acupuncture in ST_{36} in rat we observe deformation and partial destruction of the elastic and collagen fibers in the area of acupuncture channel. Changes in the structure of elastic and collagen fibers are most clearly differentiated near the channel formed by the acupuncture needle, but also occur in adjacent areas of skin.

References

1. **Dimitrov, N., D. Sivrev, N. Pirovski, A. Georgieva.** Methods for localization of BAP of the human body. – Journal of Biomedical & Clinical Research, **2**(1) Supplement 1, Pleven, 2009, 19-21.
2. **Dimitrov, N., D. Sivrev, Y. Staykova, Z. Goranova.** Comparative analysis of biological active channeles in humans and animals. – Proceedings of Scientific conference with international participation, Stara Zagora, **3**(1), 2008, 351-357.
3. **Duncan, G.** The connective tissue hypothesis for acupuncture mechanisms. – Journal of Chinese Medicine, **93**, 2010, 14-21.
4. **Jiang, X., X. Zhang, Y. Zhen, C. Jiu.** Advances in the study on the role of connective tissue in the mechanical signal transduction of acupuncture. – Acupuncture Research, **34**(2), 2009, 136-139.
5. **Langevin, H., D. Churchill, G. Wu, G. Badger, J. Yandow, J. Fox, M. Krag.** Evidence of connective tissue involvement in acupuncture. – The FASEB Journal, **16**(8), 2002, 872-874.
6. **Langevin, H., D. Churchill, J. Fox, G. Badger, M. Krag.** Biomechanical response to acupuncture needling in humans. – J. Appl. Physiol., **91**(6), 2001, 2471-2478.
7. **Langevin, H., D. Churchill, M. Cipolla.** Mechanical signaling through connective tissue: a mechanism for the therapeutic effect of acupuncture. – The FASEB Journal, **15**(12), 2001, 2275-2282.
8. **Langevin, H., N. Bouffard, G. Badger, D. Churchill, A. Howe.** Subcutaneous tissue fibroblast cytoskeletal remodeling induced by acupuncture: evidence for a mechanotransduction-based mechanism. – J. Cell. Physiol., **207**(3), 2006, 767-774.
9. **Langevin, H., N. Bouffard, G. Badger, D. Churchill.** Connective tissue fibroblast response to acupuncture: Dose-dependent effect of bidirectional needle rotation. – J. Altern. Complement. Med., **13**(3), 2007, 355-360.
10. **Menjo, Y., M. Kobayashi, A. Hayashi, H. Nakayama, K. Kobayashi.** Ultrastructural changes of collagen fibrils in mouse dermal connective tissue after moxibustion treatment. – Journal of Anatomy, **77**(1), 2002, 7-15.
11. **Yu, J., G. Ding, W. Yao, R. Zhan, M. Huang.** The role of collagen fiber in "Zusanli" (ST_{36}) in acupuncture analgesia in the rat. – Chinese acupuncture and moxibustion, **26**(3), 2008, 207-213.

Address for Correspondence:
Dr Nikolay Dimitrov
Department of Anatomy
11 Armeyska Str.
Stara Zagora 6000
e-mail: nikolaydd@abv.bg

Institute of Experimental Morphology, Pathology and Anthropology with Museum
Bulgarian Anatomical Society

Acta morphologica et anthropologica, 21
Sofia ● 2015

The Dominance of the Left Hemisphere is the Cause of the Bilateral Asymmetry of Shoulder Girdle Bones

L. Gorbov., S. Baybakov, A. Solntseva, A. Galkina

Kuban State Medical University, Krasnodar, Russia, Dept. of Normal Anatomy

In this article there are presented the results of studying the bilateral asymmetry of the shoulder girdle bones of 13 skeletons. The measurements were taken without detaching the latter. The highest number of linear sizes that are consistently different from the Wilcoxon criterion was discovered on the humerus, less-on the radius, no consistent differences-on ulna and the scapula. The data received allows to suggest that the reason for the morphologic asymmetry is the functional asymmetry of the brain hemispheres. This leads to one hand being dominant over another and being exposed to more exercise, which leads to the prevalent formation of the bone microrelief on the dominant side.

Key words: bilateral asymmetry, upper limb skeleton.

Introduction

In the past years the attention of the researchers is more and more drawn to the study of the morphofunctional status of the organism, which is formed under the influences of the gender, age, ethnicity, ecology, alimentary habits etc. The study of the specifics of the osteometric measures of the human body give the possibility to look at the patterns of the morphofunctional status formation from a new point of view. The interest for the osteometric research is still very much alive, even due to its 200-year-old history. The anthropometric measures are applied in the production of clothes and furniture, the designing of the ergonomic machines and mechanisms, which has a crucial importance not only for the civilian life but also for the production of the military equipment, aircrafts, submarines and the piloted space satellites. A lot of attention is paid nowadays to the study of the human skeleton asymmetry [1, 3]. At the same time the question about the origin of the morphological asymmetry is still relevant. In our opinion the reason why such an asymmetry takes place is that the number of right-handed people prevails in the human population. Currently, the ratio of the right-handed and left-handed people is estimated at about 86/14 [2], which indirectly shows the benefits of using the right hand in the manual labor.

The goal of our work is to study the scapula, humerus and the forearm bones on whole skeletons. Theoretically, the basis for such a research is the reasonable sugges-

tion that each of the skeletons is composed of the bones from one particular human, which is proven through historical data and the witness testimony.

In the course of study we were also working on proven true the hypothesis, that different functional exercise of the right (dominant) and the left (usually supporting) hand would affect the osteometric measures differently. In particular, we suggested that several right hand sizes would be substantially bigger than those sizes in the left hand.

Materials and Methods

There were examined 26 scapulas (13 left and right ones), 26 humeri, 26 ulnar and 26 radial bones of the whole skeletons from the collection of the Chair of Normal Anatomy, and also those of the Chair of the Operative Surgery and Topographic Anatomy of Kuban State Medical University. Common linear sizes available for the measurements without disassembling the skeleton were being determined, using the guidelines proposed by V. P. Alekseev (1966). The sizes were being measured by a caliper and a measuring tape. 1 mm was used as a unit of measurement. All the calculations were performed in the Excel application. The statistical processing included determining the median line, upper and lower quartiles in the spreadsheet application of Excel. The data is presented in the form of Me (p25, p75), where Me is the median line of the selection, p25 and p75 – lower and upper quartiles, respectively. Determining of the bilateral differences was performed by the methods of the non-parametric statistics with the help of the Wilcoxon criterion in the Statistica 6.15 application (StatSoft, USA).

Results and Discussion

While comparing the linear sizes of the scapula we did not receive any substantial bilateral differences among any of the studied parameters. The only feature that had a tendency to be different from right to left side ($p = 0.11$) – "the width of the glenoid cavity" – on the right it equaled 31 (30; 33) mm, and on the left – 30 (30; 32) mm. While comparing the right and the left humeri there were received the differences in such parameters as the greatest length of the humerus ($p = 0.021$), which equals 33.10 (32.22; 34.38) cm on the right, 32.95 (31.38; 33.75) cm on the left, the total length of the humerus ($p = 0.024$) is on the right 32.30 (31.90; 33.65) cm, and on the left – 32.25 (31.71; 33.25) cm, the width of the humerus at the level of the anatomical neck ($p = 0.007$), which is on the right – 3.48 (3.23; 3.82) cm, and on the left – 3.28 (3.01; 3.71) cm. Also, the substantial bilateral differences were found for the size of the circumference of the midpart of humerus diaphysis ($p = 0.015$): on the right – 7.15 (6.60; 7.53) cm, on the left – 7.10 (6.26; 7.35) cm.

While determining the extent of the bilateral asymmetry of the radius the following results have been received: the distance between the head and the radial tuberosity was substantially different ($p = 0.049$) on the right – 3.70 (3.25; 4.09) cm, and on the left – 3.50 (3.18; 3.78) cm, and the width of the diaphysis midpart as well ($p = 0.050$) on the right – 1.70 (1.58; 2.13) cm, and on the left – 1.93 (1.71; 2.20) cm. Also at the level of a tendency ($p = 0.060$) there was noted the bilateral asymmetry of the physiological radius length 23.55 (21.68; 23.85) cm, and 22.95 (21.75; 23.55) cm, and the circumference of the diaphysis midpart ($p = 0.093$) 4.65 (4.52; 5.30) cm, 4.60 (4.50; 5.20) cm, on the right and the left respectively.

While determining the extent of the bilateral asymmetry of the ulna there were received the differences only at the level of a tendency: the smallest circumference of the

diaphysis differed (p = 0.066) on the right – 3.98 (3.81; 4.43) cm, and on the left – 3.85 (3.63; 4.26) cm, also there was noted a tendency for a different (p = 0.069) extent of the ulnar diaphysis deviation from back to front – 20.48 (20.04; 21.04) cm on the right, and 19.90 (19.61; 20.93) cm on the left.

As it can be seen from the data presented, in all the cases except one – the width of the radial diaphysis midpart – the greater linear sizes were noted on the right, which allows to consider the above-mentioned hypothesis true. The lack of the substantial bilateral differences in the linear sizes of the scapula allows to suggest that the position close to the axial skeleton causes the bone to be less mobile and, consequently, lessens the differences in how the dominant and the codominant hands affect it. At the same time it is important to note that even though the forearm is much more mobile compared to the shoulder, the motor skills of the bones and the muscles in it are finer and the strain is much less. This is why the differences between the ulnar and the radial bones from different limbs are less prominent, the level of importance is much higher and the substantiality of the differences is lower than that in the study of the humerus bilateral asymmetry. Probably it is related to a higher level of physical exercise performed by the muscles attached to a humerus and, thus, more prominent bilateral differentiation of those bones.

Conclusion

Thus, the data received allows to reasonably suggest that the bilateral asymmetry of the upper limb skeleton may be related to the functional asymmetry of the brain hemispheres, which leads to one hand being dominant and also, taking into account the shift of the binomial distribution towards the right-handed individuals, to an increase of some linear sizes of the right hand in the population as a whole. Although the absolute value of the asymmetry is small, it is necessary to take it into account in the medical field, in designing of the clothing, creating the ergonomic systems etc.

References

1. **Гайворонский, И. В., Е. И. Дубовик, И. В. Крайник, Е. А Дергачева.** Асимметрия лицевого черепа у взрослого человека и возможности ее оценки (The asymmetry of the facial skull of an adult and the possibility of its evaluation). – Вестник Российской военно-медицинской академии, **1**, 2009, 140-144.
2. **Маркова, Д. А., М. О. Проскурякова, А. В. Горбунов.** Определение количественного соотношения левшей и правшей на примере дошкольников 6-7 лет в ДОУ г. Тамбова (Determination of the proportion lefties and righties for example preschoolers 6-7 years in preschool educational institution in Tambov). – Вестник Тамбовского университета. Серия: Естественные и технические науки, **18**(1), 2013, 280-281.
3. **Сидорович, С. А., Я. Е. Смолко, В. В. Гончарук.** Краниометрическая характеристика некоторых размеров глазницы (Craniometrical some characteristic size of the orbit). – Журнал Гродненского государственного медицинского университета, **3** (31). 2010, 89-91.

Institute of Experimental Morphology, Pathology and Anthropology with Museum
Bulgarian Anatomical Society

Acta morphologica et anthropologica, 21
Sofia ● 2015

Anthropometric Survey of 18-20 Years Old Adolescents from Varna

D. Naidenova, D. Stavrev, M. Yaneva

Medical University, Varna

Deviations from the normal weight are important for identifying metabolic risk. In practice, the categorization of body weight is mostly based on body mass index (BMI). The aim of this study is to obtain updated information on anthropometric status of young people aged 18-20 years from the town of Varna, to compare results with those collected 7 years ago and to match them with the standards for body weight. Deviations from normal BMI at 18-20 years old adolescents are decreased in recent years. This applies both to underweight and overweight. Obesity is a problem typical for a later age, which could be explained by the cumulative effect of years and of accumulated behavioral risk factors.

Key words: anthropometry, BMI.

Introduction

Anthropometry is one of the most accessible and informative methods for assessing growth, nutritional and health status of the individual. Modern health care systems of the past 200 years evaluate in a standardized way growth and nutrition of people with the help of anthrometric measurements [5, 6]. Deviations from the normal weight are important for identifying metabolic risk. Overweight and obesity in adolescence is associated with adverse consequences [4]. Identification of individuals with metabolic risk is done with the help of anthropometric indicators and categorization of weight as normal, overweight or obese [2]. Healthy weight determines the physical shape, greatest capacity, best health and likelihood of longest life [1, 7]. In practice, the categorization of body weight is mostly based on body mass index (BMI).

The aim of this study is to obtain updated information on anthropometric status of young people aged 18-20 years from the town of Varna, to compare results with those collected 7 years ago and to match them with the standards for body weight.

Materials and Methods

In 2013 the height and weight of 184 young people from the district of Varna were measured. Growth is measured with a precision of 1 mm using a portable stadiometer (Seca Ltd., Hamburg, Germany) in a standardized way according the procedure

of WHO. Weight was determined to the nearest 0.1 kg using a calibrated electronic scale (TANITA BC-420) in light clothing of the participants. BMI was calculated using the standard formula, introduced more than 100 years and continuously used to assess body mass and the degree of malnutrition and obesity: BMI = weight (kg)/height (m^2). Underweight, overweight or obesity were determined by applying the WHO criteria for BMI in a population aged over 18 years:

- Normal weight: 18.5 to 24.99 kg/m^2;
- Overweight: 25-29.9 kg/m^2;
- Obesity: over 30 kg/m^2;
- Risk of malnutrition: under 18.5 kg/m^2.

Surveyed adolescents represented 12% of the 12th grade pupils attending state schools in the region of Varna, according to the Regional Education Inspectorate, which makes the sample representative of the region. The study included only healthy subjects aged 18-19 years without chronic conditions limiting physical activity and capacity, and without physical abnormalities. The values were included in worksheets and analyzed.

Data was compared with results based on a similar survey conducted in 2006 among 179 young people from the same age group in Varna. The results were analyzed statistically.

Data was referred to the current WHO criteria for BMI in the population aged over 18 years, differentiated by age and sex based on international reference population [3].

Results

The analysis of the two cohorts found that one in ten young people are with underweight body weight (**Table 1**). Data from 2006 show that 12.29% of the young people have a BMI below 18.5 against 10.87% in 2013 (**Fig. 1**). The incidence of malnutrition in this age group decreased by nearly 20% over seven years.

Table 1. Representation of body weight results

Categories of body weight –WHO 1995	BMI	2013		2006	
	limit	number	%	number	%
Underweight	<18.5	20	10.87	22	12.29
Normal weight	18.5-24.99	123	66.85	110	61.45
Overweight	24.5-29.99	31	16.85%	34	18.99
Obesity I degree	30-34.99	9	4.89	7	3.91
Obesity II degree	35-39.99	1	0.54	3	1.68
Obesity III degree	40 +			3	1.68

With normal body weight were approximately 2/3 of males in both studies. This difference in the two cohorts was insignificant (61.45%-66.85%).

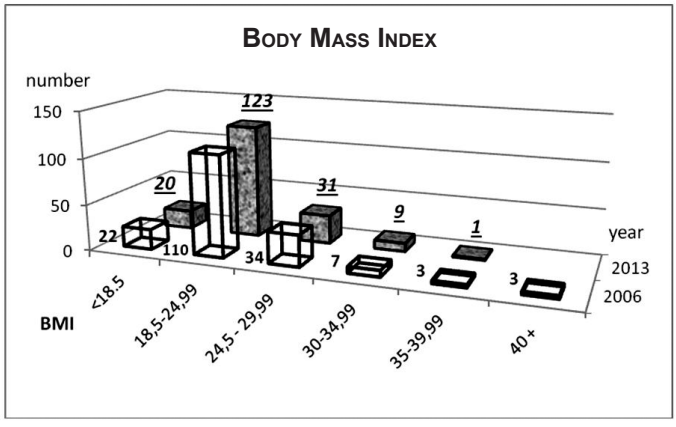

Fig. 1. Graphical representation of the body mass index results

The results for the categories overweight and obesity are intriguing. In 2006, 18.99% of the Varna adolescents were overweight compared to 16.85% of those measured in 2013 with a marked difference of 11.27% in a trend of reducing overweight. Similar is the data on obesity prevalence. The overall percentage of obese adolescents is similar in our two measurements (5.43% in 2013 against 6.27% in 2006). In the last (2013) measurement 9/10 of the adolescents with a BMI over 30 are with the lightest, first degree obesity. In the study from 2006 the distribution of light / medium / severe obesity is 2/1/1. Our results are similar to those found by the National survey of dietary intake and nutritional status of pupils in Bulgaria, conducted under the guidance of prof. Petrova and published in 2003: 19.2% of 18-19-year-olds have a BMI over 25, and 2.1% are with a BMI over 30 [3, 8].

Analysis and Conclusion

The reported results lead to the following conclusions:

1. Deviations from normal BMI at 18-20 years old adolescents are decreased in recent years. This applies both to underweight and overweight.

2. Subjects with severe obesity, referred to as "morbid obesity" are almost absent in the later study of 2013.

We can consider the conclusion that growth of individuals with overweight in recent decades should be carefully considered by the positioning of the various criteria. It should always be taken into account cultural influences and impact of public awareness of the topic "overweight". The truth is that this topic is repeatedly attracting attention and discussed in public.

Although the data of many authors about the increase of the prevalence of overweight among young people, our study found a trend to reduction of overweight in the population in the study. Obesity is a problem typical for a later age, which could be explained by the cumulative effect of years and of accumulated behavioral risk factors.

References

1. **Hershkovich, O., MD, A. Friedlander, B. Gordon et al.** Association between body mass index, body height, and the prevalence of spinal deformities. – The Spine Journal, 19 October 2013 (In press).
2. http://apps.who.int/bmi/index.jsp?introPage=intro_3.html
3. http://ncphp.government.bg/files/National%20Survey_Schoolchildren_Report++-(1).pdf
4. **Wang, L. Y., D. Chyen, S. Lee.** The association between body mass index in adolescence and obesity in adulthood. – Journal of Adolescent Health, **42,** 2008, 512-518.
5. WHO. Obesity: preventing and managing the global epidemic. Report of a WHO Consultation. WHO Technical Report Series 894. – Geneva, World Health Organization, 2000.
6. WHO. Physical status: the use and interpretation of anthropometry. Report of a WHO Expert Committee. WHO Technical Report Series 854. – Geneva, World Health Organization, 1995.
7. WHO. Report of a Joint WHO / FAO Expert Consultation. Diet, Nutrition and Prevention of Chronic Diseases. TRS 916. – Geneva, WHO, 2003.
8. Хранене и хранителен статус на учениците на възраст 7–19 години в България. Ред. С. Петрова. София, МЗ и НЦООЗ, Пропелер, 2007.

Institute of Experimental Morphology, Pathology and Anthropology with Museum
Bulgarian Anatomical Society

Acta morphologica et anthropologica, 21
Sofia ● 2015

Wormian Bones in the Coronal Suture

S. Nikolova[*], D. Toneva[*], I. Maslarski[**]

[*]*Department of Anthropology and Anatomy, Institute of Experimental Morphology, Pathology and Anthropology with Museum, Bulgarian Academy of Sciences, Sofia*
[**]*Department of Anatomy, Histology and Pathology, Faculty of Medicine, University of Sofia, Bulgaria*

The sutural bones, also known as Wormian bones, are inconstant, but of frequent occurrence. They are variable according to their shape and size. Wormian bones are defined as accidental or intercalated ossicles located in or between the cranial sutures and fontanels and have no relation to their normal ossification centers. The aim of this study is to compare the frequency, localization, sexual and intergroup differences in the Wormian bones within the coronal suture among three different cranial series. Our results show that the presence of Wormian bones in the coronal suture is a comparatively rare anatomical variation, but yet the most common pattern of distribution is a single Wormian bone localized in the C2 section. Besides, there are no significant bilateral, sexual or intergroup differences in the Wormian bones distribution in the coronal suture.

Key words: Wormian bones; coronal suture; anatomical variation.

Introduction

The sutural bones, also known as Wormian bones (Wbs), are named after the Danish anatomist Olaus Wormius, who described them in 1644. In spite of their frequent occurrence, they are inconstant and variable according to their shape and size. Wbs are defined as accidental or intercalated ossicles located in or between the cranial sutures and fontanels and have no relation to their normal ossification centers [9, 13]. It is established that Wbs most commonly appear in the lambdoid suture as they can be unilateral, bilateral or median [4, 9, 10, 13, 14, 15, 16, 17]. According to some researchers the Wbs also display a sexual dimorphism with respect to overall incidence, number, and location [2, 7, 14]. Therefore, the aim of our study is to compare the frequency, localization, sexual and intergroup differences in the Wbs within the coronal suture (CS) among three different cranial series.

Materials and Methods

The study was performed by macroscopic observation of 512 adult skulls from both sexes. The skulls were grouped into three different series: a contemporary male series

(CMS), a medieval male series (MMS) and a medieval female series (MFS). The CMS was consisted of 200 almost entirely preserved skulls from the ossuary of Bulgarian National Museum of Military History. The MMS (156 skulls) and MFS (156 skulls) were part of the bone collection of Institute of Experimental Morphology, Pathology and Anthropology with Museum, Bulgarian Academy of Sciences. The age and sex of the individuals from the medieval series were previously determined.

The presence and localization of Wbs within the sections of the CS (C1, C2 and C3) were designated as follow: **0.** Absence of Wbs within the CS; **1.** Wbs within the section C1 of the CS; **2.** Wbs within the section C2 of the CS; **3.** Wbs within the section C3 of the CS; **4.** Wbs simultaneously localized in the C1 and C2 sections of the CS; **5.** Wbs simultaneously localized in the C1 and C3 sections of the CS; **6.** Wbs simultaneously localized in the C2 and C3 sections of the CS; **7.** Single Wbs in the C1, C2 and C3 sections of the CS; **8.** Wbs along the entire length of the CS.

Results

According to our results, Wbs in CS are uncommon. Notwithstanding, if there is Wbs in CS, they are presented mainly in the C2 section, except for the CMS, where single cases of Wbs in the C1 section are established. It should be noticed, that Wbs are always single. Cases of Wbs, simultaneously placed in different sections of CS, are not observed (**Table 1**). There are no established bilateral, sexual or intergroup differences in Wbs distribution as well.

Table 1. Wormian bones in the coronal suture

Codes for designation	Contemporary male series				Medieval male series				Medieval female series			
	D		S		D		S		D		S	
	n	%	n	%	n	%	n	%	n	%	n	%
0	197	98.50	197	98.50	155	99.36	153	98.08	151	96.79	151	98.05
1	1	0.50	1	0.50	0	0.00	0	0.00	0	0.00	0	0.00
2	2	1.00	2	1.00	1	0.64	3	1.92	5	3.21	3	1.95
3	0	0.00	0	0.00	0	0.00	0	0.00	0	0.00	0	0.00
4	0	0.00	0	0.00	0	0.00	0	0.00	0	0.00	0	0.00
5	0	0.00	0	0.00	0	0.00	0	0.00	0	0.00	0	0.00
6	0	0.00	0	0.00	0	0.00	0	0.00	0	0.00	0	0.00
7	0	0.00	0	0.00	0	0.00	0	0.00	0	0.00	0	0.00
8	0	0.00	0	0.00	0	0.00	0	0.00	0	0.00	0	0.00
Total	200	100.00	200	100.00	156	100.00	156	100.00	156	100.00	154	100.00

Discussion

According to a previous investigation of Kadanov and Mutafov [9], Wbs are common, but most frequently presented in the lambdoid and coronal sutures. The Wbs greatly differ in their number, shape, localization and laterality. In other words, there is no specific pattern in Wbs distribution [9]. Our investigation shows that the presence of Wbs in CS is a comparatively rare variation, and Wbs are most commonly localized in the C2 section of the CS.

There is no agreement according to the Wbs aetiology. The mechanism of their formation is not entirely known as well. Some authors supposed that the Wbs are developed in consequence of external influence [1, 8, 16], while others assumed that they derived from normal development processes and are genetically determined [6, 11, 12, 18]. The association of Wbs with some pathological conditions is also widely discussed [3, 5, 19]. In addition, the knowledge of Wbs morphology, and the knowing of their frequency and localization within the cranial sutures and fontanels, as well as their pattern of distribution are of great importance for many scientific disciplines and that could be useful in the clinical practice.

Conclusion

The presence of Wbs in CS is a relatively rare anatomical variation, but yet the most common pattern of distribution is a single Wb localized in the C2 section. Besides, there are no significant bilateral, sexual or intergroup differences in the Wbs distribution in the CS.

Acknowledgments: This work was supported by the European Social Fund and Republic of Bulgaria, Operational Programme "Human Resources Development" 2007-2013 framework, Grant No BG-051PO001- 3.3.06-0048 from 04.10.2012.

References

1. **Bennett, K. A.** The etiology and genetics of wormian bones. – Am. J. Phys. Anthropol., **23**, 1965, 255-260.
2. **Brasili, P., L. Zaccagni, E. Gualdi-Russo.** Scoring of nonmetric cranial traits: a population study. – J. Anat., **195**, 1999, 551-562.
3. **Burgener, F. A., M. Kormano, T. Pudas.** Bone and joint disorders. Georg Thieme Verlag, Stuttgart, 2006.
4. **Da Mata, J. R., F. R. da Mata, T. A. Aversi-Ferreira.** Analysis of bone variations of the occipital bone in man. – Int. J. Morphol., **28**, 2010, 243-248.
5. **Cremin, B., H. Goodman, J. Spranger, P. Beighton.** Wormian bones in osteogenesis imperfecta and other disorders. – Skeletal Radiology, **8**, 1982, 35-38.
6. **El-Najjar, M., G. L. Dawson.** The effect of artificial cranial deformation on the incidence of Wormian bones in the lambdoidal suture. – Am. J. Phys. Anthropol., **46**, 1977, 155-160.
7. **Gualdi-Russo, E., M. A. Tasca, P. Brasili.** Scoring of nonmetric cranial traits: a methodological approach. – J. Anat., **195**, 1999, 543-550.
8. **Hess, L.** Ossicula Wormiana. – Human Biology, **18**, 1946, 61-80.
9. **Kadanov, D., S. Mutafov.** The human skull in a medico-anthropological aspect: form, dimensions and variability. – Sofia, Prof. Marin Drinov Academic Publishing House, 1984.
10. **Khan, A. A., M. A. Asari, A. Hassan.** Unusual presence of Wormian (sutural) bones in human skulls. – Warszawa, Folia Morphol., **70**, 2011 291-294.
11. **Pal, G. P., R. V. Routal.** A study of sutural bones in different morphological forms of skulls. – Anthropol. Anz., **44**, 1986, 169-173.

12. **Pal, G. P., S. S. Bhagwat, R. V. Routal.** A study of sutural bones in Gujarati (Indian) crania. – Anthropol. Anz., **44**, 1986, 67-76.
13. **Parker, C. A.** Wormian bones. Chicago, Roberts Press, 1905.
14. **Patil, M., S. Sheelavant.** Sexual dimorphism among the Wormian bones in adult human skulls. – J. Indian Acad. Forensic Med., **34**, 2012, 124-127.
15. **Murlimanju, B. V., L. V. Prabhu, C. M. Ashraf, C. G. Kumar, R. Rai, C. Maheshwari.** Morphological and topographical study of Wormian bones in cadaver dry skulls. – J. Morphol. Sci., **28**, 2011, 176-179.
16. **Sanchez-Lara, P.A., J. M. Jr. Graham, A. V. Hing, J. Lee, M. Cunningham.** The morphogenesis of wormian bones: a study of craniosynostosis and purposeful cranial deformation. – Am. J. Med. Genet. A., **143A**, 2007, 3243-5321.
17. **Wafae, N., C. R. Ruiz, L. A. Pereira, M. R. Nunes, E. Toito, J. A. Gomes.** Quantitative analysis of the sutural bones in adult human skulls. – Arq. Med. ABC, **32**, 2007, 67-69.
18. **White, C. D.** Sutural effects of fronto-occipital cranial modification. – Am. J. Phys. Anthropol., **100**, 1996, 397-410.
19. **Wolpowitz, A., A. Matisonn.** A comparative study of pycnodysostosis, cleidocranial dysostosis, osteopetrosis and acro-osteolysis. – S. Afr. Med. J., **48**, 1974, 1011-1018.

Institute of Experimental Morphology, Pathology and Anthropology with Museum
Bulgarian Anatomical Society

Acta morphologica et anthropologica, 21
Sofia ● 2015

Sacrifice – Crime or Burial Ritual. Pits with Human Remains. Recent Field Investigations

V. Russeva

Institute of Experimental Morphology, Pathology and Anthropology with Museum, Bulgarian Academy of Sciences

Many archaeological complexes present human bones in context, which to some point contradicts known outlines of the burial ritual for the investigated period. New investigations on the construction site of the Hemus highway, namely Site 6, pit N 69 and site 7, pits N 1 – square 110/20 and N 1 – square 185/5 present new similar finds in the area of the present north-east Bulgaria. Here in complex of pits, as characteristic for Iron Age are found human skeletons of four individuals**.**

Key words: Iron Age pit complex, human remains.

Materials and Methods

The site is situated by the quarter of Makak, Shumen district. During the excavations of the Iron Age pits two of them, both numbered as N 1, square 110/10 and N 1, square 185/5, presented human remains [10]. Present investigation is held in two stages. First, field one, aims strict registration of the situation of found human remains, stressing on the anatomical position and completeness of skeletons. The second laboratory, stage, aims anthropological identification of individuals, presented in excavated skeletal material. In the anthropological identification of age and sex of individuals are used following methods: epiphyseal fusion and pubic symphyseal surface relief after Todd [5], cranial sutures obliteration [9, 7]; complex of sexual dimorphism on pelvic and cranial bones [1, 7, 5], standard tables for diameters of femoral, humeral and radial heads, femoral and humeral bicondylar breadth and clavicle length [2, 3, 8].

Results

In the pit N 1, square 110/10 is registered a relatively well preserved human skeleton (**Fig. 1**). Here the skeleton is at a very unusual and unnatural position. It is relatively well preserved with some missing bones from feet and hands, explainable with the natural decomposition and taphonomic factors, which acted after the deposition of the body. Long

Fig. 1. Position of human remains in the pit N 1, square 185/5

Fig. 2. Position of human remains in the pit N 1, square 110/10

bones of limbs, vertebral column and the skull are relatively well preserved and they are found in situ in articulation in joints. The skeleton shows a strong twist of the body in deposition in the pit or, while the bones of pelvic girdle, lumbar vertebrae and lower thoracic vertebrae lie on their back (posterior sides) after rotation in the vertebral column, the bones of pectoral girdle show position of the body in that area at its left side, or lying on the bones of the left scapula and left humerus, the right humerus and right scapula covering the bones of thoracic cage. Cervical vertebrae and the skull lie on their left sides. The mandible is found in articulation with the skull. Right humerus, radius and ulna are placed with strong flexion in the elbow, wrist and hand bones being found in front of the face area of the skull. Right ulna and radius, again after a flexion in elbow, are situated over the right humerus after both hands were crossed in arms. Left wrist and hand bones are not found in the material, explicable with taphonomic destruction. The most unusual in the position of the skeleton appears the position of the lower limbs. Being in articulation in hip joints after strong flexion the bones of lower limbs lie over the bones of the trunk. After strong flexion in the knee joint the right leg was compressed over the left hip and the bones of left foot are found in the pelvic area. Left leg, after flexion in the hip joint remained extended in the knee joint being discovered with the posterior sides upward and lying over the remaining bones of the skeleton – the bones of right lower limb, the trunk and hands and bones of left foot being found in front of the face area of the skull, at a little distance from the bones of right hand.

Other case of human remains in a pit from the investigated area presents pit N 1 in square 185/5 (**Fig. 2**). Field situation shows position of bones in articulation at joints, or undisturbed anatomical position of the dead body, respectively skeleton. Bone positions present a twist and while the pelvis is situated on its right side after the twisting in the vertebral column in lumbar area, the thoracic cage and shoulders, arms and hands and the skull are placed on their anterior/face sides towards the floor of the pit. Bones

of lower limbs are positioned on their right sides and present flexion in the knee joints. After the bones of thoracic cage were removed, position of the bones of the upper limbs is registered. Both of them are flexed in the elbows, the right one located under the thoracic cage. While the left arm should have been flexed in the wrist and twisted, with final placing of the hand on its left side, the bones of the right hand show its position as palmary oriented to the pit's floor (after the position of the metacarpals and phalanges with their anterior side to that direction).

The preservation of the anthropological material for laboratory investigation is appraised as poor, the skulls are in fragmentary state, which doesn't allow reconstruction, some of the long bones of limbs don't allow reconstruction in full length as well (**Table 1**), none of the pelvic girdles can be reconstructed.

Table 1. Long bones dimensions in *mm*. D – diameter of head; B – bicondylar breadth; stature in *cm* after Tr-Gl – Trotter-Glaeser and P-L – Pearson-Lee formulae

	pit N 1, square 185/5			pit 1	110	/10
Bone	L	D	B	L	D	B
Femur dx		39.7	7.37	415		
Femur sn	446					
Tibia dx				353		
Tibia sn	306			347		
Humerus dx			57	302		
Humerus sn		41.4***	56			
Radius dx	234	2		2285		
Radius sn				222		
Cl dx	<122			137		
Cl sn	148			142		
Stature Tr-Gl	160.13*			160.98**		
P-L	155.26			155.91		

*(156.35÷163.9); **(157.11÷164.85); ***vertical

In both cases sex identification determined female sex. The age of the individual from the pit N 1, square 185/5 is ascertained at about 20 years of age (18-20 up to 25) after the epiphysis synostosis soon before death of most of long bones of limbs and unfinished synostosis of the medial epiphysis of clavicles and epiphyses of the iliac bones. The age of the individual from the pit N 1, square 110/10 is ascertained to be a little more advanced and to had reached about 30-35 up to 40 years of age at time of death after the symphyseal surface relief and cranial sutures closure. Fragments of both skeletons don't present any perimortem traumatic lesions. Pathological changes can be appraised as insignificant in comparison for known for the period and characteristic to relatively young age of the individuals.

Discussion

The situation regarded in the pit N 1, square 185/5 gives some possibilities (situation of right hand with palmar side to the floor of the pit and left one remaining in convulsive position) for interpretation of the complex as a homicide at the place. Pit 1 in square

110/10 presents a situation, which can be explained only with a deposition of strongly and neglectfully wrapped dead body, possibly right after the death before any rigidity to initiate. Many authors stressed that human remains in the pits in such complexes can't be interpreted as ordinary burials, but are result of sacrifice [4, 6]. Nevertheless, from the anthropological point of view it can't be stressed on one quality of the individuals, which to be shared in all cases. On the investigated complex both individuals are from female sex, it could be, but it is still hardly to be accepted that both individuals shared one age specific group from the point of view of age-depending social organization in the period, as one of the females is much younger. Both complexes show different situation, which testifies, that the individuals/their death bodies had been subjected to different actions before final deposition in the pits.

Conclusions

Being an unusual situation, contrasting to regular burial, the presence of human remains in both pits could be regarded as deposition of bodies of individuals shared possibly unusual/unnatural death. Possibly both complexes were result of a homicide which gives some speculations that a penalty act happened. The deposition of bodies in the pits could be a result of an attempt for giving religious significance of sacrifice as an act of penalty or needs of purification of remains of individuals subjected to such acts.

References

1. **Acsádi, G., J. Nemeskéri.** History of human life span and mortality. Budapest, Akademiai Kiado, 1970, 333.
2. **Bass, W.** Human osteology: a laboratory and field manual of the human skeleton. University of Missury, 1971, 281.
3. **Kühl, R.** Skelettreste aus prähistorische Brandbestattungen und ihre Aussagemöglichkeiten, mit Hinweisen auf spezielle Fragestellungen in Schleswig-Holstein. – MAGW, **115**, 1985, 113-137.
4. **Nekhrizov, G., J. Tzvetkova.** Ritual pit complexes in Iron Age Thrace: the case study of Svilengrad. In Anatolian Iron Ages 7. – The Proceedings of the Seventh Anatolian Iron Ages Colloquium Held at Edirne, 19-24 April 2010, 2012, 177-209.
5. **Schwartz, J.** Skelleton Keys (An introduction to human skelletal morphology, development and analysis). New York, Oxford Press, 1995.
6. **Tonkova, M.** On human sacrifice in Thrace (On archaeological evidence). Tracii si vechi in antichitate *(The thracians and their neighbours in antiquity). Studia in honorem Valerii Sirbu.* (Ed. I. Cadea), Braila, Muzeul Brailei Editura Istros, 2010.
7. **White, T., P. Folkens.** The Human Bone Manual. Elsevier, 2005, 464.
8. **Алексеев, В.** Остеометрия, методика антропологических исследований. Москва, Наука, 1966, 252.
9. **Алексеев, В., Г. Дебец.** Краниометрия, методика антропологических исследований. Москва, Наука, 1964, 228.
10. **Тонкова, М., М. Тонева, Р. Георгиева, Я. Димитров.** Селище от ранноелинистическата и ранносредновековната епоха при кв. Макак, гр. Шумен (АМ „Хемус", Обект № 7). – АОР през 2012, София, № 32, 2013, 156.

Institute of Experimental Morphology, Pathology and Anthropology with Museum
Bulgarian Anatomical Society

Acta morphologica et anthropologica, 21
Sofia ● 2015

Preliminary Results from the Investigation of Human Bone Remains from South Necropolis of Roman Deultum. Complexes with Cremation Burial Ritual

V. Russeva

Institute of Experimental Morphology, Pathology and Anthropology with Museum, Bulgarian Academy of Sciences

The study includes preliminary results from the investigation of human bone remains from 28 complexes with cremation burial ritual from the necropolis of the Roman colony of Deultum.

Key words: South necropolis, Roman colony, cremations.

Materials and Methods

During archaeological excavations on the necropolis 35 complexes with cremation are investigated, dated in the 1st-2nd c. AD, which are 41.67% from graves from the Roman period [10]. The anthropological investigation is held on field and aims at deriving maximum information from this poorly preserved material. At first all the available material is collected and analyzed, aiming recognition of the anatomical specific sites of human bones on available fragments. As in most cases cremation had been performed on place, position of the recognized fragments is documented during the investigation in order of reconstruction of body position on the burial pyre.

In anthropological identification fragments with identifiable anatomical sites are used (**Fig. 1**). For age achievement are applied methods for assessment of dental development [5, 9], epiphyseal fusion [4] and cranial sutures obliteration [7, 8]. In most cases the age is identified after data for cranial sutures obliteration, or in nine individuals, 75% from the identified in more concrete age groups (**Table 1**). For three of these cases the results from the cranial sutures obliteration are supported by other features. The sexual identification is performed by complex of dimorphism on pelvic bones [1, 7], cranial bones markers [6] and standard tables for diameters of femoral, humeral and radial heads, femoral and humeral bicondylar breadth [2, 4]. The metrical methods identified 10 of the individuals, or 62% from identified, for 12% from which obtained results are supported from additional features (**Table 2**). In the preliminary investigations is included material from 28 graves with cremation burial ritual.

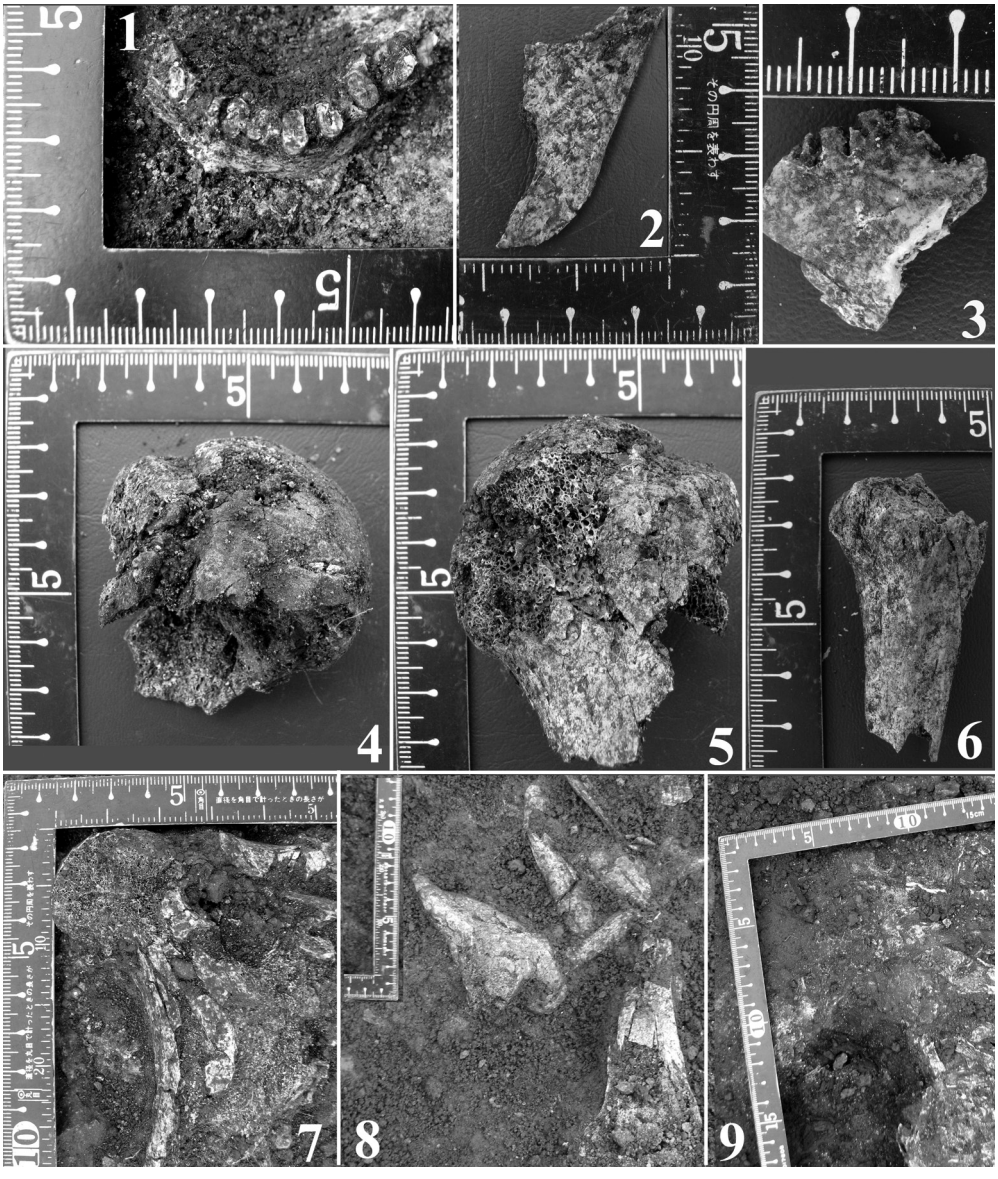

Fig. 1. Roman south necropolis, Deultum. Identifiable fragments. **1.1.** Grave N 16, field situation, mandible; present permanent teeth, pronounced mental tubers. **1.2.** Grave N 13, mandible, oval mandibular angle. **1.3.** Grave N 46, cranial fragment, parietal bone, lack of obliteration in the lambdoid suture. **1.4.** Grave N 46, head of right humerus, measurable vertical diameter, fused epiphysis. **1.5.** Grave N 46, head of left humerus, measurable vertical diameter, fused epiphysis. **1.6.** Grave N 46, head of left humerus, unfused epiphysis. **1.7.** Grave N 52, field situation, proximal part of left femur, measurable diameter of the head. **1.8.** Grave N 5, field situation, distal parts of both femurs, measurable bicondylar breadth. **1.9.** Grave N 42, field situation, left pelvic bone, narrow form of greater sciatic notch

Table 1. Distribution of the identified material in regarding to age of the individual after the available features for used methods

Age identifying features	Concrete age		Defined only as grown-ups	
	N	%	N	%
Dental development	3	25.00	1	7.14
Dental development and epiphyseal fusion		0.00		0.00
Craneal sutures obliteration	6	50.00		
Cranial sutures obliteration, epiphyseal fusion	3	25.00		
Epiphyseal fusion			13	92.86
Total	12		14	

Table 2. Distribution of the identified material in regarding to sex of the individual after the available features for used methods

Sex identifying features	N	%
Dimensions	8	50.00
Craneal feature	2	12.50
Craneal features, Massiveness, Dimensions	2	12.50
Massiveness and dimensions	2	12.50
Massivness	2	12.50
Total	16	

Results and Discussion

The investigated material allows identification of some of the individuals in broad limits of age specific groups of infants/adolescents, adults and matures for 11 complexes or 40.74% from the included in the preliminary investigation, which provide information for 12 individuals, who comprise 42.86% from defined individuals. In addition, in some more cases or 14 complexes are recognized remains, characteristic for grown-up individuals in opposite to adolescents, which couldn't obtain more precise determination of the age. Only material from eight individuals (28.7%) provide small amount of data for some more precise identification of age and sex (**Table 3**).

In age distribution is notable the small number of individuals identified as infants in the preliminary investigation (**Tables 3, 4**). This still remains a result of included material, at this stage of investigation excluding complexes, which identification was difficult on field as they presented very little number of fragments with very small dimensions. One of the explication of this state of the material in these complexes could be that they/or some of them present infant individuals. Nevertheless, without any identifying fragment their identification still remains problematic at the preliminary stage of the investigation. As in most anthropological series from the preindustrial period relative number of individuals, who died in the age of adults, between their 20-40's can be apprised as high or 66.67% in contrast to these who reached higher age at the time of death (25%) (**Table 3**). The lack of the individuals in senile age is to be explained with difficulties in recognition in the cremated material of features characteristic to that age, parallelly to the small expected number of such individuals, characteristic for preindustrial periods. The results doesn't show differences in survivorship between males

Table 3. Age and sex distribution of the identified individuals

	Infans I	Adultus		Maturus		Defined	Total
		M	F	M	F		
N	1	2	3	1	1	8	28
def %	12.50	25.00	37.50	12.50	12.50	28.57*	96.4

* – % from total investigated material.

Table 4. Age distribution of the identified individuals

	Infans I	Adultus	Maturus	Def. Age	>20 y.	Total >20 y./Inf
N	1	8	3	12	26	27
%	8.33	66.67	25.00			
%*	3.70				96.30	

* – % from identified as infants/grown-up individuals.

and females (**Tables 3, 5**), which still shell be explained more with the small number of individuals, who could receive both age and sex identification rather than with demographic specifics of the population. In individuals, who received sex identification, is visible a tendency for clear prevailer of female ones. Preliminary data from the graves with inhumation with simultaneous date with no clustering of areas of the necropolis with preference of one of the rituals [10] show possible interpretation of the latter result with preference of cremation burial ritual for females in the population. In one case (Grave N 46) was ascertained a double burial after material from an infant and a male individual (**Fig. 1**).

Table 5. Sex distribution of the identified individuals

	Adultus		Maturus		Def. Sex/ Age	Undef >20 y.		>20 y.		Def. Sex
	M	F	M	F		M	F	M	F	
N	2	3	1	1	7	2	7	5	11	16
%	25.00	37.50	12.50	12.50				31.25*	68.75*	

* – % from all individuals with defined sex.

In 24 from the studied complexes was ascertained position of the cranial fragments, which in burial ritual of the cremation on place gives some information about position of the body on the burial pyre. In directions prevail NW and SE ones with 16.67% each (**Fig. 2**). In three cases (12.5%) fragments are found at about the middle of the pit.

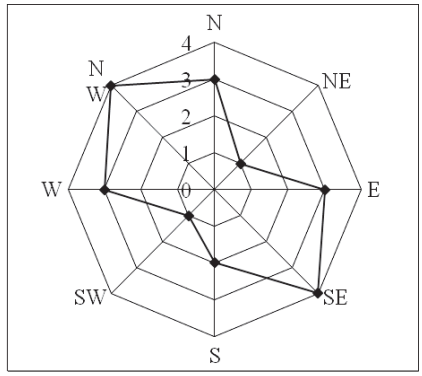

Fig. 2. Orientation of the body on the burial pyre after location of cranial fragments in grave pits

Conclusions

In spite of highly fragmentary state of the materials from graves with cremation burial ritual they could provide some information about age and sex of the individuals. These data have high value for interpretation of these complexes in the necropolis.

References

1. **Acsádi, G., J. Nemeskéri.** History of human life span and mortality. Budapest, Akademiai Kiado, 1970, 333.
2. **Bass, W.** Human osteology: a laboratory and field manual of the human skeleton. University of Missouri, 1971, 281.
3. **Kühl, R.** Skelettreste aus prähistorische brandbestattungen und ihre aussagemöglichkeiten, mit hinweisen auf spezielle fragestellungen in schleswig-holstein. – MAGW, **115**, 1985, 113-137.
4. **Schwartz, J.** Skelleton keys (an introduction to human skelletal morphology, development and analysis). New York, Oxford Press, 1995.
5. **Ubelaker, D.** Human Skeletal Remains: Excavation, Analysis, Interpretation (2nd ed.), Washington D C, Taraxacum, 1989.
6. **Walrath, D., P. Turner, J. Bruzek.** Reliability Test of the Visual Assessment of Cranial Traits for Sex Determination. – Am. J. Phys Anthropol., **125**, 2004, 132-137.
7. **White, T., P. Folkens.** The Human Bone Manual. Elsevier, 2005, 464.
8. **Алексеев, В., Г. Дебец.** Краниометрия, методика антропологических исследований. Москва, Наука, 1964, 228.
9. **Зубов, А.** Одонтология. Методика антропологических исследований. Москва, Наука, 1968.
10. **Костова, К., И. Чолаков.** Плосък римски некропол, с. Дебелт, област Бургас. – АОР през 2013, София, 2014, 297–299.

Institute of Experimental Morphology, Pathology and Anthropology with Museum
Bulgarian Anatomical Society

Acta morphologica et anthropologica, 21
Sofia ● 2015

Transatlantic Intersociety Consensus II for the Management of Peripheral Arterial Disease (TASC II for PAD) – Microscopical Structure of the Femoral Artery (FA)Wall in Patients with PAD

D. Stavrev, G. Marinov, V. Kniajhev

Medical University of Varna

The progress in medical science in the late 20th century and early 21st century made it necessary to review some of the basic guidelines of TASC for PAD, and published TASC II for PAD. One of the main ideas underlying is that due to the high individual variability of the lower limb arteries, the selection of patients requiring revascularization should be based on the presence of arterial anatomy, suitable for the intended revascularization. The study was performed on biopsies of FA from 81 patients with PAD of lower limb and on necropsies from 9 died without PAD. In patients with PAD the FA wall was remodeling. In the terminal stage of the disease differences in FA wall remodeling between the patient with revascularization and with amputation are determined much more by changes in the thickness and variability of the media than similar changes in the intima.

Key words: TASC for PAD, lower limb arteries, revascularization.

Introduction

PAD of the lower extremities occurs due to the continuous violation of their blood flow of highway arteries. The syndrome occurs mainly in men as compared to their proportion in women – 9:1 [1]. With age the incidence of the syndrome increases affecting 20% of the population of 70 years or more [9]. At the end of the last century, leading experts from Europe and North America created a TASC for PAD [6, 7, 8]. Significant progress in medical science and technology in the late 20th century and early 21st century made it necessary to review some of the guidelines and objectives of this document and published a new TASC II for PAD [4]. One of the main ideas that lie at the heart of the TASC II for PAD is that due to the high individual variability of the lower limb arteries, the selection of patients requiring revascularization should be based on the availability of anatomy of the lower limb arteries, suitable for the intended revascularization. In all studied patients with PAD, the average thickness of the media at the FA is greater than the average thickness of the intima [2, 3, 5]. In this study, the changes in the structure of the FA wall in patients with PAD of the lower limb were examined.

Materials and Methods

The biopsies of FA from 81 patients with PAD of lower limb were studied. The biopsies were taken in University Clinic of Vascular Surgery, St. Anna Hospital, Varna, from patients with PAD II-III or III-IV degree during the reconstruction of the arterial vascular bed, as well as from patients with PAD III-IV or IV degree during the amputation of the gangrened limbs. In all studied patients with PAD, the average thickness of the media at the FA is greater than the average thickness of the intima. As controls, the necropsies of FA taken from 9 cadavers without evidence of vascular disease in the Departments of Forensic Medicine, Pathology and Anatomy, Histology and Embryology, Prof. Dr. P. Stoyanov Medical University – Varna were used. Histological sections 7 μm thick, colored with Hematoxylin-eozin, Orcein, AZAN and by Van Gieson and Mallory methods, were examined using a microscope OLYMPUS BX50 equipped with a video camera Ikegami. Filming of 10-50 images of each vessel studied at different magnifications are then stored in digital form. The study was conducted by following all requirements and standards for the Ethical Treatment of patients and research biopsy and necropsy material.

Results

Thrombus formation in the FA is a multistep process, that is why along with the newly formed thrombi, old thrombi in different stages of organization are identified and incorporated. As a result it was established partial or full restoration of the lumen. In patients with reconstruction accessible area of the lumen is at least 1/3 of the cross-section, while in patients with amputation it is less than 1/5 of the cross-section. In some cases this process may lead to severe thinning of the wall of the FA and/or inability to distinguish the thrombus of the intima and the individual envelopes therebetween. In the thrombus-free areas the endothelial cells are partially preserved (**Fig. 1**), while in patients with amputation they are significantly reduced. In the thrombus-free areas of the FA intimal smooth muscle cells (SMC) are located mainly close to the media. In

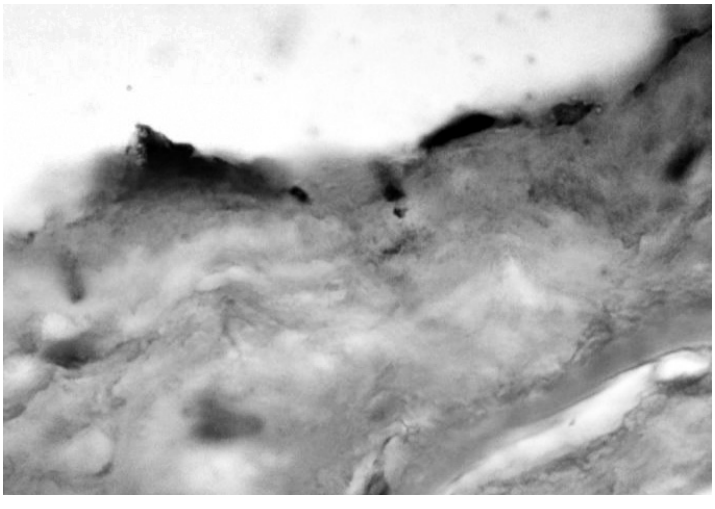

Fig. 1. Microphotographs of the wall of the Femoral artery (FA): luminal surface of FA in PAD preserved Commission. HE × 1000

all studied patients with PAD, the average thickness of the media at the FA is greater than the average thickness of the intima with longitudinal orientation. In patients with amputation their amount is reduced, they are placed more irregularly and can change their longitudinal orientation.

Intimal elastic fibers (EF) of FA in PAD are grouped subendothelially and at the border with the media form Internal elastic lamina (IEL). In thrombotic masses EF are missing. Therefore splitting between IEL establishes zones in which EF are missing. Perhaps these alternating zones are places of thrombi incorporation. Such flakings in IEL of FA in the control group are missing. Collagen fibers (CF) dimensional network formed through the thickness of the intima of the FA.

Media showed a significant resistance to the processes of remodeling. It is built mainly from transversally orientated to the longitudinal axis of the vessel SMC. They form a well-developed circular muscle layer, which is not significantly different from that in controls. The extracellular matrix between smooth muscle cells of the media is scarce. EF in uncommitted with organized thrombus wall sections are scarce and are single or rarely grouped in bundles. They do not differ from EF in the media of control arteries. At the boundary between media and adventitia the amount of fiber-like connective tissue structures increases significantly and forms pronounced fibroelastic layer. This layer passes without sharp boundary in the adventitia.

SMC in the adventitia of FA in PAD are not found. EF in this layer are thick, the amount varies, as in the inner tangential to the media areas dominated by longitudinally oriented EF. Adventitia is rich in thick CF organized in large bundles of different diameter (**Fig. 2**).

In PAD sections of the FA are with significant deformation of the wall, so that its thickness was measured only in the areas in which this shell was sufficiently well preserved structure. The points of attachment of blood clots were excluded, as in these sections organizing thrombus deleted boundary between it and the underlying part of the wall, and in some cases, the boundaries between shells. FA intimal increases its

Fig. 2. Microphotographs of the wall of the Femoral artery (FA): EF in the media and adventitia of FA in PAD. Orcein × 400

thickness. Its average thickness in patients with reconstruction exceeds that of the control and is 141% and in those with amputation is 131% against it (**Fig. 3**). FA media initially retains its thickness, but with the progress of PAD it significantly reduces. In patients with reconstruction it is 104% against it. In patients with amputation media is significantly less – 63% against it (**Fig. 4**). The intima/media (I/M) thickness is: reconstruction – 0.44, amputation – 0.97, controls – 0.34.

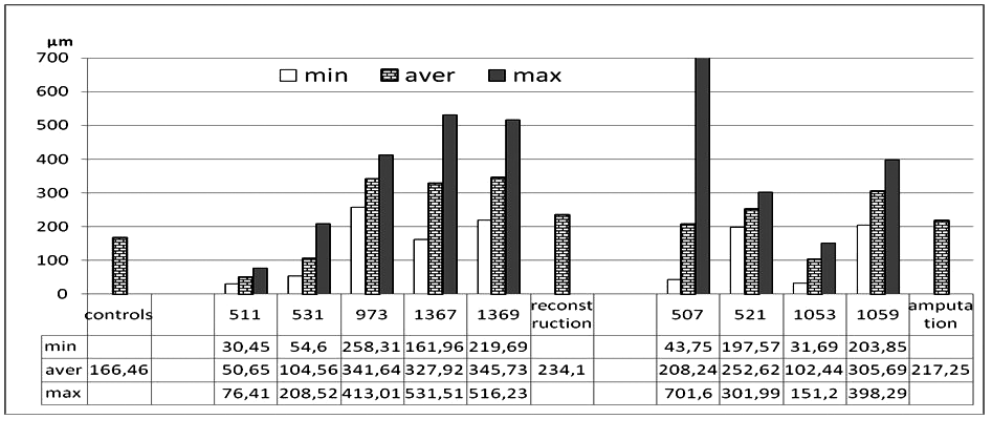

	controls		511	531	973	1367	1369	reconstruction		507	521	1053	1059	amputation
min			30,45	54,6	258,31	161,96	219,69			43,75	197,57	31,69	203,85	
aver	166,46		50,65	104,56	341,64	327,92	345,73	234,1		208,24	252,62	102,44	305,69	217,25
max			76,41	208,52	413,01	531,51	516,23			701,6	301,99	151,2	398,29	

Fig. 3. Intima thickness in µm

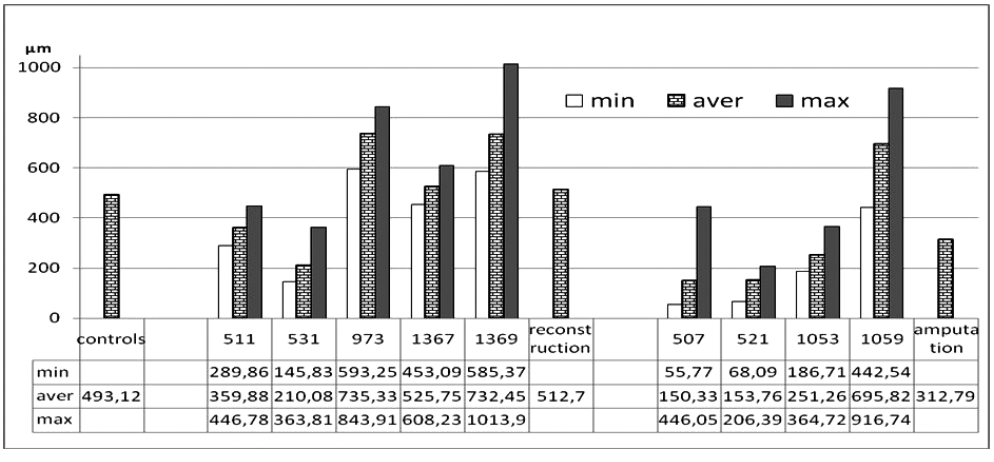

	controls		511	531	973	1367	1369	reconstruction		507	521	1053	1059	amputation
min			289,86	145,83	593,25	453,09	585,37			55,77	68,09	186,71	442,54	
aver	493,12		359,88	210,08	735,33	525,75	732,45	512,7		150,33	153,76	251,26	695,82	312,79
max			446,78	363,81	843,91	608,23	1013,9			446,05	206,39	364,72	916,74	

Fig. 4. Media thickness in µm

Discussion

In patients undergoing surgical treatment for PAD of lower limb, the wall of FA was remodeling. The process progresses with the development of the disease. The results obtained showed that in patients undergoing surgical treatment for PAD of lower limb this process has specific characteristics in terms of both location and specificity, as well as their degree of expression in the various coatings on the wall. Generally, the thickness

of the intima of FA increases with disease progression, while the media back decreases. However, in all studied patients with PAD, the average thickness of the media at the FA is greater than the average thickness of the intima The average thickness of intima in patients with reconstruction exceeds that of control – 141%. In patients with amputation intima less exceeds that of the control – 131%. Media of FA initially retains its thickness, but with the progress of PAD it significantly reduces. In patients with reconstruction it is close to that of the control - 104% against it. In patients with amputation media is significantly less – 63% against it.

In medico-biological and clinical studies evaluating of only absolute terms increases the risk of "distortion" or errors due to age, gender, racial, and other individual characteristics of the patients studied. Technological features associated with the technique and the conditions of taking material, which are also not subject to 100% uniformity and can lead to possible differences in metric reporting. For these reasons, evaluation of metric (quantitative) changes we introduced index expressing the thickness divided by intima/media (I/M) thickness. Index value I/M in patients with major amputation is twice larger than those in patients with reconstruction. In the terminal stage of the disease differences in arterial wall remodeling of FA in PAD between the two patient groups are determined much more by changes in the thickness and variability of the media than similar changes in the intima. Conducted researchs on the microscopic anatomy of the FA in patients with PAD of the lower limb showed significant variability in structural changes in the wall of this artery that must be considered when planning and performing reconstructive surgery in this area.

References

1. **Andreev, A.** Vascular deseases and applied vascular surgery. Sofia, Znanie, 2007, 72-80.
2. **Brewster, D. C.** Direct reconstruction for aortoiliac occlusive disease. – In: Vascular Surgery (Ed. Rutherford R. B.) 5th edition, Philadelphia W. B. Saunders, 2000, 943-972.
3. **Matos, J., C. F. Bechara, N. R. Barshes, B. Lowery, G. Pisimisis, S. Sharath, P. H. Lin, P. Kougias.** Comparison of outcomes between bare metal and covered nitinol stents in the treatment of TASC C and D superficial femoral artery (SFA) and popliteal lesions. – J. Vasc. Surg., **57**(5), 2013, 63S-64S.
4. **Norgren, L., W. R. Hiatt, J. A. Dormandy, M. R. Nehler, K. A. Harris, F. G. R. Fowkes** (on behalf of the TASC II working group). Inter-Society Consensus for the Management of Peripheral Arterial Disease (TASC II). – J. Vasc. Surg. 2007, **45**(1, Suppl. S), S5A-S67A.
5. **Sultan, S., W. Tawfick, N. Hynes.** Ten-year technical and clinical outcomes in TransAtlantic Inter-Society Consensus II infrainguinal C/D lesions using duplex ultrasound arterial mapping as the sole imaging modality for critical lower limb ischemia in a high-volume specialist center. – J. Vasc. Surg., **57**(4), 2013, 1038-1045.
6. TASC. Management of peripheral arterial disease (PAD). TransAtlantic Inter-Society Consensus (TASC). Eur. J. Vasc. Endovasc. Surg., **19**(Suppl. A), 2000, SI-XXVIII, S1-250.
7. TASC. Management of Peripheral Arterial Disease (PAD). TransAtlantic Intersociety Consensus (TASC). J. Vasc. Surg., **31**(1 part 2), 2000, S1-287.
8. TASC. Management of peripheral arterial disease (PAD). TransAtlantic Inter-Society Consensus (TASC). Int. Angiol., **19**(1 Suppl. 1), 2000, I-XXIV, 1-304.
9. **Андреев, А.** Съдови заболявания. София, АИ „Проф. М. Дринов", 1998. 310 с.

Institute of Experimental Morphology, Pathology and Anthropology with Museum
Bulgarian Anatomical Society

Acta morphologica et anthropologica, 21
Sofia ● 2015

Physical Development and Social Status in University Students in 1980s

R. Stoev, L. Yordanova

Institute of Experimental Morphology, Pathology and Anthropology with Museum, Bulgarian Academy of Sciences, Sofia

The purpose of this paper is to light the connections between social conditions and physical development in young adults. Data, collected in 1986 from university students in Sofia are analyzed. Although the university students are not random sample of all Bulgarian society and social differentiation in them will be rather smoothed, the analysis discovers significant social differentiation in the physical development of these students, including differences in age at menarche, height, body mass index, somatotype.

Key words: University students, age at menarche, height, body mass index, somatotype.

Introduction

The social differentiation in the physical development of young adults has established itself as a measure of the social welfare and social inequalities in the last decades [1, 2, 4, 5, 6].

The purpose of this paper is to study the social differentiation in the physical development of young adults at the end of the so called socialist period in the history of Bulgaria, in 1980s.

Materials and Methods

The individual data of 295 male and 572 female university students, investigated in 1986 in Sofia are analyzed in this study.

Their basic social characteristics were valued as follows:

1. a) Education of the parents: 1 – elementary; 2 – basic; 3 – secondary; 3,5 – college; 4 – university; 5 – scientific degree.

2. b) Birthplace and residence: 1 – village, 2 – small town (up to 25 thousands), 3 – medium town (25-100 thousands); 4 – city; 5 – Sofia.

3. c) Number of the siblings (brothers or sisters of the student).

A generalized index of social status (GISS) has been calculated by the formula:

GISS = father's education + mother's education + (birthplace + residence)/2 – number of siblings

If data of the education of one of the parents are missing (usually of the father), the value of the education of the other has been duplicated.

In practice GISS in the students varied between 4 and 12.

Then the basic anthropometric characteristics in both sexes and of age at menarche in female students were analyzed in connection with GISS.

Results and Discussion

The analysis shows strong correlations between social status and physical development, i.e. = significant social differentiation in the conditions for biological development and growth of the university students in this period.

Since the volume of this presentation is limited, the results are presented only by some graphs.

The social differences in mean age at menarche reach 0.75 year. Such differences in Europe in the 1980s were considered as very significant (**Fig. 1**).

The social differentiation of the stature is also significant, about one usual standard deviation (**Figs. 2**, **3**). The connection between GISS and body mass index (BMI) is also clear, excluding the male students of highest social status (**Figs. 4**, **5**).

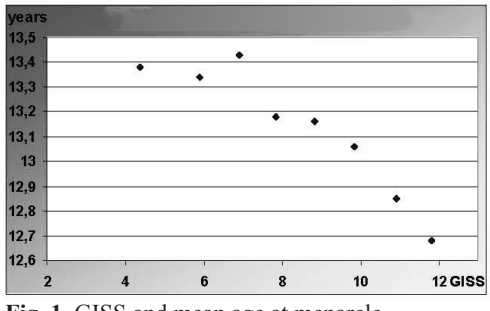

Fig. 1. GISS and mean age at menarcle

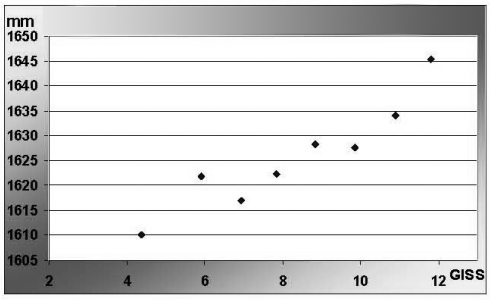

Fig. 2. GISS and mean height – female students

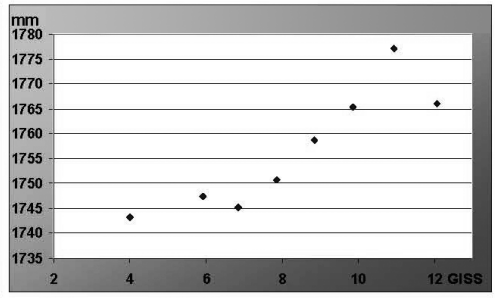

Fig. 3. GISS and mean height – male students

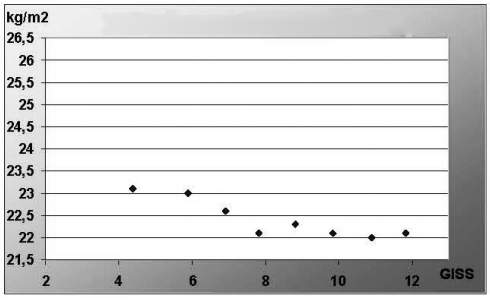

Fig. 4. GISS and BMI – female students

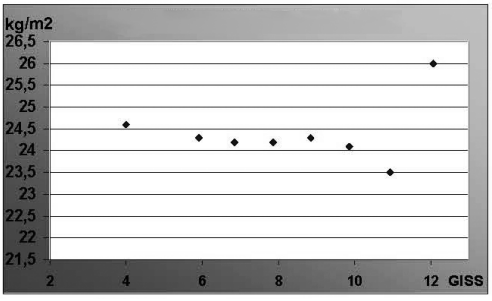

Fig. 5. GISS and BMI – male students

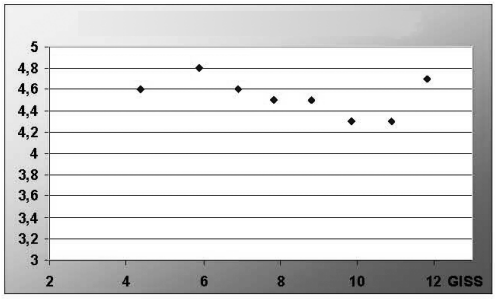

Fig. 6. GISS and endomorphy – female students

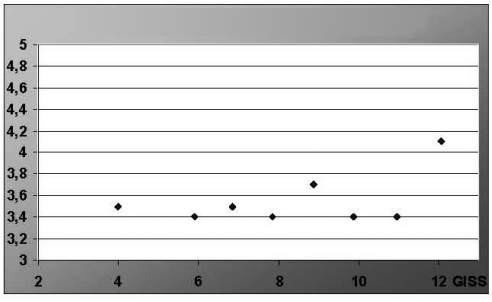

Fig. 7. GISS and endomorphy – male students

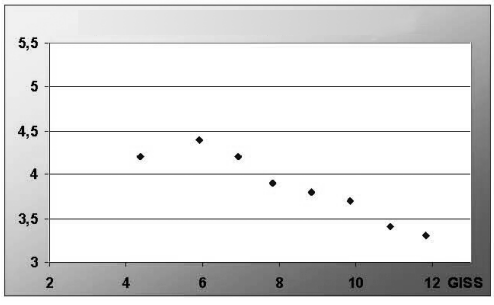

Fig. 8. GISS and mesomorphy – female students

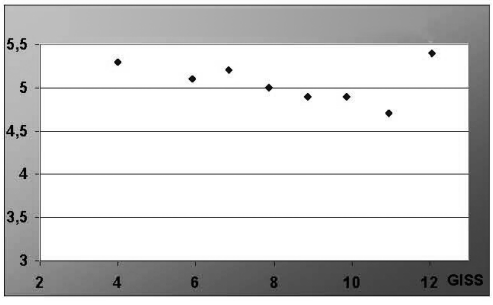

Fig. 9. GISS and mesomorphy – male students

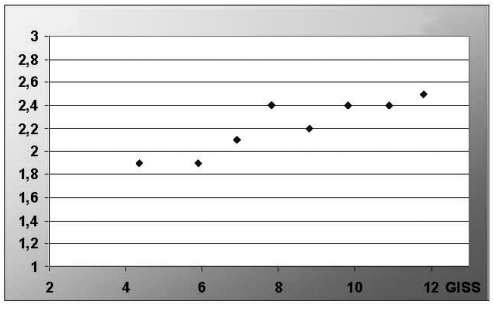

Fig. 10. GISS and ectomorphy – female students

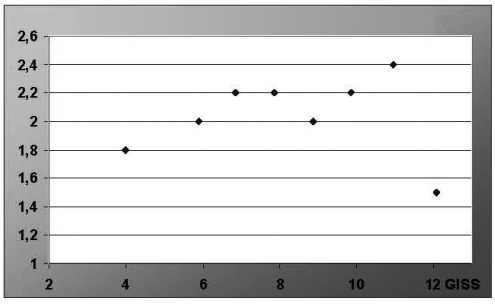

Fig. 11. GISS and ectomorphy – male students

Since BMI depends on the somatotype we shall be not surprised to find differences also in the somatotype components: endomorphy (**Figs. 6, 7**), mesomorphy (**Figs. 8, 9**), ectomorphy (**Figs. 10, 11**).

Both BMI and somatotype show that students of lower social status are more robust than these of higher social status. The same phenomenon was found in schoolchildren from the same period, 1984-1987 [3].

Since the university students are not random sample of all the Bulgarian society and social differentiation in them will be rather smoothed, and the analysis discovers significant social differentiation in their physical development, the social differentiation in the physical development of all Bulgarian youth in this period must have been very significant. So it was not a period of social equality and homogeneity as it was declared (and still is considered as such by some people).

Conclusion

In 1980s there are significant differences in the physical development of the university students in Sofia in dependence on the social environment. This fact indicates that the social environment was not homogenous and there were unfavorable conditions for children's and adolescents' growth and development in some social strata.

Since social differences have multiplied in the following 30 years (which is a well known fact), there is a pressing need similar investigations to be carried out on the influence of the social environment on the growth and development of the contemporary children and adolescents.

References

1. **Baten, J., M. Blum.** Growing taller, but unequal: Biological well-being in world regions and its determinants, 1810-1989. – Economic History of Developing Regions, **27**, 2012, 66-85.
2. **Komlos, J. D.** History of Human Height from the 17th to the 21st Century. – Paper presented on the Vth International Anthropological Congress of Ales Hrdlicka, Praha-Humpolec, 2009.
3. **Stoev, R.** Somatotype in adolescents from a big city and a smaller town. – Papers on anthropology (Tartu, Estonia), XIV, 2005, 344-352.
4. **Tanner, J. M.** Growth as a mirror of conditions in society. – In: Lindgren, G. (Ed.). Growth as a mirror of conditions in society. Stockholm Inst. Education Press, Stockholm, 1990, 9-70.
5. **Година, Е. З.** Ауксология человека – наука XXI века: проблемы и перспективы. – В: Антропология на пороге III тысячелетия (Ред. Т. И. Алексеева, Е. В. Балановская, Е. З. Година, Н. А. Дубова). **2**, М. Российское отделение ЕАА, 2003, 529-566.
6. **Миронов, Б. Н.** Благосостояние населения и революции в имперской России: XVIII – начало XX века. Москва, Новый хронограф, 2010, 1-911.

Institute of Experimental Morphology, Pathology and Anthropology with Museum
Bulgarian Anatomical Society

Acta morphologica et anthropologica, 21
Sofia ● 2015

Lower Division of the Common Carotid Artery – A Case Report

J. Stoyanov, D. Sivrev, I. Ivaniova, N. Dimitrov, A. Georgieva

Department of Anatomy, Faculty of Medicine, Stara Zagora, Bulgaria

Expressed variations in division of the common carotid artery are not rare. Low division (30% of the variations) is usually at the level of the middle part of the larynx. The dividing at the level of the annular cartilage is very rare and we found only one reported case of separation below the annular cartilage – at the base of the neck. The aim of the study was to determine, analyze, document and assess the presence of a rare variation – lower division of common carotid artery discovered during a dissection. Cadaveric dissection material was used. We detected a low separation of the common carotid artery – below the level of the lower edge of the annular cartilage. Knowledge of the variations of the common carotid artery and its branches is required, as in the diagnosis of disease in the neck and head, and in carrying out manipulations in these areas.

Key words: common carotid artery, division, variations, hyoid bone, neck.

Introduction

Expressed variations in the division of the common carotid artery are not rare in Europeans [9] and Africans [1]. Of these, the most common is high separation [3, 6, 16] of the artery – at the level of or above the hyoid bone (70% of variations). Furukawa et al. publish results of an investigation about variation of the carotid artery bifurcation level [5]. Low division (30% of the variations) is usually at the level of the middle of the larynx [8, 12].

Cakirer et al. [4] using MR inform for separate origins of the left internal and external carotid arteries from the aortic arch. Roberts and Gerald use X-ray and find an absence of both common carotid arteries [11]. Vitek et al. discover a thoracic bifurcation of the common carotid artery [17]. Many authors report about anomalous branching patterns of the carotid arteries [7, 10, 13, 15] and high carotid bifurcation but we found only two reported cases of separation below the annular cartilage – at the base of the neck and a thoracic bifurcation. The aim of the study was to determine, analyze, document and assess the presence of a rare variation – lower division of common carotid artery discovered during dissection exercises. For the implementation of the objective identified the following main tasks: 1) by preparation of anatomical objects in the division to determine the presence of vascular deviation from accepted norms; 2) to analyze the case and compare with similar abnormalities.

Materials and Methods

It was used cadaveric dissection exercises material on which the method is applicable "taxidermy anatomical objects". Detected features are observed, analyzed and a picture is taken. In the analysis, a comparison with other similar cases is described in the accessible literature. Researched and expert opinion published in specialized journals on clinically relevant, we open to variation.

Results and Discussion

We detected a low separation of the common carotid artery – below the level of the lower edge of the annular cartilage (**Figs. 1, 2**).

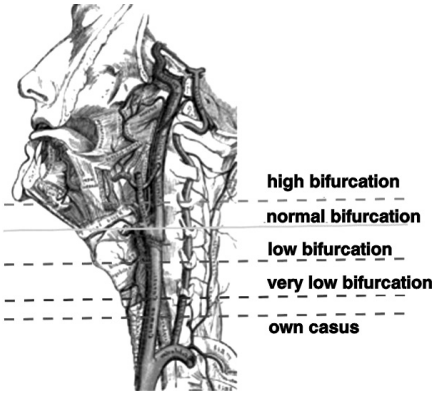

Fig. 1. Bifurcation levels of the common carotid artery

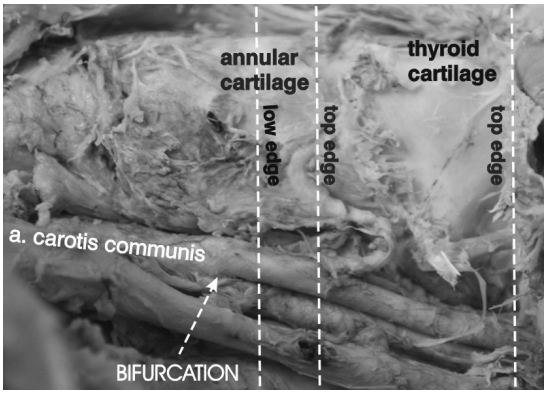

Fig. 2. Bifurcation of the left common carotid artery (an own case)

The division of the common carotid artery is about 2.5-3.0 cm below the lower edge of the annular cartilage. Regardless of the different rate variability, which indicates, according to most researchers division of a. carotis communis below the level of the thyroid cartilage is rare [8, 15].

All researchers agree that variations in the division of the common carotid artery are important [14] for the manipulation in the neck – ligation of vessels and arteriectomy, surgery of adjacent tissues, as well as diagnostics – interpretation of digital angiography, Doppler and others [9, 14].

Conclusions

1. Low division of the common carotid artery is rare.
2. Vascular variations in the neck are associated with the occurrence and development of many diseases – both vascular and surrounding structures.
3. Knowledge of the variations of the common carotid artery and its branches is required, as in the diagnosis of disease in the neck and head, and in carrying out manipulations in these areas.

References

1. **Anangwe, D., H. Saidi, J. Ogeng, K. Awori.** Anatomical variations of the carotid arteries in adult Kenyans. – East African Medical Journal, **85**(5), 2008, 244-247.
2. **Anu, V., M. Pai, R. Rajalakshmi, V. Latha, V. Rajanigandha, D'Costa.** Clinically-relevant variations of the carotid arterial system. – J. Singapore Med., **48**(6), 2007, 566.
3. **Avadhani, R., T. Chelvakumaran.** An abnormally high bifurcation of the common carotid artery. – Anatomical Adjuncts, **2**, 1995, 29-33.
4. **Cakirer, S., E. Karaarslan, M. Kayabali, I. Rozanes.** Separate origins of the left internal and external carotid arteries from the aortic arch: MR angiographic findings. – AJNR, **23**, 2002, 1600-1602.
5. **Furukawa, S., L. Wingenfeld, A. Takaya, T. Nakagawa, I. Sakaguchi and K. Nishi.** Morphological variation of the carotid artery bifurcation level. – OMICS, 2012. (http://www.omicsonline.org/scientific-reports/2155-6148-SR135.pdf).
6. **Gluncic, V., Z. Petanjek, A. Marusic, I. Gluncic.** High bifurcation of common carotid artery, anomalous origin of ascending pharyngeal artery and anomalous origin of ascending pharyngeal artery and anomalous branching pattern of external carotid artery. – Surg. Radiol. Anat., **23**, 2001, 123-125.
7. **Kishve, P., S. Kishve, M. Joshi, S. Aarif, P. Kalakoti.** An unusual branching pattern of the common and external carotid arteries in a human cadaver: A case report. – Australian Medical Journal, **4**(4), 2011, 180-182.
8. **Lo, A, M. Oehley, A. Bartlett, D. Adams, P. Blyth, S. AI-Ali.** Anatomical variations of the common carotid artery bifurcation. – ANZ Journal of Surgery, **76**(11), 2006, 970-972.
9. **Lucev, N., D. Bobinac, I. Maric, I. Drescik.** Variations of the great arteries in the carotid triangle. – Otolaryngol Head Neck Surg., **22**, 2000, 590-591.
10. **Mamatha, T., L. Rajalakshmirai. V. Prabhu, G. Hadimani, P. Jiji, M. Prameela.** Anomalous branching pattern of the external carotid artery: A case report. – Romanian Journal of Morphology and Embryology, **51**(3), 2010, 593-95.
11. **Roberts, L., K. Gerald.** Absence of both common carotid arteries. – Am. J. Roentgenology, **130**, 1978, 981-982.
12. **Schwartz, R., K. Jones, D. Chernoff, S. Mukherji, R. Khorasani, H. Tice, S. Kikini, P. Stieg, V. Polak.** Common carotid bifurcation: Artery evaluation with spiral CT. – Radiology, **185**(2), 1992, 513-519.
13. **Thwin, S., M. Soe, M. Myint, M. Than, S. Lwin.** Variations in the origin and the branches of external carotid artery in a human cadaver. – Singapore Med. J., **51**(2), 2010, 40-42.
14. **Trigaux, J., F. Delchambre, B. van Beers.** Anatomical variations of the carotid bifurcation: implications for digital subtraction angiography and ultrasonography. – Br. J. Radiol., **63**, 1990, 181-185.
15. **Ursula, G., R. Schulz, P. Rothwell.** Major Variation in Carotid Bifurcation Anatomy. – Stroke, **32**, 2001, 2522-2529.
16. **Vinaitha, D., K. Anandhi, R. Saran, L. Ramanathan, A. Subramaniam.** High bifurcation of the common carotid artery and looping of the external carotid artery: a case report. – Journal of Clinical and Diagnostic Research, **6**(3), 2012, 462-464.
17. **Vitek, J., P. Reaves.** Thoracic bifurcation of the common carotid artery. – Neuroradiology, **5**, 1973, 133-139.

Address for correspondence:
Dimiter Sivrev
Department of Anatomy
Faculty of Medicine
11 Armeyska Str.
Stara Zagora 6000
Bulgaria
e-mail: dsivrev@abv.bg

Institute of Experimental Morphology, Pathology and Anthropology with Museum
Bulgarian Anatomical Society

Acta morphologica et anthropologica, 21
Sofia ● 2015

Index Characteristics of Human Clavicle

D. Toneva[*], S. Nikolova[*], I. Maslarski[**]

[*]*Department of Anthropology and Anatomy, Institute of Experimental Morphology, Pathology and Anthropology with Museum, Bulgarian Academy of Sciences, Sofia*
[**]*Department of Anatomy, Histology and Pathology, Faculty of Medicine, University of Sofia, Bulgaria*

The aim of the present study is to determine the sexual differences in the form and proportionality of the clavicle on the basis of its index characteristics. A total of 433 adult clavicles were investigated. Eight indexes were calculated on the basis of 9 clavicular measurements. The significance of the sexual differences is determined by Student's t-test. The index characteristics show sexual differences in the form and proportionality of the clavicle. Statistically significant differences are established in the indexes characterizing the massiveness and bending of the bone.

Key words: clavicle, index, sexual differences.

Introduction

The index characteristic is an important part of the anthropometric characterization of the separate bones, which gives additional information about the differences in the form and proportionality in either sexual or bilateral aspect.

The aim of the present study is to determine the sexual differences in the form and proportionality of the clavicle on the basis of its index characteristics.

Materials and Methods

The anthropological investigation was performed on osteological material from archaeological excavations of medieval necropoles in the territory of Northeastern Bulgaria. A total of 433 clavicles (107 right and 104 left male clavicles; 115 right and 107 left female clavicles) were investigated. The sex and age of the individuals were previously determined by standard anthropological methods. Eight indexes were calculated on the basis of 9 clavicular measurements [2, 3]. Two of the measurements are introduced by the authors. The independent-sample t-test was used in order to determine the significance of the sexual differences.

Results

Basic statistics on the indexes of male and female clavicles are presented in **Table 1.**

Table 1. Basic statistics on the indexes of male and female clavicles

Indexes	Laterality	Male clavicles			Female clavicles			Sexual differences	
		n	$\bar{x}$	SD	n	$\bar{x}$	SD	t-test	p-value
Length-thickness index (6:1)	Right	96	27.0	2.6	96	25.7	2.4	3.454	0.001*
	Left	86	26.0	2.3	89	24.7	2.2	3.686	0.000*
Middle index (4:5)	Right	107	87.4	13.5	113	89.6	14.9	–1.136	0.257
	Left	103	88.5	13.3	106	90.5	14.7	–1.050	0.295
Index of the vertical diameter (4:1)	Right	96	7.5	0.9	96	7.3	1.0	1.718	0.087
	Left	87	7.4	0.9	90	7.1	1.0	2.171	0.031*
Index of the sagittal diameter (5:1)	Right	96	8.8	1.0	96	8.2	0.9	4.184	0.000*
	Left	87	8.4	0.9	89	7.9	0.9	3.888	0.000*
Index of the corpus curve (2a:1)	Right	71	20.4	2.0	83	19.4	1.8	3.025	0.003*
	Left	66	19.6	1.9	70	19.4	2.2	0.788	0.432
Index of the corpus curve I (2:3)	Right	82	8.3	2.5	94	8.5	2.5	–0.473	0.637
	Left	80	8.1	2.4	90	9.0	2.6	–2.354	0.020*
Index of the sternal curve depth	Right	67	12.5	1.7	70	12.7	1.8	–0.792	0.430
	Left	59	12.5	1.7	62	12.9	1.7	–1.316	0.191
Index of the acromial curve depth	Right	67	9.2	1.4	77	8.9	1.3	1.042	0.299
	Left	68	9.2	1.5	68	8.6	1.6	2.249	0.026*

* – statistically significant difference

The length-thickness index /6:1/ and the middle index /4:5/ are main indexes, characterizing the massiveness of the clavicle. The length-thickness index (robustness index) has significantly greater values for both right and left clavicles of male skeletons. The greater values in the male skeletons show that their clavicles have relatively thicker *corpus claviculae* in relation to the greatest length, i.e. they are more massive in comparison with the female bones. According to Jit and Singh [1], the length-thickness index is not useful for sex determination, but this is not confirmed by our results, showing statistically significant sexual differences at $p \leq 0.001$.

The middle index has greater mean values in the female clavicles. However, the sexual differences are not statistically significant. The greater values of the middle index in the female skeletons show that the vertical diameter in the middle of their clavicles is relatively greater in relation to the sagittal one, compared with the proportion between both measurements in the male clavicles.

The index of the vertical diameter /4:1/ and the index of the sagittal diameter /5:1/ determine the relative part of the vertical and sagittal diameter, respectively, in relation to the greatest clavicular length. Both indexes show greater values in favor of the male skeletons. The index of the vertical diameter has statistically significant sexual differences only in the left clavicles, whereas the index of the sagittal diameter shows very

strong sexual differences bilaterally. The results of these two indexes corroborate the greater massiveness of the male clavicles than the female ones, because both diameters in male clavicles have greater share in relation to the length.

The index of the corpus curve (2a:1) and index of the corpus curve I (2:3) characterize the curve of the clavicle corpus, according to Martin-Saller [2] and Alekseev [3], respectively. The first index represents the proportionality between the height of the corpus curve (2a) and the greatest length of the clavicle, and the second one – the relation between the height of the corpus curve (2) and the length of the curve basis.

The values of the index of the corpus curve (2a:1) are greater in the male clavicles. This means that the height of the corpus curve in male clavicles is proportionally greater in relation to the clavicular length. The sexual differences are statistically significant only on the right side. However, the index of the corpus curve I (2:3) is greater in the female clavicles, but statistically significant sexual differences are observed only in the left bones. The result shows that the curve in the female clavicles is relatively higher in relation to the length of corpus curve basis, i.e. the female clavicles have a higher curve with a shorter curve basis, compared to the male clavicles.

The index of the sternal curve depth and the index of the acromial curve depth reflect the relative part of the depths of the sternal and acromial curves in relation to the greatest clavicular length. The index of the sternal curve depth has greater values in the female clavicles, which shows the relatively deeper sternal curve in the female clavicles. The sexual differences are not statistically significant. The means of the index of the acromial curve depth are greater in the male clavicles. Statistically significant sexual differences are observed only in the left bones. The greater values in the male clavicles determine the relatively more curved acromial part of their clavicles.

Conclusion

The index characteristics show sexual differences in the form and proportionality of the clavicle. Statistically significant differences are established in the indexes characterizing the massiveness and curve of the bone. As a whole, our results show that male clavicles are more massive with relatively bigger dimensions in the middle of the bone, more curved with a relatively deeper acromial curve in relation to the clavicular length. Female clavicles are more gracile, higher and narrower in the middle of the bone and with a relatively deeper sternal curve in relation to its length.

Acknowledgments: This work was supported by the European Social Fund and Republic of Bulgaria, Operational Programme "Human Resources Development" 2007-2013 framework, Grant No BG-051PO001- 3.3.06-0048 from 04.10.2012.

References

1. **Jit, I., S. Singh.** The sexing of the adult clavicles. – Indian Journal of Medical Research, **54**, 1966, 551-571.
2. **Martin, R., K. Saller.** Lehrbuch der anthropologie in systematischer Darstellung. Band I. Stuttgart, Gustav Fischer Verlag, 1957.
3. **Алексеев, В. П.** Остеометрия. – Москва, Наука, 1966.

Institute of Experimental Morphology, Pathology and Anthropology with Museum
Bulgarian Anatomical Society

Acta morphologica et anthropologica, 21
Sofia ● 2015

Growth and Proportionality of Body and Extremities' Length during Childhood

I. Yankova, Y. Zhecheva

Institute of Experimental Morphology and Anthropology with Museum, Bulgarian Academy of Sciences

The aim of the study is to analyse the metrical data of body and extremities lengths, their proportionality and growth during childhood. Object of the study are 219 fullterm and healthy newborns (110 boys and 109 girls) investigated within 24 hours after birth, and 640 preschool children aged 3-6 years (320 boys and 320 girls). The anthropometrical measurements are taken using the classical methods of Martin-Saller. The results show that: the stature increases most intensively between 0 and 3 years, after that it increases slowly; the length of trunk in 3-6 years old children is proportionately longer in boys; the boys have proportionately longer upper extremities and the girls have proportionately longer lower extremities; the interextremities' index values decreases with age which is associated with more rapid growth of lower extremity length during the period 3-6 years.

Key words: extremities' length, growth, proportionality, newborns, 3-6 years old children.

Introduction

Peculiarity of physical development of neonates and children from early childhood is the specific proportionality between their body parts, which is different from those in adults. Body proportionality is indicator for assessing body structure during different periods of growth and development and characterizes the harmonic physical development in children.

In newborns the upper and lower extremities referred to the stature are relatively short (on average about 1/3 of their height), but their sizes are growing rapidly after birth [1, 3, 4]. The relative extremities' length in adults is ½ of their height.

The aim of the study is to analyse the methrical data of body and extremities lengths, their proportionality and growth during childhood.

Materials and Methods

Object of the study are 219 fullterm and healthy newborns (110 boys and 109 girls) investigated through 2001, within 24 hours after birth, and 640 preschool children aged 3-6 years (320 boys and 320 girls, evenly distributed into 4 age groups for both sexes separately) investigated through 2004-2005.

The anthropometrical measurements are taken using the classical methods of Martin-Saller [2]. The data of body and extremities' length and their growth and proportionality in children are analysed using SPSS for windows, version 13.0. The statistical significant differences are established by Student's t-test in $P < 0.05$.

Results and Discussion

The results for body lengths and their proportions are presented in **Table 1**, and results for dynamics of growth – in **Table 2**.

Table 1. Biostatistical data of body lengths and their proportions

Age	Body lengths							Body lengths proportions						
	♂			♀			Differences ♂/♀ (cm)	♂			♀			Differences ♂/♀ (%)
	n	mean	SD	n	mean	SD		n	mean	SD	n	mean	SD	
	Stature							Upper extremity length × 100 / Lower extremity length						
0	110	50.55	1.49	109	50.13	1.65	0.43*	110	95.33	3.61	109	94.17	2.98	1.16*
3	80	101.20	4.30	80	98.99	3.89	2.20*	80	78.75	1.80	80	77.25	2.79	1.50*
4	80	107.70	4.13	80	106.52	5.39	1.18	80	77.12	1.93	80	75.83	2.07	1.29*
5	80	114.66	4.97	80	113.91	4.97	0.75	80	77.39	1.82	80	76.01	1.72	1.38*
6	80	121.28	4.93	80	120.40	5.16	0.88	80	76.55	1.74	80	75.59	1.82	0.95*
	Torso length							Torso length proportion						
0	110	17.29	0.90	109	17.36	0.86	–0.07	110	34.20	1.42	109	34.63	1.39	–0.43*
3	80	30.39	2.00	80	29.43	1.54	0.96*	80	30.03	1.54	80	29.74	1.32	0.29
4	80	32.27	1.78	80	31.25	1.88	1.02*	80	29.97	1.49	80	29.35	1.33	0.63*
5	80	33.41	2.10	80	32.74	1.90	0.67*	80	29.14	1.33	80	28.74	1.08	0.40*
6	80	34.90	1.88	80	34.00	1.76	0.90*	80	28.78	1.18	80	28.24	1.07	0.54*
	Upper extremity length							Upper extremity length proportion						
0	110	21.04	0.91	109	20.72	0.79	0.32*	110	41.62	1.37	109	41.36	1.36	0.27
3	80	41.38	2.11	80	39.91	1.86	1.47*	80	40.89	0.89	80	40.32	0.94	0.57*
4	80	44.37	2.09	80	43.27	2.45	1.10*	80	41.20	0.93	80	40.62	1.03	0.58*
5	80	47.53	2.37	80	46.89	2.45	0.64	80	41.45	0.99	80	41.16	0.98	0.29
6	80	50.63	2.36	80	49.71	2.52	0.92*	80	41.74	0.82	80	41.28	0.96	0.46*
	Lower extremity length							Lower extremity length proportion						
0	110	22.08	0.83	109	22.02	0.79	0.07	110	43.69	1.36	109	43.94	1.52	–0.25
3	80	52.58	2.95	80	51.72	2.80	0.86	80	51.94	1.17	80	52.24	1.75	0.00
4	80	57.57	2.95	80	57.10	3.45	0.48	80	53.44	1.22	80	53.59	1.31	–0.15
5	80	61.43	2.92	80	61.70	3.11	–0.27	80	53.58	1.00	80	54.17	1.12	–0.59*
6	80	66.16	3.23	80	65.79	3.58	0.38	80	54.55	1.07	80	54.63	1.21	–0.08

* $P \leq 0.05$ – gender differences.

Table 2. Dynamics of growth

Age	♂		♀	
	AYA (cm)	**RYA (%)**	**AYA (cm)**	**RYA (%)**
Stature				
0-3	50.64*	66.74	48.86*	65.54
3-4	6.50*	6.22	7.53*	7.33
4-5	6.96*	6.26	7.39*	6.70
5-6	6.62*	5.61	6.49*	5.54
Torso length				
0-3	13.10*	54.93	12.07*	51.60
3-4	1.88	6.00	1.82*	6.00
4-5	1.15	3.49	1.49*	4.67
5-6	1.49	4.35	1.26*	3.76
Upper extremity length				
0-3	20.34*	65.17	19.19*	63.29
3-4	2.99*	6.97	3.36*	8.08
4-5	3.16*	6.87	3.62*	8.04
5-6	3.10*	6.31	2.81*	5.83
Lower extremity length				
0-3	30.50*	81.69	29.70*	80.56
3-4	4.99*	9.06	5.38*	9.88
4-5	3.86*	6.49	4.61*	7.76
5-6	4.73*	7.42	4.08*	6.41

* $P \leq 0.05$ – interage differences.
AYA – Absolute Year Alteration.
RYA – Relative Year Alteration.

The stature is a major anthropometric feature that has important medical and biological meaning in childhood. In the newborn, it reflected mainly hereditary granted of body sizes. During childhood stature characterized age-gender peculiarities in the child growth.

At birth and from 3 to 6 years the boys have higher values of stature than girls, as the differences are statistically significant ($P \leq 0.05$) in the newborns and in 3 years old children.

The growth of height is the most intensive between 0 and 3 years (49.0-50.0 cm), after this period up to six years of age the stature of children increases with 6.50 to 7.50 cm/year. The girls grow up more rapidly between 3 and 4 years, and the boys – between 4 and 5 years. The differences between both genders are statistically significant ($P \leq 0.05$). The relative year alteration (RYA) is in the range of 5.50% to 7.3% for the 3-6-year-olds.

The length of the trunk is the next important indicator of the body proportionality. In newborn boys and girls the difference is minimal (0.10 cm), but from 3 to 6 years the boys have statistically significant longer trunk than girls.

In both genders the length of the trunk grows most intensively during the first three years (51.6-54.9%). During the next three-year period, the relative growth in the torso

length in boys is 13.8 % and in girls is 14.4% respectively. From the third to the sixth year the increase is greatest during the first annual period when absolute year alteration (AYA) has nearly equal values in both genders. The increase of the torso length in boys is lowest between 4 and 5 years and in girls during the last one-year interval.

The data for the proportionality of the trunk length show that the torso of newborn girls related to the stature is significantly longer (with 0.43%) compared with the torso of the boys. In 3-6 years old children the torso length related to stature is greater in boys. The gender differences are not statistically significant only in 3 years of age. In the other three age groups of boys priority is statistically reliable ($P \leq 0.05$).

The length of the trunk in 3-6 years old children is proportionately longer in boys in contrast with the proportionality in adults where the torso length is longer in women. In both genders the relative length of the trunk decreases with the age and 6 years old children have the lowest values of the torso length proportion.

The metrical data for upper and lower extremities provide information on their size, proportionality and the proportionality between their parts.

The length of the upper extremities in newborns from both sexes is ½ of their stature. From birth to 6 years of age upper extremities of the boys are significantly longer compared with girls ($P \leq 0.05$). The upper extremities length grows most intensively between 0 and 3 years of age (with 19.0-20.0 cm). From 3 to 6 years it increases with 9.00 to 10.00 cm, as the growth is relatively equal during each one-year period. In both genders AYA is greatest between 4 and 5 years, and the lowest between 3-4 years in boys and 5-6 years in girls, as differences between genders are statistically significant ($P \leq 0.05$). The length of the upper extremity at the 6 years old boys is 9.25 cm (20.15%) greater than in the 3 years olds. In girls throughout the studied period between 3 and 6 years of age the length of the upper extremity is increased by 9.80 cm (21.95%).

The relative length of the upper extremity is an important indicator for determining the body proportionality and for the degree of morphological maturity in prenatal ontogenesis and earliest childhood. The newborn boys have bigger absolute sizes of feature and proportionately longer upper extremities, but gender differences are not statistically significant. Between 3 and 6 years of age boys have also proportionately longer upper extremities than girls but found gender differences are significant during all investigated ages, excepting 5-year-olds when the gender gap is smallest (0.29%).

The lower extremity length is a mean feature that determines the growth of man. A characteristic feature of the humans is that between birth and puberty the lower extremities grow relatively faster than the other post-cranial body segments.

In newborn boys and girls the lower extremities length is about ½ of their stature (22 cm) without statistically significant gender differences. In children from 3 to 6 years of age lower extremities have a greater length in boys with the exception of 5 years in which the priority is for girls. The greatest gender differences are reported in the group of three-year (0.86 cm).

From birth to 3 years the lower extremities increases in length with about 30.0 cm (81.0%) in both sexes. During the next three year period the lower extremities of boys and girls increases by 13.58 cm and 14.07 cm respectively. The increase of the lower extremity length is greatest between 3 and 4 years of age, after that growth decreases successively.

The data for the proportionality of the lower extremity show that girls from birth to 6 years of age have proportionately longer lower extremities than boys. The difference between genders is statistically significant ($P \leq 0.05$) only in 5 years old children (0.59%). In other age groups the differences between genders are insignificant (from 0.1% to 0.3%).

Interextremities index expresses the ratio between the upper and lower extremities lengths. Data from this index show that at birth and between 3 to 6 years statistically significant gender differences are available. Boys have significantly higher index values indicating that their upper extremity length relative to the lower extremity length is greater compared with girls. The values of the index decreases with age, which is associated with more rapid growth of the lower extremity length during the period between 3 and 6 years. Only between 4 and 5 years of age, the growth rate is faster in the upper extremity length, so that the index values increased slightly.

Throughout the studied age period the boys have longer upper extremities and the length of the lower extremities is approximately equal in both genders.

Conclusions

This paper contains data describing the stature, trunk length, upper and lower extremity lengths of newborns and children living in the town of Sofia.

The results obtained show that:

1. The stature increases most intensively between 0 and 3 years, after this period up to six years of age it increases more slowly;

2. The length of trunk in 3-6 years old children is proportionately longer in boys in contrast with the proportionality in adults where the torso length is longer in women;

3. The boys have proportionately longer upper extremities and the girls have proportionately longer lower extremities;

4. The interextremities' index values decreases with age, and are associated with rapid growth of the lower extremity length than upper extremity length during the period 3-6 years.

References

1. **Johnston, P. G. B.** Vulliamy's the newborn child. Edinburgh, Churchill Livingstone, 1994, 29-32
2. **Martin, R., K. Saller.** Lehrbuch der Anthropologie in systematischer Darstellung. Stuttgart, Gustav Fischer Verlag, **1**, 1957, 322-324.
3. **Nelson, S.** Nelson Textbook of Pediatrics. 14th ed. W. B. Saunders Company, 1992, 15-37.
4. **Бобев, Д., Е. Генов.** Педиатрия. София, 2000.

Institute of Experimental Morphology, Pathology and Anthropology with Museum
Bulgarian Anatomical Society

Acta morphologica et anthropologica, 21
Sofia ● 2015

Review Articles

The Role of the Beta-Amyloid Precursor Protein in the Diagnosis of Diffuse Axonal Injury

N. Davceva[*], M. Dimitrova[**], D. Kadiysky[**], M. Grozeva[***], N. Basheska[****]

[*]*Faculty of Medicine, Institute of Forensic Medicine and Criminalistics, Scopje, Macedonia*
[**]*Institute of Experimental Morphology, Pathology and Anthropology with Musem, Bulgarian Academy of Sciences, 1113 Sofia, Bulgaria*
[***]*Faculty of Medicine, St. Kl. Ohridski University of Sofia, 1407 Sofia, Bulgaria*
[****]*University Clinic of Radiotherapy and Oncology, Faculty of Medicine, Sts. Cyril and Methodius University, Skopje, Macedonia*

Diffuse axonal injury (DAI) is a distinct clinical-pathological entity in the closed head injuries, where very often, the macroscopic lesion of the brain tissue cannot be found. Hence, in those cases the microscopic examination is of a huge importance. Using the conventional staining techniques the axonal injuries can be perceived only if there has been a survival of up to 24 hours (hematoxylin and eosin staining), or 12 to 18 hours (silver impregnation methods). With the introduction of immunohistochemistry using antibodies against β-Amyloid Precursor Protein (β-APP), this period has been shortened to 3 hours, even less. In the present paper, a review on the role of β-APP immunohistochemistry in the diagnosis of DAI is presented. This review shows that β-APP immunohistochemistry can be a very powerful tool in diagnosing the axonal injuries, what is of a special significance for the forensic medicine practice.

Key words: diffuse axonal injury, β-amyloid precursor protein, immunohistochemistry, forensic medicine.

In the middle of the 20th century Sabine Strich, one of the most prominent authors in the field of the closed head injuries stated: "If we look back to the literature about the head injuries, very little has been discovered ever since 1900" [2]. However, in the last 20 years of the 20th century, there has been a rapid development in the field of neurotraumatology, mainly as a result of the introduction of the concept of the focal and diffuse brain damage. It has been cleared that the final outcome of a particular closed head injury mainly depends on the occurrence of diffuse brain injuries: diffuse axonal injury (DAI), diffuse vascular injury (DVI), diffuse brain edema and diffuse hypoxic-ischemic brain injury.

DAI is a clinical-pathological entity. Clinically, it is characterized by an immediate and prolonged unconsciousness after a mechanical impact to the head, typically without any lucid interval, leading to severe brain failure, vegetative state and death. Pathologically, DAI is defined by the feature of the diffuse damage of axonal fibers inside the white brain matter, including the fiber tracts and the brain stem [1, 7, 8]. In the last twenty years of the 20th century the knowledge about the Diffuse Axonal Injury (DAI) as a separate clinical-pathological entity matured, featuring it as an almost universal consequence in the fatal closed head injuries [10]

The Process of Diagnosing DAI

The diagnosis of DAI is clinical-pathological. In the neuropathological feature of DAI, a triad of specific pathoanatomical changes has been defined, which is the base for grading of the pathological findings of DAI that was recently conducted [6].

1. Focal lesion in the *corpus callosum*, as the 2nd grade of DAI (**Fig. 1**);
2. Focal lesion in the dorsolateral quadrant of the rostral pons, as the 3rd grade of DAI (**Fig. 2**);

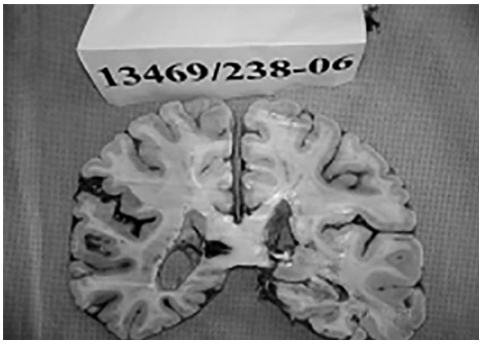

Fig. 1. Focal lesion in the *corpus callosum*, as the 2nd grade of DAI in a case with 6 days survival time

Fig. 2. Focal lesion in the dorsolateral quadrant of the rostral pons, as the 3rd grade of DAI in a case with 7 hours survival time after injury

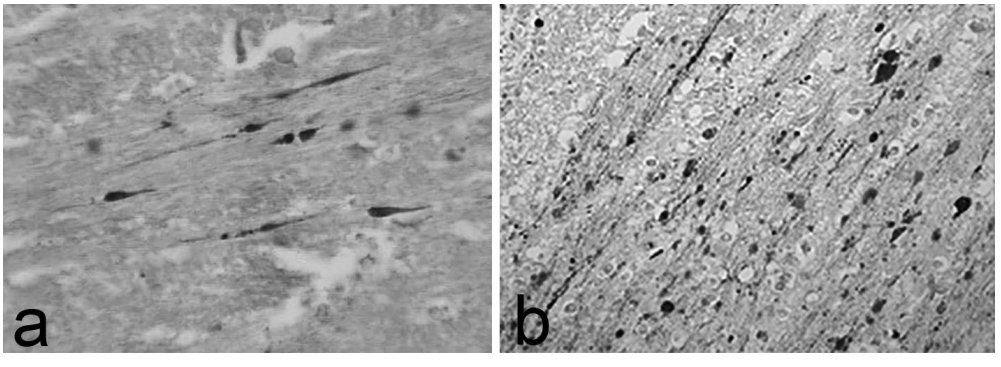

Fig. 3. Employing the method of β-APP immunohistochemistry the visualization of the damaged axons is possible even in cases with several hours of survival time: a – case with 3 hours survival time (×400); b – case with a survival time of 1.5 month (×400)

3. Microscopically detected diffuse axonal damage in the absence of any macroscopical lesion as the 1st grade of DAI (**Fig. 3**).

The main attribute in the pathological determination of DAI is the widespread and diffuse axonal damage throughout the white brain matter including the white matter bundles.

Events on the Cellular Level and Methods for the Visualization of Axonal Damage

The first considerations of the scientists pointed out that tearing of the axons with a subsequent retraction of the torn fiber into a ball, the so called "retraction ball", occurs at the moment of injury, i.e. the **primary axotomy**. However, later studies showed that axonal damage is not an immediate but rather delayed consequence of the impairment of axoplasmic transport (**secondary axotomy**) [14, 15]. With the impairment of the axonal transport, the axon is starting to swell. Such swollen axons can be seen microscopically as "sausages" or "varicosities". After that, a degeneration of the whole axon takes place with the formation of a typical "retraction balls". All these changes occur in a time period of about 12 to 24 hours, which is the reason why they cannot be visualized with the conventional histological methods. Employing the method of haematoxylin and eosin staining, the damaged axons can be seen in the time period of at least 24 hours after the injury (**Fig. 3**). Using the methods of silver impregnation, they can be detected 12 to 18 hours post injury [6, 8].

The Role of the β-amyloid Precursor Protein

The disruption of the axonal transport causes a deposition of some substances that are the normal contents of axolemma and normally are moving through it by anterograde axonal transport, as is the **ß-amyloid precursor protein (β-APP)**.

β-APP is a transmembrane glycoprotein, widely distributed in the central nervous system and involved in many normal cellular functions. In the neuron, β-APP is synthesized in the pericarion and then, by a fast anterograde transport (100-400 mm/day) it moves through the neuron [13]. In normal circumstances β-APP is not accumulated to such a degree to be detected in the tissue. However, in the condition of a structural axonal injury, an accumulation of β-APP happens to a degree to be detected by immunohistochemistry [13]. The immunohistochemical technique using antibodies to β-APP [9], enables the visualization of damaged axons as early as 2 to 3 hours post injury, and sometimes even earlier [12]. This method proved to be a highly specific and extremely sensitive, targeting selectively damaged axons. Application of antibodies to β-APP makes the visualization of axons possible, even in cases of short survival (2-3 hours), unlike the conventional methods. Our own results on a series of 60 cases with closed head injuries have shown that β-APP-immunoreactivity can be observed about 2-3 hours post injury, and the longest survival time has been 1.5 month where β-APP has been still visible [3, 5].

Pattern and Distribution of the ß-APP Immunoreactivity as Indicator for the Traumatic Axonal Damage

Some time ago, when for the visualization of the damaged axons only conventional staining techniques were available, the axonal damage in the white brain matter was considered as an indicator of traumatic damage of the brain. With the introduction of the immunohistohemistry in the process of diagnosing of DAI [9] it became clear that the axonal damage is not occurring only as a result of trauma, but can be caused by other conditions, such as: hypoxia and ischemia, multiple sclerosis, HIV-encephalitis, infarcts, hypoglycemia [16], as well as intoxication.

Nowadays, all the efforts are aimed at establishing diagnostic criteria for DAI [3, 5]. It is widely accepted that for diagnosing DAI, a correlation between a well-documented clinical history of a head trauma and certain neuropathological features is essential. Pathologically, there must be found a widespread diffuse axonal damage in no less than three different brain regions, at least one of which located above and one beneath the tentorium, including also the tracts of axonal fibers as are *corpus callosum* and the internal capsule [7].

Furthermore, prominent authors have reported that there are certain differences in the pathological findings indicative for axonal damage. Thus: "Linear or geographical patterns of β-APP accumulation are more likely to represent damaged axons at the edge of a focus of early ischemia, while scattered or groups of immunoreactive axons, particularly involving single white matter bundle (*corpus callosum*, internal capsule), probably indicate traumatic damage" [8]. In this respect, there are differences in the appearance, distribution and pattern of the axonal damage that is indicative of a traumatic or ischemic etiology. In the pathological determination of DAI, in addition to the macroscopic features like focal lesions in the *corpus callosum* and dorsolateral quadrant of the rostral pons, only the finding of single positive axons or small groups of scattered and diffusely arranged β-APP positive axons, seen as "sausage-like" or "varicosity-like" swollen axons or as "retraction balls", can be considered as confirmation of the traumatic etiology of axonal damage [11]. A finding of circumscribed foci or a linear pattern frequently described as a "zigzag" or "Z-shaped" pattern of β-APP positive axons [4], which in our experience are never big and are not as neatly shaped as the diffusely arranged traumatically damaged axons, was considered a predominantly hypoxic-ischemic finding and was not considered as a proof of traumatic axonal damage [3, 5].

Conclusion

From this review it becomes clear that β-APP immunohistochemistry is a powerful tool in the hands of forensic pathologists which undoubtedly proves that:

1. There has been an injury of the brain. With the appropriate sampling of the brain and appropriate interpretation, it can point out the origin of the axonal damage – is it traumatic or ischemic.
2. The injury of the brain has occurred during life or intravitally, which is of a big medico-legal relevance.
3. There has been the time of survival of at least 2-3 hours post injury.
4. The time course of the axonal pathology can point to the age of the injury.

References

1. **Adams, J. H., D. Doyle, I. Ford et al.** Diffuse axonal injury: definition, diagnosis and grading. – Histopathology, **15**, 1989, 49-59.
2. **Adams, J. H., D. I. Graham, L. S. Muray, G. Scott.** Diffuse axonal injury due to non-missile head injury in humans: an analysis of 45 cases. – Ann. Neurol., **12**, 1982, 557-563.
3. **Davceva, N., V. Janevska, B. Ilievski, G. Petrushevska, Z. Popeska.** The occurrence of acute subdural haematoma and diffuse axonal injury as two typical acceleration injuries. – J. Forensic Leg. Med., (in press).
4. **Davceva, N., V. Janevska, B. Ilievski, L. Spasevska, Z. Popeska.** Dilemmas concerning the diffuse axonal injury as a clinicopathological entity in forensic medical practice. – J. Forensic Leg. Med., **19**(7), 2012, 413-418.

5. **Dolinak, D., E. Matshes, editors.** Medicolegal neuropathology. New York, CRC Press, 2002.
6. **Geddes, J. F., G. H. Vowles, T. W. Beer, D. W. Ellison.** The diagnosis of diffuse axonal injury: implications for forensic practice. – Neuropath. Appl. Neurobiol., **23**, 1997, 339-347.
7. **Geddes, J. F., H. L. Whitwell, D. I. Graham.** Traumatic axonal injury: practical issues for diagnosis in medico legal cases. – Neuropath. Appl. Neurobiol., **26**, 2000, 105-116.
8. **Gentleman, S. M., A. J. Nash, C. J. Sweeting, D. I. Graham, G. W. Roberts.** β-amyloid precursor protein (β-APP) as a marker of axonal injury after head injury. – Neurosci. Lett., **160**, 1993, 139-144.
9. **Gentleman, S. M., G. W. Roberts, T. A. Gennareli et al.** Axonal injury: a universal consequence of fatal closed head injury? – Acta Neuropathol., **89**, 1995, 537-543.
10. **Graham, D. I., C. Smith, R. Reichard et al.** Trials and tribulations of using β-amyloid precursor protein immunohistochemistry to evaluate traumatic brain injury in adults. – Forensic Sci. Int., **146**, 2004, 89-96.
11. **Hortobagyi, T., S. Wise, N. Hunt et al.** Traumatic axonal damage in the brain can be detected using β-APP immunohistochemistry within 35 min after head injury to human adults. – Neuropathol. Appl. Neurobiol., **33**, 2007; 226-237.
12. **Omalu, B. I.** Diagnosis of traumatic diffuse axonal injury. – Am. J. Forensic Med. Pathol., **25** (3), 2004, 270-273.
13. **Povlishock, J. T.** Traumatically induced axonal injury: Pathogenesis and pathobiological implications. – Brain Pathol., **2**, 1992, 1-12.
14. **Povlishock, J. T, C. W. Cristman.** The pathobiology of traumatically induced axonal injury in animals and human: A review of current thoughts. – J. Neurotrauma, **12**, 1995, 555-564.
15. **Reichard, R. R, C. Smith, D. I. Graham.** The significance of β-APP immunoreactivity in forensic practice. – Neuropath. Appl. Neurobiol., **31**, 2005, 304-313.
16. **Sheriff, F. E., L. R. Bridges, S. Sivaloganatham.** Early detection of axonal injury after human head trauma using immunocytochemistry for β-amyloid precursor protein. – Acta Neuropathol., **87**, 1994, 55-62.

Institute of Experimental Morphology, Pathology and Anthropology with Museum
Bulgarian Anatomical Society

Acta morphologica et anthropologica, 21
Sofia ● 2015

Dr. Jonas Uro Basanavichius – Regular Member of the Bulgarian Literary Society and Founder of Anthropological Researches in Bulgaria

G. Marinov

Prof. Paraskev Stoyanov Medical University, Varna

In the early period immediately after the Liberation of Bulgaria, a number of foreign representatives of different branches of science – medical doctors, archaeologists, historians, humanitarians, who reside in different time periods in Bulgaria, contributed to Bulgarian scientific and cultural development. Between them shines particularly the name of the great son of Lithuania, Dr. Jonas Uro Basanavichius (Basanavičius) (23 November 1851 – 16 February 1927) – physician, scholar encyclopaedist, politician. With brief interruption he spends 25 years of his life in Bulgaria. He has huge contributions to the development of health and medical science in Bulgaria. He published scientific papers on Archaeology, ethnography and linguistics of Bulgaria. With his fundamental work "Materials for sanitary ethnography of Bulgaria. I. Lom County /1880-1889/", Dr. Basanavichius became founder of the first established representative anthropological study of the population in Bulgaria.

Key words: Basanavichius, Anthropology, Town of Lom, Town of Varna, Ethnography.

Dr. Jonas Uro Basanavichius graduated from Medical Faculty of the Imperial Moscow University (1879) [1, 2, 10]. On January 24, 1880 arrived in Bulgaria [10]. On February 7, 1880 began working as a county doctor and as the chief physician of the hospital in Lom. For a short time he significantly enhanced the work of the hospital. His first concern was to attract local people to be treated it the hospital, because during this time the people believed that one must be going in the hospital, just to die [1, 10]. Due to political intrigues in May 1882 he left Bulgaria for almost two years. In this period he specialized medicine in Prague and Vienna. In 1884 he got married in Prague to Eleonora Gabriela Mohl – a German woman from Bohemia [10]. In 1884 he returned to Bulgaria with his wife [10]. Dr. Basanavichius was appointed county physician and head of the hospital in the town of Elena. And there he used to make a lot of efforts to attract urban and rural population to be treated in the hospital [10]. In 1885 he held position of district doctor in Lom. This coincided with the Serbian-Bulgarian War. The hospital of Lom was designed to accommodate wounded soldiers, whose number reached 200 people per day [7]. February 18, 1886 he became ill with pneumonia and fever [1, 10]. After his recovery, Dr. Basanavichius continued to perform his medical duties.

On August 7, 1887 against him was committed assault and he was wounded with two bullets, but remained alive [10]. He practised medicine in Bulgaria and Vienna, but regardless of this incident that almost cost him his life; he remained loyal and sincere friend of the Bulgarian nation and continued to work with the same dedication. In the town of Elena his wife fell ill with pulmonary tuberculosis. Due to financial difficulties and lack of resources he wasn't able to send his wife to be treated abroad. On February 16, 1889 she died at the age of 26 years, 2 months and 23 days. She was buried in the cemetery in Lom [10]. After this worst ordeal of his life he fell into a deep depression and melancholy or almost a year.

In 1891, in vol. V of "SbNUNK" was published extensive monograph of Dr. Basanavichius "Materials for sanitary ethnography of Bulgaria. I. Lom district /1880-1889/" (**Fig. 1**) [2]. This is the first fundamental study of the health status of a region of Bulgaria. Erudition and encyclopedic knowledge of the author allowed him to go beyond the ordinary sanitary survey and he gave an extensive description of the geographical, geological and climatic characteristics of the Lom County, its flora and fauna, exploring their impact on population's health status. Furthermore, he made a very accurate description of the lifestyle, habits, customs and beliefs of the Bulgarians from the region, which is a valuable contribution to the Bulgarian ethnography. The author for the first time in Bulgarian scientific literature reported data from representative anthropological study of the Bulgarian population and some minority groups living in Lom County, received from own measurements on a large contingent, including data from surveys of recruits [10]. For the first time Demographics of Lom County were brought, based on a conscientious and competent study [2]. In a letter to Prof. Konstantin Jireček, Prof. Ivan Shishmanov wrote: "In the forthcoming book (Vol. V of SbNUNK, remark GM) will print the following major works: 1. Ethnographic-sanitary description of the Lom County from Dr. Basanavichius. Huge and diligent work. Will volume about 15 [printer's] sheets. Here you will find a lot of things (that you are missing ...) ...: cranial-metric tables (yes, yes!) (indices, mindices etc.), a description of the color of hair, of eyes, on the basis of the stat.[istical] data, etc. - what do you think ... is there no progress? But Basanavichius is not Bulgarian. No harm! ... " [8]. Responding to Prof. Ivan Shishmanov Prof. Konstantin Jireček writes: "The article of Dr. Basanavichius for Lom County ... will be the first experience; nation needs such materials in order to enable to make anthropometric reasoning ..." [8]. In a review of the work of Dr. Basanavichius published in the journal "Medicine" [5, 9], the author of which is probably Dr. Stefan Vatev, is stressed that "the book of Dr. Basanavichius is a kind of encyclopedia, in which the reader will find information on all kinds of things ... The work of Dr. Basanavichius to few are known, but the way he deserves greater spread not only among doctors but also among the intellectuals at all. The author has used too much time and effort to write this work, and this is honor for him." [9]. The work of Dr. Basanavichius began often to be cited in the literature.

On September 16, 1891, the 6th National Assembly of Bulgaria accepted Dr. Basanavichius for Bulgarian citizen, which he considered to be a memorable event in their lives [10] and in 1982 received the "Order of Civil Merit Grade IV" [3]. In October 1892 he moved to work in Bulgaria, where he lived until his return to Lithuania in 1905. In Varna he continued his tireless work as a physician, scientist and public figure. He published a series of scientific works, among which are "To epigraphy and archeology Upper and Lower Moesia" (1894), written on behalf of the Ministry of Education, "Instruction collection anthropological materials in Bulgaria" (1896), published materials on anthropology and the healthy status of the population (1897), on national drugstores (1898) and others. He was elected a member of the Varna City Council (1899-1903) [2] and on his motion the Council decided to establish a museum in Varna, to collect "archaeological objects and materials for anthropology and ethnography of the current

МАТЕРИЯЛИ

ЗА

САНИТАРНАТА ЕТНОГРАФИЯ

НА

БЪЛГАРИЯ.

ЛОМСКИЯТЪ ОКРЪГЪ

(1880—1889)

ОТЪ

Д-Ръ И. БАСАНОВИЧЪ.

(Отдѣленъ отпечатокъ отъ книга V. отъ „Сборникъ за народни умотворения, наука и книжнина", издаванъ отъ Министерството на Народното Просвѣщение).

СОФИЯ
ДЪРЖАВНА ПЕЧАТНИЦА
1891.

Fig. 1.

population." In 1899 Dr. Basanavichius was involved in the resumption of activities of Varna Medical Society [6]. Co-founder of the Varna Archaeological Society [2], took part in the Bulgarian Medical Association. For his contribution to the Bulgarian science in 1898 was elected a corresponding member, and in 1902 – a real member of the Bulgarian Literary Society (today Bulgarian Academy of Sciences) [3, 10]. When he was elected a member of the Bulgarian Literary Society, he wrote to Society President: "With my election as a corresponding member of the Society proved me great honor, which allow me, Mr. Chairman in your face to speak of Management Committee my heartfelt gratitude" [4].

In the mind of Dr. Basanavichius was always his homeland Lithuania, on which at that time he dedicated a number of works [10]. Dr. Basanavichius had hypothesis about the relationship between Lithuanian and Thracian ethnicity that runs throughout its life. In his autobiography he wrote that at the first trip to Bulgaria found some words that exist in Lithuanian, but they are not present in other Slavic languages [10]. In 1989, Dr. Basanavichius published "Lithuanian-Thracian studies" and then returning to Lithuania

in 1925 published the monograph "Language kinship between old Thracian and today's Lithuanians", co-authored with A. Srba, which was evidence that more than twenty years after his departure from Bulgaria it still speaks to his mind and heart.

References

1. **Бакърджиев, В. Н.** Д-р Иванъ Юриевъ Басановичъ. – Медицински преглед, II(4), 1941-42, 278-279 и II(5), 356.
2. **Басанович, Й. Ю.** Материали за санитарната етнография на България. I. Ломският окръг (1880–1889). – СбНУНК, V, 1891, 3-186.
3. **Басанавичюс, Йонас Юрев.** 100 години БАН. 1869–1969. Том I. София, 1969, 27.
4. **Костадинова, Л., В. Флорова, Б. Димитрова.** Българо-руски научни връзки – XIX–XX век, писма и документи. София, Издателство на БАН, 1968.
5. **Маринов, Г.** Към изворите на българската научна медицинска мисъл – Ловчанската медицинска колегия и списание „Медицина" (1893–1895). – Асклепий, XII, 1999–2000, 112–115.
6. **Маринов, Г., З. Маринова.** Д-р Йонас Юро Басанавичус и неговият принос за развитието на здравното дело в Ломския окръг (1880–1892). – Асклепий, XIII, 2001, 110–115.
7. **Минков, С.** Санитарен отчет за Сръбско-българката война през 1885–1886 г. – ДВ, бр. 21, год. IX, 21 февруари 1887 г., 11–16.
8. **Миятев, П.** Иван Шишманов до К. Иречек. София, 3/15 април 1891 година стр. 269; К. Иречек до Иван Шишманов, Прага 14/26 априлий 1891, стр. 273. – В: Из архива на Константин Иречек. София, Издателство на БАН, II, 1959.
9. **Рецензии** за труда на Басанович. Материали за санитарната етнография на България. I. Ломският окръг (1880-1889). – Медицина (Ловеч), I(IV), 1894.
10. **Трояньски, Ив.** Доктор Йонас Бассанавичус и неговите спомени за България. – ИНМВ, X(XXV), 1974, 251–271.

Address for correspondence:
Georgi Rusev Marinov, MD, PhD
Medical University of Varna,
55 Marin Drinov Str.
9002 Varna
e-mail: grousmarin@yahoo.com

Institute of Experimental Morphology, Pathology and Anthropology with Museum
Bulgarian Anatomical Society

Acta morphologica et anthropologica, 21
Sofia ● 2015

Medical Errors and Negligence in Cases Versus Medical Professionals

D. Radoinova[*], *Y. Kolev*[**]

[*]*Department of Forensic Medicine and Deontology, Medical University, Varna, Bulgaria*
[**]*Department of Forensic Medicine, District Hospital MBAL, Gabrovo, Bulgaria*

Introduction

The term "medical error" (medical malpractice) is a medical rather than a legal term in Bulgaria [1]. It has a different and broader content, leading to considerable practical difficulties. Recently, in society and in law it suggests that the term "medical error" is an aggregate concept, which denotes mostly cases of negligent crime of medical professionals [5]. More severe group are intentional offenses in relation to medical practice: criminal abortions illegal, non-providing medical assistance, the repeat of secret, issuing false medical documents, illegal treatment, violation of anti-epidemic rules and regulations for use of drugs or toxic substances.

According to Bulgarian criminal law, negligence is the mildest form of guilt after intention [3]. Crimes for professional negligence are sentenced when they resulted in death or injury – art. 123 and 134 of the Penal Code[1] [2]. Negligent guilt is negligence (neglect) or conceit, which include ignorance of the medical science.

[1] Article 123 (1) of the Penal Code: "Whoever causes another's death due to ignorance or negligent performance of work or other legally regulated activity, representing a source of increased danger shall be punished with imprisonment of up to 5 years. (2) Any person who negligently causes another's death through actions belonging to a profession or activity in the preceding paragraph, it shall not be entitled to exercise, be punished with imprisonment from 1 to 5 years. (3) If, in the preceding paragraphs offender was intoxicated or if it caused death of more than one person, the punishment is imprisonment from 3 to 8 years, and in especially serious cases - imprisonment from 5 to 15 years. (4) If the perpetrator after the act has done everything depending on him to rescue the victim, the punishment shall be: 1 and 2 – imprisonment of up to 3 years under par. 3 - imprisonment of up to five years, and in especially serious cases – imprisonment of up to 3 to 10 years); Art. 134 (1) of the Penal Code: Whoever causes another severe or medium bodily injury due to ignorance or due to negligent performance of work or other legally regulated activity, representing a source of increased danger shall be punished: 1. by imprisonment of up to 3 years for severe bodily harm and 2. with imprisonment of up to two years or probation for a medium bodily injury, (2) The same punishment shall be imposed on those who negligently cause another severe or medium bodily injury through the actions belonging to a profession or activity in the preceding paragraph that he is not entitled to exercise. (3) If, in the preceding paragraphs

In almost all cases where there was injury of a living person or death, victims or their relatives complain to the Prosecution (or the Prosecution acts on its own initiative) and pre-trial investigation starts. A compulsory element is the institution of collective medicolegal investigation (expertise) involving forensic medical specialists and other medical specialists according to the specifics of the case.

Materials and Methods

The objectives of this study were cases versus medical professionals. The expertise was required to establish: what specific improper actions or inactions of the medical staff took place, what should be done but was not performed, what was the occurring prejudicial result, the existence of a causal link between medical acts/omissions and the prejudicial results; to make comparison between medical records and testimony for to show where and why there were contradictions and how reliable were they from a medical standpoint; to analyze the behavior of any medical professional who was relevant to this case, etc.

An analysis of 280 cases versus medical professionals for the last seven years in North-East Bulgaria was made.

Results and Discussion

The most common omissions and errors leading to adverse results may be summarized as:

1. Much more often than a wrong action, there was inaction of the medic, i.e. doctors have not made the necessary diagnostic and therapeutic actions **in time and adequately**. In most cases the doctor has made part of the necessary examinations and tests, but has not done everything possible (at the current level of development of medical science and according to the specific situation) for a full diagnosis and differential diagnosis. These omissions usually led to improper diagnosis, which resulted in inadequate behavior or adverse treatment or death. In surgery and obstetrics, the delay usually led to death of the patient or newborn child.

2. Conventional and repetitive medical activity and thinking rather than creative and individual approach to each patient. The lack of complex diagnostics which was a consequence of narrow specialization in modern medicine, leads ultimately to insufficient, untimely or inappropriate professional behavior towards the patient. There was no unifying doctor to analyze all done by individual counseling professionals from all examinations to decide on actual and correct diagnosis, management and treatment. Favorable factor for this result was the absence of accurate and detailed records - more frequently by private practitioners.

3. Sometimes there was insufficient analysis of all the facts – e.g., not seeking an explanation for leukocytosis or other tests that suggested a pathological process. There was underestimated the poor general condition or not searched an explanation for it in dynamics; the single result was interpreted incorrectly and out of the context of all data.

4. A typical was so called “Friday syndrome” (so named by us). These were cases in which patients with uncertain diagnosis and in serious condition were admitted in the

offender was intoxicated or if it caused damage to more than one person, the punishment is imprisonment up to 5 years for severe bodily harm and imprisonment of up to three years for medium bodily injury. (4) If the perpetrator after the act has done everything within it to assist the victim, this is taken into account as a mitigating factor for sentencing purposes.

last working day before the weekend or before a series of holidays. And there was no supervising doctor on duty every day but doctors in rotation. Later the criminal liability is determined by the poor outcome – most often the patient's death. Very often there was an insufficient collaboration both between doctors and other medical professionals – nurses, midwives and others.

5. Often there were no clear and precise internal rules and regulations in the clinic or in the whole hospital. This blurs the responsibility of the individual health professional. National medical standards of medical specialties not always offer clear and precise algorithms for work, especially in emergency situations.

6. Denial of medical care – it rarely occurred, but things are clearly defined by law. For emergency assistance it is not necessary a direction from a GP, and it doesn't matter if the patients have a health insurance or not.

7. Very often there was no collaboration between physicians whom the patient attended in primary care. So there were objective reasons – the patients themselves gave insufficient information, they visited various doctors taking different therapies, often lack documentation of these stages and it was controversial. As a result, assessing the next doctor is inaccurate, incomplete and sometimes incorrect.

8. In pre-hospital care due to lack of direction-sheets or other reasons GPs did not send the patient to consultant, did not appoint imaging and other tests in full or did not interpret them correctly and the correct diagnosis was delayed sometimes fatally.

9. Very common complaint from patients and their families was the lack of attention, disinterest and indifference of the doctors. These were often only an emotional perception, but the patients are entitled to have complete and understandable information presented concerning their condition, treatment and prognosis.

10. In the smaller district hospitals there was a lack of diagnostic capabilities – necessary equipment (imaging, clinical laboratory etc.), lack of skilled specialists, no presence of blood banking and more. For such reasons several mothers and newborns died. Ministry of Health was recommended to close these hospitals. Through these cases was carried out the preventive role of the medicolegal investigation of malpractice.

11. Medicolegal investigation established and specified general methodological deficiences in the organization of health care: between outpatient and inpatient care, among foster-emergency surgeries and various clinics in the hospital, between hospitals in one city etc.

12. Medicolegal investigation indicates a need for stronger internal control in each hospital by increasing the number of autopsies performed, therapeutic and supervisory committees and clinical-anatomical conferences. This will strengthen the preventive role in all health care, i.e. doctors should learn from the mistakes of their colleagues.

13. The lack of accurate and complete medical records was considered as non performed or incorrect medical act.

14. There is some conflict of interest between hospitals and the National Health Insurance Fund. For the Fund is only important documentary implementation of clinical "path" rather than the quality of medical care. This somewhat limited the doctors and they are forced to enter objectively incorrect data in reporting documents (medical records).

Serious problem in cases versus medics was the selection of experts for a collective medicolegal investigation because of the reluctance of doctors-clinicians to participate in such investigations. The authors of a study by International Institute of Healthcare and Health Insurance [5] in their conclusions also unanimously recognized that "the outcome of the trial for medical affairs depends entirely on expert witnesses."

All the analyzed cases were against health care workers but only 2 cases were against dentists and have completed by termination for lack of proof. About 85% of

the cases were terminated in the trial phase in the absence of misconduct of medical professionals because of not discovering the errors and omissions due to failure to determine the responsible medical person or for lack of a direct causal link between doctors'actions/inactions and death. About 10% of cases led to indictment and prosecution (trial proceedings) of the case. Sentences in medical cases were suspended (for 2-8 months), a fine – up to 1000 levs (500 Euro), and worst – withdrawal of the right to practice the medical profession for a period of 1 to 6 months.

Medical errors could be avoided (or at least part of them) only if they were analyzed and studied by medical professionals themselves. Therefore, doctors should become acquainted with forensic expertise, to draw conclusions, incl. for organizational shortcomings in healthcare, which play a significant role in some cases. We were establishing repeatedly that relatives with the passage of time somehow "accept" the loss of their deceased close person, but can never forgive the doctor's behavior, which was far from deontological (ethical) standards. Charity as a reality and as a concept almost disappeared from modern medical practice in stressful and difficult routine.

Conclusion

The fight against illegal medical actions can and should be conducted in various ways, including analysis of the errors and negligence. It is necessary to comply with clear and precise rules, reflected in national standards of various medical specialties as well as procedures and internal order of hospitals and clinics. Only in this way we could personify medical activities and responsibilities of medics.

References

1. **Лисаев, П.** Деонтологично-правни въпроси на медицинската практика. Плевен, ИК „Фотон и ИЯ" ООД, 2010, с. 132.
2. Наказателнопроцесуален кодекс на Р. България (www.СИЕЛА).
3. **Радойнова, Д., А. Лазарова.** Независимо съпричинителство при лекарски дела по чл. 23 от НК (от юридическа и съдебномедицинска гледна точка) – Правен свят, 8 октомври 2011, 78–83.
4. **Раданов, Ст., П. Лисаев.** Съдебна медицина и медицинска деонтология. (Ред. Ст. Раданов). София, Сиела, 2006, 596–597.
5. Т. Безлов, Р. Илкова, Д. Чинарска, А. Георгиев в проекта „Подобряване ефективността на съдебната система при решаване на дела, свързани с лекарски грешки или небрежност и повишаване на защитата на правата на пациентите" на Международния институт по здравеопазване и здравно осигуряване, София, 2010 (www.zdrave.net).

Corresponding author:
Dobrinka D. Radoinova, PhD
Chief of Department of Forensic Medicine and Deontology
Medical University – Varna, Bulgaria
Phone: (+359) 879 202 927
E-mail: dradoinova@mail.bg

Institute of Experimental Morphology, Pathology and Anthropology with Museum
Bulgarian Anatomical Society

Acta morphologica et anthropologica, 21
Sofia ● 2015

In memoriam

Professor Wolfgang Kühnel (1934–2015)

On August 21st, 2015, after serious illness, passed away at the age of 81 years the exceptional anatomist, the long-standing Secretary General of the Anatomische Gesellschaft and Director of the Institute of Anatomy of the Medical University in Lübeck/Germany, Prof. Dr. Wolfgang Kühnel. We will remember Prof. Kühnel as an unusual person, rich in ideas scientist, outstanding morphologist, who evoked respect with his multiple interests and large number of engagements, which he realized with pedantic accuracy as well as for his important contributions for the Bulgarian anatomy.

Wolfgang Kühnel was born on January 10th, 1934 in Bad Töplitz, Saar, in a rich in traditions intellectual family. In 1946 his family ran away to West Germany – to the city of Staunau, Hessen, where in 1955 he finished the high school. During the same year he began to study medicine at the Philipps-University in Marburg/Lahn. He completed his preclinical education with excellence and continued as a scholarship holder of the Studienstiftung des Deutschen Volkes. On September 28th, 1958 he married Marianne Dietrich, famous scenic designer and artist. They had two children. During 1961 he earned his doctorate in medicine with the dissertation thesis: "Morphological and experimental studies on the hen's allantois". After that he started to work as Specializing-Doctor in the city hospital in Rendsburg.

On the January 1st, 1963 Dr. Kühnel became Assistant at the Anatomical Institute of the University of Marburg (Chairman: Prof. Dr. Gerhard Petry). During 1967 he habilitated and was appointed as prosector (senior assistant) of the Institute. In 1970 Prof. Dr. Wolfgang Bargmann appointed him as Associate Professor in the Institute of Anatomy of the Kiel University. In 1974 he was appointed as Director of the Department of Anatomy at the Technical University in Aachen, where he organized the preclinical part of the study for medical students. In 1982 he was elected, by tendering, for Chair of the Institute of Anatomy of the Medical University of Lübeck.

A substantial part of the life of Prof. Wolfgang Kühnel was connected with the Anatomische Gesellschaft. From June 5th, 1974 until 2005 he was permanent Secretary General of the largest Anatomical Society in Europe.

Prof. Kühnel held high academic posts such as: Vice-Dean of the Medical Faculty Aachen, Vice-Dean and Dean of the Medical Faculty and Vice-Rector and Rector of the Medical University of Lübeck. He was also Secretary General of the International Federation of the Anatomical Associations (IFAA) (in the period 1989-1996), and active member of many international organizations.

As a scientist Prof. Kühnel worked in the fields of the functional and experimental morphology, clinical and topographical anatomy, where he got and published important new results. He is also author and co-author of reinforced textbooks, revision books and atlases of Anatomy.

Professor Kühnel left its deep marks in the Bulgarian Morphology. As an anatomist with great experience he helped many Institutes with programs for integrated teaching in Anatomy and Histology, also provided information for current methods for fixation of corpses. He invited a lot of Bulgarian anatomists for specialization of modern methods and experimental approaches in the Institutes he worked at. His wife, Marianne Kühnel, has effectively contributed with her lovely festivities the foreign colleagues to feel very comfortable. As a result, more than 20 papers were published in prestige journals and presented at international congresses.

As Secretary General of the Anatomische Gesellschaft he markedly contributed to the rise of the international prestige of the Bulgarian morphological science and the integration of the Bulgarian Anatomical Society to the European Scientific Institutions.

Professor Kühnel invested a lot of time, efforts and organizational skills into the performance of Congresses of the Anatomische Gesellschaft in East European countries. For the first time this happened in Varna in 1981. The 76th Congress of the Anatomische Gesellschaft was held together with the 8th Congress of the Bulgarian Anatomical Society in the International Hotel in Zlatni pyasatsi (see the photo below). At the Congress more than 100 outstanding European anatomists and the same number of Bulgarian anatomists took part. The Congress had a great success. At this Congress Professor Wolfgang Kühnel was awarded Doctor Honoris Causa of the Bulgarian Anatomical Society for his contributions in the organizing of this event and its active support for the rise of the international authority of our Anatomy. He was also awarded Doctor Honoris Causa of the Medical University of Sofia.

The decease of Professor Wolfgang Kühnel is a heavy loss also for the Bulgarian Anatomical Society. We lost a very worthy, distinguished and unforgettable Person, Teacher, Scientist and a great friend of Bulgaria.

A few top publications of Professor W. Kühnel:

Kühnel W. 1965. Morphologische Untersuchungen am Amnion und an der Allantois (Kaninchen). – Z. Zellforsch., 66: 649-662.

Kühnel W., Krisch B. 1974. On the sexual segment of the kidney in the snake (Natrix natrix). – Cell Tissue Res., 148: 417-429.

Vassilev V., Andreev D., Kuehnel W. 1995. Scanning electron microscopy of the endomisial collagen in the rat paravertebral musculature. – Ann. Anat., 177: 85-87.

Wassilev W., Wassilev I., Andreev D., Kuhnel W. 2005. Morphological aspects of the problem "Anterior cruciate ligament". – Verh. Anat. Ges. (Anat. Anz. Suppl.), 187: 71.

Prof. Dr. V. Vassilev, Prof. Dr. M. Davidoff